Investigation of the prevalence and mechanisms of weight loss and muscle wasting in clinical and pre-clinical stroke

Jawzaa Alenazi

BSc, MSc

Submitted in fulfilment of the requirements of the degree of Doctor of Philosophy

School of Cardiovascular and Metabolic Health

College of Medical, Veterinary and Life Sciences

University of Glasgow

December 2025

Abstract

Stroke survivors often face complications that hinder recovery and reduce quality of life. These complications include weight loss (or cachexia) and muscle wasting (or sarcopenia), which are both linked to poor stroke outcomes. While cachexia and sarcopenia are well documented in other clinical conditions such as cancer and heart failure, their prevalence and underlying mechanisms in stroke remain largely unexplored. Some obvious factors that may contribute to post-stroke weight and muscle loss include impaired feeding and malnutrition, paresis and physical inactivity. Preclinical studies have shown that experimental stroke induces marked weight loss in rodents, which involves global wasting of lean and fat tissue. As such, it has been hypothesised that post-stroke weight loss and muscle wasting arise from catabolic overactivation and anabolic blunting driven at least in part by systemic pathophysiological mechanisms triggered by the ischaemic insult. Such systemic pathophysiological mechanisms include inflammation and sympathetic activation, which are both known to alter catabolic and anabolic balance. Importantly, however, the relationship between ischaemic infarct and post-stroke weight loss remains unclear, and it is unclear whether the weight loss is induced by these systemic responses triggered by stroke or by secondary factors.

The overarching aim of this thesis is to address key knowledge gaps regarding post-stroke weight loss and muscle wasting. Firstly, it was hypothesised that post-stroke weight loss and sarcopenia are under appreciated complications but are prevalent within the stroke population. Secondly, it was hypothesised that post-stroke weight loss in pre-clinical stroke models is dictated by stroke severity and/or the anatomical location of the infarct supporting the notion that mechanisms triggered by the brain injury contribute to body weight loss. Finally, it was hypothesised that stroke leads to an upregulation of genes in skeletal muscle involved in the catabolic pathway and a downregulation of genes involved in protein synthesis and anabolic pathways, contributing to muscle wasting.

In this thesis, the systematic review and meta-analysis of clinical studies demonstrate that the pooled prevalence of post-stroke weight loss and stroke-related sarcopenia is 31% and 36% respectively, among stroke survivors. Furthermore, both conditions were linked to poor clinical and functional

outcomes, and a more extended hospital stay. Our preclinical data using the middle cerebral artery occlusion (MCAo) and photothrombotic (PT) models found that profound weight loss occurred in the acute phase after stroke, which was characterised by marked visceral fat loss, and skeletal muscle loss in both hindlimbs (stroke-affected and non-affected side) of mice. Importantly, water and food intake did not differ significantly between stroke and sham mice, suggesting that reduced food or water consumption alone is insufficient to explain weight loss after experimental stroke. Our data subsequently found a significant, moderate positive correlation between infarct volume and weight loss, indicating that larger infarcts are associated with greater weight reduction. Furthermore, in exploratory analyses, no association was found between infarct location and weight loss, suggesting that lesion size, rather than its anatomical position, is a determinant of the extent of post-stroke weight loss. Using non-targeted metabolomics, we next assessed the metabolic response to stroke in young and aged mice. Multivariate and univariate analyses revealed no differences among sham or stroke mice and between the age groups. However, using a linear model we found potential stroke-associated metabolic alterations in metabolites involved in lipid, fatty acid, and tryptophan metabolism. Finally, we found that weight loss in mice after experimental stroke (transient MCAo [tMCAo]) persisted up to ~21 days after stroke onset whereas the loss of skeletal muscle mass was evident only of days 3 and 7 post-stroke induction. Furthermore, the loss of skeletal mass after experimental stroke (transient MCAo) in young and aged mice was associated with upregulation of catabolic genes (e.g., MuRF-1) in the acute phase after stroke, consistent with gene expression patterns observed in age-related sarcopenia. Lastly, there was evidence for increased gene expression of the pro-inflammatory cytokine TNF-α in the skeletal muscle of both hindlimbs supporting the potential involvement of inflammatory mechanisms in post-stroke muscle wasting.

In conclusion, this thesis demonstrates that post-stroke weight loss or muscle wasting are prevalent in the stroke population, and our pre-clinical work suggests that this may be dictated, at least in part, by stroke severity. These findings indicate that post-stroke weight and muscle loss is a multifactorial and complex process, underscoring the importance of recognising and addressing these conditions as a significant clinical issue after stroke and highlighting the need for

more studies to target systemic mechanisms to better understand mechanisms and improve recovery.

Table of contents

List of Tables

List of Figures

Acknowledgements

First and foremost, I express my heartfelt gratitude to Allah for giving me the strength, patience and faith to complete this journey. I would also like to thank my primary supervisor, Dr Alyson Miller, for her endless support, encouragement and guidance. I honestly can't find the right words to describe how grateful I am for everything you have done for me. My sincere thanks also go to my second supervisor, Professor Jesse Dawson, for the great help and advice during my journey.

I'm truly thankful to all the former members of Miller lab- Alex, Gabbie, Arun, and Nicola – for your help, kindness and thoughtful discussion we shared in the lab. I also extend my sincere thanks to Yasmin Amer in the animal unit for her kindness and for providing assistance with my work.

A very special thanks to my dear friend Sarah Alanazi, who made this journey brighter and full of laughter. I also want to thank my friends Eman, Rawabi and Ruqqayah for their constant support.

Finally, and most importantly, I want to express my deepest love and gratitude to my family. To my backbone, my husband, Amer, thank you for your endless patience, understanding and for continuous love and support throughout this journey. To my precious children, Ward, Ziyad and Hattan, you are the light of my life. Every smile and hug from you kept me going. You are my greatest motivation and inspiration. I'm especially grateful for my mother, whose endless prayers, love and encouragement have been my greatest source of strength throughout this journey.

Author's Declaration

I declare that this thesis was written by myself and provides a record of research performed by myself and has not been submitted for any other degree at the university of Glasgow or any other institution. For certain experiments, others were involved in practical aspects of the work:

Dr Alyson Miller performed stroke surgeries (transient middle cerebral artery occlusion) for Chapters 4-6 with anaesthetic assistance from me.

Dr Arun Flynn (transient middle cerebral artery occlusion) and Dr Alexandra Riddell (permanent middle cerebral artery occlusion) performed stroke surgeries, brain sectioning, and thionin staining for Chapter 4.

Dr Adrian Knezic performed stroke surgeries (photothrombotic), brain sectioning, and thionin staining for Chapter 4.

Ms Yasmin Amer assisted with cardiac puncture for Chapter 5

Mrs Erin Kerr conducted LC-MS experiments for Chapter 5, and Dr Clement Regnault provided training on metabolomic analyses.

Jawzaa Alenazi

3/12/2025

Abbreviations

AD	Alzheimer's disease
ADL	Activities of daily living
AgRP	Agouti-Related Peptide
AKT	Protein kinase B
ALM	Appendicular Lean mass
ANOVA	Analysis of variance
ARC	Arcuate Nucleus
ARRRIVE	Animal research: reporting of in vivo experiments
ASM	Appendicular skeletal muscle mass
ATP	Adenosine triphosphate
AWERB	Animal welfare and ethics review board
AWGS	Asian working group for sarcopenia
BAT	Brown adipose tissue
BBCAs	Branched-chain amino acids
BIA	Bioelectrical impedance analysis
BMI	Body mass index
CBF	Cerebral blood flow
CC	Calf circumference
CCA	Common carotid artery
CIV	Corrected infarct volume
CNS	Central nervous system
CRH	Corticotropin-releasing hormone
CSA	Cross-sectional area
Ct	Cycle threshold
DAPI	4',6-diamidino-2-phenylindole
DNA	Deoxyribonucleic acid
DPBS	Dulbecco's phosphate-buffered saline
DXA	Dual energy X-Ray absorptiometry
eIF2B	Eukaryotic initiation factor 2B
EAATs	Excitatory amino acid transporters
ECA	External carotid artery
EDTA	Ethylenediamine tetraacetic acid
EIF4EBP1	Eukaryotic translation initiation factor 4E-Binding protein
ET-1	Endothelin-1
EWGSOP	European working group on sarcopenia in older people
FBXO32	F-Box protein32 (Atrogin-1)
FDA	Food and Drug Administration
FDR	False Discovery Rate
FIM	Functional Independence Measure
FOXO	Forkhead box protein O

GsK3β	Glycogen synthase kinase 3 beta
H&E	Haematoxylin and Eosin
HILIC	Hydrophilic interaction liquid chromatography
HPA axis	Hypothalamic-pituitary-adrenal axis
HPLC	High-performance liquid chromatography
ICA	Internal carotid artery
ICH	Intracerebral haemorrhage
IDEOM	Integrated differential expression and outlier metabolomics
IGF-1	Insulin-like growth factor 1
IL-1β	Interleukin-1 beta
IL-6	Interleukin-6
IS	Ischaemic stroke
IRS-1	Insulin receptor substrate 1
IWGS	International working group on sarcopenia
LC-MS	Liquid Chromatography-Mass Spectroscopy
LHA	Left hemisphere area
LMM	Low muscle mass
LMS	Low muscle strength
LOS	Length of stay
LPP	Low physical performance
Lyso PE	Lysophosphoatidylethanolamine
m/z	Mass-to-charge ratio
MARP	Monash Animal Research Platform
MCA	Middle cerebral artery
MMI	Muscle mass index
mRS	Modified ranking scale
MRI	Magnetic resonance imaging
MSTN	Myostatin
mTOR	Mammalian target of rapamycin
MuRF-1	Muscle RING Finger 1
NF-κB	Nuclear factor kappa B
NIH	National institutes of health
NINDS	National institute of neurological disorders and stroke
NMDA	N-methyl-D-Aspartate (receptor)
NOS	Newcastle-Ottawa scale
NP	Natriuretic peptide
NPY	Neuropeptide Y
OV	Oedema volume
PCA	Principle component analysis
PCR	Polymerase chain reaction
PECOS	Population exposure comparison outcome study design
PiMP	Polyomics integrated Metabolomics Pipeline

POMC	Pro-opiomelanocortin
PRISMA	Preferred reporting items for systematic reviews and meta-analysis
PSD95	Postsynaptic density protein 95
PI3K	Phosphoinositide 3-kinase
PT	Photothrombotic
PVN	Paraventricular Nucleus (of the hypothalamus)
r18s	Ribosomal 18s
rCBF	Regional cerebral blood flow
REM	Random effects model
RHA	Right hemisphere area
RIA	Right infarct area
ROS	Reactive oxygen species
RPS6	Ribosomal protein S6
RPS6K	Ribosomal protein S6 kinase
RT-qPCR	Reverse transcription quantitative polymerase chain reaction
SAH	Subarachnoid haemorrhage
SD	Standard deviation
SEM	Standard error of mean
SPPB	Short Physical Performance Battery
STAIR	Stroke therapy academic industry roundtable
TBP	TATA-Box Binding Protein
TGFβ	Transforming growth factor beta
TNF-α	Tumor necrosis factor alpha
tMCAo	Transient middle cerebral artery occlusion
tPA	Tissue plasminogen activator
TUNEL	Terminal deoxynucleotidyl transferase dUTP Nick-End Labelling
UPS	Ubiquitin-proteasome system
UPLC	Ultra-performance liquid chromatography
UTI	Urinary tract infection

Chapter 1 General introduction

1.1 Stroke

Stroke is a neurological disorder that is the second leading cause of death, and it is also a leading cause of disability worldwide (Feigin et al., 2025). A stroke occurs when there is a partial or complete interruption of the blood supply to a region of the brain. This interruption typically occurs when a thrombus or embolus occludes a cerebral artery, resulting in an ischaemic stroke (IS), or when a cerebral artery ruptures, causing a haemorrhagic stroke (intracerebral or subarachnoid) (Dirnagl et al., 1999). Globally, ischaemic stroke accounts for 65.3% of incident strokes, intracerebral haemorrhage (ICH) for 28.8%, and subarachnoid haemorrhage (SAH) for 5.8%, with ischaemic stroke representing the highest proportion in high-income countries (Feigin et al., 2025). The primary focus of this thesis is ischaemic stroke as it represents the most prevalent type of stroke. According to the World Stroke Organisation, approximately 12 million incident strokes are reported each year. Moreover, despite significant advances in medical care, stroke remains responsible for about 7 million deaths each year (Feigin et al., 2025). The global estimated cost of ischaemic stroke exceeds US$890 billion annually and is projected to nearly double by 2050 due to the ageing population (Feigin et al., 2025). Therefore, the stroke is a significant challenge for the healthcare system worldwide.

1.1.1 Stroke risk factors

A stroke risk factor is defined as any specific characteristic or condition that increases an individual's risk of stroke compared to those without that condition or characteristic (Hankey, 2006b). Stroke risk factors are generally categorised as either modifiable or non-modifiable factors. Unmodifiable risk factors include age, sex, and race (Kuriakose and Xiao, 2020, Boehme et al., 2017). The prevalence of stroke has been found to vary among different races, which may be due to genetic or environmental factors. Some data have shown that the black and Hispanic population have a higher risk of stroke than the white population (Cruz-Flores et al., 2011). The influence of sex on stroke risk appears to be age-related; the risk of ischaemic stroke is lower in premenopausal women than in young men and after menopause, older women have a higher risk than men (Branyan and Sohrabji, 2020). Moreover, the death rate for stroke is found to be higher among women. For example, a report from the United States in 2019 found

that stroke is responsible for 6.2% of all deaths in women and 4.4% in men (Heron, 2021). Factors such as the use of hormonal therapy, contraceptive and preeclampsia are believed to contribute to the increased risk of stroke in women (Xu et al., 2015, Yoon and Bushnell, 2023).

Modifiable risk factors are those factors that are due to lifestyle choices and environmental factors and can be prevented or reduced by healthcare interventions and education. These factors include medical conditions such as hypertension, type II diabetes, atrial fibrillation or lifestyle choices such as cigarette smoking, obesity, physical inactivity, and alcohol consumption. Among the medical conditions, hypertension is the major modifiable risk factor for ischaemic stroke; a meta-analysis study demonstrated that a 10 mmHg reduction in systolic blood pressure was linked to a 27% decrease in stroke risk (Ettehad et al., 2016). Similarly, diabetes is considered an independent risk factor for ischaemic stroke and is associated with a twofold increase in the ischaemic stroke risk, and accounts for about 20% mortality in diabetic patients (Vermeer et al., 2006). Atrial fibrillation is also a major risk factor, increasing the risk for ischaemic stroke by approximately fivefold (Marini et al., 2005). These findings highlight the importance of targeting modifiable risk factors through proper prevention and management approaches to reduce stroke burden.

1.1.2 Pathogenesis of ischaemic stroke

Ischaemic brain injury develops rapidly, occurring within minutes of an interruption in cerebral blood flow caused by arterial occlusion. The area of the brain immediately upstream of the occluded cerebral artery is referred to as the ischaemic or infarct core (Dirnagl et al., 1999). In the infarct core, the majority of cells undergo irreversible death. Surrounding this region is the ischaemic penumbra, which receives blood supply from collaterals and is an area of potentially salvageable cells, representing the primary target for therapeutic intervention (Majumder, 2024). Cerebral ischaemia causes brain injury through a complex cascade of pathophysiological events that include excitotoxicity, oxidative stress, neuroinflammation, necrosis, and apoptosis (Dirnagl et al., 1999, Majumder, 2024). A fundamental initiating event in this cascade is the disruption of cerebral perfusion, because brain tissue relies on a continuous blood supply of oxygen and nutrients for brain survival and function, as it has limited energy

reserves. When a major cerebral artery becomes occluded, perfusion to the impacted region is reduced, leading to energy failure caused by a reduction of oxygen and glucose leading to impaired ATP production. As a result, ionic gradients are disrupted, affecting ion transport mechanisms such as the calcium/sodium exchanger and the sodium/potassium ATPase pump on neuronal plasma and organelle membranes, leading to loss of membrane potential and anoxic depolarisation (Majumder, 2024, Dirnagl et al., 1999). Failure of the ionic pumps and resultant anoxic depolarisation also promotes excessive calcium influx into neurons which in turn causes persistent release of excitatory amino acids, such as glutamate, into the synaptic cleft and extrasynaptic space. Furthermore, the accumulation of glutamate in the synapse is accentuated by the failure of Na+-dependent excitatory amino acid transporters (EAATs), which normally reuptake glutamate into the presynaptic neuron. These events drive excitotoxicity and resultant neuronal cell death, mediated by overactivation of glutamate receptors such as N-methyl-D-aspartate receptors (NMDA) on postsynaptic neurons (Dirnagl et al., 1999). The mechanisms underpinning glutamate-mediated excitotoxicity are complex, involving the activation of several calcium-dependent and -independent intracellular complexes. For example, following NMDA receptor activation, excess influx of calcium activates the enzyme neuronal nitric oxide synthase, which then couples to the scaffolding protein postsynaptic density protein 95 (PSD95). The formation of this complex in turn triggers the sustained production of nitric oxide, which at high concentrations causes mitochondrial dysfunction and cell death, particularly when it reacts with reactive oxygen species (ROS) such as superoxide to form peroxynitrite (Kamel et al., 2025).

Additionally, Cerebral oedema develops in distinct stages over time, beginning with an early cytotoxic phase and followed by a vasogenic phase (Stokum et al., 2016, Simard et al., 2007). Cytotoxic oedema occurs within minutes of ischaemic injury and develops without BBB breakdown. It is usually driven by depletion of ATP and failure of various ion channels and transporters that normally maintain ionic balance (Liang et al., 2007). One key example is the Na^+/K^+-ATPase pump, which, under normal conditions, transports sodium out of the cell and potassium into it. This failure eventually leads to excess Na+ within the cell and retention of water molecules. In addition, the sulfonylurea receptor 1–transient receptor potential melastatin 4 (SUR1-TRPM4) channel contributes to the formation of

cytotoxic oedema (Simard et al., 2012). Although not normally expressed in healthy brain tissue, this channel is upregulated following cerebral ischaemia, promoting further sodium influx, water retention, and cell swelling (Simard et al., 2012). This phase primarily reflects a redistribution of water from the extracellular to the intracellular compartment rather than an overall increase in total brain water. As a result, swelling occurs at the cellular level without significant expansion of overall brain volume or an increase in intracranial pressure. Cytotoxic oedema affects all brain cell types, with particularly marked swelling in astrocytes (Keep et al., 2017). Vasogenic oedema, in contrast, results from damage to the cerebral vasculature and is characterised by disruption of the blood–brain barrier (BBB). This leads to leakage of plasma proteins and fluid into the extracellular space. Altered sodium transport across the BBB plays an important role in the formation of this phase of oedema (Stokum et al., 2016, Keep et al., 2017).

Neuroinflammation has also been implicated as a key pathophysiological mechanism in both the acute and chronic phases of stroke (Majumder, 2024, Dirnagl et al., 1999). Furthermore, ROS play an important role as signalling molecules that initiate an inflammatory response. Inflammatory mediators, such as tumour necrosis factor α (TNF-α), platelet-activating factor, and interleukin-1β (IL-1β), are released by damaged brain cells. Consequently, the adhesion molecules on the surface of the endothelial cells are induced, leading to leukocyte infiltration into the brain and the breakdown of the blood-brain barrier, which promotes further neuronal damage (Majumder, 2024). Additionally, some studies have suggested that cerebral ischaemia acts as a stressor capable of activating the sympathetic nervous system and hypothalamic–pituitary–adrenal (HPA) axis to protect the body from severe damage (Fassbender et al., 1994). Research shows that in cases of acute severe illness, the activation of the HPA axis results in higher cortisol levels, which are directly related to the severity of the disease. This activation provides many physiological advantages such as mobilising glucose from hepatic and adipose stores (Barugh et al., 2014, Munck and Náray-Fejes-Tóth, 1994, Fassbender et al., 1994). Notably, some researchers believe that the HPA axis can be directly triggered by high levels of inflammatory cytokines such as TNF-α and IL-6 (Johansson et al., 1997, Szczudlik et al., 2004).

1.1.3 Treatment of ischaemic stroke

To date, there are only two approved treatments for ischaemic stroke to restore blood flow, which are intravenous thrombolysis and intra-arterial mechanical thrombectomy (Salaudeen et al., 2024, Berge et al., 2021). Tissue plasminogen activator (tPA) is used for thrombolysis, and alteplase is the most common form (Baig and Bodle, 2020). It acts by converting plasminogen in the blood clot to soluble plasmin, a proteolytic enzyme that degrades fibrin and fibrinogen within the thrombus, which blocks the cerebral artery. Its effectiveness in acute ischaemic stroke was demonstrated in 1995, in a study conducted by the National Institute of Neurological Disorders and Stroke (NINDS) (Disorders and Group, 1995, Liaw and Liebeskind, 2020). Although tPA is the only drug approved by the FDA for ischaemic stroke treatment, only 10% of stroke patients are believed to meet the criteria for using tPA as a treatment for ischaemic stroke because many restrictions and complications limit its clinical use (Fugate and Rabinstein, 2014). It has a short treatment window. Thus, it must be administered within 4.5 h of stroke onset to be effective, which is challenging in clinical practice. Furthermore, tPA can result in severe side effects such as intracerebral haemorrhage, and the risk of the haemorrhage increases with delayed administration of the drug, which further constrains its utility (Liaw and Liebeskind, 2020, Berge et al., 2021). The other treatment is mechanical thrombectomy (MT), which was first approved in 2015 after the publication of results from five clinical trials demonstrating its efficacy within 6-8 hours of the onset of ischemic stroke. However, recent studies have extended the treatment window up to 24 h after stroke onset based on meeting certain criteria (Jovin et al., 2015, Liaw and Liebeskind, 2020, Nogueira et al., 2018, Albers et al., 2018). Notably, however, whilst both treatments effectively restore blood flow to the brain and improve patient outcomes (Hurd et al., 2021), they do not directly target ensuing mechanisms of the ischaemic cascade or directly promote reparative mechanisms. As a result, only 50% of the patients can achieve functional independence after stroke treatment (Samaniego et al., 2018). This highlights the necessity for new effective and safe therapeutic strategies to be identified and validated for use in ischaemic stroke patients.

1.1.3.1 Challenges for improvements of novel therapy for ischaemic stroke

Given that only a small number of stroke patients are eligible for recanalization therapy with rt-PA or by mechanical thrombectomy after ischaemic stroke onset, there is an urgent need to develop alternative effective therapeutic strategies that can be used in a larger number of stroke patients. Extensive research has focused on developing neuroprotective strategies to protect the brain from damage, with particular attention paid to saving the penumbra. A range of neuroprotective agents have demonstrated promising efficacy in animal models of stroke. However, nearly all of these interventions have failed to show efficacy in clinical stroke trials (Savitz et al., 2017, Pérez-Mato et al., 2024). The key reasons that impede the successful translation of pre-clinical findings into effective clinical therapies include the use of young, healthy animals with no comorbidities and the homogeneity of the study sample in preclinical studies. In contrast, in humans, stroke is heterogeneous, and patients typically have associated risk factors and comorbidities (Xu and Pan, 2013). Another key factor is flaws in the design of preclinical and clinical studies, including a lack of blinding and randomisation. In addition, the therapeutic time window during which agents are administered prior to or immediately after stroke induction, whereas in clinical trials, a longer duration is required for diagnosis and imaging (Xu and Pan, 2013). Furthermore, often the models used do not mimic the exact pathophysiological features of human stroke, which also contributes to clinical failure (Sutherland et al., 2012, Pérez-Mato et al., 2024). To surmount translational failure, a new approach was adopted by the Stroke Therapy Academic Industry Roundtable (STAIR) which brought together industry, basic and clinical researchers, National Institutes of Health (NIH) representatives and regulators to establish guidelines for the preclinical development of neuroprotective agents before trying them in clinical trials (Fisher et al., 2009, Fisher, 2011). They recommended the use of transient occlusion models in rodents; that other conditions and comorbidities should be included in the animal models; findings should be reproduced in at least one other species; characteristics of the agents, such as pharmacokinetics and interaction with other drugs, should be investigated; and finally functional outcome should be measured in short and long-term and some regulations related to methodology (Lapchak et al., 2013).

1.1.4 Stroke complications

Many stroke patients develop a range of complications that can emerge or persist for months to years after a stroke. It has been reported that stroke patients who experience complications have higher rates of in-hospital and 3-month mortality and disability than those who do not experience complications (Al-Khaled et al., 2013). The most common complications stroke survivors may experience include infections due to immunosuppression, increased intracranial pressure, depression, altered nutritional status, and body weight and muscle loss. For example, a recent systematic review found pneumonia and urinary tract infection (UTI) to be the most prevalent infections in stroke survivors, with reported rates of 12.4% and 8.31% respectively (Awere-Duodu et al., 2024). The research showed that post-stroke infections resulted in a 16% death rate, and pneumonia-specific mortality reached 21.6% which reflects its critical clinical effects on stroke outcome (Awere-Duodu et al., 2024). Post-stroke depression is also documented and estimated to occur in approximately one-third of stroke patients at any time (Hackett and Pickles, 2014). Stroke survivors with depression have been found to have poorer functional and neurological outcomes (Sibolt et al., 2013, Ayerbe et al., 2014). Other complications such as fever, pain, urinary and faecal incontinence are also reported among the stroke survivors (Jacob and Kostev, 2020). While these complications have been relatively well-documented in the literature, post-stroke weight and muscle loss remain inadequately investigated, despite their clinical importance. Indeed, as discussed below, recent evidence indicates that weight and muscle loss after stroke affect recovery and functional outcomes, highlighting the need for further investigation.

1.2 Body weight and stroke

Excess body weight is recognised as an established risk factor for stroke. Current guidelines recommend weight reduction after a stroke to reduce the risk of a secondary event by improving obesity associated risk factors (Kleindorfer et al., 2021a). However, the beneficial effect of weight reduction after stroke to avoid recurrent stroke or cardiovascular events and to improve functional recovery remains largely unproven (Curioni et al., 2006). Additionally, evidence from a prospective, multicentre Chinese study revealed that underweight patients after ischaemic stroke had a significantly higher risk of death and dependency at 3 and 12 months post-stroke, while these outcomes in overweight and obese stroke patients did not differ from those with normal body weight (Sun et al., 2017). Furthermore, an emerging body of clinical studies suggests a survival benefit among overweight patients after ischaemic stroke. For example, a recent Japanese study assessed the prognostic impact of body weight after ischaemic stroke on clinical outcomes, found that patients with lower body mass index (BMI) were associated with unfavourable functional outcomes and high mortality compared with patients of normal BMI, whereas overweight patients were associated with favourable outcomes (Miwa et al., 2024). This phenomenon is referred to as the "obesity paradox," which was first recognised and reported in cardiovascular diseases, but is less acknowledged in other diseases (Gruberg et al., 2002).

1.2.1 Obesity paradox

In stroke, the obesity paradox has been observed in numerous studies. An inverse correlation between BMI and mortality after stroke was first reported in a cohort study conducted by Olsen and colleagues (2008). In this study, they found that the underweight patients exhibited a higher mortality rate, while the overweight and obese patients had a lower mortality rate compared to patients of normal weight after stroke (Olsen et al., 2008). Additionally, similar findings indicating a protective effect of obesity on the mortality of stroke patients have been reported by various studies (Doehner et al., 2013, Andersen and Olsen, 2015, Vemmos et al., 2011). However, some studies found a U-shaped association between BMI and mortality after stroke (Skolarus et al., 2014, Zhao et al., 2014). In this U-shaped relationship, patients with a BMI of 35kg/m^2 had the lowest mortality rate, while

those with a BMI of>38 or <31 kg/m² experienced a higher mortality risk (Skolarus et al., 2014). In contrast to these findings, Razinia and colleagues (2007) reported that obese stroke patients may experience prolonged hospital stays after stroke and reduced chances of home discharge. Similarly, Bazzano and colleagues (2010) found that the mortality after stroke increases in patients with elevated BMI (Bazzano et al., 2010). Nevertheless, a very recent umbrella review synthesising evidence from seven systematic reviews concluded that underweight patients (BMI < 18.5 kg/m²) are associated with increased mortality and poor functional outcomes, whereas excess body weight appears to be associated with decreased mortality relative to normal weight (Holland et al., 2024). However, a key limitation that may raise questions about the validity of the obesity paradox findings in stroke studies is that BMI is widely used to determine body size and weight in the vast majority of these studies and classifying individuals as underweight, normal weight, overweight or obese. It is noteworthy that BMI is not an accurate tool for assessing excess body weight or obesity, as it does not provide information on fat distribution within the body and is unable to distinguish between adipose (fat) and lean (muscle) mass (Romero-Corral et al., 2008).

Little is known about the mechanism underlying the obesity paradox after stroke; several hypotheses have been proposed to explain the protective effect of obesity. One of the proposed explanations of the protective effect of obesity on patients' outcomes is that stroke seems to induce catabolic metabolism and reduce anabolic effects leading to post-stroke weight loss and cachexia (see Section 1.3). Therefore, individuals with excess body weight possess better metabolic reserves, allowing them to better withstand the catabolic burden of stroke compared with underweight patients (Scherbakov et al., 2011a). However, a recent study of the high-fat diet model of obesity found that obese mice lost significantly more body weight than lean controls up to 50 days after stroke onset, which was accounted for by a greater reduction in adipose tissue (Haley et al., 2020b). Another suggested explanation is that adipose tissue, recognised as an endocrine organ, releases soluble TNF-α receptors that bind to and neutralise the effect of TNF-α, thereby dampening harmful inflammatory responses, which are activated in stroke (Oreopoulos et al., 2008).

1.3 Post-stroke weight loss or cachexia

Cachexia is a term that originated from Greek words, which means bad (kakos) and habit (hexis). It is characterised by a state of unintentional weight loss attributed to an underlying disease that can't be restored through nutritional support or alterations in dietary intake alone (Ebner et al., 2013). Various diagnostic criteria are utilised to diagnose cachexia. The most used definition considers many aspects of the condition. For example, Evans and colleagues (2008) developed a set of criteria at a consensus meeting to diagnose cachexia. These criteria include a body weight loss of 5% or more during a period of 12 months or less, accompanied by any three of the following criteria: muscle loss, reduction in muscle strength, anorexia, fatigue, and abnormal biochemistry characterised by anaemia, inflammation, or hypoalbuminemia (Evans et al., 2008). Body weight loss or cachexia has been observed after a stroke in both animal and clinical studies and it typically encompasses a loss of both fat and lean tissue indicating global tissue wasting (Jo̲nsson et al., 2008, Springer et al., 2014a, Yang et al., 2019). A multitude of mechanisms, as described below, may contribute to metabolic imbalance after stroke. The net effect of these mechanisms leads to catabolic overactivation and an anabolic deficit, and resultant global wasting of tissue which manifests as generalised weight loss (cachexia) or muscle loss (sarcopenia).

Importantly, clinical studies provide evidence that weight loss or cachexia after stroke is associated with poor clinical outcomes and higher dependency. For example, Scherbakov and colleagues (2019) revealed that stroke survivors who developed cachexia (21%; n=67) within 12 months of stroke onset were more severely disabled as determined by higher modified Ranking Scores, lower Barthel Index scores, and lower handgrip strengths compared with patients who experienced moderate weight loss or patients who experienced stable or weight gain. Moreover, a population-based study found that the mortality was 14% in stroke patients who lost more than 3 Kg within 1 year and just 4% in patients without weight loss (Jo̲nsson et al., 2008). As mentioned, body weight loss also observed in rodents after experimental stroke (Yang et al., 2019, Springer et al., 2014a, Haley et al., 2020b). Springer and colleagues (2014) reported a profound reduction in body weight in mice after transient middle cerebral artery occlusion (tMCAo) compared with sham controls, which was attributed to loss of both fat

and lean tissue. Similarly, Haley and colleagues (2020) observed prolonged weight loss in mice after experimental stroke, which persisted until the experimental endpoint at 2 months (Haley et al., 2020b).

Despite evidence that body weight loss occurs after stroke, no studies to date have systematically quantified the prevalence of post-stroke weight loss. Notably, however, Scherbakov and colleagues (2019) reported that approximately 21% of stroke survivors developed tissue wasting (cachexia) within 12 months of stroke occurrence, suggesting it may be a common post-stroke complication. However, the study was limited by a relatively small sample size (n=67) and only included patients with mild to moderate stroke deficits, which restricted the generalisability of the study findings to the broader stroke population (Scherbakov et al., 2019a). The lack of epidemiological evidence underscores the need for a systematic, comprehensive analysis to establish the actual burden of this condition and enhance understanding of its impact on clinical outcomes. In addition, the underlying mechanisms of post-stroke weight loss or cachexia and their functional significance remain inadequately defined in stroke.

Although post-stroke weight loss or cachexia has not been extensively investigated in the context of stroke, it is well documented and studied in other chronic diseases such as cancer and heart failure, chronic obstructive pulmonary disease and chronic kidney disease. For example, it is reported that approximately 70% of cancer patients experience cachexia, which affects them negatively as it reduces the quality of life due to frailty, decreases the efficacy of cancer therapies and correlates with increased mortality (Berriel Diaz et al., 2024). Up to 22% of cancer-related fatality is considered to be a consequence of cachexia (Fearon et al., 2012). Moreover, it is reported that approximately 50% of patients with chronic kidney disease have cachexia (Fearon et al., 2012). These observations emphasise the significant clinical impact of body weight loss or cachexia in chronic diseases and highlight the necessity for greater attention to its prevalence and consequences in stroke patients.

1.4 Sarcopenia

Sarcopenia is a disorder of skeletal muscle characterised by an accelerated decline in muscle mass, strength or function, leading to increased risk of fractures, falls and physical disability (Cruz-Jentoft et al., 2019). Sarcopenia is classified into primary and secondary sarcopenia. Primary sarcopenia is used to describe the loss of muscle mass and function that develops gradually because of ageing, and it is more prevalent in elderly people. On the other hand, secondary sarcopenia often refers to loss of muscle mass and strength caused by any underlying illness (Cruz-Jentoft et al., 2019). Despite growing recognition of sarcopenia as a significant health concern, its definition and diagnostic criteria remain inconsistent. For example, the International Working Group on Sarcopenia (IWGS) uses two criteria to define sarcopenia: low muscle mass and low muscle strength. At the same time, the European Working Group on Sarcopenia in Older People (EWGSOP) uses a decline in muscle strength as a primary and most important indicator to diagnose the condition as probable sarcopenia. The diagnosis is supported and confirmed by the presence of muscle mass loss and classified as severe sarcopenia when it is accompanied by low physical performance (Feigin et al., 2022, Cruz-Jentoft et al., 2019). The Asian Working Group on Sarcopenia (AWGS) defines the condition as a reduction in muscle mass and strength, with or without a decrease in physical performance, and has adopted cut-off values for sarcopenia diagnostic criteria customised for Asian individuals (Chen et al., 2020). Importantly, stroke survivors represent a population who are at increased risk of developing secondary sarcopenia due to inactivity and disuse atrophy. Ryan and colleagues (2011) reported that in stroke patients, the hemiplegic thigh exhibits a 20-24% decline in muscle area and volume, as well as a 17% increase in intramuscular fat, compared to the unaffected thigh (Ryan et al., 2011a). Interestingly, another study found that muscle atrophy, intramuscular fat deposition and a reduction of muscle strength in the hemiplegic limb after stroke were also observed in the contralateral limb within 3 weeks to 6 months after the stroke (Carin-Levy et al., 2006). However, English and colleagues (2010) conducted a systematic review, demonstrating that stroke survivors exhibit significantly lower muscle mass in both limbs (ipsilateral and contralateral to the ischaemic lesion) compared with healthy adults (English et al., 2010). In recent years, this kind of muscle mass and functional loss after stroke has been referred to as “stroke-related sarcopenia” or

“stroke-induced sarcopenia” (Scherbakov et al., 2013). Since ageing is considered a non-modifiable risk factor for both stroke and sarcopenia, older people are more vulnerable to this condition. While muscle wasting is well-recognised after stroke, the molecular mechanisms underpinning this loss remain unclear. It is well established that skeletal muscle homeostasis relies on a dynamic balance between anabolic and catabolic signalling pathways that control muscle growth, as described later. However, it remains unclear if this dynamic balance is disrupted after a stroke.

1.4.1 Muscle structure

A basic knowledge of muscle structure and physiology is essential for understanding the mechanisms of muscle wasting and sarcopenia, which is characterised by reductions in muscle fibre size and number. Skeletal muscle is made of different fibre types: slow-twitch type I fibres, which efficiently utilise oxygen to sustain prolonged contractions, and fast-twitch type II fibres, which primarily depend on anaerobic metabolism (Scott et al., 2001, McCuller et al., 2023). Each muscle fibre contains many myofibrils that include multiple myofilaments, called actin and myosin. The interaction between myosin and actin filaments facilitates the contraction of skeletal muscle. When ATP binds to myosin, it detaches from actin; subsequent hydrolysis of ATP triggers a conformational change that allows myosin to reattach to another actin filament. Myosin subsequently reverts to its initial conformation, allowing the actin filament to slide and generating contraction (Scott et al., 2001).

During oxidative phosphorylation, mitochondria generate approximately 90% of the ATP essential for cellular activity. Type I fibres exhibit a high oxidative capacity due to the availability of numerous mitochondria, abundant myoglobin (helps to improve oxygen delivery) and high capillary supply. Furthermore, type I fibres display a relatively low level of ATPase, glycolytic activity and creatin kinase. These oxidative characteristics enhance fatigue resistance, thereby contributing to greater exercise capacity (Scott et al., 2001, McCuller et al., 2023). Conversely, type II muscle fibres are characterised by a high level of creatine kinase, ATPase, and glycolytic anaerobic activities, making them fatigue quickly and thus suitable for short periods of activity (McCuller et al., 2023). One of the features of the muscle fibres is that they are capable of adapting and

transforming in response to any external stimuli. For example, in response to reduced physical activity in human, muscle fibres shift from slow-twitch (type I) to fast-twitch (type II) fibres (Jansson et al., 1978). In contrast, increased physical activity induces the opposite transformation, from fast-twitch to slow-twitch fibres (Hultman, 1995, Plotkin et al., 2021). In ageing, a shift from fast-twitch to slow-twitch fibres was reported in old rats (Holloszy et al., 1991). This shift in fibre type occurs due to motor unit denervation followed by reinnervation from nearby intact muscle fibres (Scherbakov and Doehner, 2011). However, an inverse shift from slow-twitch to fast-twitch that are highly fatigable has been reported in stroke survivors (De Deyne et al., 2004).

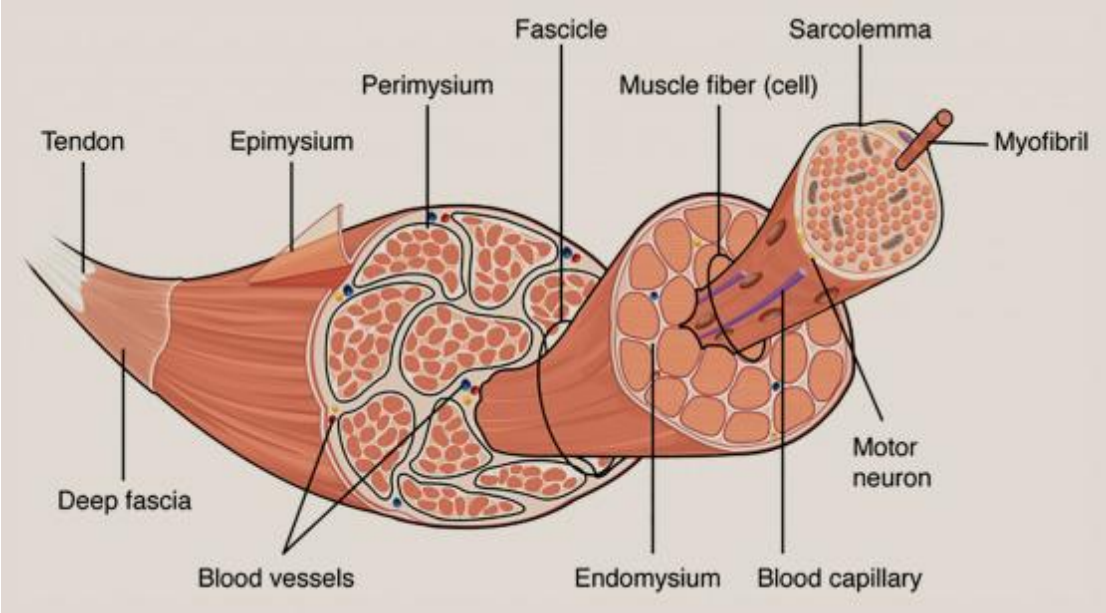

Figure 1-1 Skeletal muscle anatomy. Myofibrils consist of actin and myosin myofilaments, which are responsible for the contraction of muscle; Myofibrils form muscle fibres. Muscle fibres are surrounded by endomysium. A group of muscle fibres forms a fascicle. A group of muscle fascicle are surrounded by perimysium. A group of muscle fascicles forms muscle bundles. The muscle bundle is surrounded by epimysium. Image taken from (Allen et al., 2024).

1.4.2 Mechanisms controlling skeletal muscle mass

Muscle mass is controlled by the balance between pathways that regulate protein synthesis and degradation. The best-known anabolic signalling pathway that results in protein synthesis in skeletal muscle is the phosphoinositide 3-kinase–serine/threonine-protein kinase–mammalian target of rapamycin (PI3K–AKT–mTOR) pathway (Bodine et al., 2001b, Sandri, 2008). The anabolic stimuli in skeletal muscles, including insulin-like growth factor-1 (IGF-1), testosterone, leucine and exercise, cause activation of the pathway. When IGF-1 binds to its receptor, the insulin receptor substrate 1 (IRS-1) undergoes phosphorylation, leading to the activation of the PI3K–AKT–mTOR pathway(Bodine et al., 2001b, Sandri, 2008). This pathway also leads to the inhibition of glycogen synthase kinase 3β (GsK3β) and forkhead box protein O (FOXO) through the AKT pathway (Rommel et al., 2001). GsK-3β acts by negatively regulating the translation initiation of mRNA through phosphorylation and inhibition of the eukaryotic initiation factor 2B (eIF2B), which is needed to initiate the translation process of mRNA (Webb and Proud, 1997). Therefore, inhibition of GsK3β causes the dephosphorylation of eIF2B, which subsequently enhances the initiation of protein synthesis (Webb and Proud, 1997). On the other hand, another pathway that regulates muscle mass maintenance and is involved in protein degradation is the myostatin–Smad2/3 pathway (Sandri, 2008). Myostatin (MSTN) is one of the transforming growth factor-β (TGFβ) family members, which is released by muscle cells and produces its effect by binding to the activin-A receptor, leading to the phosphorylation of transcription factors Smad2 and 3. Notably, its role in human muscle atrophy remains undefined. However, it is suggested that it works as a muscle negative regulator through downregulating the AKT1 pathway and reducing satellite cell numbers (Sandri, 2008). Additionally, other pathways that contribute to muscle protein breakdown include the ubiquitin–proteasome system (UPS) and autophagy. The UPS functions as the primary cellular system for protein degradation, as it identifies cell cycle regulators, misfolded proteins, and transcription factors that have received ubiquitin tags for destruction through the ubiquitination process (Glass, 2010). E3 ubiquitin–protein ligases function as the rate-limiting enzyme in protein ubiquitination. They selectively recognise and attach the ubiquitin molecule to target proteins to mark them for degradation. Muscle RING Finger 1 (MuRF-1) and muscle atrophy F-box (FBXO32, also known as Atrogin-1) represent the two ligases that play the most significant role in muscle atrophy (Passmore

and Barford, 2004, Bodine et al., 2001a). The expression of *MuRF-1* and *Atrogin-1* is regulated by a transcription factor FOXO and nuclear factor-κB (NF-κB). Another mechanism is autophagy, which, under normal physiological conditions, functions as a nonselective degradation process that eliminates excess and nonfunctional cellular components, including damaged organelles and proteins (Sandri, 2013).

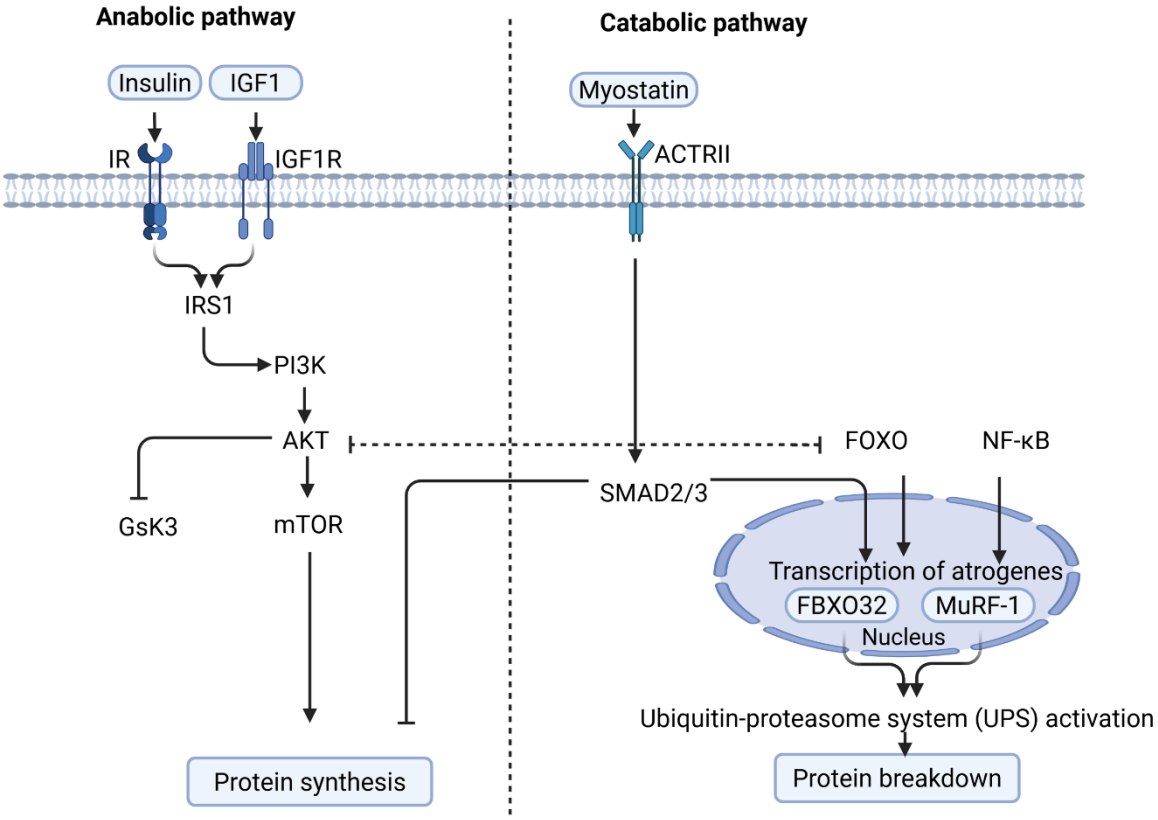

Figure 1-2 Anabolic and catabolic pathways regulating skeletal muscle mass. A diagram illustrating the key signalling pathways involved in muscle homeostasis. The two main pathways are IGF-1-PI3K–Akt–mTOR (acts as a positive regulator to increase protein synthesis) and myostatin–Smad2/3 pathway (acts as a negative regulator to inhibit protein synthesis and enhance protein degradation). Figure created in Biorender.com

1.5 Potential mechanisms of post-stroke weight loss and muscle wasting

The mechanisms underpinning wasting of fat and muscle after stroke are not well understood, and relatively little attention has been paid to it, with limited literature currently available on this complication. Some obvious factors that may contribute to post-stroke weight loss and muscle wasting include impaired feeding and malnutrition due to dysphagia, which is characterised by swallowing difficulty induced by nerve injury that may lead to malnutrition (Figure 1-3) (Scherbakov et al., 2011a). Indeed, malnutrition is a common complication in post-stroke survivors, affecting about 49% of individuals (Foley et al., 2009). Furthermore, dysphagia has been reported to occur in about 24.3-52.6% of stroke survivors and affects overall recovery (Foley et al., 2009).

Inactivity due to bed rest and/or paralysis is also proposed to contribute to tissue wasting after stroke. Indeed, it is reported that an approximate 30% reduction in muscle protein synthesis within 10 days of bed rest in healthy older adults (Kortebein et al., 2007). This reduction in muscle mass also led to a 16% decline in muscle strength. Notably, in stroke, a study indicated that hospitalised stroke survivors engage in physical activity for <40 minutes each day, and therefore their activity levels are low even in patients with mild stroke (Bernhardt et al., 2004). Clearly, reduced physical activity, which increases the risk of muscle atrophy, together with feeding impairment, might be major contributors to muscle and weight loss.

In addition to these obvious causes, it is proposed that some pathophysiological mechanisms (e.g., dysregulation of the HPA axis) triggered by the brain injury may induce tissue wasting. The HPA axis is a crucial component of the neuroendocrine system, regulating internal homeostasis and stress response and linking the periphery to the central nervous system (CNS) (Smith and Vale, 2006). Indeed, in response to physiological or psychological stressors and tissue trauma, the HPA axis is activated leading to the release of glucocorticoids from the adrenal gland. Experimental studies have shown that the HPA axis is activated in the acute phase of stroke, and that it may aggravate stroke pathology and worsen outcomes (Kim et al., 2022a, Anne et al., 2007). Furthermore, it has been shown that there is an elevation in cortisol levels during the first week of stroke in humans (Barugh et

al., 2014). The catabolic effects of glucocorticoids are well documented. Much of the literature indicates that glucocorticoids induce lipolysis by upregulating the transcription and expression of lipase enzymes responsible for lipid breakdown (Xu et al., 2009, Campbell et al., 2011). Moreover, glucocorticoids induce proteolysis by upregulating myostatin, a negative regulator of skeletal muscle, and antagonises the anabolic actions of insulin (Wang et al., 2016). A recent pre-clinical stroke study demonstrated that corticosterone is involved in body weight loss during the acute phase after stroke onset (Yang et al., 2019). Interestingly, however, they provided evidence that body weight loss after stroke might be an essential catabolic event for immunity and survival. Specifically, they showed that the extent of weight loss determined the mobilisation of monocytes/macrophages from the spleen and ultimately their infiltration into the ischaemic brain. Furthermore, bilateral adrenalectomy, which removes the primary source of endogenous glucocorticoids, increased mortality after stroke; 7 out of 8 mice with stroke that were subjected to adrenalectomy died, whereas all nine shams with adrenalectomy survived, indicating that the glucocorticoid-mediated catabolic process is essential for survival after stroke (Yang et al., 2019).

Natriuretic peptides (NPs) are peptide hormones secreted mainly by the heart and have also been reported to increase after stroke. They are known for their cardiovascular and renal actions, including lowering arterial blood pressure and reducing sodium reabsorption and have recently been found to have potent lipolytic properties (Schlueter et al., 2014). Another mechanism triggered by stroke is the activation of the sympathetic nervous system and the release of catecholamines, which increase energy expenditure. Furthermore, catecholamines such as epinephrine and norepinephrine are considered lipolytic agents that stimulate lipolysis by activating ß-adrenergic receptors in adipocytes (Schlueter et al., 2014). Notably, however, Springer and colleagues (2014) reported that targeting sympathetic overactivation after ischaemic stroke in mice did not alleviate weight loss. Their study showed that overall weight loss, as well as lean and fat mass loss, were unaffected by sympathetic suppression with propranolol, except for a slight reduction in fat loss in the propranolol-treated group.

As mentioned, inflammation is a key mechanism involved in the pathophysiology of ischaemic stroke and importantly modulates proteolysis and lipolysis (Zhang et

al., 2002, García-Martínez et al., 1993). Elevated levels of proinflammatory cytokines such as interleukin-1ß and TNF-α have been reported in some forms of cachexia, such as cancer and cardiac cachexia (Kim et al., 2012, Torre-Amione et al., 1996). Cytokines play a key role in immune regulation and have been implicated in the development of weight loss, anorexia, and cognitive dysfunction (Roubenoff et al., 2003). These proinflammatory cytokines stimulate nuclear factor κB (NF-κB), and activate the UPS in muscles, which is a key system involved in muscle proteolysis, thereby reducing muscle protein synthesis (García-Martínez et al., 1993).

In summary, in addition to obvious causes such as impaired feeding and immobility, there are several mechanisms triggered by the ischaemic brain that may contribute to catabolic overactivation and anabolic blunting and resultant body weight loss (Figure 1-3). If so, then one might would expect the extent of brain injury to dictate body weight loss after stroke, however, in terms of pre-clinical work weight loss does not always correlate with the infarct size (Yang et al., 2019, Springer et al., 2014a, Haley et al., 2020b). Therefore, it is conceivable that factors secondary to ischaemic injury may also contribute (Springer et al., 2014a, Haley et al., 2020b).

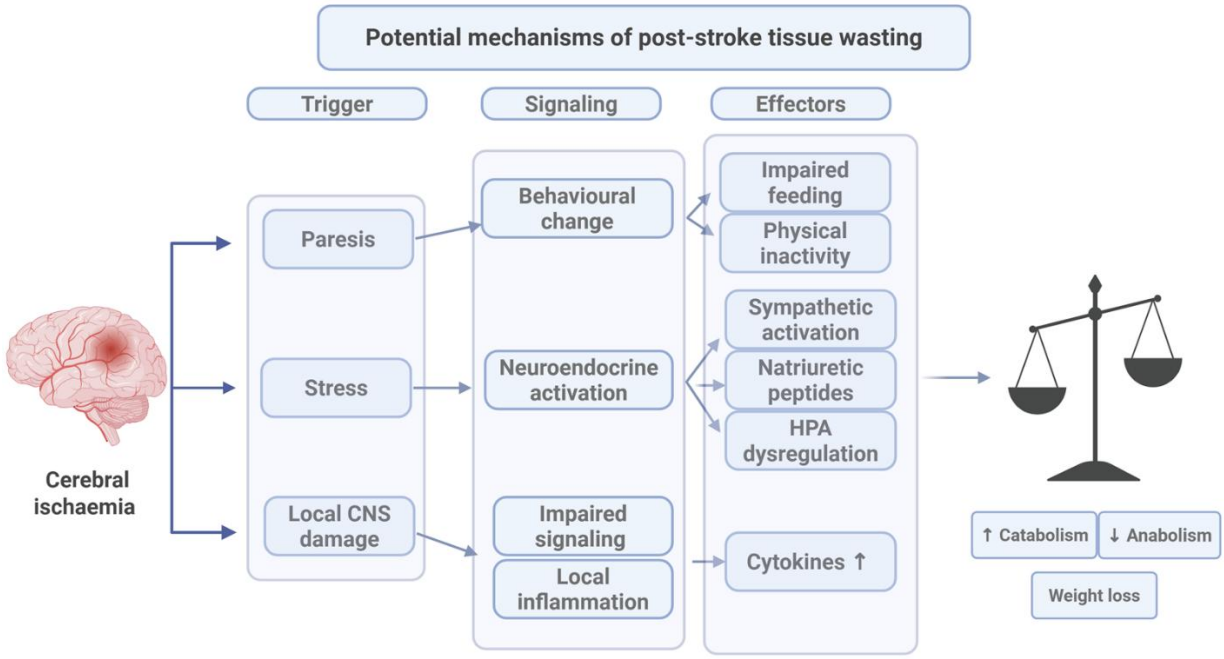

Figure 1-3 Schematic overview of the potential mechanisms of post-stroke weight loss. Factors such as impaired feeding, immobility, activation of the sympathetic nervous system, dysregulation of the hypothalamus-pituitary-adrenal axis and inflammation are proposed to be involved in mechanisms of post-stroke weight loss, figure adapted from (Scherbakov et al., 2011a)

1.6 Hypothesis and aims

As discussed, stroke survivors often face complications that hinder recovery and reduce quality of life. These complications include weight loss (or cachexia) and muscle wasting (or sarcopenia), which are both linked to poor stroke outcomes. However, despite its potential clinical importance, there is no available data regarding its prevalence among stroke survivors. Furthermore, while cachexia and sarcopenia are well documented in other chronic conditions such as cancer and heart failure, their occurrence and underlying mechanisms in stroke remain largely unexplored. Current evidence from some clinical studies indicates that muscle wasting occurs in both limbs (English et al., 2010). Also, pre-clinical studies show that weight loss encompasses both lean and fat tissue (Springer et al., 2014a, Haley et al., 2020b). Based on these observations, it is hypothesised that weight loss and muscle wasting arise from catabolic overactivation and anabolic blunting driven at least in part by systemic mechanisms triggered by the ischaemic insult. The overarching aim of this thesis is to address key knowledge gaps regarding post-stroke weight loss and muscle wasting by carrying out the following specific aims:

1. Determine the prevalence of weight loss and sarcopenia after stroke and assess their impact on patient outcomes by performing a systematic review and meta-analysis (Chapter 3).

2. Using two experimental models of ischaemic stroke, determine if there is a relationship between infarct size/location and body weight loss, with the goal of elucidating if these factors dictate the extent of post-stroke weight loss (Chapter 4).

3. Using non-targeted metabolomics, assess and compare the systemic metabolic response to ischaemic stroke in young and aged mice (Chapter 5).

4. Characterise the effect of experimental ischaemic stroke on skeletal muscle mass and expression of genes involved in muscle homeostasis in the acute, sub-acute and chronic phases after stroke onset; and determine whether any such changes resemble those found in age-related sarcopenia (Chapter 6).

Chapter 2 Materials & Methods

2.1 Materials

2.1.1 Reagents and chemicals

A detailed list and description of all reagents and chemicals used in this thesis are provided in Table 2-1.

Table 2-1 Reagents and chemicals used in this project

Chemical/reagent	Manufacturer/catalogue number	Description
Dulbecco's Phosphate-buffered saline (DPBS)	Thermo Fisher scientific, gibco #14190094	1X; Without Calcium and Magnesium
4% paraformaldehyde (PFA)	Sigma-Aldrich #P6148	4g PFA powder dissolved in 100mL PBS
Poly-L-Lysine solution	Sigma-Aldrich #P8920	0.1% (w/v) in H_2O
EDTA	Thermo Fisher scientific, Invitrogen #15575038	UltraPure™ 0.5M EDTA, pH 8.0
Chloroform	Sigma-Aldrich #366927	1X
Methanol	Fisher Chemical™ #1910333	1x
Ethanol	Sigma-Aldrich, Supelco #1009832500	absolute
Xylene	Sigma-Aldrich #78475	Xylene substitute
DPX	CellPath #03817913	Phthalate-free mounting medium
Triton	Sigma-Aldrich #T8787	100X
Vectashield® Antifade mounting media	Vector Laboratories #H-1000	With DAPI
QIAzol® Lysis Reagent	Qiagen #79306	1X
haematoxylin	CellPath # RBA420100A	
Eosin Y stain	Tcs Biosciences #HS250	1% (Aqueous)

2.1.2 Kits

A detailed list and description of all kits used in this thesis were provided in Table 2-2

Table 2-2 Kits used in this project.

Kit	Manufacturer/ catalogue number	Description
In Situ Cell Death Detection kit (TUNEL)	Roche, Merck #11684795910	Fluorescein
RNeasy® Mini Kit	Qiagen #74104	For RNA extraction
QuantiTect Reverse Transcription kit	Qiagen #205311	For cDNA conversion from RNA
QuantiNova® SYBR Green PCR Kit	Qiagen #208054	For RT-qPCR

2.2 Animals and related experiments

2.2.1 Ethics and regulatory approval

All experimental procedures involving animals were carried out under the Animals (Scientific Procedures) Act 1986, under UK Home Office Project Licence (P486284C3 and PP1054605), and personal licence (Jawzaa Alenazi: I59187411). These experiments were also covered by Glasgow Experimental Request Form (GERFs) numbers 141, 223 and 244 and received ethical approval from the University of Glasgow's Animal Welfare and Ethics Review Board (AWERB). Young male C57BL/6J mice (7 weeks old) were obtained from Envigo (Blackthorn, UK), while aged male C57BL/6J mice (17–18 months old) were purchased from Charles River (Margate, UK). All animals were acclimatised for a minimum of one week before the start of the experiments. Mice were housed under standard housing conditions, with a humidity level of approximately 55%, a temperature of approximately 21°C, and a 12-hour light/dark cycle. They had free access to standard rodent chow (special diet services, UK) and water *ad libitum*. To ensure animal welfare, aged mice were monitored twice a week using our Home Office approved aged health scoring sheet to evaluate their appearance, weight, behaviour and mobility for any signs of reluctance to move, ruffling of fur, hunched posture, weight loss and diarrhoea. Any aged mouse exhibiting a combined score of >3 or a single score of 3, or ≥20% weight loss, was euthanised immediately.

2.2.2 Cerebral ischaemia models

Given that one of the aims of this thesis was to study the relationship between post-stroke weight loss and infarct size and location, it was important to select appropriate experimental models. The middle cerebral artery occlusion (MCAo) and the photothrombotic (PT) models were chosen for this purpose. The MCAo is the most common model of cerebral ischaemia, which induces focal cerebral ischaemia by introducing a monofilament into the internal carotid artery to occlude the origin of the middle cerebral artery (MCA). This model is characterised by its ability to simulate permanent and transient ischaemia with varying occlusion durations (Koizumi, 1986). As most human infarcts occur in the MCA territory, this model closely resembles the localisation of human stroke (Ng et al., 2007, Olsen

et al., 1985). The PT model, in contrast, yields well-defined cortical ischaemia through systemic administration of a photosensitive dye followed by skull illumination. This leads to activation of the dye and the formation of ROS, which cause endothelial injury, platelet aggregation, and thrombus formation (Labat-Gest and Tomasi, 2013). The advantage of this model is its ability to yield ischaemic lesions in any cortical area of interest with minimal variation in infarct size. Together, these two models allow examination of both cortical and subcortical infarcts and variable infarct sizes, facilitating the study of the impact of location and infarct size on the outcome of interest.

2.2.2.1 Mouse model of focal cerebral ischaemia by middle cerebral artery occlusion (MCAo)

Surgeries were conducted under sterile conditions, utilising aseptic techniques that included the use of sterile instruments, drapes, surgical gowns, and gloves. First, mice were anaesthetised using isoflurane (3% for induction and 2% for maintenance) delivered in 97–98% oxygen via an oxygenator (Zoetis Ltd., UK). The fur at the site of incision on the head and neck was shaved using a clipper. Local anaesthetic Ropivacaine (4 mg/kg, s.c.; AstraZeneca, UK) was applied to incision sites and mice received 1 ml of saline (s.c.) pre-operatively for hydration. The mouse's body temperature was monitored using a rectal probe (Testronics, Victoria, Australia) and maintained at approximately 37±0.5°C throughout the surgery. To monitor regional cerebral blood flow (rCBF) and confirm successful occlusion of the right MCA, a laser-Doppler flowmetry probe (Perimed, Sweden) was placed on the skull ~5 mm lateral and ~2 mm posterior to Bregma. For probe placement, a small crescent-shaped incision was made in the scalp between the right ear and eye, exposing the skull over the territory supplied by the right MCA. The probe was then secured to the skull using medical adhesive (Figure 2-1). A midline neck incision (~2 cm) was then made and using a microscope, the right common carotid artery (CCA), external carotid artery (ECA) and internal carotid artery (ICA) were separated and dissected away from the surrounding membranes and connective tissue. Two silk suture loops with a small space between them were placed around the ECA and tied off to ligate it. Next, a cut was made between the sutures to create an ECA stump. The surgical technique for occluding the ICA involves making a slit in the stump to insert the filament. Therefore, to protect against severe bleeding and control blood flow to the ECA during surgery,

a suture was placed around the ICA and secured to a haemostat. Therefore, by applying gentle pressure to the haemostat and placing a vessel clamp on the CCA, the blood flow to the artery was restricted, allowing for the insertion of the filament. A silicon-coated nylon monofilament with a diameter of 0.21 mm (6-0 medium MCAO suture L12 PK10; 602312PK10), 0.23 mm (6-0 medium MCAO suture L12 PK10; 602312PK10) or 0.25 mm (6-0 large MCAO suture L12 PK10; 602512PK10) were used for mice weighing 21-25 g, 25-30 g, or >30 g, respectively (Doccol Corporation, US). The monofilament was then inserted into the stump of ECA, followed by the release of the pressure to the haemostat and the removal of the clamp to maintain the blood flow to the CCA. The filament was then advanced into the ICA to the origin of the MCA (approximately 11 mm) until a sharp reduction in rCBF was observed. Successful occlusion of the origin of the MCA was determined by a ≥70% drop in the rCBF reading. In this project, we used both the reperfused (transient MCAo; tMCAo) and non-reperfused (permanent MCAo; pMCAo) models of MCAo. In the tMCAo model, after ischaemia, the filament was retracted into the ECA to allow for reperfusion of cerebral blood flow into the MCA. Restoration of >80% of baseline rCBF withing 10 minutes of filament withdrawal confirmed successful perfusion. In contrast, in the pMCAo model, the filament remained in place, maintaining the occlusion of the MCA until the experimental endpoint was reached. Details of tMCAo durations and experimental end-points are given in the methods section of the relevant results chapters. Buprenorphine (0.05 mg/kg; Ceva Animal Health Ltd., UK) and 0.5 ml saline were delivered to each mouse at least 10 min before the end of the surgery. After surgery, the incision at the neck was closed, the laser-doppler probe removed, and the incision on the head was sutured using simple interrupted Vicryl-coated 5-0 nylon sutures (Nu-Care Products Ltd., UK). Sham-operated mice were subjected to the same surgical procedures; however, the filament was not inserted (Figure 2-1).

After surgery, mice were allowed to recover on a heated pad and closely observed for at least 4 hours until they were fully recovered. To support feeding and hydration after the surgical procedure, all mice were given a fresh diet daily consisting of softened chow, baby food (Sainsbury's little ones, UK), and hydration gel (HydroGel®, US) ad libitum. All mice were observed for at least 4 hours after surgery and monitored daily using our clinical severity scoring system until the

experiment endpoint. This assessment included evaluation of the following criteria: body weight, appearance, hunching, facial grimacing, provoked behaviour and clinical signs such as breathing behaviour, pale eyes, and diarrhoea. In addition, faecal and urinary output, appetite and incision sites were examined daily to detect any signs of infection. Each parameter was scored on a scale from 0 to 4, and the overall severity score was calculated. Mice were immediately euthanised if they met any of the following criteria: a score of 4 in any single category, the weight loss ≥20% of baseline body weight or a total score from all categories of ≥10. Animals with a moderate score (6–9) were monitored multiple times daily, while those with a score of 0–5 were monitored once daily.

Surgeries were performed by Dr Alyson Miller (tMCAo), Dr Arun Flynn (tMCAo), and Dr Alexandra Riddell (pMCAo) whereas the pre-surgical preparation of mice, post-surgical care, monitoring and all the analyses related to the experiments were performed by me.

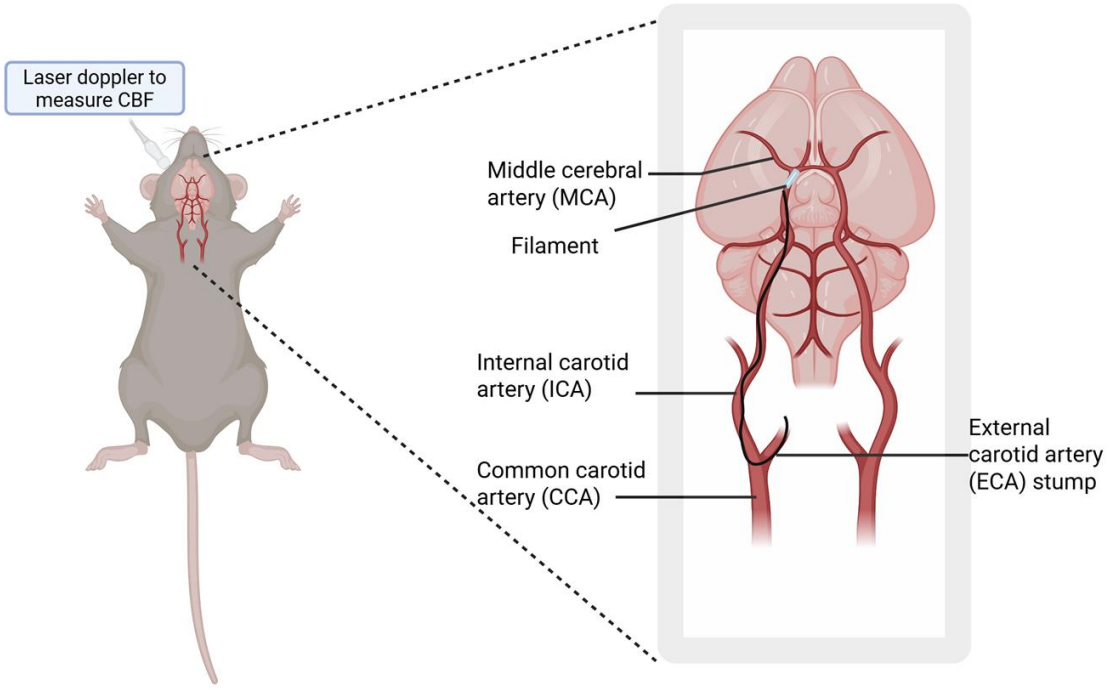

Figure 2-1 Schematic of induction of ischaemia by middle cerebral artery occlusion (MCAo). A schematic depicting the arteries involved in the induction of cerebral ischaemia. A filament is introduced into the ICA and advanced to the origin of the MCA at the circle of Willis to occlude the origin of the MCA. Regional cerebral blood flow (CBF) at the cerebral territory of the MCA is monitored using Laser Doppler Flowmetry. Original diagram made by author, created in BioRender.com

2.2.2.2 Mouse model of photothrombotic (PT) stroke

Surgeries were carried out by Dr Adriana Knezic and her team at Monash University, as detailed in Knezic et al. (2022). Dr Adriana Knezic shared the data with the author, and the experimental datasets were then analysed by the author as detailed in the results section of Chapter 4.

All experimental procedures were approved by the Monash University Ethics Committee (MARP/2017/144 and MARP/23298) and were conducted under the guidelines of the National Health and Medical Research Council of Australia and the ARRIVE guidelines for the ethical care and use of animals in research. Male C57Bl/6 mice aged 8 to 12 weeks were sourced from the Monash Animal Research Laboratory (Clayton campus, Monash University, Australia). Mice were housed in specific pathogen-free conditions, maintained on a 12-hour light/dark cycle, and provided with free access to food pellets and water.

Mice were anaesthetised using isoflurane inhalation (5% for induction and 1.5% for maintenance, Issorane, Baxter, Baxter Healthcare Pty. Ltd). Body temperature was monitored using a rectal probe and maintained at 37.0±0.5°C with the aid of an electric temperature controller (Harvard Apparatus, Cambridge, UK) throughout the surgical procedure. the mouse was positioned in a stereotaxic frame. Next, the scalp was shaved, and an incision was made over the skull. A 5 mm objective lens connected to a source of cold light (KL 1600 LED, Schott, Mainz, Germany, luminuous flux: 680lm, colour temperature: 5600K) was positioned precisely over the left sensorimotor cortex (M1 region). Then, the mouse was given an injection of Rose Bengal solution intraperitoneally (0.2 mL; 10 mg/mL in distilled water; Sigma, St. Louis, USA). After 5 minutes, the skull overlying the M1 region was illuminated for the needed duration, depending on the experimental group, either 15, 18 or 20 minutes (Figure 2-2). Then, the light was turned off, and the mouse was carefully removed from the frame. The head incision was closed using skin adhesive (Vetbond, 3M Animal Care Products, MN, USA), and the mice were then allowed to recover under a heat lamp. Sham-operated mice underwent the same surgical procedure; except they did not receive a Rose Bengal injection. All animals were monitored daily till the experimental endpoint.

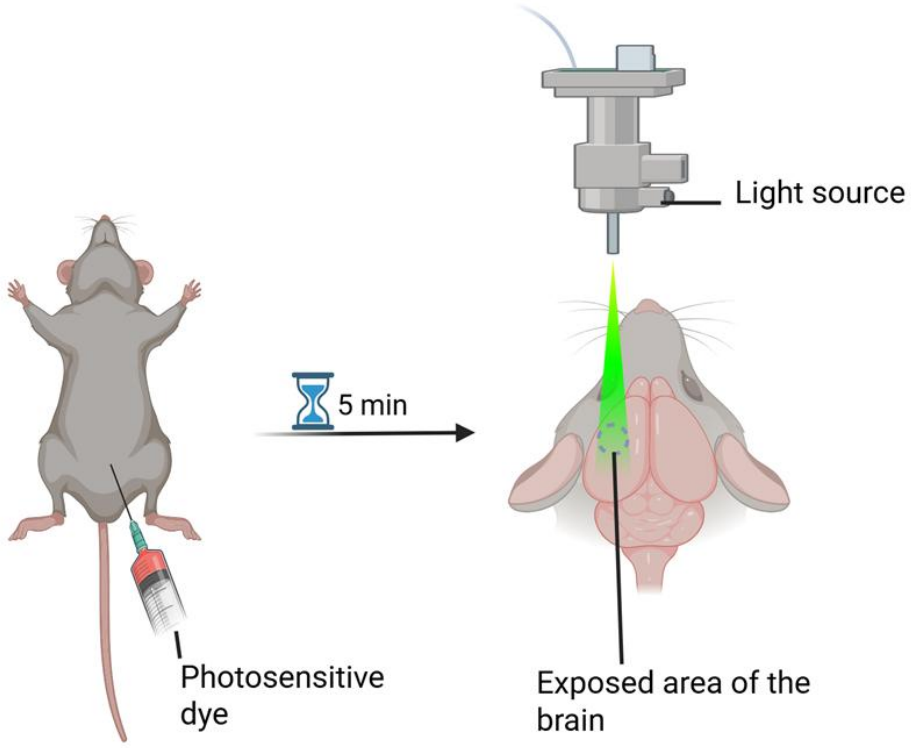

Figure 2-2 Schematic of photothrombotic model of stroke. Mice were injected with Rose Bengal dye solution (i.p.), and after 5 minutes, the skull was illuminated for the **15, 18 or 20 minutes**. Original diagram made by the author, created in BioRender.com

2.2.3 Weight, food and liquid intake monitoring

To follow ethical requirements, the weight of the mice was regularly monitored before surgery (baseline) and daily for the first week after surgery, then twice weekly if the study lasted for an extended period. Since this thesis is interested in weight loss after stroke, the weight loss is presented as a percentage relative to the baseline body weight, which was calculated using the following equation:

% body weight loss= (current weight-baseline body weight)/baseline body weight *100

The food and water intake were also monitored and calculated. Each mouse was housed in an individual cage after surgery, and the rodent food was prepared and weighed daily, and the mice's intake was recorded. The water was also monitored daily. The volume of water provided to each mouse was measured before administration and again after 24 hours to determine the total volume change. To account for potential water loss unrelated to consumption (e.g. leakage), a

‘dummy cage’ equipped with an identical water bottle was kept under the same conditions. The volume of water lost from the ‘dummy cage’ bottle was recorded and subtracted from the total decrease in each experimental bottle, allowing for an estimate of the actual water intake by each mouse.

2.2.4 Forelimb grip strength test

Forelimb grip strength was evaluated using a BIO-GS3 grip strength meter (BioSeb, UK) before surgery and post-operatively on day 2. Mice were gently held at the tail and lowered toward the T-bar of the device. Upon grasping the bar with both forelimbs, the animal was steadily pulled backwards in a horizontal direction until grip release occurred for both forelimbs, at which point the peak force exerted was recorded. Only measurements are considered when both forepaws are released simultaneously. If one forepaw was released and the other maintained grip, the measurement was repeated until both forepaws were released. The measurement was performed three times for each mouse, with a 5-to 10-minute break between each measurement, and the average value was used for analysis.

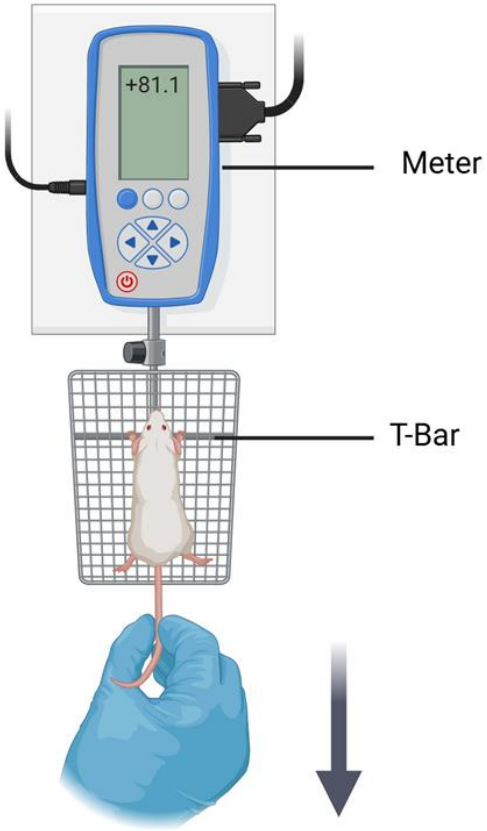

Figure 2-3 Forelimb grip strength test. Diagram depicting the assessment of grip strength, where the mouse grasps the T-bar and the researcher pulls the mouse backwards until maximum strength is reached before the grip is released. The figure created by BioRender.com

2.2.5 Tissue harvesting

At the experiment endpoint, mice were euthanised by overdose of an anaesthetic agent (isoflurane) or by a rising concentration of CO_2 (Schedule 1 method). Brains were subsequently extracted and slowly frozen over liquid nitrogen, then stored at -80 °C until further analysis. The skeletal muscles (gastrocnemius and tibialis anterior) from the limbs were excised and weighed. Gastrocnemius samples were stored in a microcentrifuge tube and immediately snap frozen in liquid nitrogen, then stored at -80 °C until use for RT-qPCR. The tibialis anterior samples were placed in a microcentrifuge tube containing 4% paraformaldehyde (PFA) and stored at 4°C for 24 hours and subsequent use in histology.

Adipose tissue is classified into white adipose tissue (WAT) or brown adipose tissue (BAT). The majority of body fat is WAT, which acts as energy storage and is composed of unilocular (single) lipid droplets and is found under the skin or in visceral areas (mesenteric, renal and gonadal). In contrast, BAT acts to maintain

body temperature by dissipating energy as heat (thermogenesis) and is mainly located in areas like the shoulders, under the skin and neck (Ibrahim, 2010, Cinti, 2006, Verma et al., 2017). In this thesis, mesenteric, renal, and gonadal fat were collected and weighed from mice subjected to tMCAo or sham surgery.

2.2.6 Ischaemic mouse brains

2.2.6.1 Cryosectioning of the brains

Frozen brains were embedded in OCT compound and coronally sectioned using a cryostat. Fifteen sections were collected at a 10 µm thickness, covering three brain regions (striatum, depth: +2.8 to +0.76 mm; hippocampus 1, depth: +0.25 to -1.79 mm; and hippocampus 2, depth: -2.3 to -4.34 mm; relative to Bregma). From each brain region, five representative sections (spaced apart by 420 µm) were collected in 9 replicates. The collected sections were mounted onto glass slides coated with poly-L-lysine and stored at -80°C until further use (Figure 2-4). Accordingly, for each area of the brain, a total of 9 slides, each containing five sections reflecting the whole region of the brain, were obtained. Of these, the first three slides were used for infarct volume analysis using thionin staining, while the remaining six slides were used for various experiments, including the TUNEL assay.

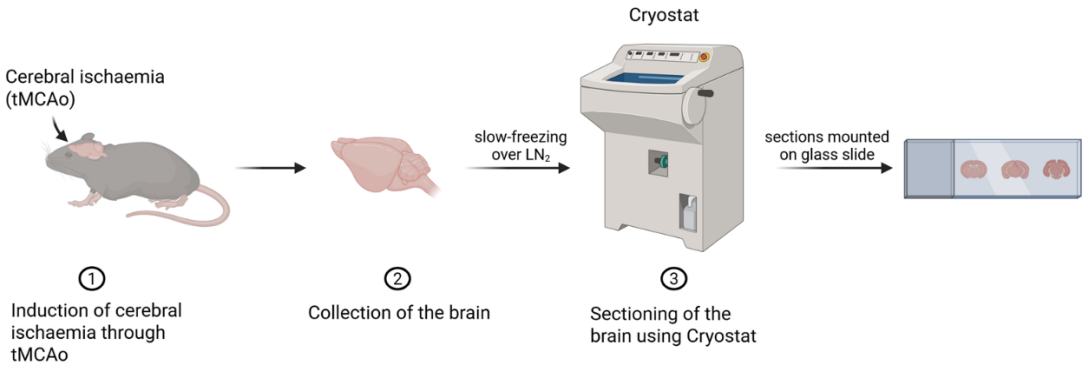

Figure 2-4 Diagram of the mouse brain collection and sectioning using a cryostat. Upon reaching the experimental endpoint, the brains were collected and sectioned by cryostat. Original diagram made by the author, created in BioRender.com

2.2.6.2 Thionin staining

Staining of Nissl bodies using thionin is a standard histological method used to visualise healthy neuronal cell bodies in brain tissue sections. In this method, thionin, a basic (cationic) dye, selectively binds to the negatively charged molecules of Nissl bodies (clusters of ribosomes and rough endoplasmic reticulum), causing them to appear blue or purple. In contrast, the infarct area of the brain appears colourless due to the cell death and degradation of cellular components that thionin binds to (Larson, 2025). Therefore, this method allows for delineation and identification of the infarct. In this thesis, brain sections were stained by placing them in a 0.125% thionin solution for 7 minutes followed by two rinses in distilled water (dH_2O). Next, for dehydration, the sections were placed in a graded series of ethanol- first in 70% ethanol for 2 minutes, then in 100% ethanol for an additional 2 minutes. Tissue sections were allowed to air dry at room temperature. Then, the sections were cleared in xylene and mounted with DPX mounting media on cover slips. CCD digital camera (Canon, Japan) was used to image thionin-stained sections.

2.2.6.3 Quantification of cerebral infarct and oedema volume after experimental stroke

Thionin-stained brain sections were subsequently used to quantify infarct and oedema volumes. Images of the stained sections were analysed using ImageJ software (ImageJ2, v. 2.14.0, NIH, US). Total infarct and oedema volumes were calculated based on the following equations where LHA represents the area of the left hemisphere, RHA the area of the right hemisphere, and RIA the infarct area:

Corrected Infarct Volume (CIV) = (LHA – (RHA – RIA)) × (section thickness + distance between sections)

Oedema Volume (OV) = (RHA – LHA) × (section thickness + distance between sections)

2.2.6.4 TUNEL assay

Terminal deoxynucleotidyl transferase dUTP nick end labelling (TUNEL) is a method used for the detection of DNA fragments (breaks), which is a well-recognised hallmark of late-stage apoptosis (programmed cell death). The

technique requires labelling the free 3'-hydroxyl ends of fragmented DNA using the enzyme terminal deoxynucleotidyl transferase (TdT). This enzyme adds a modified nucleotide (deoxyuridine triphosphate nucleotide tagged with a fluorescent label) to the free 3'-hydroxyl ends of DNA. This labelling allows for the detection and visualisation of apoptotic cells (Loo, 2002). Brain sections from the tMCAo and pMCAo models used for the TUNEL assay were sectioned by Dr Arun Flynn and Dr Alexandra Riddell, respectively. In this thesis, frozen Coronal brain sections encompassing the hypothalamic brain region (-0.5 to -2.5 mm relative to Bregma) were selected and allowed to thaw at room temperature. Then, they were fixed with 4% paraformaldehyde (PFA) for 20 minutes. The sections were washed three times with PBS and then incubated with a permeabilisation solution (0.1% Triton in PBS) for 2 minutes on ice. The slides were washed with PBS and placed on a foil-covered (or darkened) humidified tray. The TUNEL reaction mixture (In Situ Cell Death Detection kit, Roche, UK) was then added to each brain section and incubated for approximately 1 hour at 37°C. The slides were then washed with PBS and covered with glass coverslips using mounting media containing DAPI (Vectashield® Antifade). They were then left to dry overnight. Stained sections were visualised and imaged using a ZEISS LSM 900 confocal microscope with 25X oil immersion objective (Carl Zeiss Microscopy, US). Stained images were analysed using ImageJ software (ImageJ2, v. 2.14.0, NIH, US). For the analysis, five fields were imaged from each mouse brain section and TUNEL-positive cells were counted using the Cell Counter function on the software. The average number of TUNEL-positive cells across the five images was then calculated and expressed relative to the brain area ($TUNEL^+$ cells/mm^2).

2.3 Molecular methods

2.3.1 RNA extraction & cDNA synthesis

RNA extraction from tissue samples was conducted in a fume hood using a phenol-chloroform method. Briefly, the tissue sample was placed into a microcentrifuge tube containing a 5 mm stainless steel beads, followed by the addition of 1mL Qiazol reagent. Then, the tissue sample was disrupted and homogenised using the Tissue Lyser LT (Qiagen, UK) for 5 minutes at a frequency of 30 Hz. After 5 minutes of incubation at room temperature, 200 µL of chloroform was added, and the mixture was vigorously shaken for 15 seconds. The sample was then incubated for

an additional 3 minutes at room temperature before being centrifuged at 13,000 × g for 15 minutes at 4°C. The upper aqueous phase was carefully transferred to a new microcentrifuge tube, followed by precipitation of RNA using 70% ethanol. Total RNA was subsequently purified using the Qiagen RNeasy Mini Kit (Qiagen, UK), following the manufacturer's instructions (Figure 2-5).

The concentration and purity of the isolated RNA for all samples were assessed using a NanoDrop spectrophotometer (ThermoFisher, UK). Reverse transcription was then performed to synthesise cDNA from all samples by converting 1 µg of isolated RNA using the QuantiTec Reverse Transcription Kit (Qiagen, UK), following the manufacturer's instructions.

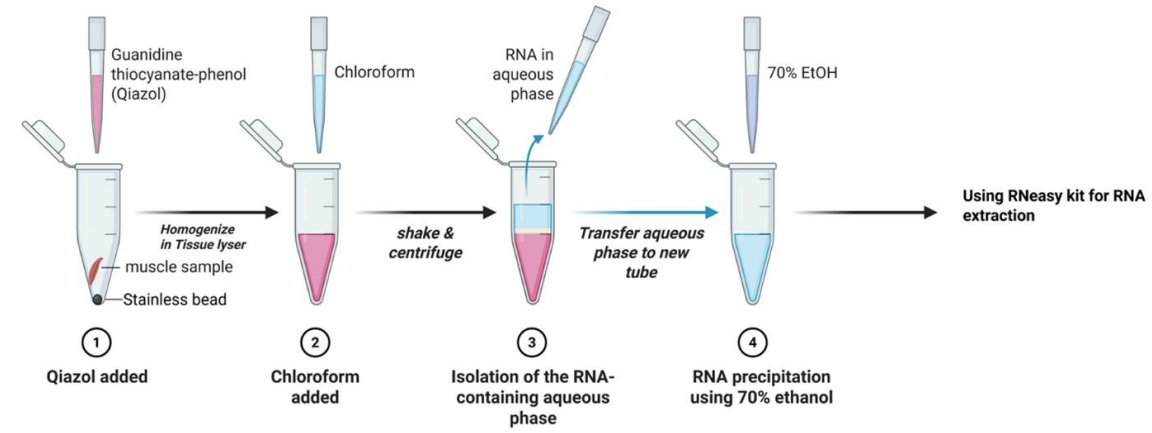

Figure 2-5 RNA extraction from tissue following a phenol-based method. Original image made by author, created in BioRender.com

2.3.2 Real-time quantitative polymerase chain reaction (RT-qPCR)

SYBR Green was used in this thesis as the fluorescent dye for all RT-qPCR assays following the manufacturer's instructions. Each reaction was prepared in a 348-well PCR plate (Applied biosystems, UK) with a total volume of 10µL containing template cDNA (1.5µL), SYBR Green (5µL), forward and reverse primers (1µL), and nuclease-free water to reach the final volume. Cycling conditions were as follows: an initial denaturation at 95°C for 10 minutes, followed by 40 amplification cycles consisting of denaturation at 95°C for 15 seconds and annealing/extension at 60°C for 60 seconds. This was followed by a continuous melting curve analysis with steps at 95°C for 15 seconds and 60°C for 60 seconds. A final dissociation stage was performed at 95°C for 15 seconds. Gene expression analysis was performed

using the$2^{-\Delta\Delta Ct}$ formula, as described by Livak and Schmittgen (2008). First, the C_t value of the target gene was normalised to that of the housekeeping gene (r18s) to calculate the ΔCt. The ΔCt of each sample was then subtracted from the ΔCt of a reference control (sham's value) to obtain the ΔΔCt. Finally, the relative expression level was determined using the $2^{-\Delta\Delta C}$ method.

2.3.2.1 Primers

A detailed list of all primers and their description is provided in Table 2-3.

Table 2-3 List of primers used in this thesis

Gene	Primer ID	Catalogue No.	Manufacture
r18s	MM_RN18S	2524400	Qiagen
TBP	MM_TBP	2243910	Qiagen
AKT1	MM_AKT1	2264612	Qiagen
mTOR	Customised: Forward_Mouse (GCCACATCTAGCAACGTGAG) Reverse_Mouse (CTGGTCATAGAAGCGCGTAG)	10336022	Invitrogen, ThermoFisher
AKT2	MM_AKT2	249900	Qiagen
RPS6K	MM_RPS6KA4	2066436	Qiagen
RPS6	MM_RPS6	1941272	Qiagen
GsK3B	MM_GSK3B	2106573	Qiagen
EIF4EBP1	MM_EIF4EBP1	2310315	Qiagen
FOXO1	MM_FOXO1	2039358	Qiagen

MSTN (Myostatin)	MM_MSTN	2128872	Qiagen
FBXO32 (Atrogin-1)	MM_FBXO32	2024057	Qiagen
TRIM63 (Murf-1)	MM_TRIM63	1947054	Qiagen
TNF-a	Customised Forward_Mouse (CAAACCACCAAGTGGAGGAG) Reverse_Mouse (GTGGGTGAGGAGCACGTAGT)	Unknown _requested by past researcher (Erika Trabold)	Invitrogen, ThermoFisher
IL-6	Customised Forward_Mouse (CCGGAGAGGAGACTTCACA) Reverse_Mouse (TTCTGCAAGTGCATCATCGT)	Unknown _requested by past researcher (Erika Trabold)	Invitrogen, ThermoFisher

2.4 Histology

2.4.1 Haematoxylin and Eosin (H&E) staining

Tibialis anterior muscles were fixed in 4% PFA for 24 hours, followed by incubation in 70% ethanol. Tissues were then embedded in paraffin and sectioned at a thickness of 5µm using a Leica microtome (Leica Biosystems, UK). Sections were mounted onto silane-coated glass slides, baked at 60°C for 2 hours, and then incubated overnight at 40°C (Techne, UK). For H&E staining, tissue sections were deparaffinised in xylene, rehydrated through a series of decreasing ethanol concentrations (100% to 70%), and rinsed in dH_2O. Sections were then stained with haematoxylin to visualise nuclei, rinsed under running water for 5 minutes, and briefly dipped in alcohol for 30 seconds. Cytoplasmic staining was performed using eosin, followed by dehydration through increasing concentrations of ethanol (95% and 100%), and clearing in xylene. Coverslips were applied using DPX mounting medium. Stained sections were scanned using a slide scanner (NanoZoomer, Hamamatsu, Japan) and analysed with ImageJ software (ImageJ2, v. 2.14.0, NIH,

US). For quantification of muscle fibre cross-sectional area (CSA), approximately 200 fibres were randomly selected and assessed per muscle sample.

2.5 Metabolomics

2.5.1 Plasma extraction

On day 1 after tMCAo and sham surgeries, blood was collected (~1mL) via cardiac puncture with the help of Ms. Yasmin Amer from the Cardiovascular Research Unit at the University of Glasgow. The mice were anaesthetised using isoflurane (3% for induction and 2% for maintenance). Once the mouse was deeply anaesthetised, a 26G needle was inserted into the heart, and the blood was withdrawn slowly into a 1 mL syringe. It was then immediately transferred into a microcentrifuge tube containing the anticoagulant 0.5M EDTA. The tube was gently inverted several times to ensure the anticoagulant was mixed with the blood. Next, the blood was centrifuged at 3,000 × g for 10 minutes, which allowed the plasma to separate from the blood cells. After centrifugation, the plasma was carefully aspirated using a pipette and placed into a new, labelled microcentrifuge tube and stored at -80°C.

2.5.2 Sample preparation for metabolomics analysis

The plasma samples were then defrosted at room temperature. Approximately 25 µL of the plasma was mixed with extraction solvent (chloroform/methanol/dH_2O; 1:3:1 ratio) at 4°C. Next, the samples were centrifuged at 13,000 × g for 3 min at 4 °C. The supernatants were collected and transferred into a screw top vial (Simport® cryovial, 2 mL, Simport® Scientific Inc., Canada). They were sent on dry ice to Glasgow Polyomics for analysis by Liquid Chromatography–Mass Spectrometry (LC-MS). I performed the plasma extraction and sample preparation for metabolomics analysis. Mrs Erin Kerr conducted all the LC-MS experiments, and Dr Clement Regnault and I analysed the data.

2.6 Power Calculations and Statistical Analysis

Power calculations are described in the methods section of each results chapter. Statistical analysis was conducted using GraphPad Prism (version 10.4.1, GraphPad Software Inc, San Diego, CA). Data are presented as mean ± SEM, and statistical significance was considered when $P<0.05$. Group numbers and specific statistical tests used for each data set are described in each corresponding chapter's methods and figure legends.

Chapter 3 Prevalence of post-stroke weight loss and sarcopenia in clinical stroke: systematic review and meta-analysis

3.1 Introduction

After a stroke, patients may experience complications that adversely affect their recovery and diminish their quality of life. These complications include cognitive impairment, depression, infection, and changes in body weight (Nakling et al., 2017, Shi et al., 2018). Body weight and muscle loss are reported to occur in patients after stroke and are linked to poor prognosis(Scherbakov et al., 2019c, Kim et al., 2015a, Jonsson et al., 2008). The mechanisms underlying body weight and muscle loss after stroke are complex and not fully understood but are believed to involve factors such as inactivity due to paresis, reduction in food intake due to loss of appetite or dysphagia. Also, it is proposed that systemic mechanisms such as sympathetic overactivation and inflammation triggered by the cerebral infarction lead to metabolic imbalance resulting in catabolic overactivation and anabolic deficit (Scherbakov et al., 2011b, Jonsson et al., 2008). Consequently, increased degradation of muscle and fat can develop, leading to muscle wasting (sarcopenia) or overall body weight loss (cachexia). Tissue wasting (cachexia) is a complex syndrome characterized by an unintentional loss of body weight and skeletal muscle mass, with or without a reduction in adipose tissue that cannot be completely reversed by standard nutritional support. Patients with cachexia are identified as those who suffer a chronic disease and experience a loss of more than 5% of their body weight within 12 months or less (Morley et al., 2006). This condition is well documented in chronic diseases such as heart failure and cancer. In cancer, it is claimed that tissue wasting or cachexia affects around 70% of patients and is estimated to contribute to up to 22% of cancer-related deaths (Thibaut et al., 2021). In heart failure, a recent systematic review and meta-analysis revealed that the prevalence of weight loss (cachexia) in heart failure patients is 31%, and it is considered an independent predictor of all-cause mortality among the patients (Prokopidis et al., 2024). Despite the recognition of weight loss in other chronic diseases, comparatively little attention was paid to its prevalence and impact on patients after stroke. However, in rodents, substantial body weight loss is commonly observed in different models of ischaemic stroke, starting within 1 day after ischaemia induction and peaking up to 20% within 3 days (Dirnagl, 2010, Springer et al., 2014b, Yang et al., 2019, Haley et al., 2020a).

Dr. Irwin Rosenberg first defined sarcopenia as a skeletal muscle disorder associated with aging, characterized by a progressive loss of muscle mass and strength. Primary sarcopenia refers to muscle loss that occurs as a natural consequence of the aging process without any other identifiable underlying cause, and it is commonly observed in the older adult population. In contrast, secondary sarcopenia is used to describe muscle wasting due to factors other than aging, such as physical inactivity, chronic disease, or malnutrition (Li et al., 2020). Stroke patients have an increased risk of developing sarcopenia because of muscle atrophy associated with inactivity, denervation, inflammatory response, and paralysis (Scherbakov et al., 2013). Muscle weakness that occurs after a stroke plays a significant role in reducing physical function or disability and reducing patients' quality of life (Bohannon, 2007). Traditionally, muscle atrophy and disability following stroke have been mainly attributed to brain injury (Li et al., 2018), whereas little attention has been given to the metabolism, structure, and function of muscle tissue following stroke. Recently, muscle wasting and functional decline following stroke have been referred to as “stroke-related sarcopenia” (Scherbakov et al., 2015, Scherbakov et al., 2013, Li et al., 2020). Importantly, however, although there is evidence that sarcopenia is reported to affect patient outcomes, little is known about its prevalence after stroke. A previous systematic review documented that sarcopenia occurred in 42% of stroke patients (Su et al., 2020). The review included only seven studies because the literature was scarce. The stroke-related sarcopenia term emerged recently while sarcopenia research continues to gain momentum. The growing interest in sarcopenia research will likely produce additional studies which will enable us to update and expand previous findings. A follow-up systematic review becomes essential at this time to analyse the developing evidence base while providing a detailed prevalence assessment and improved clinical care for stroke survivors with sarcopenia.

In this study, we aimed to systematically review articles and identify studies that recorded the prevalence of weight loss or sarcopenia after stroke and calculate the pooled prevalence of both post-stroke weight loss and sarcopenia. Furthermore, we aimed to examine the impact of post-stroke weight loss and sarcopenia as well on stroke patients' outcome. We hypothesise that post-stroke weight loss and sarcopenia are very common among stroke patients and negatively affect patients' prognosis.

3.2 Methods

The research methods of this review were conducted according to the Preferred Reporting Items for Systematic Reviews and Meta-analyses (PRISMA) guidelines (Moher et al., 2009). The protocol for the review was registered in PROSPERO (CRD420251114372) and is available at https://www.crd.york.ac.uk/PROSPERO/view/CRD420251114372.

3.2.1 Inclusion and exclusion criteria

The inclusion and exclusion criteria for this review were performed using the Population Exposure Comparison Outcome Study design (PECOS) framework (Morgan et al., 2018).

3.2.1.1 Participants

Stroke survivors aged 18 years or over with no sex and ethnicity limitations. Any studies that recruited patients other than stroke survivors were excluded from the analysis.

3.2.1.2 Exposure

The exposure in this review was stroke. The articles were eligible when they studied stroke survivors; any study with other diseases or that did not consider stroke patients was excluded.

3.2.1.3 Outcome

This review focuses on post-stroke weight loss and sarcopenia. Therefore, the eligible type of outcome was unintentional weight loss or sarcopenia. For the studies to be included in the meta-analysis, they had to meet the following criteria: (1) weight loss had to be reported after stroke, (2) used validated diagnostic criteria for sarcopenia as defined by the International Consensus on Sarcopenia (ICS) or the European Working Group on Sarcopenia in Older People (EWGSOP) or the Asian Working Group for Sarcopenia (AWGS). These criteria included low muscle strength (LMS), low muscle mass (LMM), and/or low physical performance (LPP). Any studies that did not clearly report the diagnostic criteria

of sarcopenia or did not report weight loss after stroke occurrence were excluded. Studies were included if they reported the prevalence or the proportion of patients who lost weight or had sarcopenia after a stroke. As this review also examined the impact of weight loss and sarcopenia after stroke on patients' prognosis, any articles reporting functional outcomes, mortality rate, and/or length of hospital stay were included in this review.

3.2.1.4 Study types

Studies were considered if they had an observational, case-control, or cross-sectional design. Any reviews, conference abstracts, book chapters, pre-clinical studies, and letters were excluded.

3.2.1.5 Language

Only studies written in the English language were included in this review. Articles that were written in other languages were excluded.

3.2.2 Databases and search strategy

The search was conducted in 2024 using four databases to identify all relevant studies with no year restriction: Cochrane Library, MEDLINE (OVID), Scopus, and Web of Science.

Search key terms were created utilizing medical subject headings (MeSH) and text words related to stroke, weight loss, and sarcopenia. In addition, to assist with the development of the key search terms for this review, published systematic reviews on stroke, intentional weight reduction after stroke, or sarcopenia were examined (Curioni et al., 2006). Truncation was implemented to capture all studies with a title related to the search keywords (stroke, weight loss, and sarcopenia) by inserting a symbol ($) at the end of the keywords. Boolean operators were used to combine the keywords. The advanced search was limited to studies of humans and published in English. The search strategy for this review is shown in more detail in Table 3-1.

Table 3-1 Keywords use for database search

#	Keywords
1	exp carotid artery thrombosis/
2	exp cerebrovascular accident/
3	exp Ischemic attack, transient/
4	exp cerebral infarction/
5	exp intracranial aneurysm/
6	exp "Intracranial Embolism and Thrombosis"/
7	exp cerebral hemorrhage/
8	exp basal ganglia hemorrhage/
9	exp putaminal hemorrhage/
10	exp intracranial hemorrhage, hypertensive/
11	exp subarachnoid hemorrhage/
12	(stroke$ or apoplex$ or post-stroke or poststroke).tw.
13	or/1-12
14	exp Weight Loss/
15	exp body mass index/
16	body mass ind$.tw.
17	cachexia
18	or/14-17
19	exp sarcopenia/
20	(sarcopeni$ or myopeni$ or dynaponi$).tw.
21	(muscle atroph$ or muscle wasting$ or muscle weak$ or muscle loss$ or muscular atroph$ or muscular wasting$ or muscular weak$ or muscular loss$).tw.
22	Or/19-21
23	18 or 22
24	13 and 23

3.2.3 Study selection

The search was applied to all selected databases, and all retrieved articles were imported into EndNote for further examination and to delete duplicates. Then, screening was conducted in two stages: title and abstract screening followed by full-text articles screening for the articles that met the predefined inclusion criteria. The screening was performed independently by myself and Dr. Alyson Miller. Any disagreement was resolved by discussing it with a third reviewer (Professor Jesse Dawson).

3.2.4 Data extraction

The data extraction form was developed based on the necessary information to be collected. A standardised Microsoft Excel 2010 worksheet was utilised to extract data from the eligible studies for data synthesis. The extracted information from studies on weight loss includes the first author with publication year, study design, sample size, country, sex, age, stroke subtype, time since stroke onset, length of follow-up, prevalence of weight loss, cut-off value, and outcome of interest. Similar information is extracted from studies on sarcopenia, including the first author with publication year, study design, sample size, country, sex, age, stroke subtype, time since stroke onset, length of follow-up, prevalence of sarcopenia, diagnostic criteria with cut-off value, and interested outcomes.

3.2.5 Assessment of methodological quality

The risk of bias for included studies was independently assessed by myself and Dr Alyson Miller. The assessment was conducted using the Newcastle-Ottawa Scale (NOS), applying the appropriate tool for cohort, case-control, or cross-sectional studies and adjusting the anchoring statements to align with the review question. NOS is a validated eight-item tool designed to assess the quality of non-randomised studies. It employs a star-based rating system, with a maximum of nine stars distributed across three key domains (Wells et al., 2014). The first domain evaluates the selection of study groups, awarding up to four stars. The second domain, with a maximum of two stars, assesses the comparability of study groups by ensuring that confounding factors are adjusted for the analysis. The third domain assigns a maximum of three stars to assess how the study determines the

outcome (for cohort and cross-sectional studies) or how the study ascertains the exposure in case-control study designs (Wells et al., 2014). Studies were classified as good, fair, or low quality based on their scores, with 7-9 stars indicating good quality, 4-6 stars representing fair quality, and 0-3 stars denoting low quality.

3.2.6 Statistical analysis

STATA 18 (version 18, StataCorp, College Station, TX, USA) was used to conduct the meta-analysis. The number of patients who had weight loss or sarcopenia after stroke and the total number of patients recruited from all studies were extracted and entered into the software calculator. Heterogeneity in a systematic review refers to any form of variation among the included studies (Borenstein et al., 2010); Cochran's Q test was employed to evaluate heterogeneity among studies, with a P-value < 0.1 considered statistically significant. Furthermore, the I^2 statistic test was used to measure the extent of heterogeneity (Higgins and Thompson, 2002). The I^2 value ranges from 0% to 100%, where 0% signifies no observed heterogeneity, and higher values (≥50%) indicate increasing levels of heterogeneity (Higgins and Thompson, 2002). The pooled prevalence of post-stroke weight loss or sarcopenia, along with 95% confidence intervals (CIs), was estimated using a random-effects model (REM) when significant heterogeneity was detected (as determined by Cochran's Q test). If no significant heterogeneity was present, a fixed-effects model was applied instead. To explore possible sources of heterogeneity, subgroup analyses were conducted based on gender, location, diagnostic criteria or cut-off values, and time since stroke onset. Furthermore, subgroup analyses were used to determine whether the prevalence of post-stroke weight loss or sarcopenia varied based on different characteristics of the included studies and participants. A sensitivity analysis was conducted to evaluate the impact of each study on the overall pooled prevalence by systematically excluding one study at a time. Egger's test was used to evaluate the publication bias, with $P<0.05$ indicating significant publication bias.

3.3 Results

3.3.1 Search process

The initial search for published articles was conducted across four databases. In total, 18,716 articles related to stroke and weight loss, or sarcopenia, were identified. After eliminating duplicate records, the titles and abstracts of 12,890 studies were thoroughly screened, resulting in the exclusion of 12,658 irrelevant articles. A total of 232 relevant articles were selected for full-text screening, out of which 200 studies were excluded. The reasons for exclusion are outlined in the flowchart Figure 3-1. Finally, 32 studies were included in this review, of which 9 articles related to post-stroke weight loss and 23 articles related to stroke-related sarcopenia.

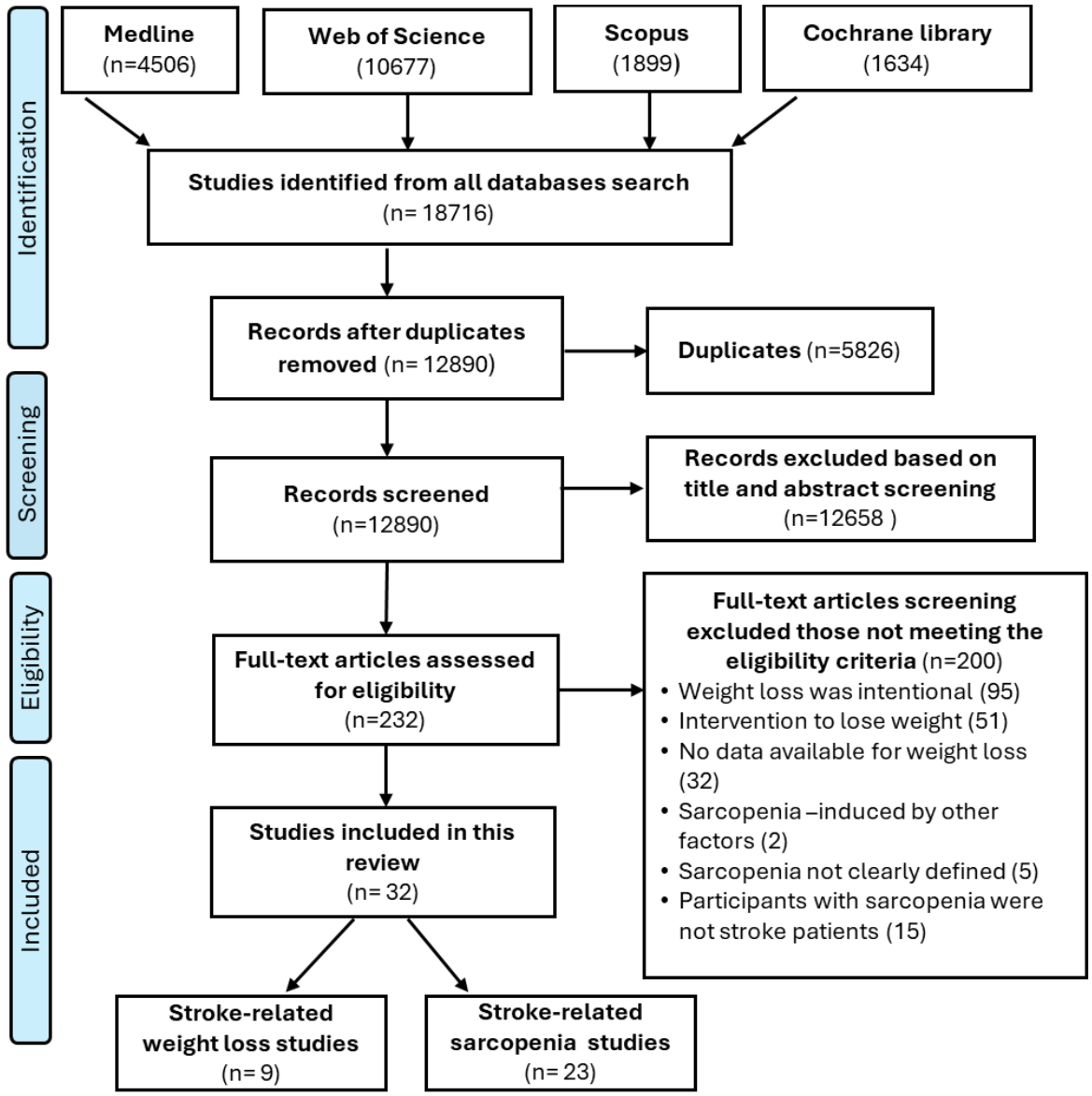

Figure 3-1 PRISMA study flow chart for the process of the eligible studies selection

3.3.2 Post-stroke weight loss

3.3.2.1 Characteristics of included studies for post-stroke weight loss

The basic characteristics of the included studies are summarised in **Table 3-2.**

A total of 9 eligible studies enrolling a total of 2,046 participants, with an average age ranging from 66 to 73 years, were included in the review. Seven studies employed a cohort design, one used a case-control design, and one was a cross-sectional study. Four studies were conducted on patients with ischaemic stroke, and another four studies were done on mixed cohorts, such as ischaemic, haemorrhagic and subarachnoid haemorrhage stroke. Five studies were carried out in Europe (Huppertz et al., 2022, Jonsson et al., 2008, Scherbakov et al., 2019c, Rodriguez-Castro et al., 2019, Wohlfahrt et al., 2015) and 4 in Asia (Kim et al., 2015b, Kishimoto et al., 2022, Mogamiya et al., 2022, Yamamoto et al., 2022). Five studies recruited participants within one week of stroke onset (Jonsson et al., 2008, Kim et al., 2015b, Scherbakov et al., 2019c, Yamamoto et al., 2022, Rodriguez-Castro et al., 2019), and two studies focused on individuals who were more than one month post-stroke (Huppertz et al., 2022, Kishimoto et al., 2022). Five studies used an unintentional weight loss of more than 3 kilograms (Kg) as a cut-off value to define the weight loss post-stroke (Huppertz et al., 2022, Jonsson et al., 2008, Mogamiya et al., 2022, Wohlfahrt et al., 2015, Rodriguez-Castro et al., 2019) , whereas three studies defined post-stroke weight loss as a loss of more than 5 % of the baseline body weight (Kishimoto et al., 2022, Scherbakov et al., 2019c, Yamamoto et al., 2022).

Table 3-2 Characteristics of the included study (weight loss)

Study	Location	Study design	N	Men (%)	Age Mean(years)/BMI	Type of stroke	Time since onset of stroke	Length of follow-up	Weight loss definition	Prevalence
(Huppertz *et al.*, 2022)	Netherlands	Cross-sectional study	42	76.2	69.1/ 26.8	NR	≥6 months	NR	>3 kg in the past month	16.7%
(Jonsson *et al.*, 2008)	Sweden	Prospective cohort study	305	60	72.5/ 25.8	IS/ HS/ SAH	24 h	16 months	>3 kg	26%
(Kim *et al.*, 2015)	Korea	Retrospective observational study	654	61.5	66.7/ 21-24.2	IS	7 days	3 months	loss >0.05 kg per baseline BMI-unit or ≥ -2 Kg	24.6%

Study	Location	Study design	N	Men (%)	Age Mean(years) /BMI	Type of stroke	Time since onset of stroke	Length of follow-up	Weight loss definition	Prevalence
(Kishimoto *et al.*, 2022)	Japan	Retrospective cohort study	293	60.8	69/ 22.1	IS/HS/SAH	36 days	1 month	>5% within the past 6 months	39.9%
(Mogamiya *et al.*, 2022)	Japan	Retrospective cohort study	81	58	73/ 22.4	IS/HS/SAH	NR	3 months	>3 kg	76.5%
(Scherbakov *et al.*, 2019)	Germany	Prospective observational study	67	58	69/ 27	IS	48 h	1 year	loss ≥5% within 1 year	21%

Study	Location	Study design	N	Men (%)	Age Mean(years)/BMI	Type of stroke	Time since onset of stroke	Length of follow-up	Weight loss definition	Prevalence
(Rodriguez-Castro *et al.*, 2019)	Spain	Prospective case-control study	98	54.1	69.3	IS	24 h	3 months	>3 kg within 3 months	NR
(Wohlfahrt *et al.*, 2015)	Czech Republic	Retrospective cohort study	351	60	66/ 29.3	IS	NR	21 months	>3 kg within 16 months	21%
(Yamamoto *et al.*, 2022)	Japan	Prospective-cohort study	155	67.7	72/ 24	IS/HS	48 h	NR	loss ≥5% in 1 month	19%

Abbreviations: BMI, body mass index; HS, haemorrhagic stroke; IS, ischemic stroke; NR, not reported; SAH, subarachnoid haemorrhage

3.3.2.2 Quality of included studies

NOS scale was used to assess the quality of the included studies. The detailed risk of bias assessment is provided in Table 3-3. Most of the studies meet the criteria for high quality. However, four studies were identified with at least one domain classified as high risk, primarily due to limitations in patient selection. This issue stemmed from factors such as single-centre study designs.

Table 3-3 Summary table of quality assessment of included studies

Study	Design	Selection				Comp		Outcome		Score
Author (year)		1	2	3	4	5	6	7	8	
(Huppertz *et al.*, 2022)	Cross-sectional study	*		*	*	*	**	*	-	Good
(Jonsson *et al.*, 2008)	Cohort study	*	*	*	*	*	*	*	*	Good
(Kim *et al.*, 2015)	Cohort study	*	*		*	*	*	*	*	Good
(Kishimoto *et al.*, 2022)	Cohort study		*	*	*	*	*	*	*	Good
(Mogamiya *et al.*, 2022)	Cohort study		*		*		*	*	*	Poor
Scherbakov *et al.*, 2019)	Cohort study		*	*	*	*	*	*	*	Good
(Wohlfahrt *et al.*, 2015)	Cohort study	*	*	*	*	**	*	*	*	Good
(Yamamoto *et al.*, 2022)	Cohort study		*	*	*	**	*	*	*	Good

3.3.2.3 Prevalence of post-stroke weight loss

Among the nine studies investigating patients with stroke, one study was excluded from the analysis due to an unreported proportion of patients who experienced weight loss (Rodriguez-Castro et al., 2019). In the remaining eight studies, the prevalence of patients who experienced unintentional weight loss after stroke exhibited considerable variation, ranging from 16.7% to 76.5%, as shown in Table 3-2. The meta-analysis was conducted to calculate the pooled prevalence using random-effects model due to the presence of high heterogeneity (I^2=97.8%, P<0.01). The pooled prevalence of post-stroke weight loss was 31% (95% CI 17-44%) (Figure 3-2).

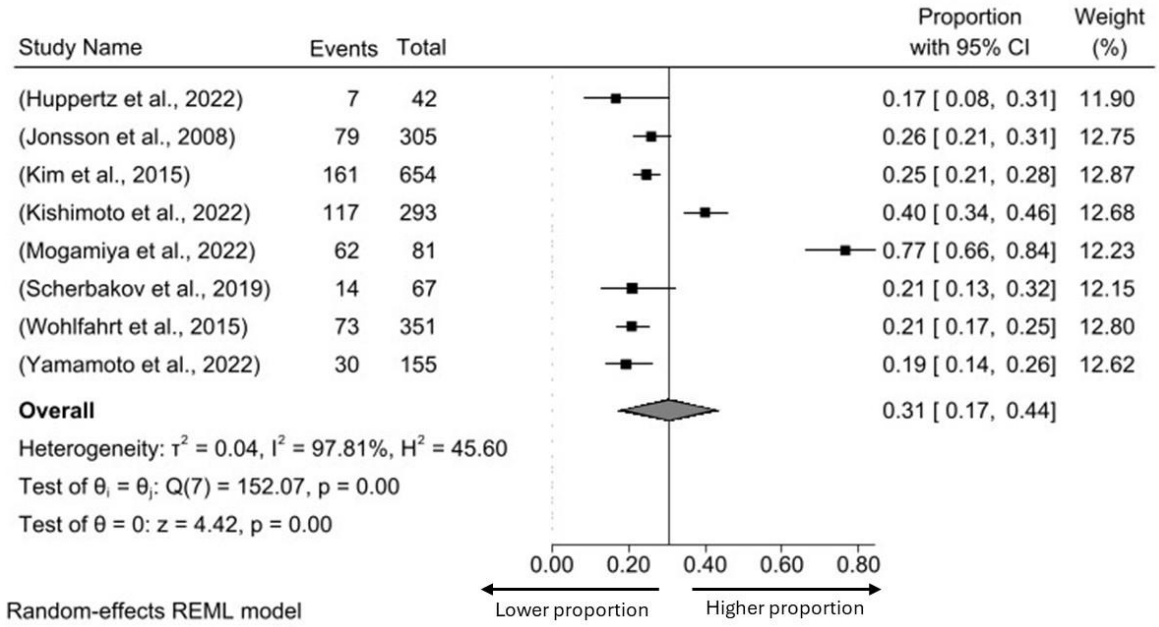

Figure 3-2 Forest plot showing the pooled estimate prevalence of unintentional weight loss among patients after stroke.

3.3.2.4 Sensitivity analysis and publication bias

Figure 3-3 shows the results of sensitivity analysis that assessed the influence of individual studies on the pooled prevalence by sequentially excluding one study in each turn. None of the studies significantly influenced the overall estimated prevalence. However, by excluding Mogamiya et al (2022) study, the estimated pooled prevalence drops from 31% to 24% (95% CI 19-30%). A visual assessment of the funnel plot reveals an imbalance in the distribution of the studies across the plot, which may suggest the potential presence of publication bias (Figure 3-4). However, Egger's test showed no statistically significant result (ß=2.48, p=0.6), indicating that there is no publication bias present.

3.3.2.5 Subgroup analysis by sex, time since onset of stroke, stroke type, and cut-off value

The analysis was stratified according to sex, time since onset of stroke, stroke type and cut-off value to detect the source of heterogeneity (Table 3-4).

Five studies reported data for the proportion of patients who had lost weight unintentionally after stroke in both male and female participants. The pooled prevalence of post-stroke weight loss in men was estimated at 25% (95% CI 15-35%), demonstrating substantial heterogeneity (I^2=91.73%, p<0.01). Similarly, the pooled prevalence among the women was 25% (95% CI 19-30%). Although the heterogeneity decreased slightly, it still exhibited a high level of heterogeneity (I^2=55.7%, p=0.07). The result showed no sex difference in the prevalence of post-stroke weight loss.

Data for the time of stroke onset were available in 6 studies. The prevalence of unintentional weight loss in patients during one week of stroke onset was 24% (95% CI 21-26%). The assessment of heterogeneity showed no statistically significant heterogeneity between studies (I^2=0.10%, p=0.36). However, significant heterogeneity was observed between studies when the time of stroke onset was ≥ 1 month (I^2=92%, p=0.00), with pooled prevalence set at 29% (95% CI 6-52%). The results indicated no statistically significant difference between the subgroups (p = 0.67).

Three studies had been done on patients with ischaemic stroke, and the prevalence of weight loss among the patients was 23% (95% CI 20-26%). No statistically significant heterogeneity was found between the studies (I^2=26.5%, p=0.34). However, four cohorts were conducted on mixed stroke types such as ischaemic, haemorrhagic and subarachnoid haemorrhagic stroke. The prevalence of weight loss in mixed cohorts was 40% (95% CI 15-65%) with significant heterogeneity detected between studies (I^2=98%, p=0.00). However, the difference in effect size between the groups is not statistically significant (p=0.17).

Furthermore, a stratified analysis was conducted based on the cut-off value used to define weight loss after stroke. Three studies used an unintentional weight loss of more than 3 kg as a cut-off measure to consider post-stroke weight loss as an interesting outcome, while three other studies used a loss of 5% or more of the baseline body weight as a cut-off value. The prevalence of post-stroke weight loss of more than 3kg was 22% (95% CI 18-27%), and no significant heterogeneity was observed between studies (I^2= 42.6%, p =0.18). However, the pooled prevalence of post-stroke weight loss of≥5% of the baseline body weight was estimated at 27% (95% CI 14-40%) with a high level of heterogeneity (I^2= 90.9%, p =0.00). The result showed that there was no significant difference between the two groups (P=0.51)

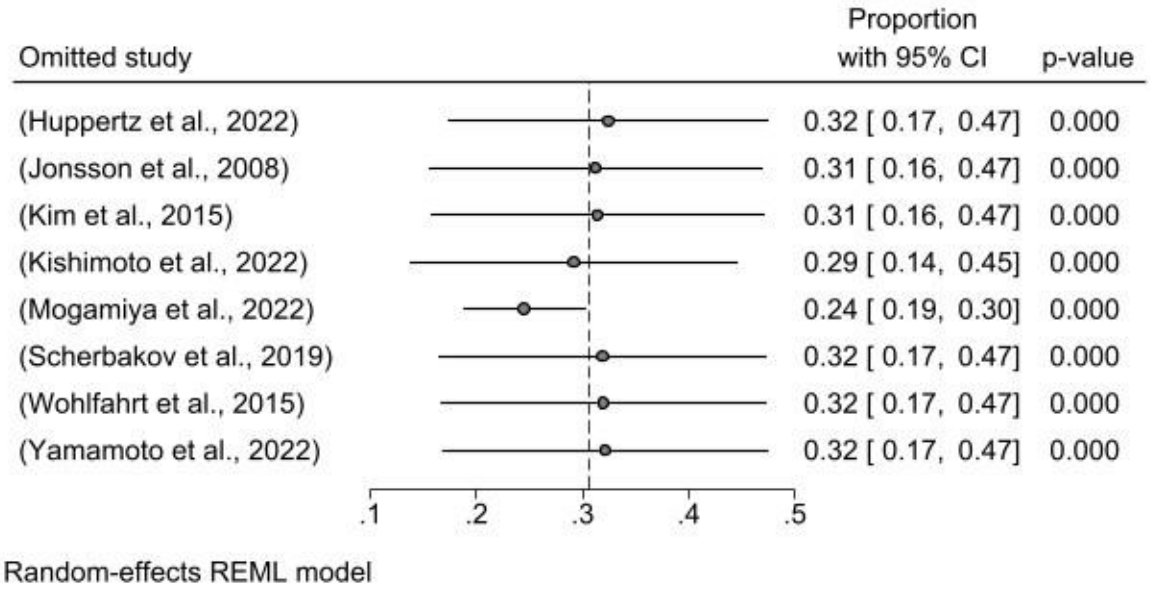

Figure 3-3 Sensitivity analysis excluding one study in each turn (leave-one-out meta-analysis).

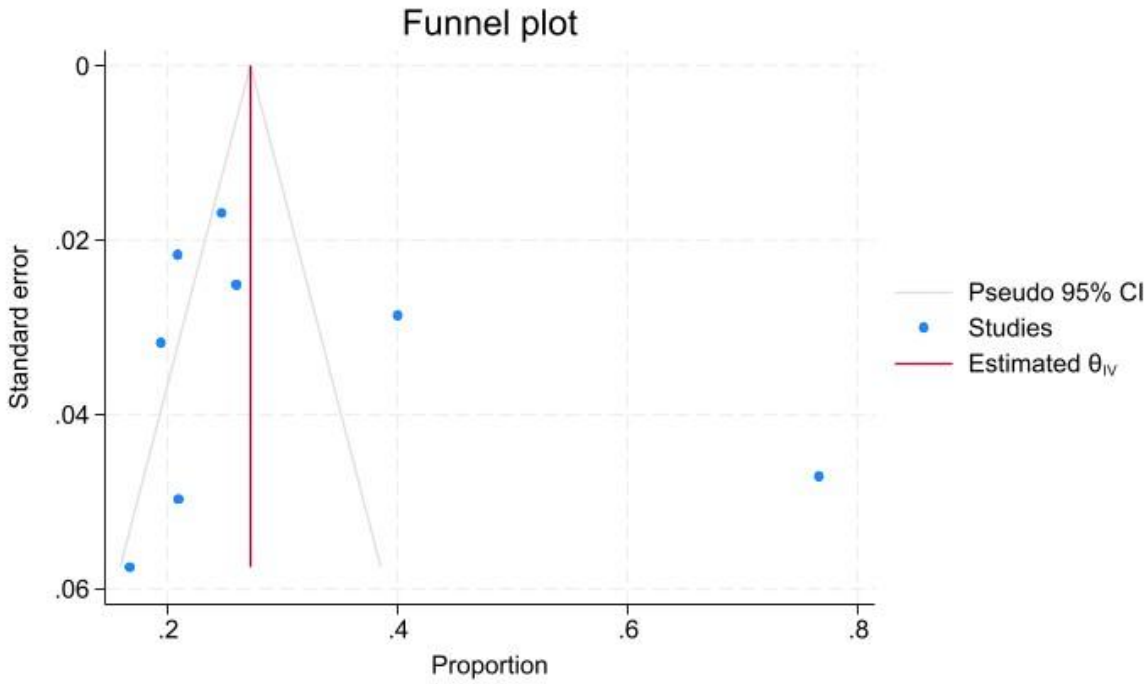

Figure 3-4 Funnel plot of the included studies examining the publication bias.

Table 3-4 Subgroup analysis of the prevalence of weight loss in the included studies

Subgroup		Number of studies	Events	Total	Pooled prevalence	95% CI	P-value for heterogeneity	I^2 (%)	Between-group P-value
Sex	Male	5	250	939	25%	15-35 %	0.00	91.73	
	Female	5	145	581	25%	19-30 %	0.07	55.73	
Time since stroke onset	≤ 1 week	4	284	1181	24%	21-26 %	0.36	0.10	0.67
	≥ 1 month	2	124	335	29%	6-52 %	0.00	92.38	
Type of stroke	IS	3	248	1072	23%	20-26%	0.34	26.52	0.17
	Mixed cohort	4	288	834	40%	15-65%	0.00	98.45	
Cut-off value	>3 kg	3	159	698	22%	18-27 %	0.18	42.56	0.51
	≥ 5% baseline BW	3	161	515	24%	17-31 %	0.00	90.92	

Abbreviations: BW, body weight; CI, confidence interval; IS, ischaemic stroke

3.3.2.6 Impact of post-stroke weight loss on patient outcomes

Functional outcome: Five studies examined the impact of post-stroke weight loss on functional outcomes using various measures to assess functional and physical performance, including the Modified Rankin Scale (mRS), motor Functional Independence Measure (FIM) gain, and Activity of Daily Living (ADL) scores. The mRS was examined in three studies for short and long-term outcomes. Two studies showed that patients who experienced weight loss demonstrated poorer functional outcomes as assessed by mRS in the short and long term compared to those with stable or gained weight group (Kim et al., 2015b, Scherbakov et al., 2019c). Moreover, one study found that reductions in body weight were significantly greater in the group with poor outcomes at three months post-stroke (Rodriguez-Castro et al., 2019). The motor FIM gain was assessed as the outcome of interest in one study (Kishimoto et al., 2022). This study also reported that the weight-stable or gain group showed a greater improvement in motor FIM gain scores compared to the weight loss group, although this difference was not statistically significant. Nevertheless, after adjusting for potential confounders, the weight-stable group demonstrated a significant positive association with motor FIM gain (Kishimoto et al., 2022). Only one study evaluated the association between post-stroke weight loss and independence of ADL. The study indicated that body weight loss is more strongly associated with dependence in ADL among patients with mild to moderate stroke (Mogamiya et al., 2022).

Mortality: Two studies examined the association between weight loss after stroke and mortality risk. Post-stroke weight loss was independently associated with an increased risk of mortality in one study (Wohlfahrt et al., 2015). Another study reported on mortality and found that substantial weight loss within the first four months following an ischemic stroke was more frequently observed in patients who died within the first year post-stroke compared to those who survived (Jonsson et al., 2008).

Length of hospital stay (LOS): Only one study examined the relationship between post-stroke weight loss and LOS and found that patients with weight loss experienced a significantly longer LOS and a lower discharge rate to home (Yamamoto et al., 2022). A summary of the impact of weight loss after stroke on outcome is presented in Table 3-5.

Table 3-5 Impact of Weight loss after Stroke on Patients' Outcomes

Outcome	studies	Findings
Functional outcome	(Kim *et al.*, 2015)	Patients who experienced weight loss demonstrated significantly poorer functional outcomes at three months post-stroke than those with stable weight ($p < 0.001$).
	(Kishimoto *et al.*, 2022)	A greater improvement in motor FIM scores was observed in the stable or gain weight group compared to the Weight Loss (WL) group. However, this difference was not statistically significant in the unadjusted analysis, but after adjustment, the difference became statistically significant.
	(Mogamiya *et al.*, 2022)	The study indicated that body weight loss is more strongly associated with dependence in ADL among patients with mild to moderate stroke.
	(Scherbakov *et al.*, 2019)	Patients who experienced weight loss demonstrated poorer functional outcomes, as assessed by the mRS, in the long term compared to those in the stable or gained weight groups.
	(Rodriguez-Castro *et al.*, 2019)	The reductions in body weight were significantly greater in the poor-outcome group at 3 months post-stroke.
Mortality	(Wohlfahrt *et al.*, 2015)	Post-stroke weight loss was independently associated with an increased risk of mortality.
	(Jonsson et al., 2008)	Significant weight loss within the first four months following an ischemic stroke was more frequently observed in patients who died within the first year post-stroke.
LOS	(Yamamoto *et al.*, 2022)	Patients with weight loss experienced a significantly longer LOS and a lower discharge rate to home

3.3.3 Stroke-related sarcopenia

3.3.3.1 Characteristics of the Included Study

A total of 23 eligible studies reporting stroke-related sarcopenia were identified, enrolling a total of 5,554 participants with an average age ranging from 52.8 to 79 years. The key characteristics of the included studies are presented in Table 3-6. Most studies were carried out in Japan (n=11), followed by five in South Korea, two in the United States of America, one in Turkey, one in Italy, one in Indonesia, and one study involving a multinational cohort. Twelve studies had a cohort design (Abe et al., 2023, Bise et al., 2022, Ikeji et al., 2023, Jang et al., 2020, Lee et al., 2022, Lee et al., 2023b, Matsushita et al., 2019, Nagano et al., 2020, Park et al., 2019b, Siotto et al., 2022, Yoshimura et al., 2019b), nine studies utilised a cross-sectional design (Aydin et al., 2021, Inoue et al., 2021, Jang et al., 2021, Kanai et al., 2023, Li et al., 2022, Mohammed and Li, 2022, Ryan et al., 2017, Shiraishi et al., 2018, Sosiawati et al., 2021, Yoshimura et al., 2018), and two were conducted as case-control studies (Kameyama et al., 2022, Yao et al., 2022). Among the 23 studies included in this review, 15 utilised the Asian Working Group for Sarcopenia (AWGS) or its updated 2019 version (AWGS2019) to diagnose sarcopenia, while seven employed the European Working Group on Sarcopenia in Older People (EWGSOP) or its revised version (EWGSOP2). Most studies utilised low muscle mass in conjunction with low muscle strength to diagnose sarcopenia. However, only four studies employed comprehensive diagnostic criteria for sarcopenia, incorporating a combination of low muscle mass, low muscle strength, and low physical performance. Additionally, one study used a combination of low muscle mass and low physical performance, while another study used low muscle strength as the sole criterion to detect sarcopenia. Table 3-7, summarises the diagnostic criteria used in each study.

Table 3-6 Characteristics of included studies (stroke-related sarcopenia)

Study	Location	Population setting	Study design	N	Men (%)	Age Mean(years)	Type of stroke	Time since onset of stroke	Length of follow-up	Prevalence
(Abe *et al.*, 2023)	Japan	Acute care hospital	Retrospective cohort study	308	64.3	73.2	IS/HS	48 h	1 month	28.20%
(Aydin *et al.*, 2021)	Turkey	Rehabilitation hospital	Cross-sectional study	81	50.6	64.6	IS/HS	14 months	NR	1%
(Bise et al., 2022)	Japan	Convalescent rehabilitation ward	Retrospective cohort study	499	52	74	IS/HS/SAH	NR	3 months	43.28%
(Ikeji *et al.*, 2023)	Japan	Neurosurgical hospital	Prospective observational cohort study	286	67.8	72	IS/HS	48 h	NR	32.50%
(Inoue *et al.*, 2021)	Japan	Convalescent rehabilitation ward	Cross-sectional study	256	57	76.6	IS/HS/SAH	29 days	NR	63.70%
(Jang *et al.*, 2021)	South Korea	Department of rehabilitation medicine	Cross-sectional study	66	53	74.8	IS/HS	NR	NR	18.20%
(Jang *et al.*, 2020)	South Korea	Department of rehabilitation hospital	Retrospective cohort	194	59.3	64.3	IS/HS	2 weeks	6 months	41.80%
(Kameyama *et al.*, 2022)	Japan	Convalescent rehabilitation ward	Case-control study	283	56.2	76.8	IS/HS/SAH	33 days	72 days	57.60%

Study	Location	Population setting	Study design	N	Men (%)	Age Mean(years)	Type of stroke	Time since onset of stroke	Length of follow-up	Prevalence
(Kanai et al., 2023)	Japan	Convalescent rehabilitation ward	Cross-sectional study	80	47.5	72	IS/HS	NR	NR	57.5
(Lee *et al.*, 2022)	South Korea	Department of neurology at stroke center	Retrospective observational cohort study	568	64.6	65.5	IS	4 days	3 months	8.50%
(Lee *et al.*, 2023)	South Korea	Stroke center of university hospital	Prospective cohort study	653	61.7	69	IS	2 days	3 months	26.60%
(Li *et al.*, 2022)	USA	Institute of rehabilitation	Cross-sectional observational study	28	57.1	57.4	NR	> 6 months	NR	25%
(Matsushita *et al.*, 2019)	Japan	Convalescent rehabilitation ward	Retrospective cohort study	267	56.2	72.5	IS/HS/SAH	24 days	3 months	48.30%
(Mohammed and Li, 2022)	China/ Egypt	Department of rehabilitation	Prospective cross-sectional study	T=395, E=200, CH=195	62.5	Egypt = 55.5 China= 52.8	IS/HS	< 2 months	NR	Egypt = 17% China=13.8%
(Nagano *et al.*, 2020)	Japan	Convalescent rehabilitation ward	Retrospective cohort study	272	74.3	79	IS/HS/SAH	18 days	4 months	44%
(Park *et al.*, 2019)	South Korea	Rehabilitation center	Cohort study	39	50	66.5	IS/HS	15.5 days	1 month	28.60%

Study	Location	Population setting	Study design	N	Men (%)	Age Mean(years)	Type of stroke	Time since onset of stroke	Length of follow-up	Prevalence
(Ryan *et al.*, 2017)	USA	Community	Cohort study	168	69	63	IS	51 months	NR	14.3%
(Shiraishi *et al.*, 2018)	Japan	Convalescent rehabilitation ward	Cross-sectional study	202	53	72.2	HS/IS/LI/SAH	12 days	NR	53.50%
(Siotto *et al.*, 2022)	Italy	Rehabilitation department	Cohort study	61	49.2	68	IS/HS	105 days	6 weeks	29.50%
(Sosiawati *et al.*, 2021)	Indonesia	Community	Cross-sectional study	80	60	74	NR	>6 months	NR	40%
(Yao *et al.*, 2022)	China	Rehabilitation center	Case-control study	259	69.1	57	IS/HS	<6 months	42 days	46.70%
(Yoshimura *et al.*, 2018)	Japan	Convalescent rehabilitation ward	Cross-sectional study	233	42.5	74	IS/HS/SAH	15 days	NR	53.6
(Yoshimura et al., 2019)	Japan	Convalescent rehabilitation ward	Retrospective cohort study	276	41	74.9	IS/HS/SAH	15 days	NR	52.20%

Abbreviations: E, Egypt; Ch, China; h, hour; HS, haemorrhagic stroke; IS, ischemic stroke; LI, lacunar infarction; NR, not reported; SAH, subarachnoid haemorrhage; T, total.

Table 3-7 Diagnostic criteria for sarcopenia diagnosis and cut-off values of the included studies

study	Diagnostic criteria	Muscle mass	Muscle strength	Physical performance
(Abe *et al.*, 2023)	AWGS2019	(BIA) SMI <7.0kg/m^2 for men and <5.7kg/m^2 for women	Handgrip strength cut-off values were <28 kg for men and <18 kg for women	NA
(Aydin *et al.*, 2021)	EWGSOP2	(BIA) total SMM <9.2 kg/m^2 for males and 7.4 kg/m^2 for females	Handgrip strength cut-off values were <27 kg for men and <16 kg for women	gait speed- walk 6 min and (SPPB). The cutoff points for low performance were gait speed ≤0.8 m/s and SPPB ≤8 points.
(Bise et al., 2022)	AWGS2019	(BIA) SMI <7.0kg/m^2 for men and <5.7kg/m^2 for women	Handgrip strength cut-off values were <28 kg for men and <18 kg for women	NA
(Ikeji *et al.*, 2023)	AWGS2019	(BIA) SMI <7.0kg/m^2 for men and <5.7kg/m^2 for women	Handgrip strength cut-off values were <28 kg for men and <18 kg for women	NA
(Inoue *et al.*, 2021)	AWGS2019	(BIA) SMI <7.0kg/m^2 for men and <5.7kg/m^2 for women, Calf circumference (CC) Men: < 34 cm, Women: < 33 cm	Handgrip strength cut-off values were <28 kg for men and <18 kg for women.	NA
(Jang *et al.*, 2021)	AWGS2019	(BIA) SMI <7.0kg/m^2 for men and <5.7kg/m^2 for women	Handgrip strength cut-off values were <28 kg for men and <18 kg for women	NA
(Jang *et al.*, 2020)	EWGSOP with cut-off value like Asian	NA	Handgrip strength cut-off values were <26 kg for men and <18 kg for women	NA
(Kameyama *et al.*, 2022)	AWGS2019	(BIA) SMI <7.0kg/m^2 for men and <5.7kg/m^2 for women	Handgrip strength cut-off values were <28 kg for men and <18 kg for women	NA
(Kanai et al., 2023)	AWGS2019	(BIA) SMI <7.0kg/m2 for men and <5.7kg/m2 for women	Handgrip strength cut-off values were <28 kg for men and <18 kg for women	(SPPB) score ≤9 or gait speed <1.0 m/s
(Lee *et al.*, 2022)	AWGS2019	(BIA) SMI <7.0kg/m^2 for men and <5.7kg/m^2 for women	(MRC) score, cut-off values were 54 for men and 53.42 for women to define low muscle strength	NA

study	Diagnostic criteria	Muscle mass	Muscle strength	Physical performance
(Lee *et al.*, 2023)	AWGS2019	(BIA) SMI <7.0kg/m^2 for men and <5.4kg/m^2 for women	Handgrip strength cut-off values were <28 kg for men and <18 kg for women	NA
(Li *et al.*, 2022)	EWGSOP2 / AWGS2019	EWGSOP2 : (DXA _ ASM/height^2 <7 kg/m2 for men, <5.5 kg/m^2 for women) AWGS2019: (DXA_ ASM/height^2 <7 kg/m2 for men, <5.4 kg/m^2 for women)	EWGSOP2: Handgrip strength cut-off values were <27 kg for men and <16 kg for women AWGS2019: Handgrip strength cut-off values were <28 kg for men and <18 kg for women	Gait speed EWGSOP2: (≤0.8 m/s) AWGS2019: (<1 m/s)
(Matsushita *et al.*, 2019)	EWGSOP2	(BIA) SMI <7.0kg/m^2 for men and <5.7kg/m^2 for women	Handgrip strength cut-off values were <26 kg for men and <18 kg for women	NA
(Mohammed and Li, 2022)	AWGS2019	(Anthropometry) SMI <7.0kg/m^2 for men and <5.4kg/m^2 for women	Handgrip strength cut-off values were <28 kg for men and <18 kg for women	NA
(Nagano *et al.*, 2020)	AWGS2019	(BIA) SMI <7.0kg/m^2 for men and <5.7kg/m^2 for women	Handgrip strength cut-off values were <28 kg for men and <18 kg for women	NA
(Park *et al.*, 2019)	AWGS	(BIA) SMI <7.0kg/m^2 for men and <5.7kg/m^2 for women	Handgrip strength cut-off values were <26 kg for men and <18 kg for women	NA
(Ryan *et al.*, 2017)	EWGSOP	DXA _ ALM/height^2 <7.23 kg/m^2 for men, <5.67 kg/m^2 for women	NA	gait speed <0.8 m/s
(Shiraishi et al., 2018)	AWGS	(BIA) SMI <7.0kg/m^2 for men and <5.7kg/m^2 for women	Handgrip strength cut-off values were <26 kg for men and <18 kg for women	NA

study	Diagnostic criteria	Muscle mass	Muscle strength	Physical performance
(Siotto et al., 2022)	EWGSOP2	(BIA) SMI <7.0kg/m^2 for men and <5.5kg/m^2 for women	Handgrip strength cut-off values were <27 kg for men and <16 kg for women	NA
(Sosiawati et al., 2021)	AWGS	(MMI) with calf circumference: Male & Female <33 cm	Handgrip strength cut-off values were <29 kg for men and <17 kg for women	Physical performance with 6 min walking test: gait speed <0.8 m/s
(Yao et al., 2022)	AWGS2019	(BIA) SMI <7.0kg/m^2 for men and <5.7kg/m2 for women	Handgrip strength cut-off values were <28 kg for men and <18 kg for women	NA
(Yoshimura et al., 2018)	EWGS with cut-off values like Asian	(BIA) SMI <7.0kg/m^2 for men and <5.7kg/m^2 for women	Handgrip strength cut-off values were <26 kg for men and <18 kg for women	NA
(Yoshimura et al., 2019)	EWGS with cut-off values like Asian	(BIA) SMI <7.0kg/m^2 for men and <5.7kg/m^2 for women	Handgrip strength cut-off values were <26 kg for men and <18 kg for women	

Abbreviations: ALM, appendicular lean mass; ALM/height^2, appendicular lean mass/height^2; ASM/height^2,appendicular skeletal muscle mass/height^2; AWGS2019, Asian working group for sarcopenia; BIA, Bioelectric Impedance Analysis; DXA, dual energy X-ray absorptiometry; EWGSOP, European working group on sarcopenia in older people; m, meter; MRC, Medical Research Council; MMI, Muscle Mass Index; NA, not available; s, second; SMI, skeletal muscle index; SPPB, Short Physical Performance Battery.

3.3.3.2 Quality of the included studies

The risk of bias of the included studies was assessed using the NOS scale (Table 3-8). From the 23 studies included in this review, approximately 35% (8) were rated as high quality, while 48% (11) were considered fair, and 17% (4) were poor. The major problems were observed in the selection domain due to the studies being limited by the recruitment of participants exclusively from convalescent rehabilitation centres, which may affect the generalizability of the findings to broader stroke populations. The other issue was that “the demonstration that the outcome of interest was not present at the start of the study”, i.e. sarcopenia was not present prior to stroke onset was unclear in most studies. In fact, around fourteen studies did not report this information, making it difficult to determine whether sarcopenia developed before or after the stroke onset.

Table 3-8 Summary table of quality assessment of included studies

Study	Design	Selection				Comp		Outcome		Score
Author (year)		1	2	3	4	5	6	7	8	
(Abe *et al.*, 2023)	Cohort study		*	*		**	*		*	Fair
(Bise et al., 2022)	Cohort study		*	*		*	*	*	*	Fair
(Ikeji *et al.*, 2023)	Cohort study		*	*	*	**	*		*	Good
(Jang *et al.*, 2020)	Cohort study		*	*		*	*	*	*	Fair
(Lee *et al.*, 2022)	Cohort study	*	*	*		**	*	*	*	Good
(Lee *et al.*, 2023)	Cohort study	*	*	*		**	*	*	*	Good
(Matsushita *et al.*, 2019)	Cohort study		*	*		*	*	*	*	Fair
(Nagano *et al.*, 2020)	Cohort study	*	*	*		*	*	*	*	Good
(Park *et al.*, 2019)	Cohort study		*	*			*		*	Poor
(Ryan *et al.*, 2017)	Cohort study	*	*	*			*		*	Poor
(Siotto etal., 2022)	Cohort study		*	*		*	*		*	Fair
(Yoshimura etal., 2019)	Cohort study		*	*		*	*	*	*	Fair
(Aydin *et al.*, 2021)	Cross-sectional			*	*	*	**	*	-	Fair

Study	Design	Selection				Comp		Outcome		Score
Author (year)		1	2	3	4	5	6	7	8	
(Inoue *et al.*, 2021)	Cross-sectional		*	*	*		*	*	-	Poor
(Jang *et al.*, 2021)	Cross-sectional			*	*	*	**	*	-	Fair
(Kanai *et al.*, 2023)	Cross-sectional			*	*	**	**	*	-	Fair
(Li *et al.*, 2022)	Cross-sectional	*		*	*	*	**	*	-	Good
(Mohammed and Li, 2022)	Cross-sectional	*	*	*	*	*	**	*	-	Good
(Shiraishi etal., 2018)	Cross-sectional	*	*	*	*	**	*	*	-	Good
(Sosiawati etal., 2021)	Cross-sectional	*		*			*		-	Poor
(Yoshimura etal., 2018)	Cross-sectional		*	*	*	*	*	*	-	Good

3.3.3.3 Prevalence of stroke-related sarcopenia

The reported prevalence of sarcopenia across the 23 included studies ranged from 1% to 64%. Random-effects models were employed in the meta-analysis due to the presence of substantial heterogeneity among the studies (I^2 = 97.85%, p < 0.01). As illustrated in Figure 3-5, the pooled prevalence of stroke-related sarcopenia was 36% (95% CI 29-44 %).

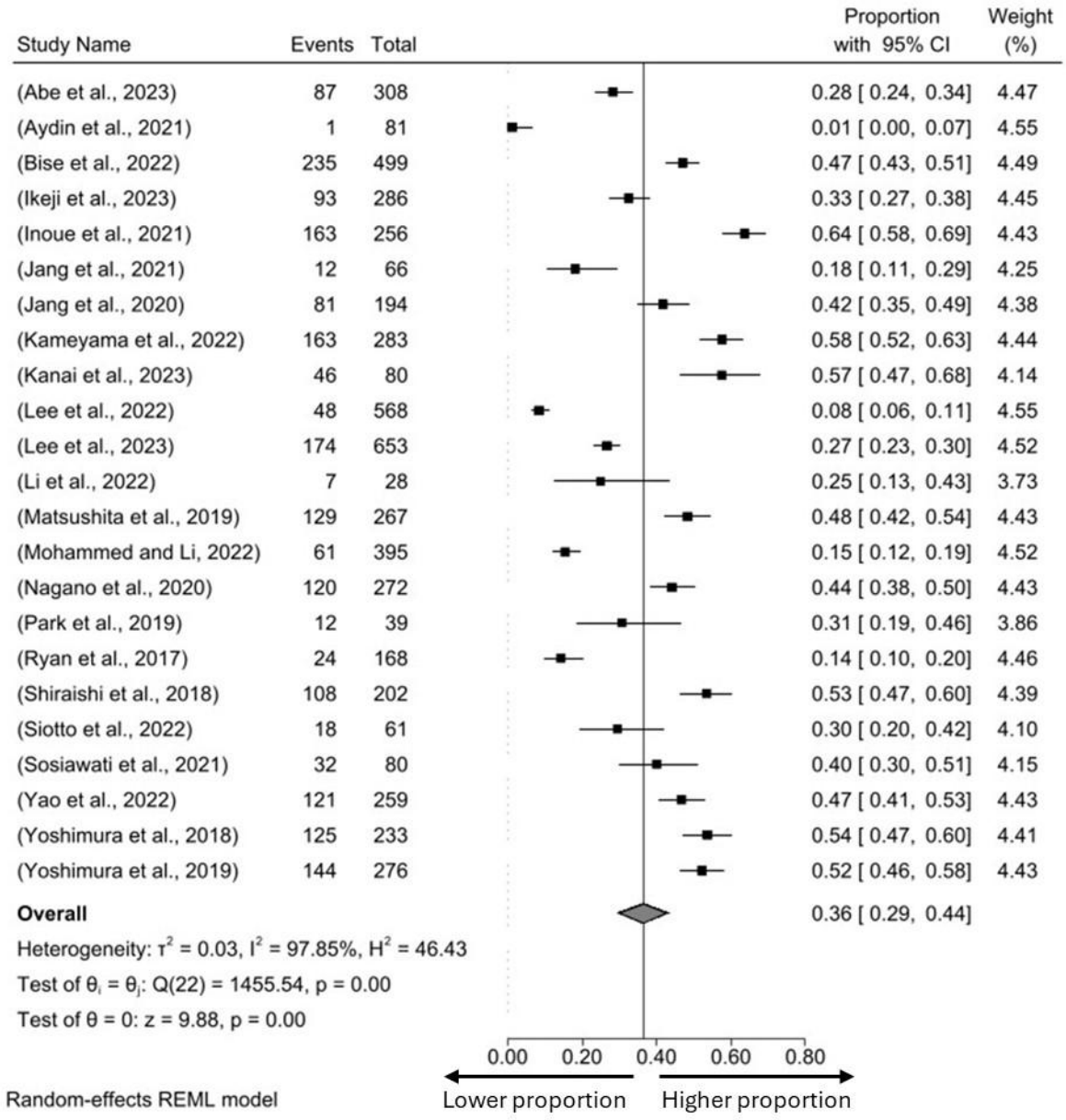

Figure 3-5 Forest plot showing the estimated pooled prevalence of stroke-related sarcopenia among 23 included studies.

3.3.3.4 Sensitivity analysis and publication bias

The sensitivity analysis was conducted using a one-study removed meta-analysis approach. The analysis revealed that the pooled prevalence of sarcopenia among stroke patients remained stable, indicating that no individual study has a significant impact on the overall estimate. Egger's test revealed the absence of publication bias (p=0.4, β=1.6).

3.3.3.5 Subgroup analysis by study location, sex, time since stroke onset, and diagnostic criteria

Table 3-9 summarises the results of subgroup analysis, which assess the robustness of the primary finding and identify the potential sources of heterogeneity among the included studies. This analysis reveals that the prevalence of sarcopenia was found to be significantly higher within the first three months following stroke onset (40%, 95% CI 31-48 %) compared to the prevalence observed beyond six months post-stroke (19%, 95% CI 3-36 %). No significant difference was observed in the prevalence of sarcopenia when the included studies adopted different definitions of sarcopenia. Indeed, when AWGS or its updated version, AWGS2019, and EWGSOP were used, the prevalence was 37% and 32%, respectively. Additionally, the subgroup analysis of stroke-related sarcopenia prevalence indicated that the observed heterogeneity was not attributable to sex, geographic location, time since stroke onset, or the diagnostic criteria used to define sarcopenia.

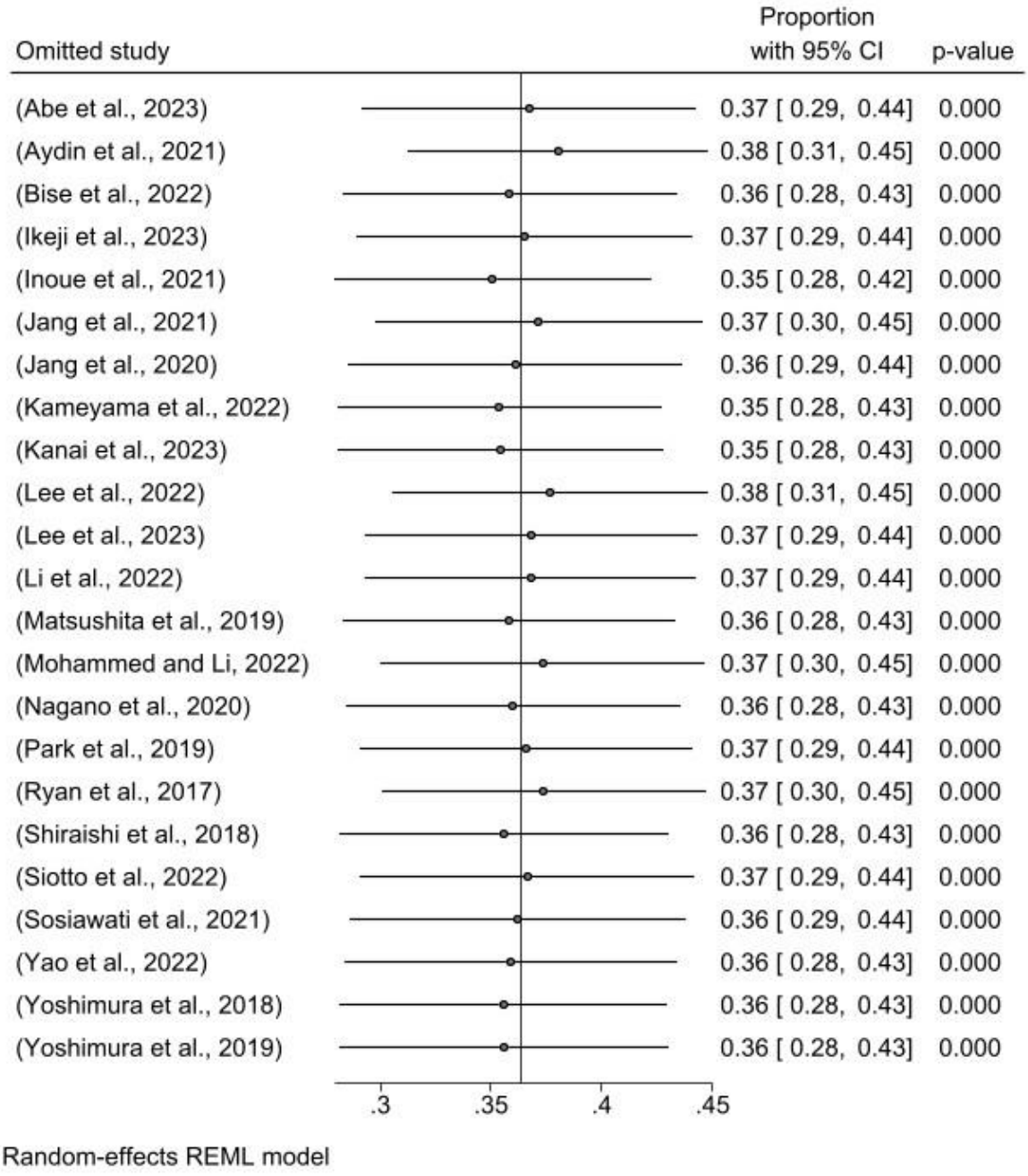

Figure 3-6 Stroke-related sarcopenia sensitivity analysis (leave-one-out) meta-analysis approach.

Table 3-9 The estimated pooled prevalence of sarcopenia according to subgroup analysis in stroke patients

Subgroup		Number of studies	Events	Total	Pooled prevalence	95% CI	*p*-value for heterogeneity	I^2 (%)	Between-group *p*-value
Sex	Male	14	679	2,229	33%	24-42 %	0.00	96.20	
	Female	14	623	1,447	43%	32-55 %	0.00	96.68	
Time since stroke onset	≤ 3 months	14	1,508	4,232	40%	31-48 %	0.00	97.78	0.03
	> 6 months	4	64	357	19%	3-36 %	0.00	96.37	
Location	China	1	121	259	47%	41-53 %			0.00
	Indonesia	1	32	80	40%	29-51 %			
	Italy	1	18	61	30%	18-41 %			
	Japan	11	1,413	2,962	49%	42-55 %	0.00	92.27	
	South Korea	5	327	1,520	25%	13-36 %	0.00	96.32	
	Turkey	1	1	81	1%	1-4 %			
	USA	2	31	196	17%	8-26 %	0.21	35.32	
Diagnostic criteria	AWGS/ AWGS2019	16	1,482	4,274	37%	29-45 %	0.00	97.47	0.56
	EWGSOP2	8	527	1,308	32%	19-46 %	0.00	97.87	

Abbreviations: AWGS, Asian working group for sarcopenia; CI, confidence interval; EWGSOP2, European working group on sarcopenia in older people

3.3.3.6 Impact of stroke-related sarcopenia on patients' outcomes

Six studies investigated the association between sarcopenia and functional outcome in stroke patients. Four studies found a statistically significant association between sarcopenia and functional outcome as assessed by FIM-m. Specifically, the studies showed that the presence of sarcopenia in stroke patients was independently associated with poor functional outcomes (Kameyama et al., 2022, Lee et al., 2022, Yoshimura et al., 2019b, Jang et al., 2020). Additionally, one study reported that the presence of sarcopenia was independently associated with lower functional outcome in male stroke patients, whereas no such association was observed in female patients (Matsushita et al., 2019). However, one study found the association between sarcopenia and poor functional outcome was statistically significant in univariate analyses, but the association was not maintained after adjusting for confounders such as age, sex, BMI, stroke severity and chronic diseases (Lee et al., 2023b). Mortality was assessed in one study, which revealed a positive association between sarcopenia and 3-month mortality. However, this association disappeared after adjusting for potential confounding variables (Lee et al., 2023b). Beyond its influence on clinical outcomes, sarcopenia has also been linked to healthcare utilisation, particularly concerning hospital stay duration. One study examined this aspect and found that stroke patients with sarcopenia had a significantly longer length of stay and fewer home discharges compared to those without sarcopenia (Ikeji et al., 2023).

3.4 Discussion

3.4.1 Post-stroke weight loss

In this systematic review and meta-analysis, our results demonstrate a pooled prevalence of post-stroke weight loss of 31%, based on data extracted from eight studies involving 1,948 stroke survivors. The findings exhibited substantial heterogeneity, which may be attributed to a combination of multiple factors or methodological differences between the included studies.

It is important to note that the search strategy was intentionally broad, focusing on unintentional weight loss following stroke without restricting the inclusion criteria to studies specifically applying cachexia definitions. Despite this broad approach, only eight articles reporting on post-stroke weight loss were identified, of which only two explicitly applied cachexia criteria. This further highlights the limited research attention given to weight loss and cachexia following stroke, while the phenomenon of weight loss is well-documented and widely recognised in other clinical populations, such as those with cancer and heart failure (Argilés et al., 2014, von Haehling et al., 2009). The underlying causes of weight loss following stroke are not fully understood but are proposed to arise from catabolic overactivation and an anabolic deficit. There are obvious causes of this metabolic imbalance which include impaired feeding due to dysphagia and inactivity due to hospitalisation and/or paresis (Scherbakov et al., 2011b). However, findings across studies have been inconsistent. In this review, two studies, Jonsson et al. (2008) and Kim et al. (2015), reported that 46% and 30% of patients who experienced weight loss following stroke, respectively, also had dysphagia, suggesting a potential role of impaired feeding in post-stroke weight loss. In contrast, in the study conducted by Scherbakov et al. (2019), none of the participants who experienced weight loss had dysphagia. Furthermore, in the study by Huppertz et al. (2022), although all participants had dysphagia, only 16.7% of these patients experienced weight loss. Collectively, the findings suggest that weight loss after stroke is a multifactorial phenomenon. Whilst dysphagia may be a factor in some patients, in others, other mechanisms likely contribute. As discussed in chapter 1, factors such as inflammation, stress-related neuroendocrine sympathetic activation, and hormonal imbalance are hypothesised to have a role in the metabolic imbalance and weight loss.

The prevalence of weight loss in the included studies generally ranged between 17% and 26%. However, one study reported a substantially higher prevalence of approximately 77% (Mogamiya et al., 2022). A closer examination of this study suggested the possibility of methodological bias. Participants in this study were divided into two groups based on their level of dependency in ADL, and body weight changes were then assessed. Notably, the distribution of participants between the two groups was unbalanced, introducing the possibility of selection bias. This imbalance in group sizes may have influenced the observed outcomes and contributed to the disproportionately high prevalence of weight loss reported in that study. To further explore the impact of this study on the overall findings, a sensitivity analysis was conducted. After excluding the study by Mogamiya et al. (2022), the pooled prevalence of post-stroke weight loss decreased to 24% (I^2 = 86.43%), although this change was not statistically significant. In addition, subgroup analyses were performed based on factors such as sex, time since stroke onset, and cut-off values to investigate potential sources of heterogeneity. However, these analyses revealed that the observed heterogeneity was not attributable to these variables, suggesting that a combination of multiple factors or methodological differences between studies, such as variations in stroke populations, stroke severity, baseline body weight, and study design, the definition of the cut-off value of weight loss among study participants may have contributed to the variability in prevalence estimates.

The impact of post-stroke weight loss on various clinical outcomes has been explored in several studies, focusing on functional recovery, mortality, and hospital stay duration. Regarding functional outcomes, five studies examined the relationship between post-stroke weight loss and functional performance using various measures. Kim et al. (2015) and Scherbakov et al. (2019) consistently found that patients who experienced weight loss had poorer functional outcomes compared to those who maintained or gained weight. Moreover, the findings of Rodriguez-Castro et al. (2019) revealed that reductions in body weight were significantly greater in the group with poor outcomes. The relationship between weight stability and functional improvement was investigated by Kishimoto et al. (2022), who evaluated motor FIM gain. Although the weight-stable or gain group initially showed greater improvement compared to the weight-loss group, the difference was not statistically significant. After adjusting for confounders such

as age, sex, stroke type, dysphagia, and BMI through multiple regression analysis, a significant positive association was observed between weight stability and motor FIM gain, reinforcing the potential benefit of maintaining body weight after stroke onset.

Regarding mortality, two studies examined the association between post-stroke weight loss and survival outcomes. Wohlfahrt et al. (2015) found that post-stroke weight loss was independently associated with an increased risk of mortality. Similarly, Jonsson et al. (2008) observed that substantial weight loss within the first four months after ischemic stroke was more common among patients who died within the first year compared to survivors, highlighting early weight loss as a potential indicator of poor patient prognosis.

3.4.2 Stroke-related sarcopenia

This systematic review found that the pooled prevalence of stroke-related sarcopenia was 36%, as determined from 23 studies recruiting a total of 5554 stroke patients. This was demonstrated in the REM, with evidence of considerable heterogeneity among the included studies (I^2 = 97.85%, p < 0.001). Considering that many of the contributing factors to sarcopenia are highly prevalent in this population, the observed high prevalence of stroke-related sarcopenia is not entirely unexpected (Ikeji et al., 2023, Yao et al., 2022). This relatively high prevalence may be attributed to a combination of multiple factors commonly encountered in the post-stroke population. Stroke often leads to reduced mobility and prolonged physical inactivity, which may accelerate disuse muscle atrophy (Ryan et al., 2000). Stroke-induced immobility can lead to changes in muscle fibre composition (Bernhardt et al., 2004). Specifically, there is often a shift from type I fibres (slow-twitch, fatigue-resistant) to type II fibres (fast-twitch, more prone to fatigue). This shift contributes to increased muscle weakness and reduced endurance in stroke patients (Greiwe et al., 2001, Landin et al., 1977). Additionally, malnutrition, frequently observed in stroke patients due to dysphagia, diminished appetite, or cognitive decline, can lead to inadequate protein and energy intake, amplifying the loss of muscle mass and function (Scrutinio et al., 2020). Moreover, a recent meta-analysis revealed that the pooled prevalence of post-stroke dysphagia was 42%, which is considered very high among stroke patients (Banda et al., 2022). However, in this review, four studies investigated the oral function status among stroke patients and its relationship with sarcopenia and found that poor oral function is associated with sarcopenia (Ikeji et al., 2023, Shiraishi et al., 2018, Siotto et al., 2022, Yoshimura et al., 2018). Interestingly, the prevalence of sarcopenia was found to be significantly higher within the first three months following stroke onset (40%) compared to the prevalence observed beyond six months post-stroke (19%). Undeniably, the number of studies that found to recruit patients in the early phase of stroke (14 studies) is greater than that in the chronic phase (4 studies), and thus, the sample size is larger in the early phase than in the chronic phase which may affect the result. However, this elevated rate in the early post-stroke phase may be attributed to several interrelated factors. For example, in the acute and subacute stages of stroke recovery, patients often experience marked reductions in physical activity and mobility, leading to rapid muscle disuse and atrophy. Muscle atrophy

resulting from physical inactivity has been linked to disuse in both healthy and critically ill patients (Kawahara et al., 2017). Moreover, a previous study involving healthy older adults found that just 10 days of bed rest could lead to a 30% decrease in muscle protein synthesis and a 6% loss of lean leg mass, resulting in a 16% decline in muscle strength (Kortebein et al., 2007). Additionally, it is reported that the changes in muscle tissue have been shown to begin as early as 4 hours after the onset of stroke (Arasaki et al., 2006). A study showed that muscle weakness can also occur in the unaffected limbs on the opposite side of the body within the first week following a stroke (Bernhardt et al., 2004). Notably, some studies have demonstrated that stroke patients may recover from sarcopenia when provided with an effective combination of therapeutic interventions, such as nutritional support, resistance exercise, and comprehensive rehabilitation programs. Matsushita et al (2021) showed that the stroke survivors who engaged in a rehabilitation program with an average of around 180 min/day and received appropriate nutritional therapy for 180 days had recovered from sarcopenia. Collectively, these factors may explain the higher prevalence of sarcopenia observed in the early phase post-stroke, and stroke patients could recover from sarcopenia in a period of 6 months if they received a good combination therapy (Matsushita et al., 2021).

The subgroup analysis revealed that there was no statistically significant difference in the prevalence of sarcopenia between studies using the EWGSOP2 criteria and those applying the AWGS or AWGS2019 definitions. The EWGSOP2 and the AWGS criteria are both widely accepted tools for diagnosing sarcopenia, though they differ slightly in diagnostic thresholds and emphasis. EWGSOP2, for instance, prioritises low muscle strength as the primary indicator, followed by assessments of muscle mass and physical performance. In contrast, AWGS/AWGS2019 incorporates similar components but uses cut-off values more suitable for Asian populations. In line with the use of region-specific diagnostic criteria, the subgroup analysis also revealed that Japan had the highest reported prevalence of stroke-related sarcopenia, with a pooled estimate of 49%. However, it is important to note that approximately 11 out of the 23 included studies were conducted in Japan, which may have disproportionately influenced the overall pooled estimate, potentially leading to an overrepresentation of the national prevalence within the broader analysis. The high prevalence of stroke-related

sarcopenia observed in this analysis may be partially explained by the study settings. Specifically, 21 out of the 23 included studies were conducted in rehabilitation centres, where patients typically present with moderate to severe post-stroke disability, a population inherently at greater risk for developing sarcopenia due to prolonged immobility and functional impairment. In contrast, only two studies assessed patients from community settings, where individuals are generally more independent and may have a lower risk of sarcopenia. This imbalance in study populations may have contributed to the elevated overall prevalence estimate. Therefore, further research involving community-dwelling stroke survivors is needed to obtain a more comprehensive and representative data sample of the true prevalence of stroke-related sarcopenia.

To explore the sources of heterogeneity in the prevalence of post-stroke sarcopenia, a subgroup analysis was conducted based on sex, geographic location, time since stroke onset, and diagnostic criteria. The results indicated that the observed heterogeneity was not significantly influenced by any of these factors. Instead, the heterogeneity may be largely explained by methodological differences across studies, including variations in patient selection, assessment tools, and measurement protocols. These findings highlight the need for the standardisation of methodologies and assessment procedures in future research to ensure more consistent and comparable prevalence estimates of stroke-related sarcopenia.

In addition to evaluating the prevalence of stroke-related sarcopenia, this systematic review also examined the impact of sarcopenia on stroke patient prognosis, including functional recovery, mortality, and length of hospital stay. Six studies investigated the association between sarcopenia and functional outcomes in stroke patients. Among these, four studies (Kameyama et al., 2022; Lee et al., 2022; Yoshimura et al., 2019; Jang et al., 2020) demonstrated a statistically significant independent association between the presence of sarcopenia and poor functional outcomes, as measured by the motor component of the FIM. These findings suggest that sarcopenia negatively impacts the rehabilitation capacity and functional recovery of stroke survivors. Additionally, Matsushita et al. (2019) reported that sarcopenia was independently associated with poorer functional outcomes in male patients, while no such association was noted in female patients. This may indicate potential sex-dependent differences

in the impact of sarcopenia post-stroke. The natural variations in muscle mass and strength in males and females might explain this. The presence of testosterone leads to greater absolute muscle mass in males than in females, regardless of age (Gallagher et al., 1997). However, the proportional reduction of muscle mass by age is more observable in males than females (Gallagher et al., 1997). However, more studies are needed to confirm the findings. Conversely, one study initially found a significant association between sarcopenia and poor functional outcomes in univariate analysis, but this association did not remain significant after adjusting for confounding variables (Lee et al., 2023).

Similarly, Mortality outcomes were assessed in a single study (Lee et al., 2023), which showed a positive association between sarcopenia and 3-month mortality. However, this association was not sustained after adjustment for potential confounders. The author attributed this to the lower statistical power of the study. In addition to its impact on functional recovery and survival, sarcopenia has been linked to increased healthcare utilisation. For instance, Ikeji et al. (2023) found that stroke patients with sarcopenia had a significantly longer hospital stay and were less likely to be discharged home compared to those without sarcopenia.

These findings suggest that given its association with poorer functional recovery, prolonged hospitalisation, and increased healthcare burden, routine screening for sarcopenia and prevention of muscle wasting should be integrated into post-stroke rehabilitation programs and stroke guidelines. However, despite the growing evidence linking sarcopenia to adverse outcomes after stroke, the current clinical guidelines still have not formally recognised or addressed sarcopenia as a target for management after stroke (Kleindorfer et al., 2021b, Fonseca et al., 2021). This gap highlights the need for stroke-related sarcopenia to be more thoroughly integrated into the interdisciplinary framework of stroke rehabilitation, with future guidelines emphasising strategies such as promoting physical activity, resistance training, nutritional support, and preventing muscle wasting as essential components of post-stroke care.

The best approach to addressing weight loss and sarcopenia might be to try several types of therapy, such as exercise training, nutritional support, and enhancing appetite. Increasing protein intake is recommended to prevent the development of sarcopenia and tissue wasting (Morley et al., 2010). Essential amino acids

supplementation and omega-3 fatty acids have been examined in several studies on patients with cachexia associated with chronic diseases and have shown positive results with respect to reduced skeletal muscle loss, weight gain and improvement of quality of life (Jonker et al., 2017, Lavriv et al., 2018). Exercise training is considered the most efficient method for addressing muscle wasting and sarcopenia. A study reported that resistance exercise interventions can help to improve muscle strength in stroke patients (Ryan et al., 2011b).

In summary, despite a scarcity of literature, we have found that post-stroke weight loss and sarcopenia are very common among stroke survivors, with a pooled estimate prevalence of 31% and 36%, respectively. Additionally, some studies have linked these two conditions with poor functional outcomes and mortality, and a more extended hospital stay, suggesting that more attention needs to be given to weight loss and sarcopenia in stroke patients.

Chapter 4 Investigating the relationship between infarct size and location, and post-stroke weight loss in pre-clinical stroke models

4.1 Introduction

Weight loss is a frequently observed phenomenon following stroke. In the previous chapter, we reported that approximately 31% of stroke patients experience post-stroke weight loss—a notably high prevalence rate. Furthermore, we highlighted that this weight loss has been consistently associated with adverse clinical outcomes. For instance, in a population-based study, Jonsson et al. (2008) found that about 25% of stroke patients lost more than 3 kg within both the short-term (4 months) and long-term (1 year) periods post-stroke. Importantly, the mortality rate among patients with substantial weight loss was 14%, compared to only 4% among those without significant weight loss (Jönsson et al., 2008). Additionally, further evidence from multiple studies indicates that post-stroke weight loss is associated with poor functional outcomes and prolonged hospital stay (Kim et al., 2015a, Kishimoto et al., 2022, Yamamoto et al., 2022, Mogamiya et al., 2022). Despite its clinical implications, weight loss following stroke remains an under-recognised and insufficiently studied phenomenon in the literature. Furthermore, the underlying mechanisms contributing to post-stroke weight loss are not fully understood. Some proposed hypotheses include obvious factors such as inactivity due to paresis, disuse atrophy and impaired feeding. Moreover, it has been suggested that systemic pathophysiological mechanisms triggered by the stroke-induced brain injury may also play an important role (Scherbakov et al., 2011b). These systemic mechanisms triggered by brain injury include sympathetic overactivation and pro-inflammatory cytokines with the net effect being increased catabolic signalling and blunting of anabolic signalling, resulting in body weight loss (Scherbakov et al., 2011b). However, it is unclear if cerebral infarction dictates the extent of weight loss. Indeed, some studies show a positive correlation between infarct size and the extent of weight loss in the middle cerebral artery occlusion (MCAo) model (Yang et al., 2019, Springer et al., 2014a), while others show no correlation supporting the role of factors secondary and unrelated to the initial ischaemic injury (Haley et al., 2020c, Haley et al., 2017). However, potential limitations of these studies are that they often comprise of small sample sizes and use only one stroke model or a single middle cerebral artery occlusion (MCAo) period. Another potential determinant of post-stroke weight loss is the anatomical location of the cerebral infarct. Substantial evidence indicates that the brain, particularly regions such as the hypothalamus, plays a critical role

in the homeostatic regulation of energy metabolism (Roh and Kim, 2016, Cowley et al., 1999, Raposinho et al., 2001). Therefore, ischaemic injury to the hypothalamus following MCAo may contribute to post-stroke weight loss. Furthermore, it is conceivable that body weight loss may arise because of injury to the motor cortex and resultant downstream denervation of motor units and muscle wasting.

In this Chapter, the overarching aim was to investigate the relationship between cerebral infarction and subsequent changes in body weight to provide insight into whether the weight loss might be caused by mechanisms triggered by cerebral injury or whether factors secondary to the initial insult are involved. We hypothesised that weight loss after stroke is dictated by stroke severity and/or the anatomical location of the infarct. However, prior to testing this hypothesis, the first specific aim was to perform a systematised search of databases (outlined in Chapter 3) to evaluate whether post-stroke weight loss is commonly reported in preclinical studies. Second, we characterised the effect of transient MCAo (tMCAo) on body weight, body composition and, food and water intake during the acute phase after stroke induction. Thirdly, we evaluated the relationship between infarct volume and the extent of post-stroke weight loss by performing retrospective analyses of a database of mice that had undergone either reperfused (tMCAo) or non-reperfused (permanent MCAo [pMCAo]) ischaemic stroke. Finally, to explore whether the location of the infarct contributes to the extent of weight loss, we employed a second experimental stroke model (photothrombotic) designed to induce infarction primarily in the brain's cortical regions, including the motor and somatosensory areas. Furthermore, we performed exploratory analyses of brain sections from tMCAo mice to examine if there is a relationship between any specific brain region affected by an infarct and the extent of weight loss.

4.2 Materials and methods

4.2.1 Systematic search

4.2.1.1 Search criteria

The search was performed using four databases to identify the relevant studies: Cochrane Library, MEDLINE (OVID), Scopus, and Web of Science. Search key terms were developed utilising medical subject headings (MeSH) and text words related to stroke, stroke models and weight loss. The search was limited to experimental animal studies and published in English. As the aim of the search was to evaluate whether post-stroke weight loss is commonly reported in preclinical research, Studies were included if animals were subjected to experimental stroke and received only a vehicle treatment. Studies involving any form of therapeutic or experimental intervention were excluded.

4.2.1.2 Data extraction

The data extraction form was developed based on the necessary information to be collected. A standardised Microsoft Excel 2010 worksheet was used to extract data from eligible studies for synthesis. The extracted information from studies includes the first author with publication year, animal species, stroke model used, duration of ischaemia, % and absolute weight loss and duration of study.

4.2.2 Experimental work

4.2.2.1 Animals

For this chapter, a total of 20 male C57BL/6J mice (8-15 weeks of age) were used to characterise the effect of 40-minute tMCAo or sham surgery on body weight, body composition (fat and skeletal muscle), food and water intake. Furthermore, a retrospective analysis was performed on a total of 65 male C57BL/6J mice who had undergone sham surgery, varying MCAo periods (30-, 40-, 50-, 60- or 70-minutes; or permanent MCAo) or photothrombotic (PT) light exposure periods (15-, 18-, and 20-minutes) to examine if there is a relationship between infarct size and post-stroke weight loss. Furthermore, a retrospective analysis was performed on the male C57BL/6J mice (8-15 weeks of age) who had undergone tMCAo (n=41;

30-, 40-, 50-, 60- or 70-minutes) to test if there is a relationship between infarct location and weight loss after stroke.

4.2.2.2 Stroke models

4.2.2.2.1 MCAo model

Mice were randomised to either MCAo or sham surgery (random.org). For the retrospective analyses, each of the mice had been studied as part of a previous study. Therefore, mice were not randomised to the varying occlusions. Mice were subjected to 30-, 40-, 50-, 60-, or 70-minutes tMCAo or permanent MCAo using a silicon-coated monofilament to occlude the origin of MCA as described in Section 2.2.2.1 of Chapter 2. Sham-operated mice were also subjected to the same surgical procedures as described in Section 2.2.2.1 of Chapter 2. It was not possible to blind the surgeons to MCAo and Sham procedures. Also, I was not blinded to the procedure post-surgery as stroke and sham mice can be readily distinguished from each other.

4.2.2.2.2 PT model

Mice were subjected to 15-, 18-, or 20-minutes of light exposure to induce stroke as described in Section 2.2.2.2 of Chapter 2. Sham-operated mice were also subjected to the same surgical procedures as described in Section 2.2.2.2 of Chapter 2.

4.2.2.3 Weight, food and liquid intake monitoring

Weight, food, and water intake were monitored as described in Section 2.2.3 of Chapter 2. Weight loss is presented as a percentage of baseline body weight.

4.2.2.4 Tissue collection

On day 3 (MCAo) or day 7 (PT), mice were euthanised by exposure to a high concentration of CO_2. The brains were collected and histological staining performed by Dr Arun Flynn, Dr Alexandra Riddell, or Dr Adrian Knezic as described in Section 2.2.6 of Chapter 2. Given the subjective nature of infarct quantification, three independent investigators, blinded to the MCAo and PT duration, performed the analyses under my supervision, and the final values were calculated by averaging the measurements across the three investigators (MCAo: myself, Cameron Thomson and Niamh Laing-Doctor; PT: myself, Lucrezia Morganti

and Rania Thompson). Additionally, the TUNEL assay was performed by me in a blinded manner as described in Section 2.2.6.4 on coronal brain sections encompassing the hypothalamic brain region (-0.5 to -2.5 mm relative to Bregma) from mice subjected to 70-minute tMCAo or pMCAo. Lastly, gastrocnemius and tibialis anterior muscles, and fat (mesenteric, gonadal and renal) tissue were collected and weighed as described in Section 2.2.5 of Chapter 2.

4.2.3 Power calculations

G*Power 3.1.9.7 software (Heinrich Heine University, Germany) estimated that n=10 per group was required for the primary endpoint of % weight loss for initial experiments characterising the effect of 40-minute tMCAo or sham surgery on body weight. A two-way ANOVA model was used, with an effect size f=0.50, a significance level (α) of 0.05, and power (1-ß) of 0.80. Consequently, group sizes ≤10 were used for % weight loss, food and water intake, body composition (fat and skeletal muscle), and grip strength. Effect size was estimated using published data of weight loss post-tMCAo (Springer et al., 2014).

4.2.4 Statistical analysis

Statistical analysis was conducted using GraphPad Prism (version 10.4.1, GraphPad Software Inc, San Diego, CA). The Shapiro-Wilk test was used to assess the normality of data; if $P>0.05$, the data were considered normally distributed. Student's t-test was used to compare means of two groups with normally distributed data, while the Mann-Whitney U test was applied for non-normally distributed data. One-way ANOVA was used to assess differences among three or more groups with a single independent variable, whereas two-way ANOVA was used when analysing two independent variables. To determine the relationship between weight loss and infarct volume in MCAo, infarct volumes and % body weight loss from mice exposed to tMCAo or pMCAo were collated and Spearman correlation analysis and simple linear regression were performed. A similar correlation analysis was performed for the PT model. Specific statistical tests and group numbers are detailed in the figure legends. Quantitative data are presented as mean ± SEM, and statistical significance was considered when $P<0.05$.

To explore the relationship between the extent of weight loss and infarct location, brain sections from each mouse were thoroughly examined to identify all regions with infarct. Then, brain regions were ranked according to the number of tMCAo mice exhibiting infarcts within each region. For regions in which infarcts were present in 10 or more mice, a univariate t-test was used to compare the extent of weight loss between mice with infarcts in that region and those without. In addition, a comparative analysis of extremes was conducted between two groups of mice: the ten mice exhibiting the greatest weight loss (top 10) and the ten mice with the least weight loss (bottom 10). For any brain region in which an infarct was present in at least five mice, this region included in the analysis. Then, Fisher's exact test was applied to test if any observed differences in the number of occurrences of an infarct in the brain region between the two groups (top and bottom 10) were related to weight loss or due to chance. To account for the increased risk of Type I error resulting from multiple comparisons, the p-value obtained from Fisher's test and univariate t-test for each brain region was adjusted using the Benjamini-Hochberg procedure to control the False Discovery Rate (FDR).

4.3 Results

4.3.1 Weight loss in pre-clinical studies (systematised search)

The search strategy and databases outlined in Chapter 3 were applied to evaluate how common post-stroke weight loss is in preclinical studies. A total of seventeen articles were identified that reported body weight loss following experimental stroke. These studies employed a variety of stroke models and species, including transient and permanent middle cerebral artery occlusion (MCAo), distal MCAo, photothrombotic stroke (PT), and endothelin-1 (ET-1)-induced stroke in mice and rats. Some studies also utilised modified versions of the MCAo model, such as MCAo with ligation of the internal carotid artery (ICA) and MCAo without ligation of the external carotid artery (ECA). Among the various models described, MCAo was the most frequently used model. Notably, weight loss was observed in all models in both rats and mice, with the highest percentage of weight loss reported following MCAo—reaching up to 33% in mice—and the lowest following ET-1-induced stroke—1 % in rats. In most of these studies, body weight and weight loss were reported primarily as indicators of animal well-being, rather than as scientific endpoints or as part of a research question. Indeed, only four out of the seventeen articles explicitly reported weight loss as an outcome of scientific interest (Table 4-1).

Table 4-1 Summary of stroke models and corresponding weight loss data in pre-clinical studies

study	Species	Model	Duration of Ischaemia	Time points post-stroke	% weight loss	Absolute weight loss	Weight loss studied as an outcome of scientific interest
(Biose et al., 2022)	Rat	tMCAo	90 min	• 24 hr • day 7 post-MCAo	• 24 hr (5.5%) • Day 1 (6%), day 3 (12%), day 7 (14%)	-	No
(Biose et al., 2023)	Mice	tMCAo	60 min	• Day 7	• Day 1 (>10%), day 3 (22%), day 7 (19%)	-	No
(Boyko et al., 2010)	Rat	Original tMCAo & Modified tMCAO (ligation of ICA)	60 min	• Day 28	• Original tMCAo: day (11%), day 7 (5%), day 28 gained (17%) • Modified tMCAo: day 1 (10%), day 7 (5%), day 28 gained (34%)	-	No
(Dettori et al., 2018)	Rat	tMCAo	60 min	• Day 7	• Day 1 (8.5%), day 5 (14.96%), day 7 (10.9%)	Day 1(23.8 g), day 5 (41.9 g), day 7 (30.6 g)	No
(Dong et al., 2020)	Mice	tMCAo & pdMCAo	60 min & permanent	• 24 h	-	tMCAo: 24 hr (3.5 g) pdMCAo: 24 hr (3 g)	No
(Esposito et al., 2013)	Rat	tMCAo	100 min	• 2 weeks	-	Day 14 (29.2 g)	No

study	Species	Model	Duration of Ischaemia	Time points post-stroke	% weight loss	Absolute weight loss	Weight loss studied as an outcome of scientific interest
(Fathali et al., 2013)	Rat	pMCAo	permanent	• Day 3	-	Day 1 (1.5 g), day 2 (0.5g), day 3 (0 g)	No
(Haley et al., 2017)	Mice	tMCAo	20 min	• 24 hr	• Control mice *ob*/-: (8.4%) • Obese mice *ob*/*ob*: (5.5%)	Control (2.9 g), obese mice (2.9 g)	Yes
(Haley et al., 2020)	Mice	tMCAo	Control_low fat diet (30 min), obese_ high-fat diet (20 min)	• 2 months	• Control: day 1 (5.8%), day 3 (14.7%), day 7 (23.5%), day 14 (29.4%), day 49 (17.6%) • Obese: day 1(4%), day 3 (12%), day 7 (26%), day 14 (34%), day 49 (32%)	Control: day 1 (2 g), day 3 (5 g), day 7 (8 g), day 14 (10 g), day 49 (6 g) Obese: day 1 (2 g), day 3 (6 g), day 7 (13 g), day 14 (17 g), day 49 (16 g)	Yes
(Knezic et al., 2022)	Mice	PT	15, 18, 20 min light exposure	• Day 7	• Day 1 (9%), day 3 (8%), day 7 (4%)	-	No
(Knezic et al., 2024)	Mice & Rat	Mice (tMCAo) rat ((ET-1)-induced MCAo)	30 min	• 24 hr (mice) • Day 3 (rat)	• Mice: 24 hr (11.6%) • Rat: day 1 (3.04%), day 3 (1%)	-	No
(Suofu et al., 2023)	Mice	tMCAo	60 min	• Day 14	• Day1 (10%), day 3 (21%), day 7 (33%), day 14 (21%)	-	No

study	Species	Model	Duration of Ischaemia	Time points post-stroke	% weight loss	Absolute weight loss	Weight loss studied as an outcome of scientific interest
(Springer et al., 2014)	Mice	tMCAo	60 min	• Day 7	• Day 1(11.4%), day 3 (21.7%), day 7 (13.9)	-	Yes
(Trotman-Lucas et al., 2017)	Mice	tMCAo & modified tMCAo (without ligation of ECA)	60 min	• 48 hr	• ECA ligated: day 1(11%), day 2 (17.05%) • ECA unligated: day 1 (9%), day 2 (12.19%)	-	No
(Wu et al., 2021)	Mice	tMCAo	50 min	• 24 hr	• 24 hr (19%)	-	No
(Xiao et al., 2021)	Mice	tMCAo	45 min	• 72 hr	• Day 1 (10.08%), day 3 (14.9%)	Day 1 (2.5 g), day 3 (3.7 g)	No
(Yang et al., 2019)	Mice	tMCAo	NR	• Day 7	• Day 1 (11%), day 3 (18%), day 7 (11%)	-	Yes

Abbreviations: ECA, external carotid artery; ET-1, endothelin-1; g, gram; hr, hour; ICA, internal carotid artery; min, minutes; NR, not reported; pdMCAo, permanent distal middle cerebral artery occlusion; pMCAo, permanent middle cerebral artery occlusion; PT, photothrombotic; tMCAo, transient middle cerebral artery occlusion.

4.3.2 Effect of sham and tMCAo surgery on body weight, food and liquid intake.

In total, 3 mice were excluded when: (1) technical complications arose during surgery (e.g., loss of >0.2 ml of blood) (n=2); and (2) there was no visible infarct following thionin staining (n=1). There were no mortalities, and no mouse had to be euthanised prior to the scientific endpoint due to reaching the severity limits of the procedure. The body weights of all mice were recorded prior to surgery, and there were no significant differences between mice randomly assigned to sham-operated or tMCAo groups (Table 4-2). However, body weight loss was observed after surgery in tMCAo and sham mice and persisted until the experimental endpoint on day 3 (Figure 4-1A). Interestingly, Mice subjected to 40-minutes tMCAo exhibited significantly greater weight loss compared with sham-operated controls at all post-surgery time points (mean±SEM; day 1: 9.3±0.5% vs 6±0.6%; day 2: 14.1±1.1% vs 5.6±0.4%; day 3: 15.4±1.6% vs 4.5±0.6%; $p<0.0001$ for all comparisons). The peak of weight loss in mice after tMCAo was on day 3 (-15.4±2%) (Figure 4-1B). Two-way ANOVA analyses revealed a significant effect of surgery and time post-surgery on % weight loss ($F(1, 132) = 114.2$, $p<0.0001$; $F(3, 132) = 78.84$, $p<0.0001$) (Figure 4-1A).

To determine if reduced food and water intake contribute to the significant weight loss in the tMCAo mice, food and water intake were monitored before and daily after surgery for both sham and stroke mice till the experimental endpoint. Prior to surgery, food intake was similar between sham and stroke mice (Figure 4-1C). As depicted in Figure 4-1C, on day 1 following sham or tMCAo surgeries, total food intake was reduced by 38.8±6.6% and 53.6±5.4% in sham and tMCAo mice, respectively, and there was no statistical difference between sham and tMCAo mice ($p>0.05$). Total food intake tended to increase on days 2 and 3 in both groups but importantly there were no statistical differences between tMCAo and sham mice (mean±SEM; day 2: 5.3±0.7 vs 7.3±0.9; day 3: 6.5±0.9 vs 7.6±0.8; $p>0.05$ for all comparisons).

For water intake, tMCAo mice consumed significantly less water on day 1 compared with sham mice (mean±SEM: 0.3±0.3 vs 1.8±0.3; $p<0.01$), whereas on day 2, sham mice consumed significantly less fluid (mean±SEM: 1.8±0.3 vs 0.5±0.2;

p<0.01) (Figure 4-1D). By day 3, tMCAo and sham mice consumed comparable amounts of water (mean±SEM: 0.7±0.5 vs 1±0.1; p>0.05). In addition, the analysis of cumulative water intake over the 3 days period revealed no significant difference between tMCAo and sham mice (mean±SEM: 2.2±0.8 vs 2.3±0.9; p>0.05) (Figure 4-1E). These data demonstrated that changes in food intake were comparable between sham and tMCAo mice, which might indicate that reduced food or water intake is not the primary cause of the significant weight loss in tMCAo mice and that other factors may play a role.

Table 4-2 Pre-surgery body weights (unpaired t-test, p>0.05)

	Sham	MCAO
Body weight (g) Mean±SEM	27.2±0.69 (n=10)	28.35±0.73 (n=10)

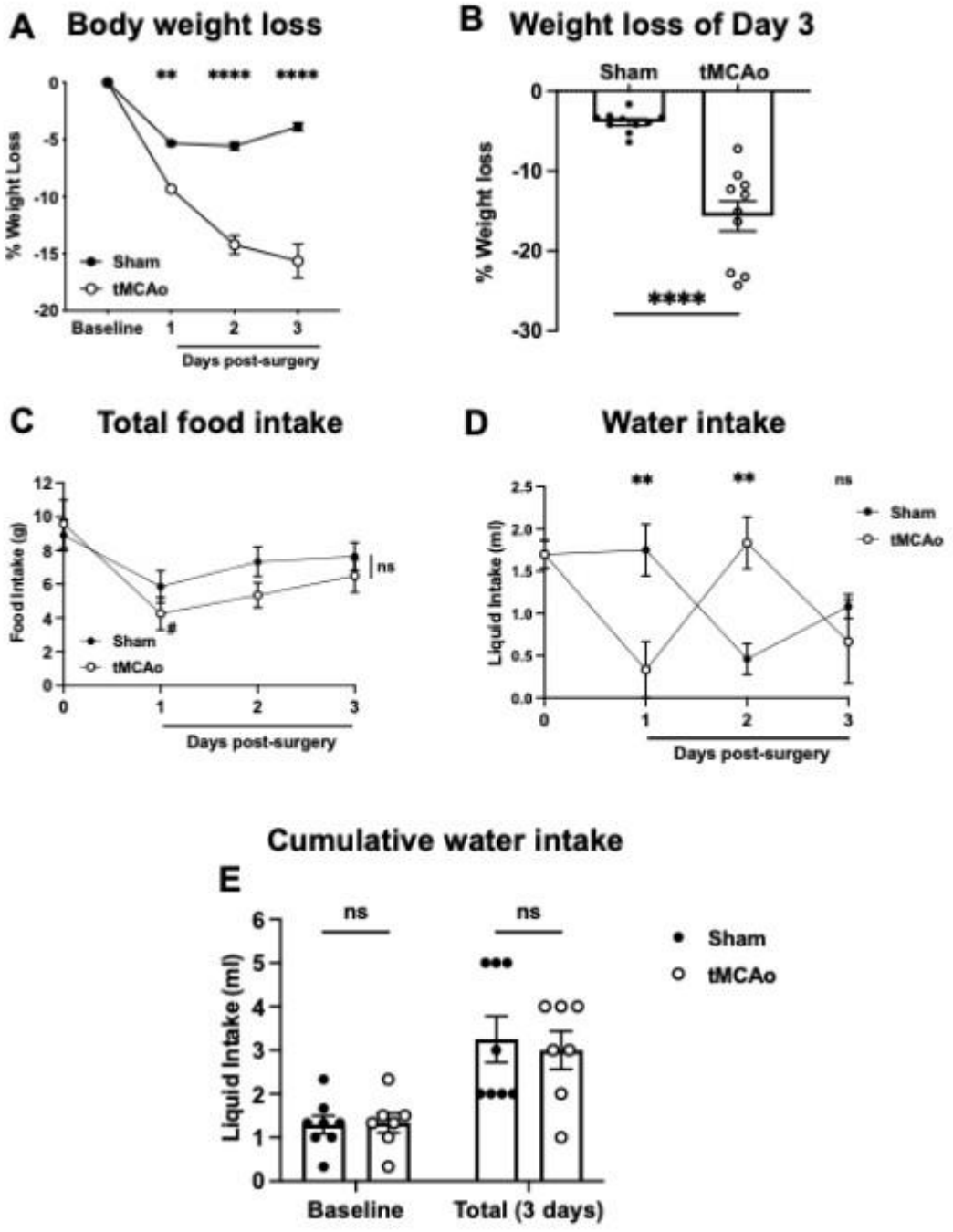

Figure 4-1 Impact of transient middle cerebral artery occlusion (tMCAo) or sham surgery on body weight, food and water intake.
Mice were subjected to tMCAo or sham surgery**;** the experimental endpoint was day 3 post-surgery. Body weights (g) were recorded before surgery (baseline) and daily thereafter until day 3 (**A**), n=10 MCAo; 10 sham. % weight loss on day 3 Body weight loss on day 3 is also expressed as a % of baseline body weights (**B**). Total food (**C**) and water intake (**D & E**) were measured at baseline before surgery for both sham and tMCAo mice and daily thereafter until the experimental endpoint of day 3 (n=7-8). Data is presented as mean ± SEM. **A**, **p<0.01, ****p<0.0001, two-way ANOVA followed by Šídák's multiple comparison test. **B**, ****p<0.0001, unpaired t-test. **C**, #p<0.05 vs baseline, ns= not significant for all time points vs sham, two-way ANOVA followed by Šídák's multiple comparison test. **D&E**, **p<0.01 vs sham, ns= not significant, two-way ANOVA followed by Šídák's multiple comparison test.

4.3.3 Effect of tMCAo or sham surgery on body composition

We observed that post-stroke weight loss resulted from fat and muscle mass loss. Indeed, tMCAo mice had significantly less mesenteric (0.29±0.01 g versus sham 0.38±0.02 g, $p<0.05$) and gonadal white adipose tissue on day 3 after surgery (0.17±0.01 g versus sham 0.25±0.03 g, $p<0.05$), whereas renal adipose tissue was comparable to that of sham mice (0.02±0.002 g versus sham 0.03±0.01 g, $p>0.05$) (Figure 4-2A). Furthermore, the amount of total adipose tissue was 26.8% less in tMCAo mice compared with shams (Figure 4-2B).

Skeletal muscles (gastrocnemius and tibialis anterior) from tMCAo mice weighed significantly less than muscles from sham mice (Figure 4-2C-D). It is also noteworthy that this loss of muscle mass was observed in both the ipsilateral and contralateral legs (stroke-affected side) of tMCAo mice (gastrocnemius sham 0.18±0.01 g vs tMCAo 0.16±0.01 g, $p<0.05$) (Figure 4-2C-D). Muscle strength was assessed by measuring forelimb grip strength in mice before and after sham or tMCAo surgeries. In sham mice, no significant difference in grip strength was observed between pre- and post-surgical assessments (107±1.4 vs 106±1.3 g; $p>0.05$). In contrast, mice in the stroke group showed a significant reduction in grip strength post-surgery compared to their baseline measurements (94±3 vs 110±1.7 g, $p<0.05$), and more importantly, grip strength was lower compared with sham mice after surgery (Figure 4-2E-F).

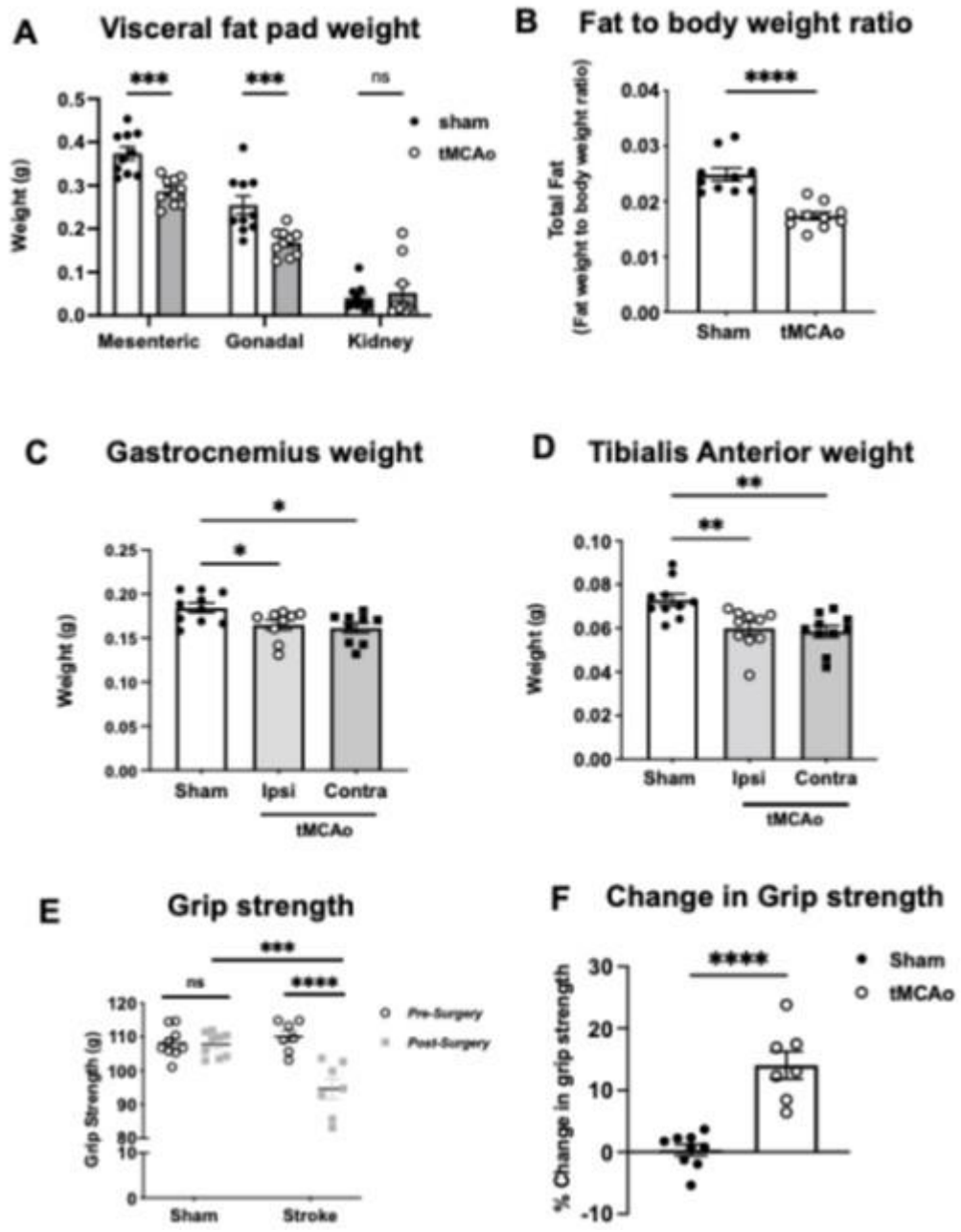

Figure 4-2 Fat and muscle weights, and forelimb grip strength on day 3 after transient middle cerebral artery occlusion (tMCAo) or sham surgery. *Ex vivo* weight of the visceral fat pads (grams, **A**), total fat (fat to body weight ratio, **B**), gastrocnemius muscle (grams, **C**), and tibialis anterior muscle (grams, **D**), grip strength of mice subjected to sham and tMCAo before and after surgery (**E**), and change in grip strength of mice subjected to sham and tMCAo (**F**). Data is presented as mean ± SEM, **A & B**, n=10 tMCAo, n=10 Sham; **C & D**, n=9-10 for both groups; **E & F**, n=7 tMCAo, n=9 Sham. **A**, ***p<0.001, two-way ANOVA followed by Šídák's multiple comparisons test; **B**, ****p<0.001, unpaired student's t-test; **C & D**, *p<0.05, **p<0.01, one-way ANOVA followed by Šídák's multiple comparison test; **E**, ***p<0.001, ****p<0.0001, two-way ANOVA followed by Šídák's multiple comparison test; F, ****p<0.0001 unpaired student's t-test. Ipsi=ipsilateral; Contra= contralateral.

4.3.4 Effect of 70-minutes tMCAo occlusion periods and pMCAo on hypothalamic neuronal apoptosis

The hypothalamus is a region of the brain that is involved in the regulation of energy balance, appetite and homeostasis (Morton, 2007, Kim et al., 2022b). Given the critical role of the hypothalamus in maintaining energy homeostasis and regulating food intake, it is conceivable that ischaemic injury or dysfunction of the hypothalamus contributes to post-stroke weight loss. Therefore, we assessed whether neuronal apoptosis occurred in the hypothalamus of mice that had undergone 70 min of tMCAo or pMCAo. We employed the TUNEL assay to identify apoptotic/necrotic cells within the hypothalamus. Therefore, to determine if there is evidence of apoptosis in the hypothalamus after MCAo, the number of TUNEL-positive apoptotic cells was identified in coronal brain sections from mice that had undergone either pMCAo or the longest transient MCA occlusion period, 70 minutes. As expected, we found TUNEL-positive cells in the infarct core of the ischaemic hemisphere in both pMCAO and tMCAo mice (Figure 4-3). Furthermore, we found evidence of TUNEL-positive apoptotic cells in the hypothalamus from pMCAo mice; however, there was no evidence of hypothalamic neuronal apoptosis in mice that had undergone 70-minute tMCAo (Figure 4-3B&D). Based on the absence of hypothalamic apoptosis at this highest occlusion duration (70 min), we inferred that shorter occlusion periods (30, 40, and 60 minutes) were also unlikely to result in hypothalamic neuronal apoptosis.

A

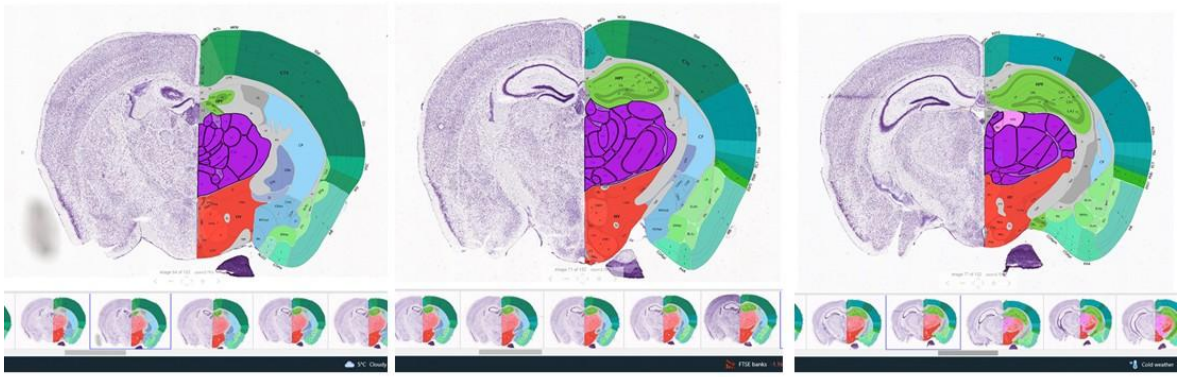

B

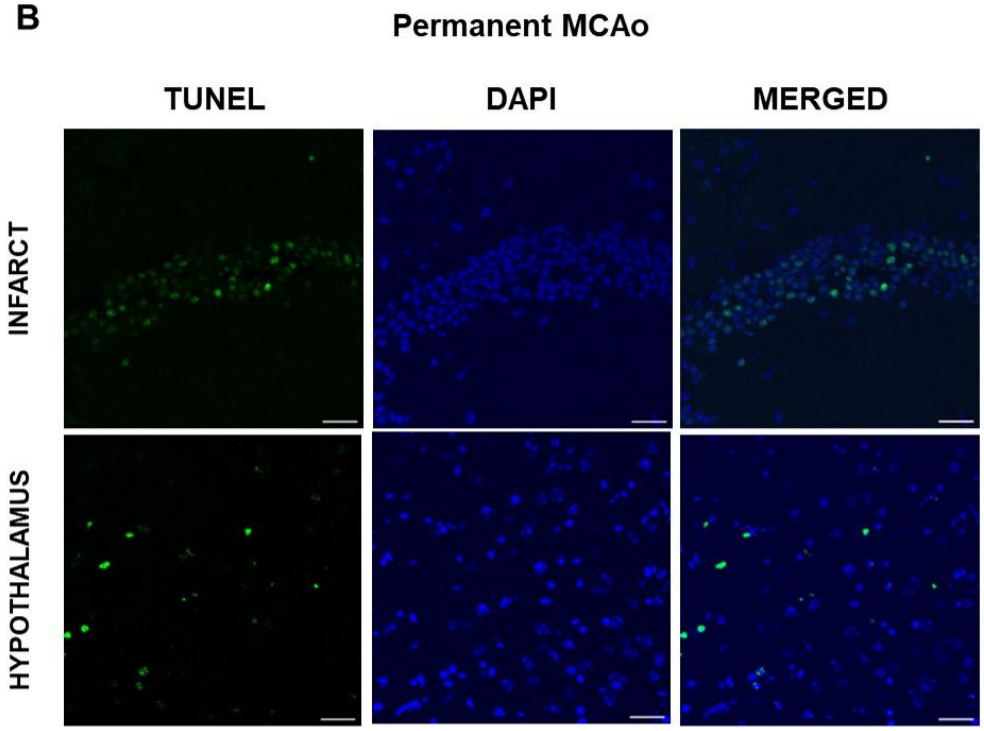
Permanent MCAo
TUNEL
DAPI
MERGED
INFARCT
HYPOTHALAMUS

C

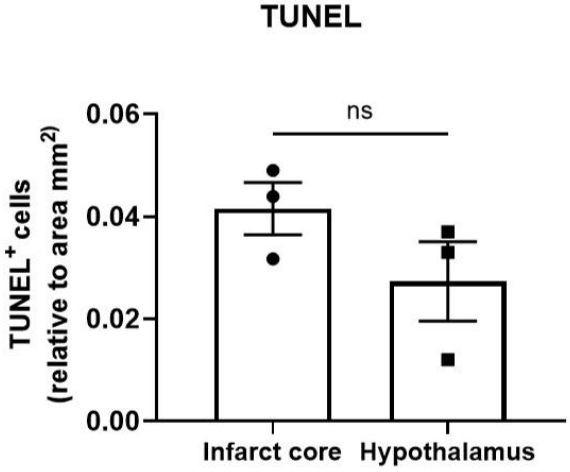
TUNEL
ns
0.06
0.04
0.02
0.00
TUNEL+ cells
(relative to area mm2)
Infarct core
Hypothalamus

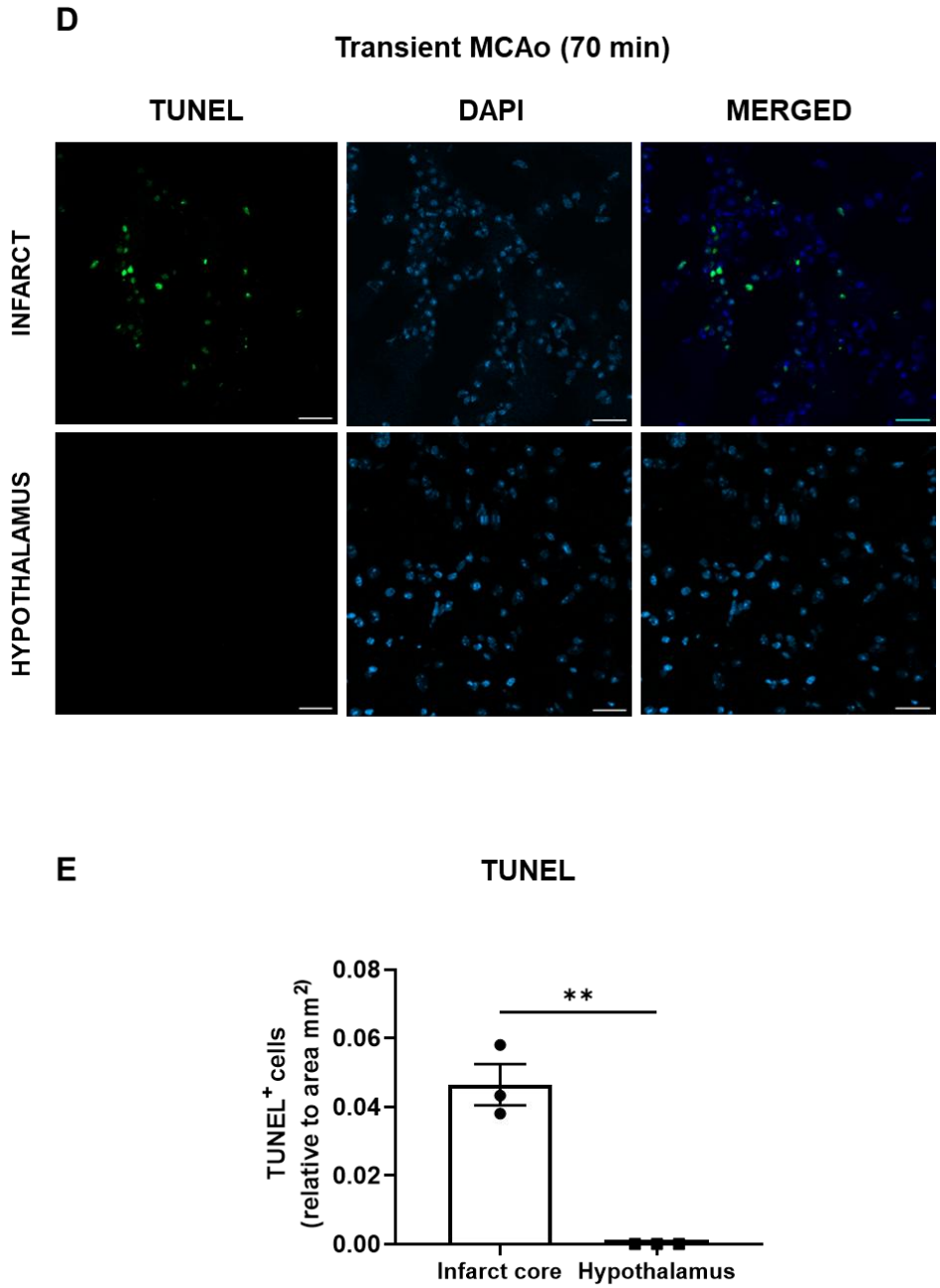

Figure 4-3 Effect of pMCAo and 70-minute tMCAo on apoptotic cell death in the infarct core and hypothalamus. The TUNEL assay was quantified in the brain sections at the level of -0.5 to -2.5 mm relative to Bregma to capture the hypothalamus (red) (**A**)**.** Reference images obtained from Allen brain atlas (available from atlas.brain-map.org). Representative images of the infarct core and hypothalamus of mice following pMCAo (**B**, n=3) or 70-minute tMCAo (**D**, n=3). TUNEL-stained (green) coronal sections were counterstained with DAPI (blue, to stain nuclei). The quantification of TUNEL-positive cells per mm² in the infarct core and the hypothalamus was performed using the cell counter tool on ImageJ software. Scale bars=30 µm. **C&E,** data is presented as mean ± SEM, ***p*<0.01, unpaired student's t-test, ns= not significant.

4.3.5 Effect of MCA occlusion periods on infarct and oedema volumes

As expected, we observed a significant effect of occlusion period on infarct volume, as shown by a One-way ANOVA ($F(5, 41) = 16.94$, $P<0.0001$). We found that mice who underwent pMCAo had the largest infarct with an average volume of 48.6±8 mm^3, which was significantly larger than that observed in the 30-, 40-, 50-, and 60-minute tMCAo groups ($P<0.0001$). Similarly, 70-minute tMCAO resulted in a significantly larger infarct size compared to 30-, 40-, 50-, and 60-minute tMCAo (31±6 mm^3, $P<0.05$). Whereas the smallest infarct size was observed after 30-minutes tMCAo (3.5±0.4 mm^3).

We found that the oedema volume was significantly larger in pMCAo compared to 30-, 40-, 50-, 60-, 70-minute tMCAo. However, no statistical difference was observed in oedema volume between other tMCAo groups ($P>0.05$, Figure 4-4 B).

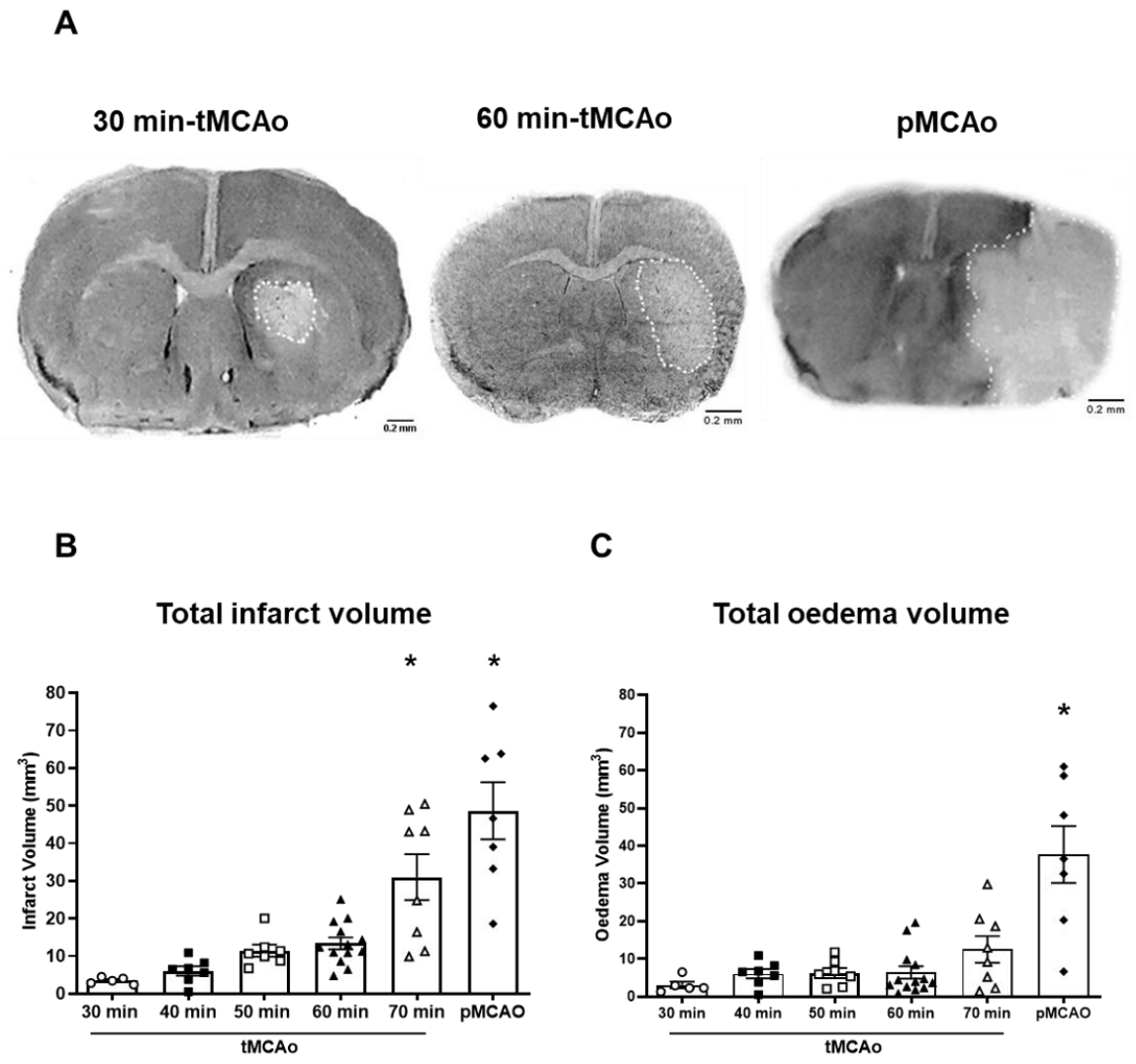

Figure 4-4 Infarct and oedema volumes in mice subjected to various middle cerebral artery occlusion periods (MCAo).
Representative images of mouse coronal brain sections after 30-, 60-min tMCAo and pMCAo **(A).** Mice subjected to different occlusion periods and the total infarct (**B**) and oedema (**C**) volumes were calculated accordingly. Data is presented as mean ± SEM. 30-minutes tMCAO n=5; 40-minutes tMCAO n=7; 50-minutes tMCAO n=7; 60-minutes tMCAO n=13; 70-minutes tMCAO n=8 and pMCAO n=7. *p<0.05 vs other tMCAo periods, one-way ANOVA followed by Šídák's multiple comparison test. Scale bar = 0.2mm

4.3.6 Effect of MCA occlusion periods on body weight loss

To determine if there is a relationship between infarct or oedema volumes and weight loss after stroke, we measured the body weights of mice subjected to sham surgery and different MCA occlusion periods, i.e., 30-, 40-, 50-, 60-, 70-minutes tMCAo and pMCAo. Weight loss was observed after MCAo for all different groups but was not observed in sham-operated mice (Figure 4-5A). The data showed a significant effect of occlusion period on body weight loss after surgery ($F(6,184) = 19.6$, $P<0.0001$, two-way ANOVA). The % body weight loss on day 3 after surgery was significantly higher in 40-, 60-, 70-minute tMCAo and pMCAo compared to sham (sham, 0.1±2; 40-minutes, 9.6±1.5; 60-minutes,13.2±1.6; 70-minutes, 11.2±1.4; pMCAo, 21.2±3.1, $P<0.05$, Figure 4-5A-B). In contrast, the weight loss was not significantly different between the 30- and 50-minute tMCAo groups compared to sham (30 minutes, 3±1.4; 50 minutes, 7.6±1.1; $P>0.05$).

Since the duration of MCA occlusion was found to influence the extent of weight loss as well as infarct and oedema volumes, a correlation was performed using infarct volume and weight loss data for all occlusion periods to ascertain how these variables change with increasing infarct and oedema volumes. As demonstrated in Figure 4-5C, no significant correlation was found between infarct volume and % weight loss on day 1 after MCAo surgery ($r=0.16$, $p=0.29$, Spearman correlation). However, we found a significant moderate positive correlation between % weight loss at day 2 and 3 post-surgery and infarct volume (day 2, $r=0.43$, $p=0.003$ and day 3, $r=0.59$, $P<0.0001$, Spearman correlation, Figure 4-5D-E). Similarly, a significant moderate positive correlation was observed between oedema volume and % weight loss after MCAo at day 3 ($r=0.53$, $P=0.0002$, Spearman correlation, Figure 4-5F).

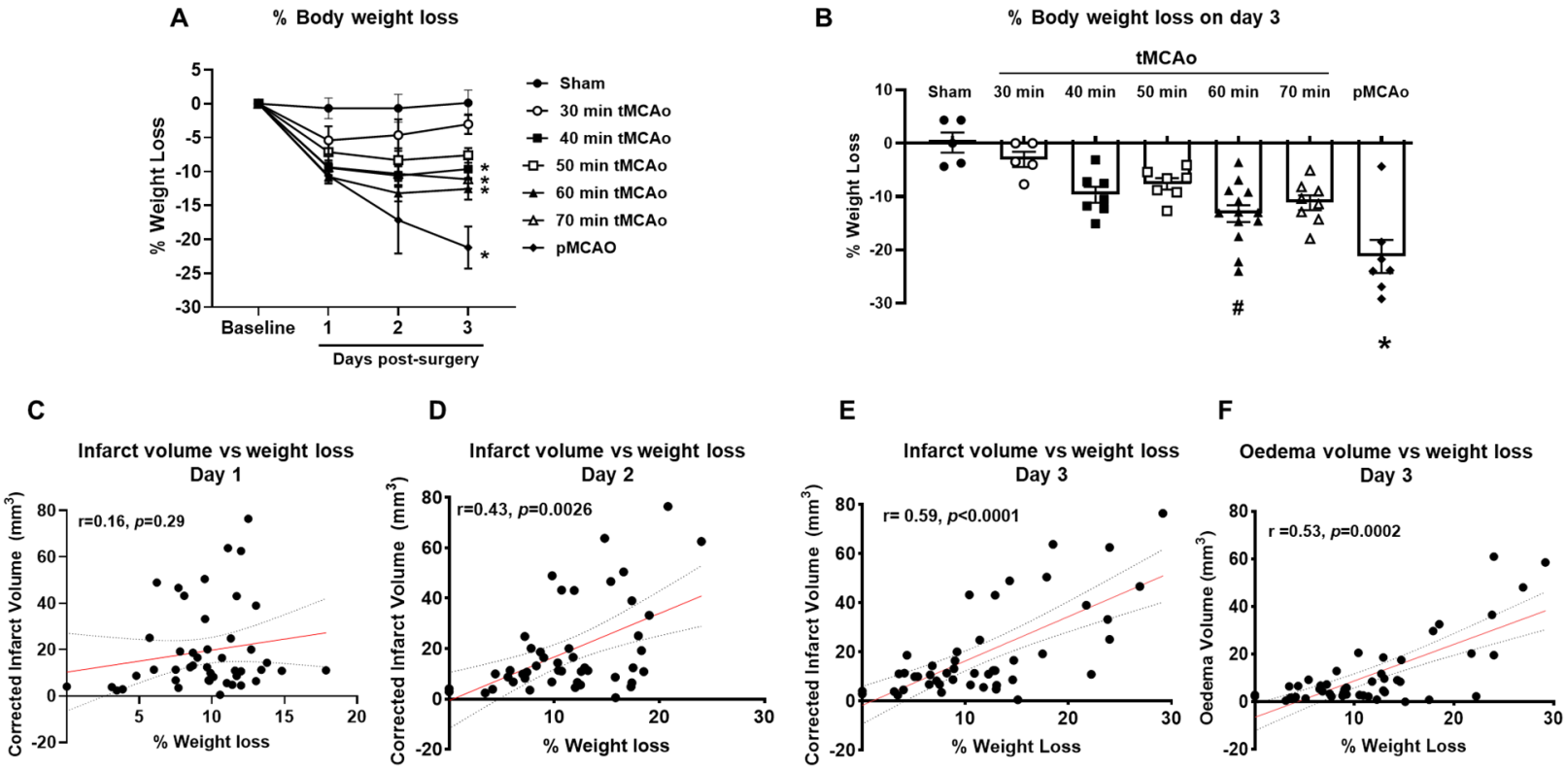

Figure 4-5 The body weight loss of mice after varying degrees of middle cerebral artery occlusion (MCAo) or sham, and the relationship between body weight loss and infarct and oedema volumes.

% weight loss of mice exposed to sham and different occlusion periods 30-, 40-, 50-, 60-, 70-minute tMCAO and pMCAO. % weight loss calculated relative to baseline weights (**A**). % Body weight loss on day 3 after sham and different occlusion periods (**B**). Scatter plots showing the correlation between weight loss and infarct volume on day 1(**C**), day 2 (**D**), and day 3(**E**); and the correlation between weight loss and oedema volume on day 3 (**F**). Data presented as mean ± SEM. Sham, n= 5; 30-minutes tMCAO, n=5; 40-minute tMCAO,n=7; 50-minute tMCAO, n=7; 60-minute tMCAO, n=14; 70-minute tMCAO, n=8 and pMCAO n=7. **A**, *p<0.05 vs sham on all time points, two-way ANOVA followed by Šídák's multiple comparison test. **B**, *p<0.05 vs sham and all tMCAo groups, #p<0.05 vs sham and 30-minute tMCAo, one-way ANOVA followed by Šídák's multiple comparison test. **C-F**, Infarct and oedema volume correlation data, n=47, Spearman correlation with simple linear regression.

4.3.7 Effect of photothrombotic stroke on body weight

Having found a significant positive correlation between infarct volume and the extent of body weight loss after MCAo, we next examined if this relationship exists in a second model of stroke (PT). This model induces a well-defined infarct in the cortical brain region through thrombus formation. The mice included in this study were part of a published work by Knezic and colleagues (2022). Inclusion criteria for that study were that mice had to survive to the experimental endpoint of day 7 post-surgery and there had to be a measurable infarct. In total, 9 mice were excluded as they did not reach these criteria or had to be culled prior to the endpoint due to animal welfare.

As demonstrated in Figure 4-6A, acute weight loss was observed in both sham-operated and PT mice after surgery. Notably, the % weight loss in shams was significantly lower than that observed in stroke mice on day 1, 3, and 7 post-stroke ($p<0.001$). The peak of weight loss was on day 3 post-surgery, with sham mice exhibiting an average weight reduction of 2.2±0.9%, whereas stroke mice exposed to 15, 18, and 20 minutes of light exposure experienced significantly greater weight loss, averaging 7.6±0.8%, 7.8±0.2%, and 9.7±0.9%, respectively. Notably, stroke mice exhibited partial weight recovery between days 3 and 7, whereas sham-operated animals fully restored body weight over the same period (Figure 4-6A).

Then, the relationship between the infarct size and % weight loss in mice subjected to the PT was examined. As observed in the MCAo model, the data from the PT model showed the presence of a significant positive moderate correlation between final infarct size and % weight loss on day 1 and day 3 (day 1, $r=0.51$, $p=0.01$; day 3, $r=0.5$, $p=0.01$, Figure 4-6B-C). However, no correlation was found on day 7 post-surgery ($r=0.09$, $p=0.7$, Figure 4-6D).

Table 4-3 Baseline body weight ($p>0.05$, one-way ANOVA)

Body weight (g)	sham	15 min (PT)	18 min (PT)	20 min (PT)
mean±SEM	26±0.43	28±1.3	26±0.6	26±1

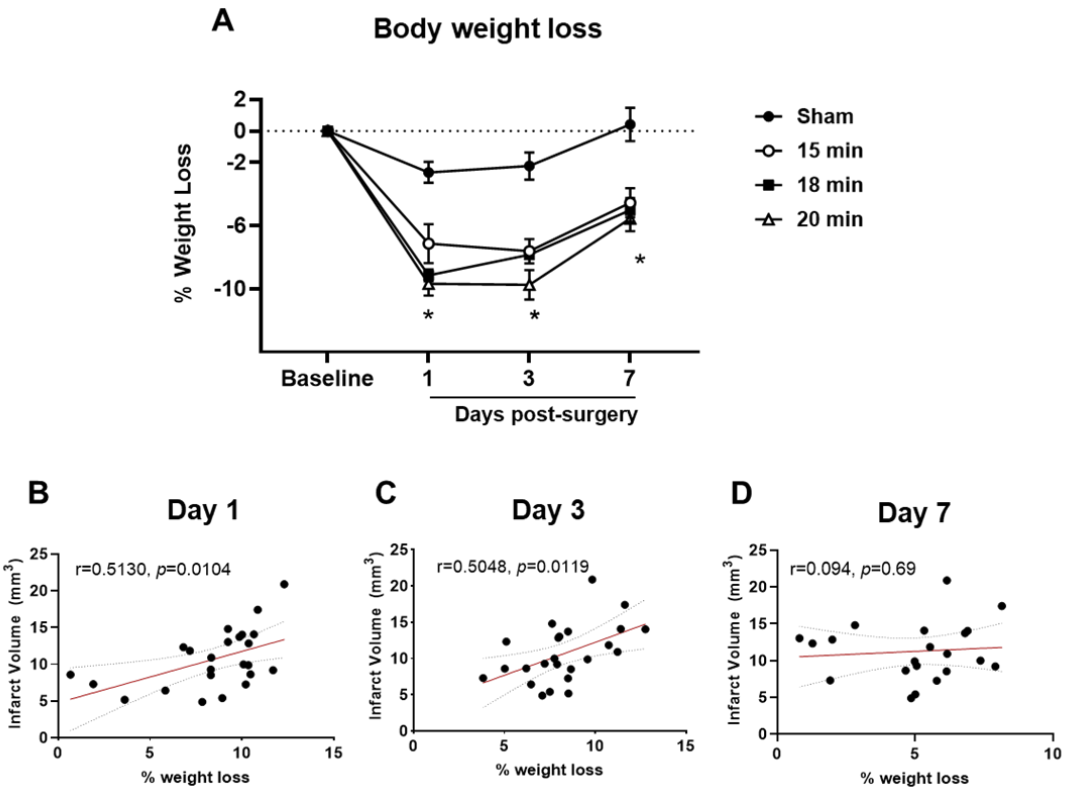

Figure 4-6 Body weight loss of mice after photothrombotic stroke (PT) or sham surgery and the relationship between body weight loss and infarct volumes. % weight loss of mice exposed to 15-, 18-, and 20-minutes of light exposure. % weight loss calculated relative to baseline weights on days 1, 3, and 7 post-surgery (sham, n=9; 15-min, n=10; 18-min, n=7; 20-min, n=7). (**A**) *p<0.05 vs sham for all groups, two-way ANOVA followed by Šídák's multiple comparisons test. Spearman correlation analysis and simple linear regression of infarct volume and weight loss on day 1 (**B**, n=24), day 3 (**C**, n=24), and day 7 (**D**, n=21).

4.3.8 The effect of the cortical and subcortical infarct on the extent of weight loss after stroke

The PT model produces infarcts in the cortical brain regions, and the tMCAo model primarily produces subcortical infarcts but when the tMCAo period is longer, infarcts also develop in the cortex. Therefore, given that we observe a positive but moderate correlation between infarct size and weight loss in both models, this suggests that infarct size, rather than location, is an important determinant of weight loss. To further verify this, we compared the weight loss between these two models. It is noteworthy that the MCA supplies a substantial portion of the cerebral cortex, including parts of the frontal, temporal, and parietal lobes, and the extent of ischemic damage following MCA occlusion is highly dependent on the duration of the occlusion (Margetis and Sánchez-Manso, 2025). Specifically, prolonged occlusion tends to result in both cortical and subcortical infarction, whereas shorter occlusion periods predominantly affect the subcortical regions. To ensure a valid comparison with the PT model, we selected tMCAo mice in which the infarct was restricted to subcortical areas, and those with infarct volumes comparable to those produced by the PT model. This approach enabled us to assess the influence of infarct localisation (cortical vs. subcortical) on post-stroke weight loss independent of infarct size. Furthermore, to control for potential confounding effects of surgical intervention and anaesthesia, for each model, the weights of stroke mice were normalised by subtracting the weights of sham-operated mice. Since the peak of weight loss in both models was on day 3, and the infarct is fully developed by day 3 (Liu et al., 2009a), we choose this time point. As demonstrated in Figure 4-7, the infarct size was comparable between mice subjected to PT or MCAo ($p=0.34$). The mean infarct size in PT and tMCAo mice was 10.69±0.81 and 9.49±0.92 mm^3, respectively. However, this study found no significant difference in % weight loss in mice with a stroke induced by PT or tMCAo ($p=0.85$). The mean weight loss in PT and tMCAo was 6.12±0.45% and 6.17±1.25%, respectively.

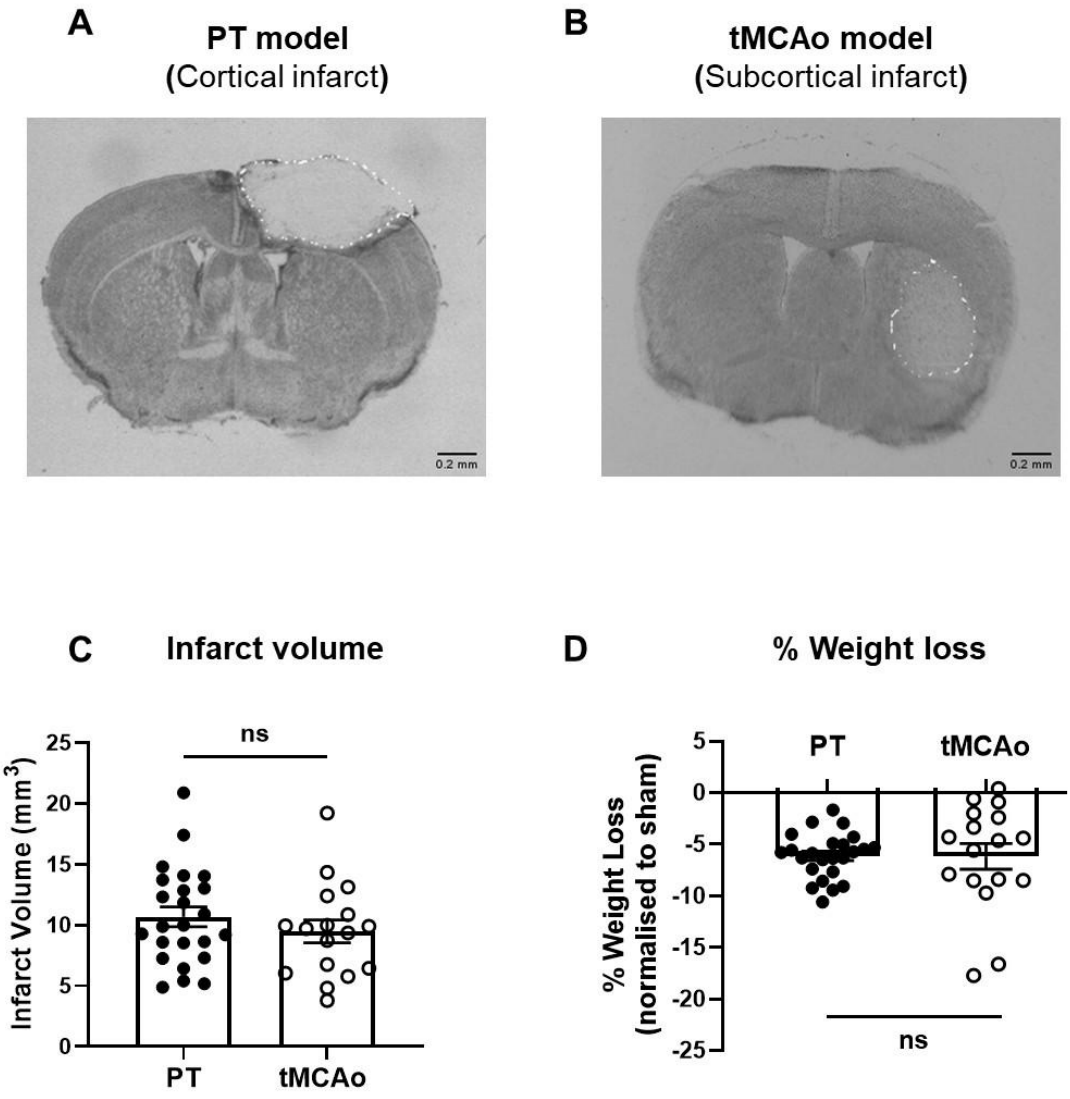

Figure 4-7 The infarct volume and weight loss in PT and MCAo models. Representative images of PT model with infarct only in cerebral cortex (**A**) and tMCAo model with a sub-cortical infarct (**B**). Total infarct volume in mice subjected to PT and tMCAo (**C**). The % weight loss in mice induced by PT and tMCAo (**D**). Data presented as mean ± SEM, PT (n=24) tMCAo (n=17). unpaired t-test, ns=not significant. Scale bar = 0.2mm.

4.3.9 The relationship between infarct location and the extent of weight loss after stroke

To further investigate whether a particular infarcted brain region influences the extent of post-stroke weight loss, all brain sections for each tMCAo mouse were checked to identify the regions that had an infarct. Only regions that had an infarct in at least 10 mice were included in the analyses. A total of 13 regions were found to contain an infarct in 10 or more mice. Then each region from those was tested individually by comparing the weight loss of mice with an infarct in that region to those without. After correction for multiple comparisons, none of the examined regions showed a statistically significant difference in weight loss between these two groups of mice (Table 4-4).

A comparative extremes analysis was also performed to further assess the effect of brain regions on weight loss. We included the top 10 mice that had the greatest weight loss and the bottom 10 mice that had the lowest weight loss. Regions that had an infarct in at least 5 mice were included in the analysis. For each region, we recorded the number of mice from the top or bottom group with an infarct in that region versus those without. Fisher's exact test was used to test for differences between groups. After p-value correction, no significant difference was observed, indicating that no significant association between the infarcted regions and weight loss (Table 4-5).

Table 4-4 Univariate analysis of the differences in weight loss between mice with and without infarcts in the most common infarcted brain areas (statistical test: two-tailed t-test and Mann-Whitney U tests, the p-values were adjusted for multiple comparisons using the Benjamini-Hochberg false discovery rate (FDR) correction)

Brain region	N of mice with an infarcted brain region	Adjusted p-value
Nucleus Accumbens	36	0.15
Globus Pallidus	31	0.26
Endopiriform nucleus	31	0.09
Claustrum	25	0.17
Piriform area	25	0.17
Agranular insular area	20	0.09
Substantia Innominata	19	0.19
primary somatosensory area	18	0.10
Olfactory tubercle	15	0.12
Striatum-like amygdalar nuclei	14	0.51
Fundus of striatum	13	0.28
Gustatory area	11	0.07
Visceral area	10	0.08

Table 4-5 Fisher's exact tests of the differences in weight loss considering locations affected by infarct in mice with greatest and least weight loss (extreme analysis). Statistical analysis: Fisher's exact tests were performed, the p-values were adjusted for multiple comparisons using the Benjamini-Hochberg false discovery rate (FDR) correction

Brain region	N of mice with an infarcted brain region	Adjusted p-value
Nucleus Accumbens	12	0.15
Globus Pallidus	10	>0.9999
Fundus of striatum	10	>0.9999
Endopiriform nucleus	9	0.21
primary somatosensory area	9	>0.9999
Substantia Innominata	8	>0.9999
Claustrum	7	0.52
Piriform area	7	0.26
Olfactory tubercle	6	>0.9999

4.4 Discussion

This study firstly performed a systematised literature review to investigate how widely post-stroke weight loss is reported in preclinical research. Our findings revealed that weight loss is frequently reported following experimental stroke across various animal models and species. A second objective was to explore the relationship between infarct size and location, and weight loss, to provide insight into how these factors influence post-stroke weight loss. Using tMCAo and PT models in mice, we observed that mice who had undergone stroke induction exhibited significantly greater body weight loss compared to sham-operated controls. Importantly, reduced food or water intake did not appear to be the primary contributor to this weight loss. We further tested the hypothesis that infarct size and location influence the extent of weight loss. Our data demonstrated a significant, moderate, positive correlation between infarct volume and weight loss, indicating that larger infarcts are associated with greater weight reduction. However, in our exploratory analyses, no association was found between infarct location and weight loss, suggesting that lesion size, rather than its anatomical position, is a determinant of the extent of post-stroke weight loss.

In the previous chapter, we examined the prevalence of post-stroke weight loss in clinical stroke. In the current chapter, we sought to determine whether this post-stroke complication is widely documented and studied in preclinical research. To address this, we conducted a systematised review of the literature and identified 17 experimental studies that reported body weight loss following stroke in animals. Weight loss reached concerning levels in some studies—with mice losing up to 33% of their body weight (Suofu et al., 2023). Furthermore, a study reported that animals experiencing significant body weight loss during the acute post-stroke period exhibit increased mortality rates (Verma et al., 2016). Indeed, in most cases, weight loss was reported solely as part of routine animal welfare monitoring, rather than being examined as a primary or secondary outcome to investigate its underlying causes or implications. In addition, it is widely accepted that some surgical approaches to induce MCAo, such as the ECA-ligation model, contribute to the body weight loss observed in experimental animals after MCAo (Dittmar et al., 2003). Studies have shown that ligation of ECA affects the blood supply to its downstream territory, causing impairment in the swallowing and masticatory muscles. This thereby reduces food intake and leads to increased

weight loss in experimental animals (Dittmar et al., 2003). However, modified MCAo approaches that avoid ECA ligation, such as CCA repair or CCA ligation models, in which the filament is introduced via the CCA and the vessel is subsequently either repaired or ligated following reperfusion, do not consistently result in improved weight loss. For instance, Trueman and colleagues (2011) compared three surgical approaches and reported that animals subjected to ECA ligation exhibited the greatest weight loss, whereas those undergoing reperfusion via the CCA-based approach produced the least weight loss over a 90-day period after MCAo surgery (Trueman et al., 2011b). In contrast, Trotman-Lucas and colleagues (2017) compared the loss in body weight between the ECA-ligation technique and ECA-unligation (either CCA-ligation or CCA-repair) model. Their results revealed a trend towards reduced weight loss in the ECA-intact model within the first 2 days after MCAo, although the difference between the two groups did not reach statistical significance (Trotman-Lucas et al., 2017). Similarly, a more recent study indicates that the CCA-repair approach does not confer a significant advantage over the traditional ECA-ligation model in terms of weight loss, failing to ameliorate the loss in body weight associated with ECA ligation (Hu et al., 2023). Furthermore, an alternative surgical approach targeting the ICA has also been explored. Boyko and colleagues (2010) reported that while ICA-based occlusion produced comparable weight loss to the ECA-ligation model during the acute phase (days1-7) after MCAo, it resulted in reduced weight loss at later time points (day 28) after surgery (Boyko et al., 2010). Collectively, these findings suggest that although ECA ligation may contribute to post-stroke weight loss through impaired feeding behaviour, avoidance of ECA disruption does not eliminate this effect.

Next, we aimed to characterise the effect of tMCAo on body weight and composition, and food and water intake. In alignment with previous findings (Springer et al., 2014a, Haley et al., 2020c), we observed a significant reduction in body weight following MCAo (15.4%), whereas sham-operated animals exhibited significantly less weight loss (4.5%). Given that the sham mice underwent the same surgical procedures and length of exposure to anaesthesia, this indicates that the excess (i.e. above what the sham lost) weight loss is related to the stroke and not due to exposure to anaesthesia or pain arising from the incisions or surgical stress. Notably, this weight loss was associated with marked alterations in body

composition, characterised by bilateral skeletal muscle atrophy affecting both the ipsilateral and contralateral limbs, as well as a significant depletion of visceral fat stores. As discussed in Chapter 3, muscle wasting is often attributed to disuse of the paretic limb following stroke (English et al., 2010), together with published findings (Springer et al., 2014), our data challenge this assumption and reveal a more widespread pattern of atrophy. Specifically, both the paretic and non-paretic limbs exhibited muscle atrophy and reduced grip strength during the acute phase after stroke induction, suggesting a systemic response rather than localised disuse alone. Reduced food or water intake is common in rodents following surgical procedures resulting in body weight loss. Indeed, a decline in food intake was observed in both sham and stroke groups on day 1 post-surgery. However, food consumption progressively increased over the subsequent days in both sham and tMCAo mice, and importantly, no significant differences in food intake were detected between the groups. Despite this, stroke animals continued to lose significantly more weight, with the most pronounced reduction occurring on day 3 post-stroke.

Additionally, water intake was monitored in this study. It is noteworthy that the distribution of water intake appeared bimodal, suggesting the potential presence of two distinct subpopulations of mice. As this was observed in both sham and stroke mouse groups, this may suggest that this pattern is not solely attributable to stroke effects. Instead, it likely reflects inter-individual variability in drinking water behaviour, as well as the potential influences from housing conditions, circadian factors, or measurement variability. Notably, accurately quantifying water intake using standard cage bottles was challenging. The use of metabolic cages would have provided more accurate measurements; however, this method was considered inappropriate for stroke mice due to ethical considerations.

An important methodological issue in the MCAo model is the ligation of the external carotid artery (ECA), which has been proposed to contribute to post-surgical feeding difficulties and, consequently, weight loss in rats (Trueman et al., 2011a). For example, Trotman and colleagues (2017) found that mice subjected to tMCAo with ECA ligation exhibited a 17.5% loss in body weight, compared with a 12.9% loss in mice that underwent the procedure without ECA ligation. In our study, to control for this potential confounder, sham-operated mice underwent the same ECA ligation procedure. However, sham mice displayed minimal weight

loss compared with tMCAo mice, suggesting that ECA ligation alone does not account for the observed weight reduction in MCAo. Furthermore, as discussed above although food intake was reduced on day 1 in sham and tMCAo mice, food intake progressively increased thereafter. Notably, dysphagia is reported to affect stroke patients, resulting from weakness or paralysis of the muscles involved in swallowing, which in turn may contribute to post-stroke weight loss (González-Fernández et al., 2013). However, as discussed in Chapter 3, significant weight loss was also reported in stroke patients without dysphagia (Scherbakov et al., 2019b). Taken together, our findings demonstrate that global tissue wasting occurs after ischaemic stroke, as evidenced by the loss of fat and skeletal muscle on both the stroke-affected and non-affected side. This widespread atrophy cannot be solely explained by the obvious factors alone, such as a reduction in the liquid and food intake. To better understand the underlying contributors to this global tissue wasting, we next examined whether post-stroke weight loss was associated with the severity or location of the infarct.

The hypothalamus plays a central role in regulating feeding behaviour, metabolism, and energy expenditure (Tran et al., 2022). Within the hypothalamus, the arcuate nucleus (ARC) contains two key populations of neurons that exert opposing effects on energy homeostasis: pro-opiomelanocortin (POMC) neurons, which are anorexigenic, and neuropeptide Y (NPY)/agouti-related peptide (AgRP) neurons, which are orexigenic (Cansell et al., 2012). Activation of POMC neurons promotes satiety and enhances energy expenditure, whereas activation of NPY/AgRP neurons stimulates appetite and reduces energy expenditure (Dougherty, 2020). A key hormonal regulator of this system is leptin, which is secreted by adipose tissue and is released into the bloodstream to act on leptin receptors in the hypothalamus, particularly in the ARC (Klok et al., 2007). Through binding to these receptors, leptin conveys information about the body's energy status and modulates the activity of multiple hypothalamic neurons (Morris and Rui, 2009). Specifically, leptin inhibits the activity of orexigenic peptides such as NPY and AgRP, and stimulates anorexigenic pathways, including POMC neurons (Morris and Rui, 2009). Additionally, other neuropeptides like melanin-concentrating hormone and ghrelin—the latter produced by the stomach—modulate appetite by acting on receptors in the ARC, contributing to regulating food intake and body weight (Klok et al., 2007). Given the hypothalamus's central

role in energy balance, it is plausible that ischaemic injury to this region may contribute to the weight loss observed in mice after stroke. To investigate this possibility, we employed the TUNEL assay to detect apoptotic cell death in the hypothalamus. While apoptosis was observed following pMCAo, no evidence of hypothalamic apoptosis was found in the tMCAo model. However, it is crucial to also consider the extensive connectivity of hypothalamic neurons. The hypothalamus sends and receives projections to and from several brain regions involved in neuroendocrine regulation and metabolic control, including the pituitary gland, cerebral cortex, hippocampus, amygdala, thalamus, and brainstem (Bear et al., 2022, Tran et al., 2022, Dougherty, 2020). Therefore, damage to any of these interconnected areas by ischaemia could indirectly impair hypothalamic function, potentially contributing to post-stroke metabolic disturbances and weight loss. As such, even in the absence of overt hypothalamic apoptosis, the functional integrity of the hypothalamic network may still be compromised, and its role in post-stroke weight loss cannot be ruled out; more studies are needed to investigate this.

The intraluminal MCAo technique is a well-established experimental stroke model that allows for easy adjustment of arterial occlusion duration by retracting the monofilament (Shahjouei et al., 2016). This flexibility allows the study of both reperfused and non-reperfused cerebral ischaemic insults. To investigate the impact of stroke severity on the extent of weight loss following stroke, the varying levels of cerebral ischaemia were examined. This approach allowed for direct comparison of stroke severity and its effects on weight loss. The major new finding of this study was that the extent of weight loss is significantly positively correlated with infarct and oedema volumes. The correlation was significant on days 2 and 3 post-stroke but was moderate suggesting other factors in addition to infarct size contribute to the weight loss. Notably, however, no such correlation was observed on day 1. The reasons why there is no correlation at day 1 are unclear but it might be that the weight loss is driven primarily by reduced food intake, however, as mentioned above tMCAo mice experienced a similar decrease in food intake to sham mice. In rodents, the vast majority (~70-80%) of the infarct development occurs during the first day (Lansberg et al., 2001, O'Collins et al., 2017, Liu et al., 2009a). Therefore, other factors independent of those triggered by the brain injury appear to contribute to early post-stroke weight loss in mice. To further

validate these findings, we analysed data from an additional stroke model, the PT stroke model. Similar to the tMCAo model, mice subjected to PT-induced stroke exhibited weight loss, whereas sham-operated mice demonstrated only minimal weight reduction. Also, we found that infarct volume in the PT model was significantly but moderately correlated with weight loss on day 1 and 3 post-stroke, whereas no significant correlation was detected between infarct size and weight loss on day 7 post-stroke. Collectively, these findings suggest that systemic factors triggered by the initial ischaemic injury may play an important role in post-stroke weight loss. However, given the correlation was moderate in both models indicates that factors secondary to the initial injury also contribute.

To investigate whether infarct localisation influences the extent of post-stroke weight loss, we utilised two distinct stroke models: the PT model, which primarily induces cortical infarcts, and the tMCAo model, which typically results in subcortical infarction with short occlusion periods. To ensure that infarction in the MCAo group was restricted to the subcortical region, only animals with subcortical infarcts comparable in size to those induced by the PT model were included. This approach allowed us to assess the effect of the infarct location without the influence of the stroke size or severity. Additionally, to control for the potential confounding effects of surgical intervention and anaesthesia, weight loss data from both stroke models were adjusted by subtracting the corresponding weights of sham-operated controls. Since the peak of weight loss in both models occurred on day 3 post-stroke — a time point that coincides with the infarct being fully developed (Li et al., 2014a)— this time point was selected for analysis. Our data showed no significant difference in weight loss between the two models. After accounting for the effects of surgery and anaesthesia, weight loss was comparable, suggesting that the location of the infarct does not significantly impact the extent of post-stroke weight loss under the conditions tested. In addition to comparing overall infarct localisation across stroke models, we further examined whether ischemia in specific brain regions was associated with post-stroke weight loss. Two analytical approaches were employed. First, we independently assessed the most frequently affected brain regions—defined as those infarcted in at least 10 animals—to determine whether their involvement was linked to greater weight loss. Second, we conducted an extreme-group comparison, identifying the brain regions most commonly affected in animals with

the greatest weight loss and comparing them to those with the least weight loss. In both analyses, no statistically significant association was found between infarction in specific regions and the extent of weight loss. These findings further support the conclusion that infarct location, whether broadly or regionally defined, does not appear to be a primary determinant of post-stroke weight loss.

This study however has some limitations: first, it used only male mice, which limits the ability to assess potential sex-specific differences. Second, the PT model differs from the MCAo model in the method of stroke induction, and narrow light exposure periods were used. Third, measuring water intake was challenging without using metabolic cages. In addition, the correlation analyses between infarct size and weight loss were conducted at different time points, with brains collected on days 3 and 7 for the MCAo and PT models, respectively. Future studies could address this limitation by using a more robust approach, such as magnetic resonance imaging (MRI), to assess the correlation over time.

In conclusion, our findings demonstrate that although post-stroke weight loss is consistently reported in various stroke models and species, it remains an underappreciated outcome in preclinical research. Our data provide clear evidence of global systemic tissue wasting following stroke, characterised by significant losses in both skeletal muscle and adipose tissue. Importantly, this wasting was found to be positively correlated with infarct volume, while infarct location was not. Furthermore, commonly considered confounding factors—such as reduced food or liquid intake, anaesthesia, or surgical procedures—were insufficient to fully account for the extent of this global catabolic response, suggesting the involvement of systemic mechanisms triggered by the ischaemic brain injury. However, the systemic metabolic pathways mediating this response remain unclear. Given that stroke is known to induce widespread weight loss, further investigation is required to elucidate this process. Therefore, the following chapter aims to examine the metabolic response to ischaemic stroke using untargeted metabolomics in order to identify potential pathways underlying post-stroke weight loss.

Chapter 5 Effect of ischaemic stroke on the metabolic response in aged and young mice

5.1 Introduction

Metabolomics is a subdivision of the omics field that integrates high-throughput analytical methods with bioinformatics analysis. It involves qualitative and quantitative analysis of metabolites, which function as key intermediates and final products of metabolic processes, reflecting the organism's phenotypes at a particular moment (Zhang et al., 2014). In addition, metabolites are generally small molecules (molecular weight<1500 Da) and display heterogeneity in terms of chemistry as well as physical properties such as solubility, polarity and volatility. Metabolomics can provide a snapshot of cellular physiological status, revealing how the metabolic profile of an organism's complex biological system changes when it is under stress conditions such as environmental alterations, adverse conditions or diseases. Therefore, metabolomics analysis enables the differentiation between normal, abnormal, or pathological pathways, thereby aiding in disease diagnosis, prognosis prediction, and offering insights into the underlying pathophysiological mechanisms, which improves understanding of the pathological process (Zhang et al., 2015). Metabolomics methods have been extensively utilised to study neurological, cancer, metabolic, and cardiovascular diseases, resulting in a significant improvement in the identification of biomarkers associated with these conditions. For example, it has been suggested that obesity-associated insulin resistance is strongly linked to elevated concentrations of branched-chain amino acids (BCAAs), namely valine, leucine and isoleucine (Newgard et al., 2009). Additionally, by using a metabolomics approach in Alzheimer's disease (AD), Researchers identified a set of approximately ten lipids that contribute to AD pathophysiology and can predict progression to mild cognitive impairment or AD in cognitively normal older individuals within a period of 2-3 years with accuracy exceeding 90% (Mapstone et al., 2014). This highlights the importance of this approach in a clinical setting.

Profiling of the metabolome is typically performed using analytical platforms such as mass spectrometry (MS) or nuclear magnetic resonance (NMR) spectroscopy. In MS, metabolites are separated based on their mass-to-charge ratio, while in NMR, separation is achieved by the metabolites' magnetic resonance shift. NMR is characterised by requiring minimal sample preparation, being reproducible, and not being destructive to the sample, but it has low sensitivity (i.e., it cannot detect low-abundance metabolites). On the other hand, MS is known as a highly

sensitive technique; however, it is also a challenging method to quantify, destructive to the sample, and time-consuming (Sussulini, 2017). In MS, the sample is subjected to ionisation at the MS source, and the resulting ionised molecules are then directed to the mass analyser, where they are separated based on their mass-to-charge ratio (m/z). This produces a mass spectrum displaying the relative intensity of detected ions versus their m/z. However, in the MS, a previous separation step is required to reduce ionisation suppression effects and minimise sample complexity to enhance sensitivity. Separation methods coupled to MS, include high-performance liquid chromatography (HPLC) or ultra-performance liquid chromatography (UPLC), gas chromatography (GC) and capillary electrophoresis coupled to mass spectrometry (CE-MS). Notably, due to the diversity of chemical metabolites, a combination of analytical platforms is typically used to cover the entire metabolome (Sussulini, 2017). The approach selected for metabolomics analysis can be targeted or untargeted. Untargeted metabolomics is used to identify as many metabolites as possible in the extracted sample, whereas targeted analysis aims to detect specific molecules or a class of metabolites. It is noteworthy that the degree of confidence in metabolite identification differs across analytical techniques, ranging from identities confirmed using authentic reference standards to putative annotations suggested based on database m/z matching, and in some cases, to signals that remain classified as unknown (Sussulini, 2017).

As discussed in Chapter 1 of this thesis, it is proposed that stroke has a catabolic effect on metabolism as well as having a negative effect on anabolism. Consistent with published literature (Yang et al., 2019, Springer et al., 2014a, Haley et al., 2020b), we showed in the previous chapter that mice who had undergone transient middle cerebral artery occlusion (tMCAo) experience significantly more body weight loss compared with control mice despite food and water intake being comparable. Furthermore, this profound weight loss encompasses a loss of both fat and muscle, consistent with a global catabolic effect of stroke with global tissue wasting. The mechanisms responsible for weight loss after stroke are not fully understood; however, understanding the effects of ischaemic stroke on metabolism could be a step towards addressing this knowledge gap. Many studies focused on comparing metabolic profiles of stroke patients to those of the control population with the goal of identifying metabolomic biomarkers for predicting

stroke outcomes (Wang et al., 2020). Pre-clinical stroke studies have reported metabolic changes after tMCAo. For example, a study using untargeted metabolomics found evidence of acute and long-term changes in metabolic pathways in tMCAo mice including BBCAs, corticosterone, tyrosine, and tryptophan metabolic pathways (Yoon et al., 2022). Furthermore, fat loss after tMCAo in mice is associated with long-term changes in adipokine production in the adipose tissue and plasma of mice after tMCAo (Haley et al., 2020c). Also, a study has shown that although obese mice do not experience more weight loss in the acute period after tMCAo, the metabolic response to tMCAo is altered in obese ob/ob mice (Haley et al., 2017).

Given that ischaemic stroke is more prevalent in aged individuals, the first aim of this study was to firstly examine the impact of ageing on the extent of body weight loss and muscle wasting after stroke. We hypothesised that ageing would accelerates muscle wasting after stroke due to the likely presence of age-related sarcopenia however given aged mice typically have greater adipose tissue and therefore energy reserves, we hypothesised that ageing might protect against post-stroke weight loss. Therefore, the second aim was to examine the systemic metabolic response to ischaemic stroke in young and aged mice.

5.2 Materials and methods

5.2.1 Animals

A total of 36 male C57BL/6J mice were used for sham and tMCAo surgery in this study comprising of n=18 young mice (7-15 weeks of age) and n=18 aged mice (17-18 months of age). Those mice were used for the assessment of body weight, food intake, as well as muscle and fat mass. For metabolomics analyses, 15 of these mice were used, including n=8 aged mice (n=4 sham and n=4 tMCAo) and n=7 young mice (n=3 sham and n=4 tMCAo). Mice's brains were collected 24 hours post-surgery and sectioned. Infarct volume was quantified using thionin-stained brain sections and analysed with ImageJ, as described in section 2.2.6 of the general methods (Chapter 2). Animals were then selected such that infarct volumes were comparable between young and aged groups. Specifically, only mice with infarct sizes within ±10-20% of the mean infarct volume were included to minimise potential confounding effects of infarct size on metabolic responses.

5.2.2 Determining the effect of sham and tMCAo on body weight and composition of young and aged mice

5.2.2.1 Transient MCAo

Aged and young mice were subjected to tMCAo as described in section 2.2.2.1 in General methods (Chapter 2). Mice were randomised to either MCAo or sham surgery (random.org). Evidence from the literature shows that the aged mice can paradoxically experience less infarct injury than young mice at 24 h after stroke (Ritzel et al., 2018, Liu et al., 2009b, Manwani et al., 2013). In contrast, ageing female mice demonstrate an exacerbation of ischaemic injury relative to their younger counterparts (Liu et al., 2009b). These findings contribute to the growing recognition that stroke is a sexually dimorphic condition, both in experimental models and clinical settings (Branyan and Sohrabji, 2020), although the underlying mechanisms driving these sex differences remain insufficiently understood. Importantly, this difference tends to be more closely associated with oestrogen loss. Supporting this, studies have shown that infarct volumes in young ovariectomized female mice are comparable to those observed in aged females, whereas infarct size in aged females treated with oestradiol replacement is reduced back to levels similar to those seen in young females without ovariectomy

(Liu et al., 2009b, Toung et al., 2004). Despite these insights, the mechanisms underlying the reduced infarct size observed in aged male mice compared to young male mice remain unclear. One potential explanation may involve age-related alterations in excitotoxic signalling (Wenk et al., 1991). For instance, earlier research showed a widespread reduction in the binding to the NMDA receptor in aged male rats relative to younger animals (Wenk et al., 1991, Gonzales et al., 1991). However, it remains uncertain if a similar decline in excitotoxic susceptibility occurs in the brain of aged female mice.

As shown in Chapter 4, there is a positive correlation between infarct volume and weight loss, and therefore infarct size could be a confounding factor for the metabolic response. Therefore, to produce a similar infarct volume in aged and young mice, the MCA was occluded for 50 minutes in aged mice and 40 minutes in young mice. Moreover, given the physiological differences between mice and humans, particularly the markedly higher heart rate in mice (~500 beats per minute) and a metabolic rate about seven times higher in mice than that of humans (Janssen et al., 2002, Demetrius, 2005, Janssen et al., 2016), the post-stroke pathophysiological changes in mice are likely to occur more rapidly. Consequently, early time points after stroke induction are critical for capturing any changes in metabolism. Thus, we selected the 24 h post-stroke time point for metabolomics analysis. It was not possible to blind the surgeons to MCAo and Sham procedures. Also, I was not blinded to the procedure post-surgery as stroke and sham mice can be readily distinguished from each other.

5.2.2.2 Weight, food and liquid intake monitoring

The weight of the mice was recorded before surgery and 24 hours after; food and liquid intake were also monitored at baseline and 24 hours after surgery as described in Section 2.2.3 in General Methods (Chapter 2). Weight loss is presented as a percentage of baseline body weight.

5.2.2.3 Forelimb grip strength test

Forelimb grip strength was evaluated using a BIO-GS3 grip strength meter before and after stroke induction or sham surgery as described in Section 2.2.4 in General methods (Chapter 2).

5.2.2.4 Tissue harvesting

At the experimental endpoint (24 h), the mice were anaesthetised with isoflurane (3% for induction and 2% for maintenance) delivered in oxygen. The blood was collected via cardiac puncture as described in section 2.5.1 in General methods (Chapter 2), then the mice were euthanised by using an overdose of isoflurane. Subsequently, the brains were collected and slowly frozen in liquid nitrogen, then stored at -80 °C for sectioning, as described in section 2.2.6.1 of General methods. Skeletal muscles and white adipose tissue were also collected, weighed and stored at -80 °C.

5.2.2.5 Metabolomics

The plasma was extracted from the blood by centrifugation, and the samples were prepared for untargeted metabolomics as described in Section 2.5.2 in General methods.

Hydrophilic interaction liquid chromatography (HILIC) was carried out on a Dionex UltiMate 3000 RSLC system (Thermo Fisher Scientific, Hemel Hempstead, UK) using a ZIC-pHILIC column (150 mm × 4.6 mm, 5 µm column, Merck Sequant), which was maintained at 25 ºC. The elution of the samples was performed with a linear gradient (20 mM ammonium carbonate in H_2O, A and acetonitrile, B) over 26 min at a flow rate of 0.3 ml/min as follows: 0 min 20% A, 15 min 80% A, 15 min 95% A, 17 min 95% A, 17 min 20% A, 26 min 20% A. An injection volume of 10 µL was used, and the samples were kept at 5 °C before injection. For the Mass spectrometry (MS) analysis, a Thermo Orbitrap QExactive (Thermo Fisher Scientific) was operated in polarity switching mode, and the MS settings were as follows: Resolution 70,000, AGC 1e6, m/z range 70–1050, Sheath gas 40, Auxiliary gas 5, Sweep gas 1, Probe temperature 150°C, Capillary temperature 320°C. For positive mode ionisation: source voltage +3.8 kV, S-Lens RF Level 30.00, S-Lens Voltage 25.00 (V), Skimmer Voltage 15.00 (V), Inject Flatapole Offset 8.00 (V), Bent Flatapole DC 6.00 (V). For negative mode ionisation: source voltage, -3.8 kV. The calibration mass range was extended to cover small metabolites by inclusion of low-mass calibrants with the standard Thermo calmix masses (below m/z 138), butylamine (C4H11N1) for positive ion electrospray ionisation (PIESI) mode (m/z 74.096426) and COF3 for negative ion electrospray ionisation (NIESI)

mode (m/z 84.9906726). To enhance calibration stability, lock-mass correction was also applied to each analytical run. Then, the Instrument raw files were converted to positive and negative ionisation mode mzXML files. These files were then analysed using IDEOM (Creek et al., 2012) and Polyomics integrated metabolomics Pipeline (PiMP) (Gloaguen et al., 2017) with the FrAnK in-house fragmentation data analysis software. Erin Kerr conducted all the LC-MS experiments, and Dr Clement Regnault and I analysed the data.

5.2.3 Power calculations

G*Power 3.1.9.7 software (Heinrich Heine University, Germany) estimated that n=10 per group was required for the primary end point of % weight loss for initial experiments examining the impact of ageing on post-stroke weight loss and muscle wasting. A two-way ANOVA model was used, with an effect size f=0.50, a significance level (α) of 0.05, and power (1 − β) of 0.80. Consequently, group sizes ≤10 were used for % weight loss, food and water intake, body composition (fat and skeletal muscle), and grip strength.

5.2.4 Statistical analysis

GraphPad Prism (version 10.4.1, GraphPad Software Inc, San Diego, CA) was used to analyse and present all data relating to body weight, food and water intake, and fat and skeletal muscle mass. The data were tested for normal distribution using the Shapiro-Wilk test. Results are presented as mean ± SEM. For assessing differences between three or more groups involving a single independent variable, one-way ANOVA was used, while two-way ANOVA was applied when considering two independent variables. Specific test and group numbers are detailed in the corresponding figure legends. Statistical significance was defined as a p-value <0.05.

For metabolomic analyses, a principal component analysis (PCA) was generated in MetaboAnalyst 6.0 on $\log_{10}$-transformed data obtained in PiMP to assess clustering and separation within each sample group, and a heat map was generated using unsupervised hierarchical clustering analysis. Four group-wise univariate comparisons (fold-change) across the entire metabolome were also performed using an unpaired t-test, and p-values were adjusted using the Benjamini-

Hochberg procedure to control the False Discovery Rate (FDR). Peaks with an FDR-adjusted $p<0.05$ were considered significant, Lastly, a linear model was applied in MetaboAnalyst 6.0 to identify metabolites significantly associated with ischaemic stroke. Statistical significance was defined as FDR-adjusted $p<0.05$.

5.3 Results

5.3.1 Mortalities and exclusions

There were no mortalities however n=5 young stroke mice were excluded from the study when: (1) technical complications arose during surgery (e.g., loss of >0.2 ml of blood) (n=3), and (2) there was no visible infarct found after sectioning and staining of the brain (n=2). For the aged mice, n=2 stroke mice were also excluded from the study when there was no visible infarct found after sectioning and staining of the brain.

5.3.2 Effect of acute tMCAo and sham surgery on body weight, food and liquid intake of young and aged mice.

The body weights of all mice were recorded prior to surgery, and as expected, aged mice assigned to sham or tMCAo surgery weighed significantly more than young mice assigned to either sham or tMCAo surgery (Table 5-1). Consistent with our results in Chapter 4, profound body weight loss was observed after tMCAo in young mice compared to sham (-11.95±1.45 vs. -2.06±1.25%, $p<0.05$). Interestingly, the percentage of weight loss was less in aged mice than in young mice after tMCAo. Specifically, no statistically significant difference in percentage weight loss was detected between aged stroke mice and sham aged controls (-5.54±0.61 vs. -2.1±1.26%; $p>0.05$, respectively) (Figure 5-1A). However, the weight loss (% and grams) was significantly lower in aged mice after stroke compared with the young stroke mice.

Food and liquid intake were also monitored after surgery in both young and aged mice. However, no significant difference in food intake was observed between young and aged mice after stroke (young, 7±1.3 g; aged, 5.5±0.85 g, $p>0.05$) (Figure 5-1B). Similarly, water intake did not differ significantly between stroke groups in either young or aged mice (Figure 5-1C).

Table 5-1 Baseline (pre-surgery) body weights (two-way ANOVA followed by Tukey's multiple comparison post-hoc test, **p<0.05 versus young mice assigned to sham or tMCAo surgery. Baseline body weights were comparable between mice assigned to sham or tMCAo surgery for both young and aged mice, p>0.05)

	Sham	MCAO
Young mice (g) Mean ± SEM	26.18±2.07	26.06±0.98
Aged mice (g) Mean ± SEM	35.66±0.78**	35.96±1.05**

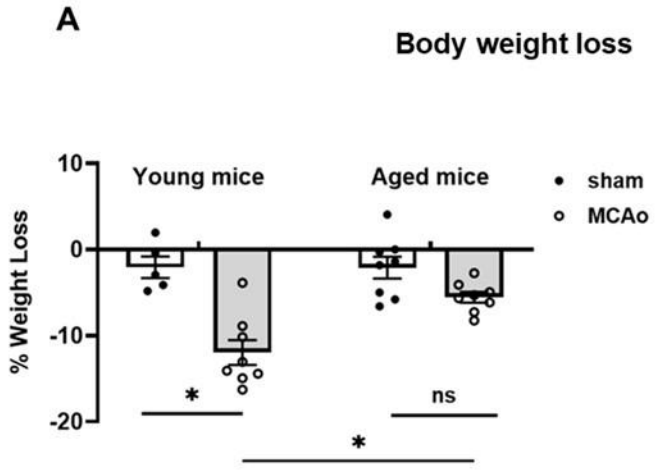

MCAo	Young	Aged
Weight loss (g)	3±0.4	1.96±0.2
Weight loss (% baseline)	11.95±1.4	5.54±0.61

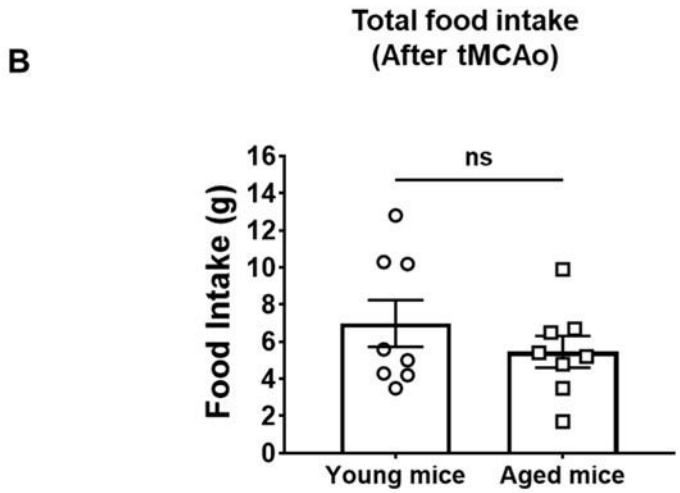

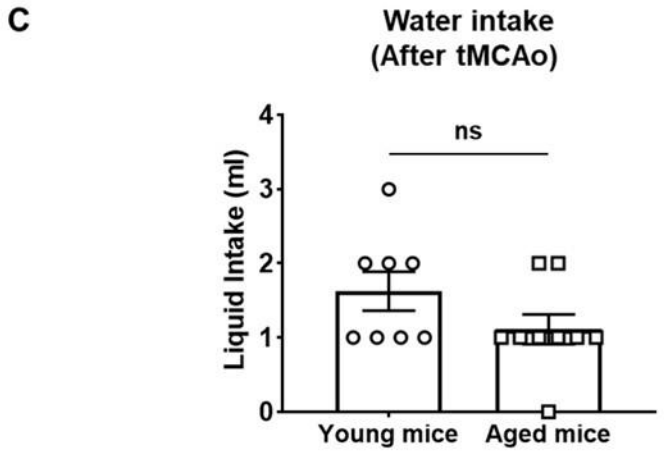

Figure 5-1 The effect of transient middle cerebral artery occlusion (tMCAo) or sham surgery on the body weight, food and water intake in young and aged mice at 24 hours after surgery. Body weight loss is expressed as a percentage relative to baseline; the table shows weight loss in grams and % weight loss (**A**). Total food (**B**) and water (**C**) intake by young and aged mice over the 24 hours after tMCAo. Young mice: n=5 sham; 8 tMCAo, aged mice: n=8 sham; 8 tMCAo. Data presented as mean ± SEM; *p<0.05, two-way ANOVA followed by Šídák's multiple comparison test; ns= not significant, unpaired student's t-test.

5.3.3 Effect of acute tMCAo and sham surgery on body composition of young and aged mice.

Weights of skeletal muscle isolated from the ipsilateral and contralateral limbs of young or aged tMCAo mice were comparable to muscles from their respective age-matched sham mice (Figure 5-2A & B, $p>0.05$). Similarly, visceral fat pad weights from young or aged tMCAo mice were not significantly different compared with fat from sham mice (Figure 5-2C, $p>0.05$). Regarding functional outcomes, despite no differences in muscle weights, aged stroke mice showed a significant decrease in grip strength compared to sham controls ($p<0.05$). In contrast, in young mice, a trend toward decreased grip strength was observed after tMCAo compared to sham controls, although this did not achieve statistical significance ($p=0.077$) (Figure 5-2D).

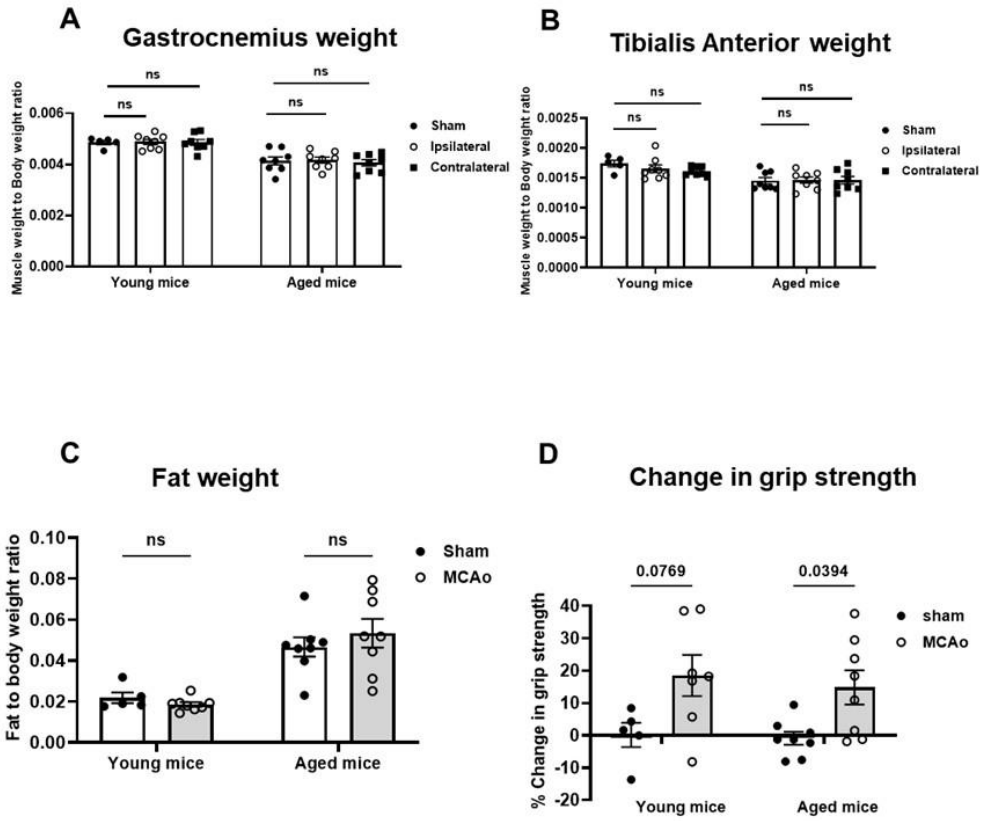

Figure 5-2 Skeletal muscles, fat weight and grip strength after transient Middle Cerebral Artery occlusion (tMCAo) or sham surgery in young and aged mice. *Ex vivo* weights of the gastrocnemius muscle (**A**), the tibialis anterior muscle (**B**), and the visceral fat pads (**C**) are expressed relative to body weight in both young and aged mice after sham or tMCAo surgery. Muscles were collected from the ipsilateral and contralateral (stroke-affected) limbs of tMCAo mice and the right limb of the sham mice. % change in grip strength of young and aged mice subjected to sham and tMCAo (**D**). Young mice: n=5 sham; 8 tMCAo, aged mice: n=8 sham; 8 tMCAo. Data presented as mean ± SEM. *p<0.05, ns= not significant, two-way ANOVA followed by Šídák's multiple comparison test.

5.3.4 Infarct volume in young and aged tMCAo mice for metabolomics analyses

Given that we demonstrated in the previous chapter that the extent of weight loss is correlated with infarct volume, and therefore to minimise the potential confounding effect of infarct volume on our results and metabolic responses to stroke, we needed to match the infarct volume between young and aged mice. Therefore, the young mice were subjected to a 40-minute occlusion period, while the aged mice underwent a 50-minute occlusion period. However, this approach was challenging due to the inherent variability in collateral blood flow, which may affect the infarct volume induced by this model, especially in young mice (Figure 5-3A). Nevertheless, for metabolomics analysis, we identified four young and aged mice with comparable infarct volumes. As depicted in Figure 5-3B, infarct volumes were comparable between these young and aged tMCAo mice. The mean infarct volume in young mice was 15.58 ± 4.7 mm^3, while in aged mice it was 15.54 ± 3 mm^3.

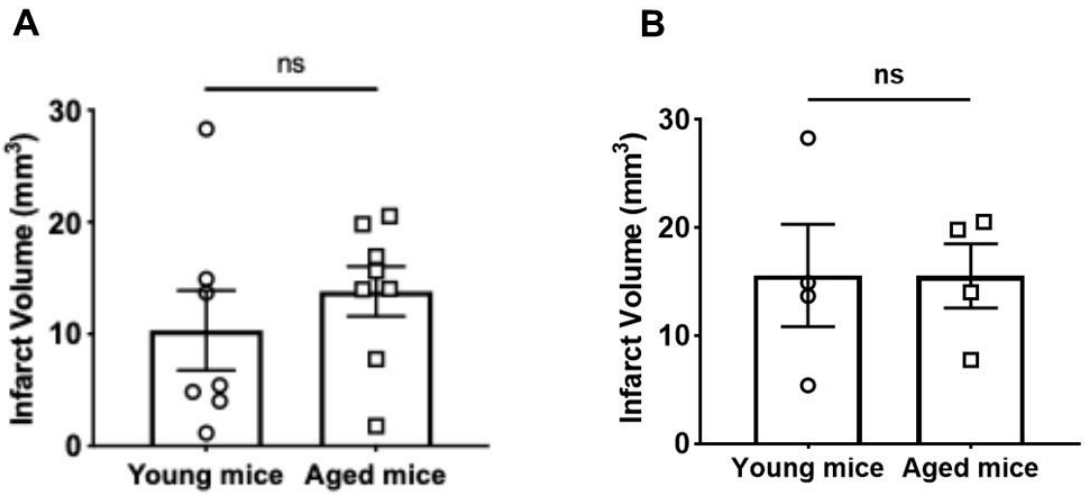

Figure 5-3 Infarct volumes after 24-hour transient middle cerebral artery occlusion (tMCAo) in young and aged mice. Young mice were exposed to 40 minutes tMCAo, whereas aged mice were exposed to 50 minutes tMCAo. Infarct volume of all mice included, n=7-8 (**A**), infarct volume of mice used for metabolomics, n=4 per group (**B**). Data expressed as mean ± SEM. ns = not significant, Mann-Whitney test.

5.3.5 Untargeted metabolomics analysis

After data processing and filtering in PiMP, 4,161 peaks were detected in the dataset. Of these, 1,638 were putatively annotated as metabolites based on m/z match to compounds in databases at the University of Glasgow MVLS Shared Facility. These 1,638 peaks were retained for downstream statistical analyses. Of these, 141 peaks were matched by retention time and exact mass to authentic standards. These are referred to as 'identified'. Additionally, fragmentation was also performed on the pooled sample, and approximately 64 signals matched to the fragmentation database.

5.3.5.1 Quality control

To assess and maintain the quality of the obtained data throughout the run, a single pooled quality control sample was analysed at regular intervals, specifically after every fifth injection. The pooled quality control samples exhibited tight clustering relative to the biological samples, indicating that the pooled samples behaved in a reproducible manner (Data is shown in Section 8.1 of the Appendix for this thesis). This also ensures that any observed differences in metabolites are attributable to biological variation rather than technical variation.

5.3.5.2 Multivariate analysis

PCA is an unsupervised method that reduces the dimensionality of the data by transforming a large set of correlated variables into a smaller set of uncorrelated components that still retain most of the original information in the large set. The first principal component captures the most significant potential variance, accounting for a substantial portion of the variability among the data. The second principal component explains the greatest amount of the remaining variance after the first component has been extracted.

PCA was conducted to qualitatively evaluate biological variation and reproducibility in the four groups – sham young, stroke young, sham aged, and stroke aged. The result from the PCA of the experimental data is shown in Figure 5-4. The first principal component (PC1) along the X-axis accounted for 29.5% of the total variance across our samples, and PC2 on the Y-axis described an additional 18.2% of the variance. Visual inspection of the PCA plot showed no

apparent clustering or clear separation of the replicates within our four groups. A heat map was then generated using unsupervised hierarchical clustering to visually organise our samples and metabolites based on the relative abundance of putatively annotated metabolites. As depicted in the Figure 5-5, no distinct visual pattern of increased or decreased metabolite levels was observed among sham and stroke mice within each age group.

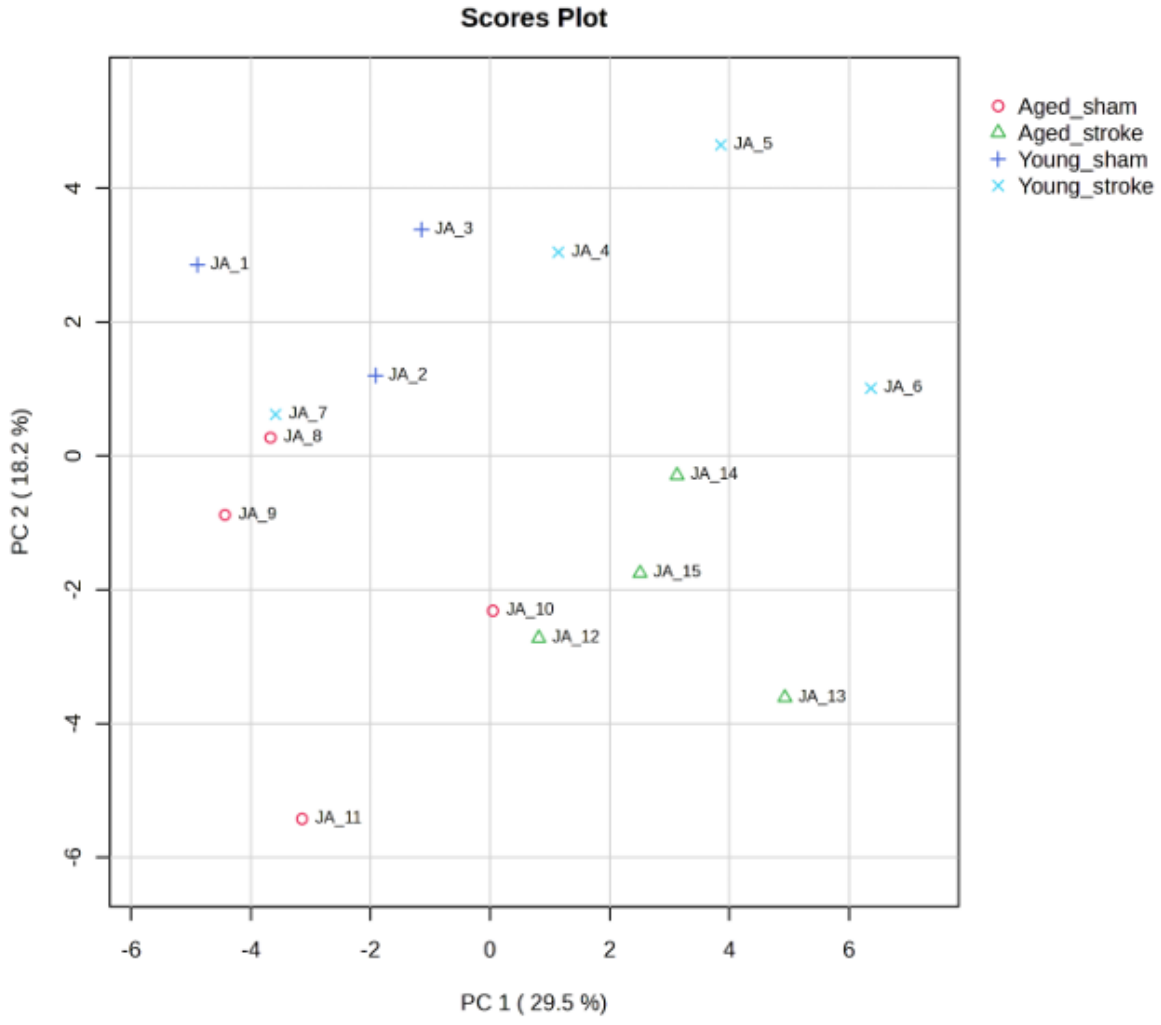

Figure 5-4 Principal component analysis (PCA) of metabolites in plasma from sham or tMCAo mice. Plot of the first two principal components calculated for the samples extracted from plasma 24 h after sham or tMCAo surgery on young and aged mice. The plot was generated in MetaboAnalyst 6.0 on log_{10}-transformed data obtained in PiMP young mice: n=3 sham, 4 tMCAo; aged mice, n=4 sham, n=4 tMCAo.

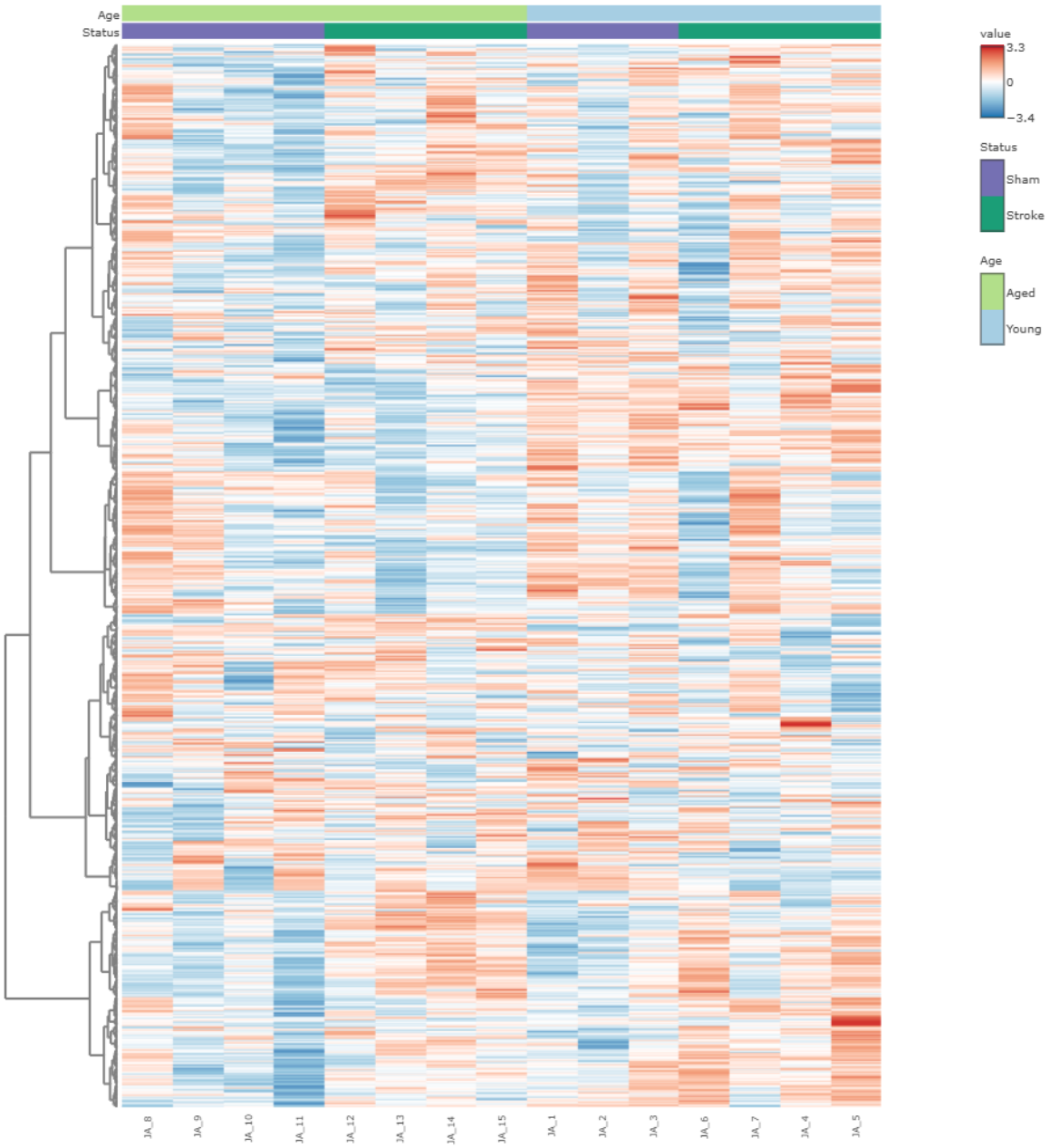

Figure 5-5 Heatmap of putatively annotated peak levels in plasma from sham or tMCAo mice. Each row corresponds to one putatively annotated peak detected in PiMP (Gloaguen, 2017), and each column one sample replicate. Metabolite levels in each sample are represented as fold changes relative to the mean and coloured according to the key (red = high abundance, blue = low abundance). Heatmap generated on $\log_{10}$-transformed data obtained in PiMP using MetaboAnalyst 6.0, young mice: n=3 sham, 4 tMCAo; aged mice, n=4 sham, 4 tMCAo.

5.3.5.3 Univariate analysis

Given the initial multivariate analysis did not reveal any apparent metabolic differences or clear group separation, we next performed four group-wise univariate comparisons (fold changes; comparison 1: young stroke vs young sham; comparison 2: aged stroke vs aged sham; comparison 3: aged sham vs young sham, or comparison 4: aged stroke vs young stroke) across the entire metabolome. The results of these comparisons are visualised in volcano plots in Figure 5-6. No statistically significant changes were found for comparison 1 (young stroke vs young sham) or comparison 2 (aged stroke vs aged sham). Also, although some fold changes were found to be significantly different in comparisons 3 and 4, most of the observed peaks remained unannotated, as they did not match any compounds in the database.

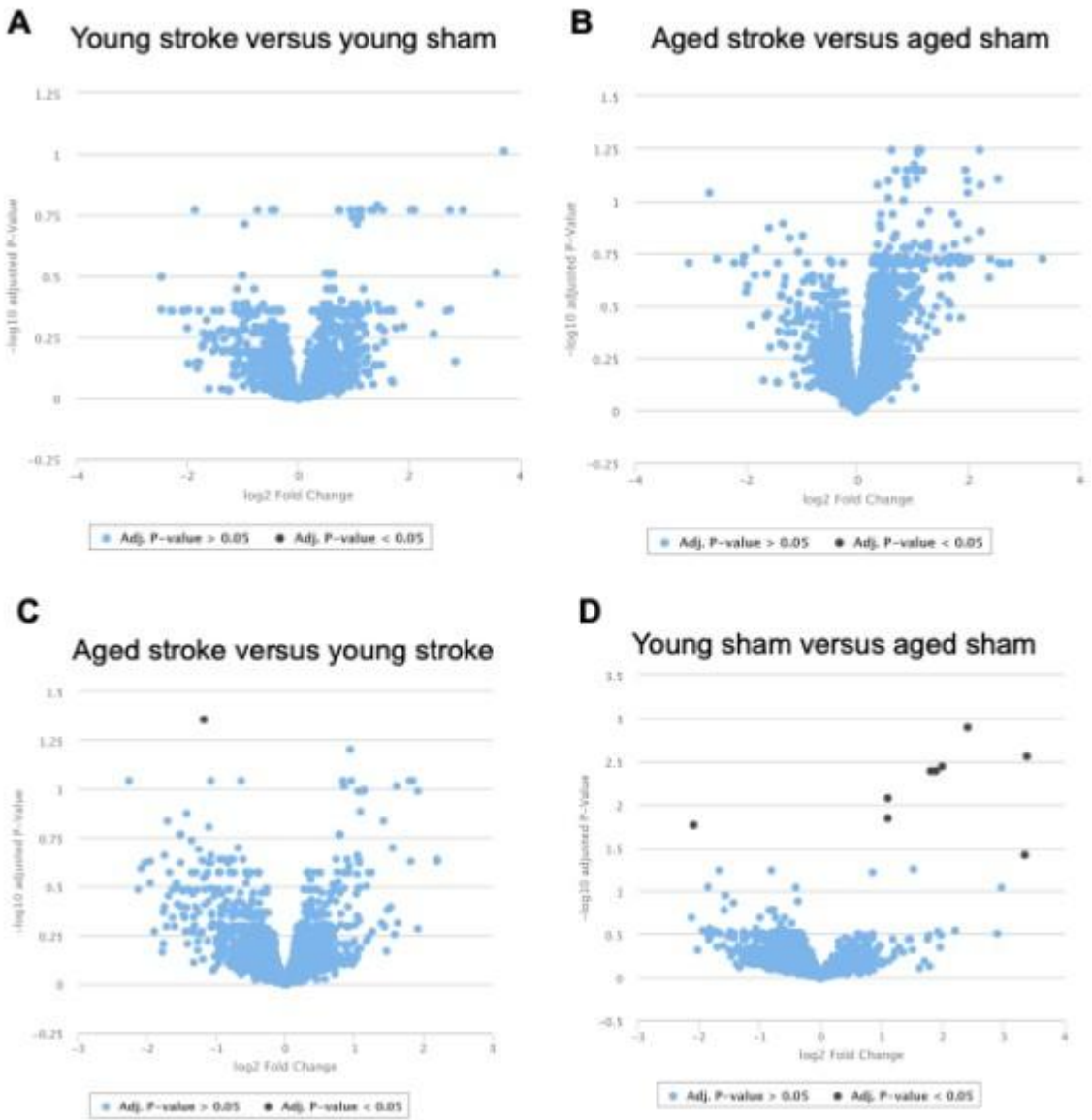

Figure 5-6 Volcano plots displaying four group-wise univariate comparisons across the entire metabolome in plasma from sham or tMCAo mice. Four-group wise comparisons were performed to identify differences (fold-change) between the groups of mice – young stroke versus young sham (**A**), aged stroke versus aged sham (**B**), aged stroke versus young stroke (**C**), and young sham versus aged sham (**D**). An unpaired t-test with Benjamini-Hochberg (BH) procedure to control the False Discovery Rate (FDR) was used. Peaks with an adjusted $p<0.05$ were considered significant. Data is presented as $\log_2$ fold change plotted against $-\log_{10}$ adjusted p value, young mice: n=3 sham, 4 tMCAo; aged mice, n=4 sham, 4 tMCAo.

In the final part of the analyses, a linear model was implemented in MetaboAnalyst 6.0. to identify if any metabolites were significantly associated with ischaemic stroke regardless of age. This led to the identification of 42 metabolites as significantly different (adjusted p-value < 0.05). The lists of putatively annotated metabolites with significantly changed (adjusted p-value < 0.05) are presented in a table in Section 8.2 of the Appendix. Among these, only the metabolites confidently identified by matching authentic standards or putatively annotated through fragmentation spectra and exhibiting well-defined peaks were discussed. These metabolites were involved in fatty acid, lipid and tryptophan metabolic pathways. The corresponding Stroke-associated metabolic alterations are illustrated in Figure 5-7.

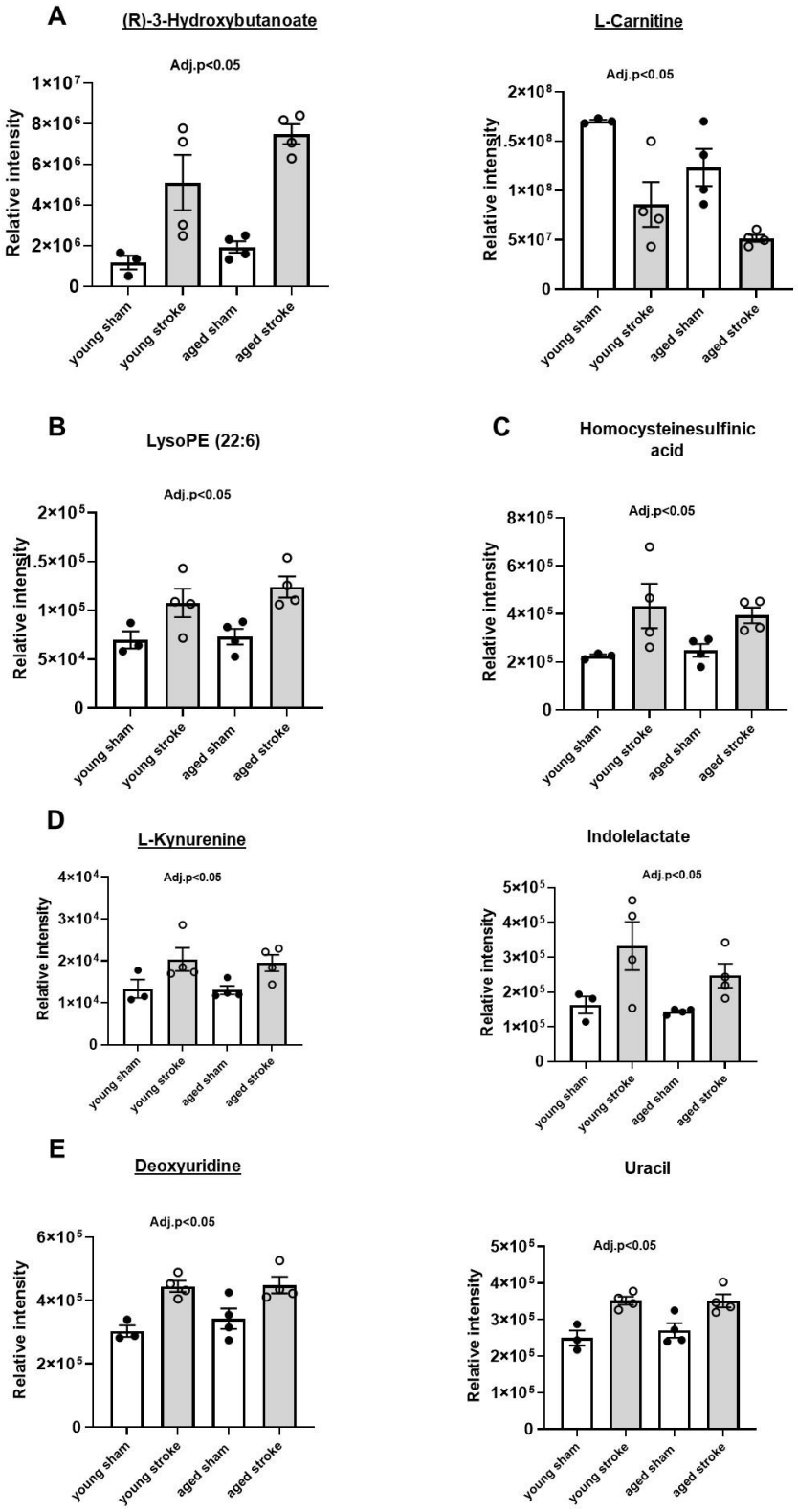

Figure 5-7 Effect of acute ischaemic stroke on the metabolic profile of mice. Bar charts showing relative peak intensities of fatty acid metabolites (A), glycerophospholipid (B), homocysteinesulfinic acid (C), tryptophan metabolites (D) and pyrimidine metabolites (E) after 24 h tMCAo and sham surgery on young and aged mice. All annotations are putative. Metabolites with their names underlined had their exact mass and retention time matched to those of an authentic standard. The data were analysed using a linear model in MetaboAnalyst 6.0. Data presented as mean±SEM, (n=3-4 per group).

5.4 Discussion

In this study, we aimed to investigate the systemic metabolic response to ischaemic stroke in young and aged mice to gain insight into the potential mechanisms underlying post-stroke weight loss. To minimise the possible confounding effect of stroke severity on metabolic responses, young mice were subjected to 40 minutes of tMCAo. In contrast, aged mice underwent 50 minutes of tMCAo, based on previous studies indicating that aged mice typically develop smaller infarcts than young mice under similar conditions. In alignment with our earlier findings, both young and aged mice lost weight after stroke. However, the extent of weight loss was significantly lower in the aged cohort. In the metabolomic study, multivariate and univariate analyses revealed no differences among sham or stroke mice and between age groups. However, using a linear model, we found evidence of stroke-associated metabolic alterations in fatty acid, lipid and tryptophan-related metabolites.

Consistent with our findings in Chapter 4, young mice lost a significant amount of weight (~12%) on day 1 after stroke, compared with sham controls (~2%). Surprisingly, aged mice showed only a slight, nonsignificant weight loss on day 1 after tMCAo (-5.5%) compared with sham mice (-2%). Notably, both young and aged stroke mice consumed comparable amounts of food and water after stroke, indicating that differences in food intake do not explain the differences in body weight loss. However, food intake in young mice after stroke exhibited a bimodal distribution, suggesting variable individual responses to the insult. As demonstrated in the previous chapter, both sham and stroke-operated mice show a reduction in food intake on day 1 post-surgery, followed by a gradual recovery and an increase in food intake over subsequent days. Therefore, perioperative factors such as surgical stress and anaesthesia may influence early feeding behaviour and cannot be ruled out. Consistent with our observation, Springer and colleagues (2014) reported an initial reduction in food intake after MCAo followed by a subsequent recovery and an increase in food intake (Springer et al., 2014a). Nevertheless, the subgroup of animals with higher food intake may reflect individuals with milder injury due to collateral blood flow or a more rapid recovery trajectory. The underlying reasons for this age-dependent difference in post-stroke weight loss are unclear. One potential explanation could be that mice typically exhibit low energy expenditure and greater energy conservation as they

age (Stern et al., 2012, Schefer and Talan, 1996). It is conceivable that this may serve as a protective metabolic adaptation after stroke, thereby limiting acute weight loss compared to younger mice. Supporting this notion, studies in humans have demonstrated that advancing age is characterised by a progressive decline in resting metabolic rate (RMR), averaging 1-2% per decade after the age of 20 (Elia et al., 2000, Kitazoe et al., 2019). Interestingly, a pre-clinical study showed that young mice experience transient reductions in energy expenditure after stroke as a compensatory response to restore body weight, however this study also showed a significant increase in locomotor activity in young animals after tMCAo (Springer et al., 2014a). In contrast, a study showed that aged mice have markedly reduced locomotor activity 24 hours after tMCAo (Manwani et al., 2011), which may further contribute to their lower overall energy expenditure and therefore weight loss. Another plausible explanation may relate to the fact that aged mice have a higher fat mass than their younger counterparts and therefore are protected from post-stroke weight loss due to excess energy resources. However, recent studies using obesity mouse models do not support this theory. Indeed, although ob/ob obese mice lose comparable weight to control mice in the acute phase after tMCAo (24 hours)(Haley et al., 2017), high-fat diet obese mice lose more weight than their lean counterparts up to 50 days after tMCAo (Haley et al., 2020c). Clinical studies have reported that increased adiposity may exert a beneficial effect on outcomes and protect from adverse effects after stroke (Scherbakov et al., 2011a, Oesch et al., 2017). However, functional recovery was not assessed in this study due to the severity limits of our Home Office Licence. Lastly, future studies are needed to examine the impact of ageing on post-stroke weight loss beyond the acute phase after tMCAo.

Although acute body weight loss was observed in both young and aged mice after the stroke, we found no significant differences in fat and skeletal muscle mass in either group. Interestingly, however, the grip strength was significantly reduced in stroke-aged mice compared to sham mice, and there was a trend of low grip strength in young stroke mice as well, compared to sham. It is unclear what is underpinning the weight loss at this early time point. As described in this Chapter and Chapter 4, water intake is comparable between sham and tMCAo on day 1, suggesting the loss of body weight is not related to dehydration. However, given

the challenges of measuring water intake (discussed in Chapter 4) we cannot rule this out.

Metabolomics analysis was conducted using group-wise univariate comparisons to assess fold changes in metabolite levels. Specifically, four comparisons were performed: (1) young stroke versus young sham, (2) aged stroke versus aged sham, (3) aged sham versus young sham, and (4) aged stroke versus young stroke. However, no statistically significant differences in metabolite levels were observed in these comparisons. The lack of significant changes could be due to the timing of sample collection post-stroke, which might have been too early to detect any effects of stroke on metabolism. Also, the impact of factors such as anaesthesia and stress relating to the procedure on metabolism cannot be entirely excluded at this early time point. However, both sham and stroke mice were exposed to the same period of isoflurane anaesthesia with isoflurane and underwent the same procedures apart from sham mice did not undergo filament insertion. Furthermore, a previous study identified significantly altered metabolites between young sham and tMCAo mice on day 1 post-surgery including alterations in fatty acid, tyrosine, tryptophan, and glucocorticoid pathways (Yoon et al., 2022). We choose to perform the metabolomic analyses on day 1 post-stroke for several practical and ethical reasons. First, for ethical reasons, given aged mice often exhibit worse neurological outcomes and higher mortality rates after experimental stroke, we were concerned that many of the aged mice may have to be culled prior to a later scientific endpoint such as day 3 or 7 post-surgery. Indeed, prior to starting this work, two of the mice from the aged cohort were found dead, highlighting the fragility of aged mice and the challenges of using them in biomedical research. Second, the physiological characteristics of mice, such as a high heart rate and metabolic rate, indicate that pathophysiological and metabolic changes will occur more rapidly than in humans, supporting the rationale for an early time point assessment in this study. Another likely explanation for the lack of significantly different metabolites is the limited sample size of n=3-4, which likely reduced the statistical power to detect subtle changes in metabolites, particularly given the natural variability in metabolomics data. However, in designing this study, we aimed to achieve comparable infarct sizes between aged and young mice to minimise the effects of differing levels of stroke severity on the metabolic response. However, this approach resulted in a

small sample size per group (3-4 mice), which may have limited the robustness of statistical comparisons.

A linear model was then used to identify metabolites that significantly associated with ischaemic stroke, regardless of age. This led to the identification of 42 metabolites significantly altered between sham and stroke mice. These metabolites were related to fatty acid, lipid and tryptophan pathways. With respect to fatty acid metabolism, we observed a significant increase in plasma 3-hydroxybutanoate in mice at day 1 after tMCAo compared with sham. 3-hydroxybutanoate - also known as ß-hydroxybutyrate (BHB)- is a ketone body that makes up approximately 70% of the total circulating ketone body pool in the blood (Dabek et al., 2020). This metabolite serves as an alternative to glucose in conditions of limited fuel supply in the brain, such as cerebral ischaemia (Møller, 2020). Ketone bodies, which are mainly derived from lipid metabolism, are generated through fatty acid oxidation. Free fatty acids that are released from adipose tissue are transported to the mitochondria of hepatocytes, where they undergo ß-oxidation to form acetyl-CoA and, ultimately, through a series of interactions leading to BHB synthesis. This metabolite is released from the liver and transported to peripheral tissues such as the brain, heart and muscle, where it is metabolised back into acetyl-CoA, which in turn can be used for ATP production (Newman and Verdin, 2017, Feng et al., 2024). This may suggest that ischaemic stroke induced lipolysis to form ketone bodies as an alternative energy source. Consistent with our observation, elevation of BHB in blood and brain after tMCAo in mice was reported in a metabolomics study (Jia et al., 2021). Notably, an increased level of BHB in the blood after stroke is reported to be associated with poor prognosis in humans (Licari et al., 2022).

We also found a significant decrease in l-carnitine in the stroke group. L-carnitine facilitates fatty acid ß-oxidation for energy production by transporting long-chain fatty acids into mitochondria (Longo et al., 2016). The reduction in l-carnitine may suggest an increased need for shuttling to meet tissue energy demand. A study demonstrates that the L-carnitine level in plasma is inversely associated with stroke recurrence and post-stroke cardiovascular events in stroke patients, and therefore may serve as a promising prognostic marker for predicting cardiovascular events in stroke survivors (Du et al., 2022). Moreover, a reduction in plasma l-carnitine is associated with a higher risk of post-stroke cognitive

impairment in ischaemic stroke patients (Che et al., 2022). Furthermore, in the stroke group, a significant increase in lysophosphatidylethanolamine (lyso PE 22:6) was observed which is derived from membrane lipid PE through hydrolysis by phospholipase A2 enzyme (Zeng et al., 2017).

A change in L-tryptophan metabolism was also observed in stroke mice, with a significant increase in the tryptophan metabolites L-kynurenine and indolelactate. Tryptophan is an essential amino acid that is absorbed from the intestine. It is metabolised via major pathways, including the kynurenine and indole pathways (Xue et al., 2023). Clinically, increased kynurenine levels have been reported as a potential diagnostic biomarker for post-stroke cognitive impairment (Liu et al., 2015). Additionally, a study showed that an elevated concentration of kynurenine after ischaemic stroke is associated with an increased risk of developing post-stroke infection among stroke survivors (Dylla et al., 2025). Our data also revealed a significant increase in homocysteine sulfinic acid in stroke mice. Although little is known about its metabolic pathway, this amino acid functions as a potent, selective agonist of metabotropic glutamate receptors, thereby increasing excitotoxicity, oxidative stress and inflammation(Santhoshkumar et al., 1994). Some studies have shown that it also activates transcription factors such as NF-κB that regulate expression of pro-inflammatory cytokines (Hankey, 2006a, Song et al., 2009). Lastly, we found evidence of alterations in nucleotide metabolism in stroke mice, with a significant increase in plasma levels of deoxyuridine and uracil, which are pyrimidine metabolites. Taken together, these findings provide evidence that ischaemic stroke induces metabolic alterations, some of which could conceivably contribute to post-stroke complications such as weight loss.

This study has some limitations: only male mice were used. Also, we did not assess neurological function and locomotor activity in mice after stroke, as it was unethical to subject the mice to multiple experiments within the same acute time window. Second, we studied only the metabolic response in the acute phase after stroke onset, without evaluating the subacute or chronic phases. Additionally, the metabolomics analysis was performed on a relatively small sample size due to challenges in obtaining comparable infarct sizes across cohorts.

In summary, we have shown that body weight loss was lower in aged mice than in young mice after stroke, despite both groups eating a comparable amount of food

after stroke. We have demonstrated that stroke induces alterations in lipid, fatty acid, and tryptophan metabolism, which may explain the loss of fat observed after stroke; however, since this study assessed the acute phase after stroke, further studies are needed to evaluate the effect in the chronic phase. Given that skeletal muscle constitutes a substantial proportion of total body mass, and that the present work demonstrates significant loss of skeletal muscle in both limbs following stroke, further investigation into muscle-specific mechanisms is warranted. Accordingly, the next chapter examines the direct effects of ischaemic stroke on skeletal muscle, with a particular focus on changes in muscle mass and the regulation of anabolic and catabolic gene expression across the acute, subacute, and chronic phases of stroke.

Chapter 6 Effect of experimental ischaemic stroke on skeletal muscle mass and expression of catabolic/anabolic genes

6.1 Introduction

Skeletal muscle, comprising approximately 30–40% of total body mass, is the most abundant tissue in the human body. It plays an essential role in regulating a wide range of physiological functions, most notably in facilitating voluntary movement and regulating metabolism (Izumiya et al., 2008). The maintenance of skeletal muscle mass depends on the balance between protein synthesis and degradation. Two key signalling pathways have been identified as central regulators of protein synthesis: the anabolic IGF-1–Akt–mTOR pathway, which acts as a positive regulator promoting protein synthesis and muscle growth, and the catabolic myostatin–Smad2/3 pathway, which is considered an inhibitory mechanism that downregulates muscle growth (Bonaldo and Sandri, 2013) (Figure 6-1). Phosphorylation of AKT enhances protein synthesis through mTOR (Mammalian target of rapamycin) activation, whose downstream targets are S6 kinase-1 (Rps6k) and eukaryotic translation initiation factor 4E-binding protein 1 (EIF4EBP1), which have been shown to increase protein synthesis by promoting translation initiation (Yoshida and Delafontaine, 2020, Leite et al., 2021). AKT1 also regulates and decreases the activity of the ubiquitin-proteasome system (UPS) through phosphorylation and inhibition of transcription factor FOXO (Stitt et al., 2004). Evidence shows that FOXO increases the expression of atrophic genes, Muscle Ringer Finger 1 (MuRF-1) and muscle atrophy F-box (FBXO32), also called Atrogin-1 (Sandri et al., 2004). A second pathway involves myostatin (MSTN), which is secreted by skeletal muscle itself and acts by negatively regulating muscle growth (Ruas et al., 2012). It produces its effect by binding to activin-A receptor, leading to phosphorylation of transcription factors Smad2 and 3, whose targets are not yet known, but it is believed that they interfere with and inhibit the AKT-mTOR axis, reduce muscle gene expression and promote proteolysis (Esser, 2008, Leite et al., 2021, Amirouche et al., 2009).

Under many pathological conditions, skeletal muscle loss occurs leading to muscle atrophy and weakness. In Chapter 3, we have shown that the prevalence of muscle wasting (sarcopenia) among stroke survivors is 36%. Moreover, it is associated with worse clinical outcomes and poor physical functioning (Park et al., 2019a, Li et al., 2020, Lee et al., 2023a). As discussed in Chapter 3, obvious factors likely contributing to post-stroke muscle wasting include immobility/disuse, malnutrition due to dysphagia, and neuromuscular disruption (denervation).

Furthermore, stroke patients demonstrate markedly lower muscle mass in both limbs compared to healthy adults (English et al., 2010), and the decline in muscle mass occurs rapidly after stroke onset along with alterations in muscle fibre structure, contrasting with ageing-sarcopenia, suggesting stroke-related disuse, denervation and/or malnutrition are not the sole contributing factors. Consistent with this, in Chapter 4 we have shown that bilateral wasting and reduced muscle strength of skeletal muscle occur in mice during the acute phase (day 3) after transient middle cerebral artery occlusion (tMCAo) in the absence of marked changes in food or water intake. Due to the differences between muscle wasting after stroke versus ageing-sarcopenia, the term 'stroke-related or -specific sarcopenia' has been proposed (Scherbakov et al., 2013). However, despite the clinical significance of post-stroke muscle atrophy, very little is known about the molecular mechanisms driving these changes, as well as the time course of these signalling pathways in skeletal muscle during stroke.

Current evidence suggests that muscle atrophy in other diseases such as age-related sarcopenia results at least in part from a disrupted balance between protein synthesis and degradation (Park et al., 2017). Springer and colleagues (2014) found evidence of caspase activation, increased proteosome activity, and increased myostatin levels in gastrocnemius muscle collected from both hindlimbs of mice in the acute phase after tMCAo, suggesting upregulation of catabolic pathways (Springer et al., 2014a). Therefore, given the central roles of the IGF-1/PI3K/AKT and myostatin/Smad2/3 signalling pathways in regulating muscle homeostasis, we hypothesised that stroke leads to an upregulation of genes involved in the catabolic pathway and a downregulation of genes involved in protein synthesis and anabolic pathways, contributing to muscle wasting. To test this hypothesis, we examined the effect of experimental stroke in mice (tMCAo) on muscle mass and on the expression of genes involved in regulating the anabolic/catabolic balance in skeletal muscle, including inflammatory genes such as TNF-α, which are known to contribute to muscle wasting in other diseases (García-Martínez et al., 1993). Furthermore, we sought to determine the time course of these effects by examining gene expression during the acute and sub-acute/chronic phase after stroke induction to determine if the alterations induced by stroke persist over time which may influence long-term functional outcomes. To examine whether stroke-related changes in anabolic/catabolic genes resemble

those found in age-related sarcopenia, we also measured gene expression of skeletal muscle from aged naïve mice. Lastly, we aimed to investigate the effects of experimental ischaemic stroke on the expression of genes regulating the anabolic/catabolic balance in aged mice, given that stroke is common in advanced age.

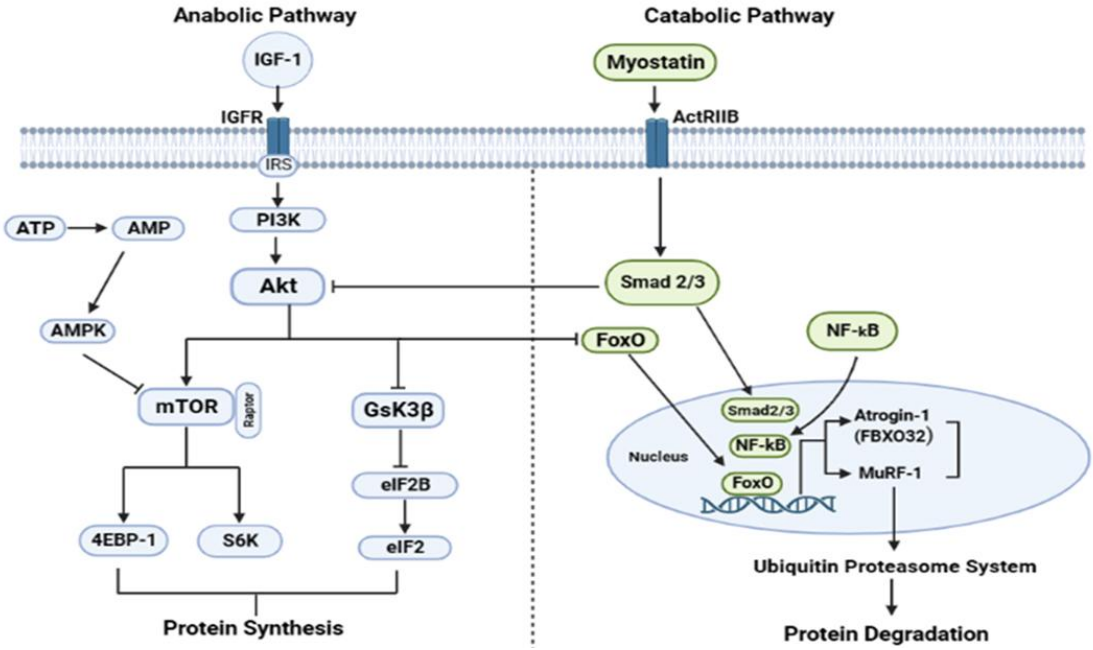

Figure 6-1 Anabolic and catabolic pathways regulating skeletal muscle mass. A diagram illustrating the key signalling pathways involved in muscle homeostasis. The two main pathways are IGF-1–Akt–mTOR (**acts** as a positive regulator to increase protein synthesis) and myostatin–Smad2/3 pathway (**acts** as a negative regulator to inhibit protein synthesis and enhance protein degradation). Figure created in Biorender.com

6.2 Materials and methods

6.2.1 Animals and study design

Within each time point, mice were randomised to either MCAo or sham surgery (random.org). It was not possible to blind the surgeon to MCAo and sham procedures. Also, I was not blinded to the procedure post-surgery as stroke and sham mice can be readily distinguished from each other. To study the effect and time course of cerebral ischaemia on the skeletal muscle wasting and genes involved in regulating muscle homeostasis, young male C57BL/6J mice (8-15 weeks of age) were subjected to transient middle cerebral artery occlusion (tMCAo) or sham surgery with the following experimental endpoints: day 1 post-surgery (n=16), day 3 (n=16), day 7 (n=16), day 14 (n=14), and 1 month (n=16). To assess whether the molecular mechanisms of muscle wasting post-stroke are similar to ageing-sarcopenia, skeletal muscles from young (8-12 weeks of age, n=8) and aged (20-22 months of age, n=8) naïve C57BL/6J mice were collected. Furthermore, to examine the effect of experimental stroke on muscle homeostasis in ageing, aged male C57BL/6J mice were subjected to experimental stroke (tMCAo) or sham surgery (n=8 per group).

6.2.2 Stroke model

40 minutes of tMCAo was used to induce stroke in young mice as described in Section 2.2.2.1 of Chapter 2, and 50 minutes of tMCAo was used to induce stroke in the aged mice. Sham-operated mice were exposed to the same duration of anaesthesia as stroke mice, as described in Section 2.2.2.1 of Chapter 2. For all mice, body weights were measured prior to surgery and then daily for the first week after surgery, then twice a week until the experimental endpoints (day 1, 3, 7, 14 and 1-month post-surgery) were reached. At the experimental endpoints, mice were euthanised by exposure to a rising concentration of CO_2 (Schedule 1 of the Animals [Scientific Procedures] Act 1986). The gastrocnemius and tibialis anterior muscles were collected, weighed and snap frozen in liquid nitrogen, then stored at -80 °C.

6.2.2.1 RNA extraction and cDNA conversion

The gastrocnemius muscle from young and aged tMCAo or sham mice, and young and aged naïve mice was homogenised by adding 1 mL of QIAzol™ reagent along with sterile beads. RNA was extracted and then converted into cDNA as described in Section 2.3.1 of Chapter 2.

6.2.2.2 RT-qPCR

mRNA levels of key genes involved in muscle homeostasis: *mTOR, AKT1, AKT2, RPS6K, RPS6, GsK3B, EIF4EBP1, FOXO1, MSTN, FBXO32*, *TRIM63, TNF-α and IL-6* were quantified using RT-qPCR as detailed in Section 2.3.2 of Chapter 2.

6.2.2.3 Haematoxylin & Eosin staining

The tibialis anterior muscles were fixed in 4% PFA at 4°C, followed by a graded ethanol series for dehydration and then rehydration after being embedded in paraffin wax. Slides were then stained with haematoxylin & eosin as described in Section 2.4 of Chapter 2. For quantification of muscle fibre cross-sectional area (CSA), approximately 200 fibres were randomly selected and quantified per muscle section/image in a blinded manner using ImageJ software.

6.2.3 Power calculations

G*Power 3.1.9.7 software (Heinrich Heine University, Germany) was used to calculate sample sizes for this study. Since we did not have pilot gene expression (primary end point) in skeletal muscle post-stroke, we used the mean and standard deviation from a previous unpublished study that examined expression of genes in skeletal muscle from aged mice. It was estimated that a minimum of 8 mice per group would be required to detect differences in gene expression across the three groups (sham muscle, stroke muscle - ipsilateral and contralateral). A one-way ANOVA model was used, with an effect size f = 0.69, a significance level (α) of 0.05, and power (1 − β) of 0.80.

6.2.4 Statistical analysis

GraphPad Prism (version 10.4.1, GraphPad Software Inc, San Diego, CA) was used to analyse and visualise the study data. Results are presented as mean ± SEM. The

data were tested for normal distribution using the Shapiro-Wilk test. For two groups comparisons, an unpaired Student's t-test was used with normally distributed data, and the Mann-Whitney U test was used for non-normally distributed data. For assessing differences between three or more groups involving a single independent variable, one-way ANOVA was used, while two-way ANOVA was applied when considering two independent variables. The statistical tests and group numbers are detailed in the corresponding figure legends. Statistical significance was defined as a p-value <0.05.

6.3 Results

6.3.1 Mortality and exclusions

There were no mortalities in this study, and no mouse had to be euthanised prior to the scientific endpoint due to reaching the severity limits of the procedure. 5 mice had to be excluded as they did not experience ≥70% drop in the regional cerebral blood flow (Day 7: n=1, Day 14: n=3, 1-month: n=1) and 1 mouse from the Day 14 group had to be excluded as the clamp time on the carotid artery was greater than 5 minutes.

6.3.2 Effect of tMCAo on body weight up to 1 month after stroke induction

In Chapter 4 of this thesis, we showed that tMCAo (40 minutes) mice experience profound weight loss during the first 3 days after stroke induction. In this Chapter, we wanted to investigate whether the effect of stroke on body weight persists beyond this acute phase by measuring body weights in sham and 40-minute tMCAo mice up to 1 month after stroke (i.e., mice in the 1-month group described in Section 6.2.1). Baseline body weights were comparable between sham and tMCAo mice (Sham: 28±0.66 versus tMCAo: 29±0.63, grams, Table 6-1, $p>0.05$). As illustrated in Figure 6-2, tMCAo mice weighed significantly less than sham mice on day 1, 3, 7, and 14, whereas body weights were not statistically different on day 21 or 1 month. Recovery of body weight started on day 4 in both sham and tMCAo mice, however, body weights in tMCAo mice did not stabilise until >21 days post-surgery.

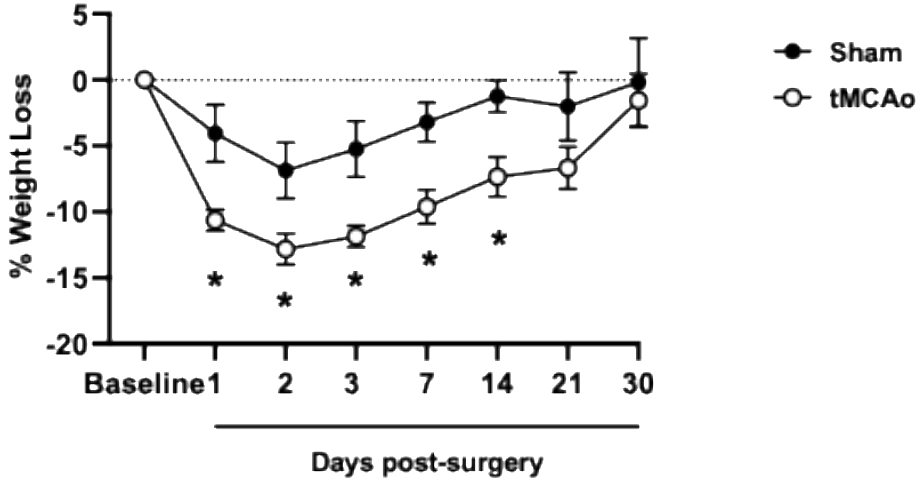

Figure 6-2 Change in body weight over 1 month in mice after transient middle cerebral artery occlusion (tMCAo) and sham surgery. Body weights were recorded before surgery (baseline) and daily thereafter until day 30. Body weight loss is expressed as % weight loss relative to baseline. Data expressed as mean ± SEM. n=8 sham, n=8 tMCAo. *p<0.05, two-way ANOVA followed by Šídák's multiple comparisons test.

6.3.3 Effect of tMCAo on skeletal muscle mass up to 1 month after stroke induction

Skeletal muscle mass was assessed in separate groups of sham and tMCAo mice on days 1, 3, 7, 14, and 1-month after surgery. Pre-surgery body weights of sham and tMCAo mice in each of the groups are given in Table 6-1. Weights of gastrocnemius and tibialis anterior muscles from both the ipsilateral and contralateral (stroke-affected) limbs of tMCAo mice on day 1 after stroke induction were comparable to those from sham mice, whereas weights of the gastrocnemius from both limbs of tMCAo mice were significantly lower on day 3 and day 7 (Figure 6-3A-B). Furthermore, the weights of tibialis anterior from both limbs of tMCAo mice were significantly lower on day 3 compared with shams (Figure 6-3B). As shown in Figure 6-4, there were no differences in muscle weights between tMCAo and sham mice on day 14 or 1 month after surgery.

Table 6-1 Pre-surgery body weight (unpaired t-test, p>0.05), given as mean ± sem. No statistical differences between sham and tMCAo mice within each of the experimental endpoints, p>0.05, unpaired t-test.

Experimental endpoint	Day 1		Day 3		Day 7		Day 14		1 month	
	sham	tMCAo	sham	tMCAo	sham	tMCAo	sham	tMCAo	sham	tMCAo
Body weight (g)	26±2.1	25±0.4	27±0.4	28±0.6	25±0.3	25±0.1	26±1	27±1	28±1	29±0.6

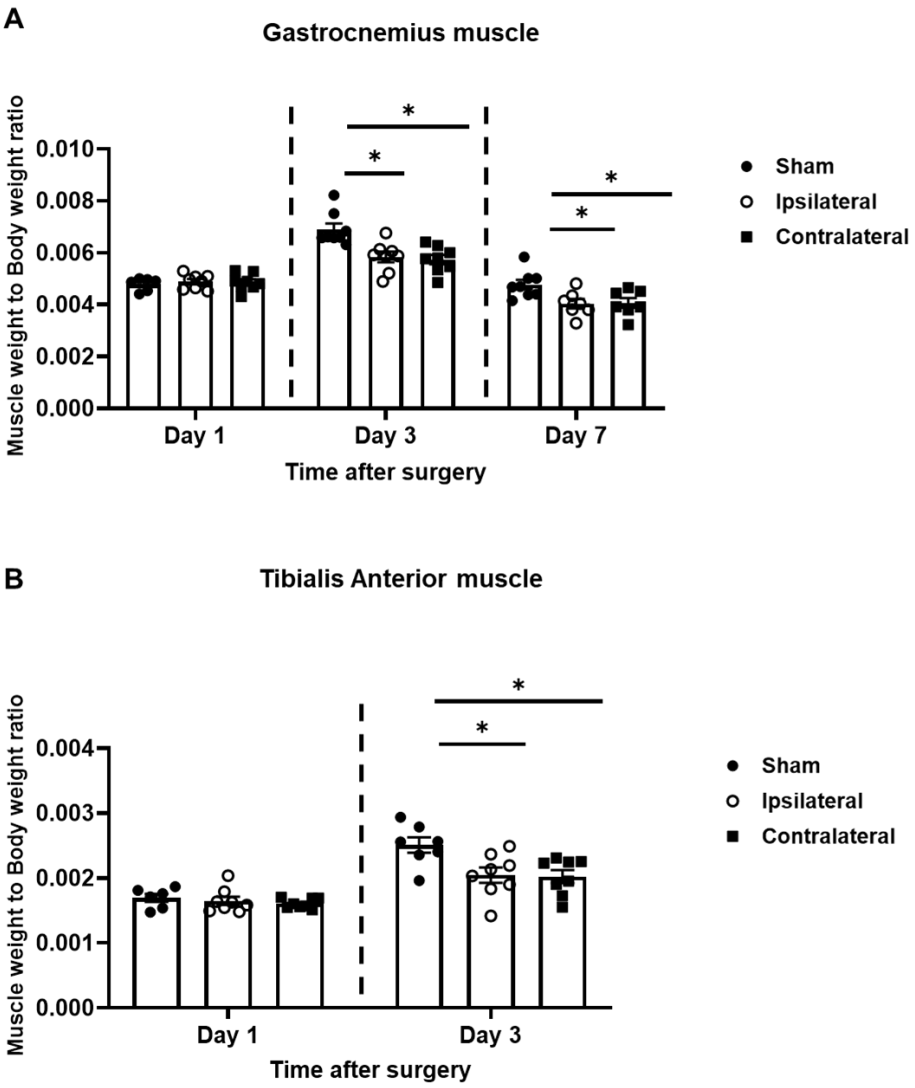

Figure 6-3 Skeletal muscle weights on day 1, 3 and 7 after transient middle cerebral artery occlusion (tMCAo) or sham surgery. *Ex vivo* weights of the gastrocnemius muscle **(A)** and tibialis anterior muscle **(B)** from sham (right hindlimb) and tMCAo mice (ipsilateral [right] and contralateral [left – stroke affected] on day 1, day 3, and day 7 post-surgery. Weights are normalised to body weight and given as mean ± SEM. **A**, Day 1: sham n=7, tMCAo n=8, Day 3: sham n=8, tMCAo n=8, Day 7 sham n=8, tMCAo n=7. **B**, n=7-8 per group for both time points. *p<0.05, one-way ANOVA followed by Šídák's multiple comparisons test.

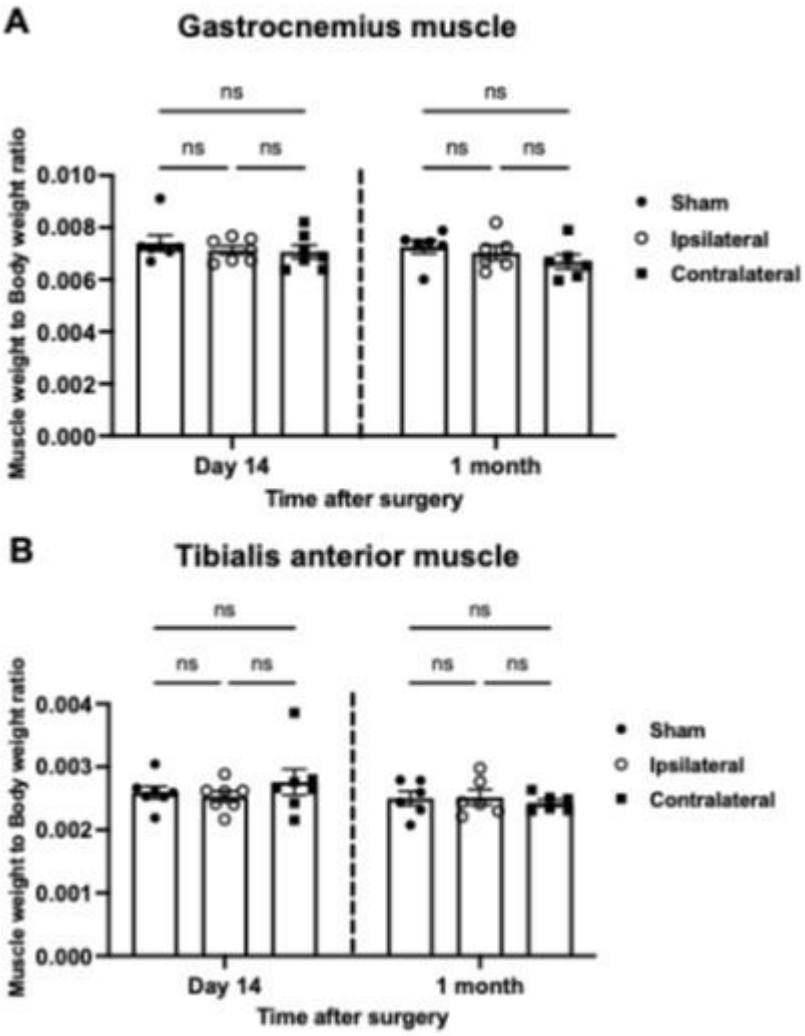

Figure 6-4 Skeletal muscle weights on day 14 or 1 month after transient middle cerebral artery occlusion (tMCAo) or sham surgery. *Ex vivo* weights of the gastrocnemius muscle (**A**) and tibialis anterior muscle (**B**) from sham (right hindlimb) and tMCAo mice (ipsilateral [right] and contralateral [left – stroke affected] on day 14, and 1-month post-surgery. Weights are normalised to body weight and given as mean ± SEM. **A** & **B**, Day 14, n=7 per group for both muscles, 1 month, n=6 per group for both muscles. ns= not significant, one-way ANOVA followed by Šídák's multiple comparisons test.

6.3.4 Effect of tMCAo on skeletal muscle cross sectional area on day 3 and day 7 after stroke induction

Muscle fibre cross-sectional area was quantified using approximately 200 muscle fibres of the tibialis anterior that were randomly selected from each mouse. As demonstrated in Figure 6-5A, there was an apparent shrinkage in the volume of muscle fibres on day 3 in both contralateral (stroke-affected) and ipsilateral muscles in comparison to the sham control. Our data showed a significant decrease in mean fibre cross-sectional area on day 3 post-cerebral ischaemia in the contralateral limb compared to the sham group ($p<0.05$). In contrast, there was no significant difference in the cross-sectional area of the ipsilateral limb, but there was a trend toward a reduction in cross-sectional area ($p=0.07$). On day 7, there were no statistical differences between tMCAo or sham mice for cross-sectional area (Figure 6-5B, $p=0.07$).

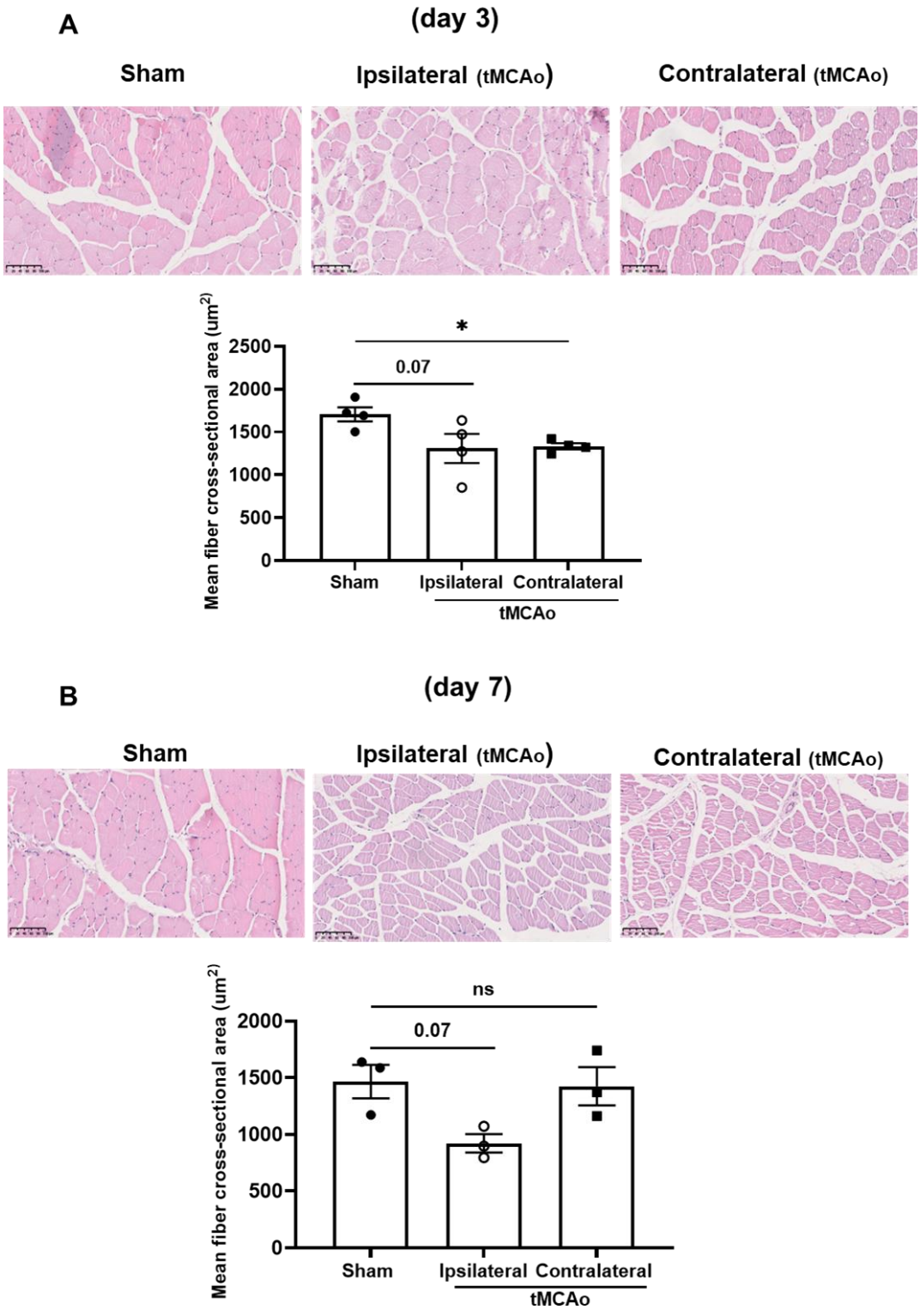

Figure 6-5 Fibre cross-sectional area of skeletal muscle from tMCAo or sham mice on day 3 and day 7 after surgery. Representative transverse sections of haematoxylin and eosin (H&E) staining of the Tibialis anterior from sham (right hind limb) and tMCAo mice (ipsilateral [right] and contralateral [left – stroke affected] on day 3 and day 7 after surgery. **A**, n=4 per group, **B**, n=3 per group. Data expressed as mean ± SEM. *p<0.05, ns= not significant, one-way ANOVA followed by Dunn's multiple comparisons test. Scale bar = 100 µm.

6.3.5 Validation of the housekeeping genes for RT-qPCR normalisation

The accuracy and reliability of data obtained by RT-qPCR significantly depend on normalising target gene expression to the internal control, commonly referred to as the housekeeping gene (Dheda et al., 2004). These genes are essential for basic cellular function and typically their expression remains stable in different cell types. The ideal housekeeping gene should be sufficiently expressed in the tissue of interest and show minimal changes under different experimental conditions (Thellin et al., 1999). However, previous studies have shown that some housekeeping genes experience changes in expression levels when samples undergo physiological alterations or receive external treatments (Deindl et al., 2002, Zhong and Simons, 1999, Glare et al., 2002). Therefore, selecting an appropriate housekeeping gene was essential for this study, given that the samples were collected from both stroke and sham-operated mice. Two housekeeping genes used by our laboratory were assessed: the ribosomal 18s (r18s) gene and the TATA-binding protein (TBP) gene. Compared to TBP, r18s was detected earlier in the skeletal muscle tissue. The C_t values for r18s were (mean ± SEM: 17.13±0.17 vs. 26.33±0.24). The standard deviation (SD) was calculated for each housekeeping gene to evaluate the variability in skeletal muscle (gastrocnemius) from naïve, sham, and 40-minute tMCAo mice. Both genes exhibited relatively low variability across the three groups (SD for r18s was 0.52 and TBP, 0.72). Since r18s was the most stable gene across the groups and it had higher C_t values than TBP, r18s was used as the internal control in subsequent experiments.

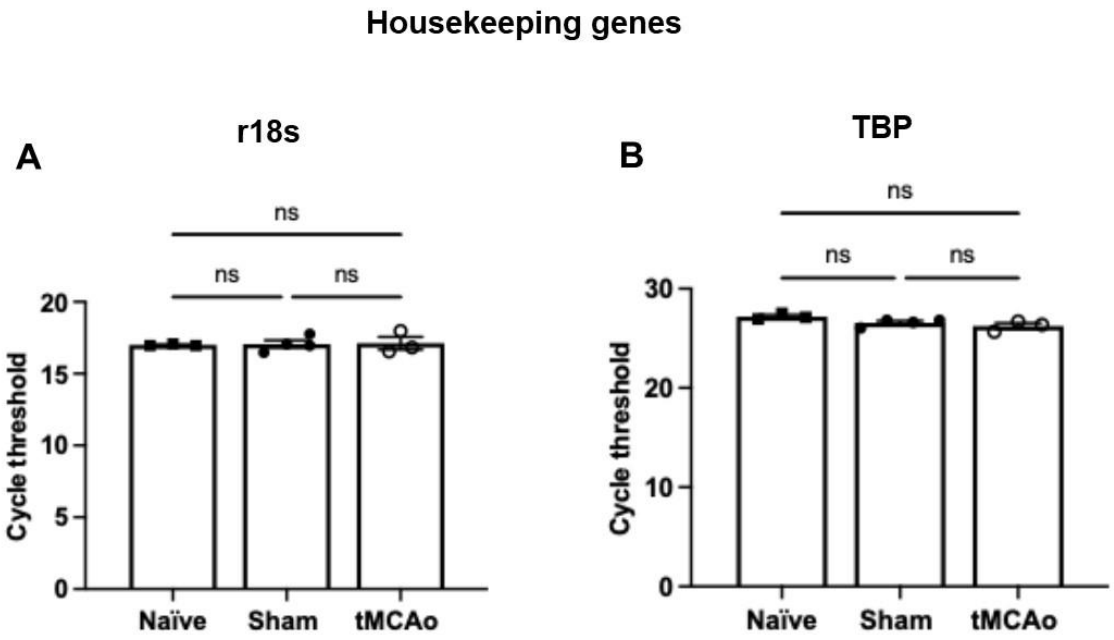

Figure 6-6 Cycle threshold (C_t) of the housekeeping genes in skeletal muscle obtained from naïve, sham and stroke-affected mice. Evaluation of the stability of *r18s* (**A**) and *TBP* (**B**) expression in the gastrocnemius muscle obtained from naïve, sham and tMCAo mice on day 3 after surgery. Data is acquired from n=3-4 biological replicates per group and expressed as mean ± SEM. ns=not significant, one-way ANOVA followed by Šídák's multiple comparisons test.

6.3.6 Effect of tMCAo on expression of genes involved in anabolic and catabolic signalling in skeletal muscle

Muscle atrophy can occur because of decreased protein synthesis and/or increased protein degradation, arising from an alteration in the catabolic/anabolic balance associated with muscle homeostasis. The aim of this work was to use SYBR Green RT-qPCR to determine if alterations to key genes involved in anabolic (*mTOR, AKT1, RPS6,* and *RPS6K*) and catabolic (*GsK3B, EIF4EBP-1, MSTN, FOXO1, TRIM63*, and *FBXO32*) signalling are associated with the muscle wasting we observed after tMCAo. We isolated gastrocnemius from sham and tMCAo (40 minutes) mice on days 1, 3, 7, 14, and 1-month post-surgery.

6.3.6.1 Day 1 and day 3 post-stroke induction

On day 1 post-stroke induction – a time point at which muscle mass was unchanged (Figure 6-3) - expression levels of genes involved in anabolic signalling - *AKT1, mTOR*, *AKT2, RPS6K and RPS6* - in gastrocnemius from the ipsilateral and contralateral hindlimbs of tMCAo mice were comparable to levels in sham mice (Figure 6-7A). With respect to catabolic genes, expression levels of *EIF4EBP-1* and *GsK3B* mRNA were significantly higher in the ipsilateral gastrocnemius of tMCAo mice compared to sham (Figure 6-7B). Furthermore, there was a significant increase (~4-fold) in *MuRF-1* mRNA in muscle from both hindlimbs of tMCAo mice (Figure 6-7B). However, there were no statistical differences between sham and tMCAo mice (both hindlimbs) for *FOXO-1, MSTN, or Atrogin-1.*

When muscle wasting becomes apparent on day 3 post-stroke induction (Figure 6-3), mRNA expression levels of *RPS6 and RPS6K* were significantly higher only in gastrocnemius from the contralateral hindlimb of tMCAo mice compared to sham mice (Figure 6-8A). However, levels of the other genes involved in anabolic signalling, *AKT1, mTOR, or AKT2*, were comparable between the groups. Consistent with day 1 post-surgery, there was evidence of upregulated levels of genes involved in catabolic signalling (Figure 6-8 B). Specifically, we found that *EIF4EBP-1* was significantly higher in gastrocnemius from both hindlimbs of tMCAo mice, whereas *FOXO1* and *GsK3B* were significantly higher only in muscles from the contralateral hindlimb. There were no statistical differences between the groups for expression levels of *MSTN, TRIM63*, or *FBXO32* mRNA (Figure 6-8B).

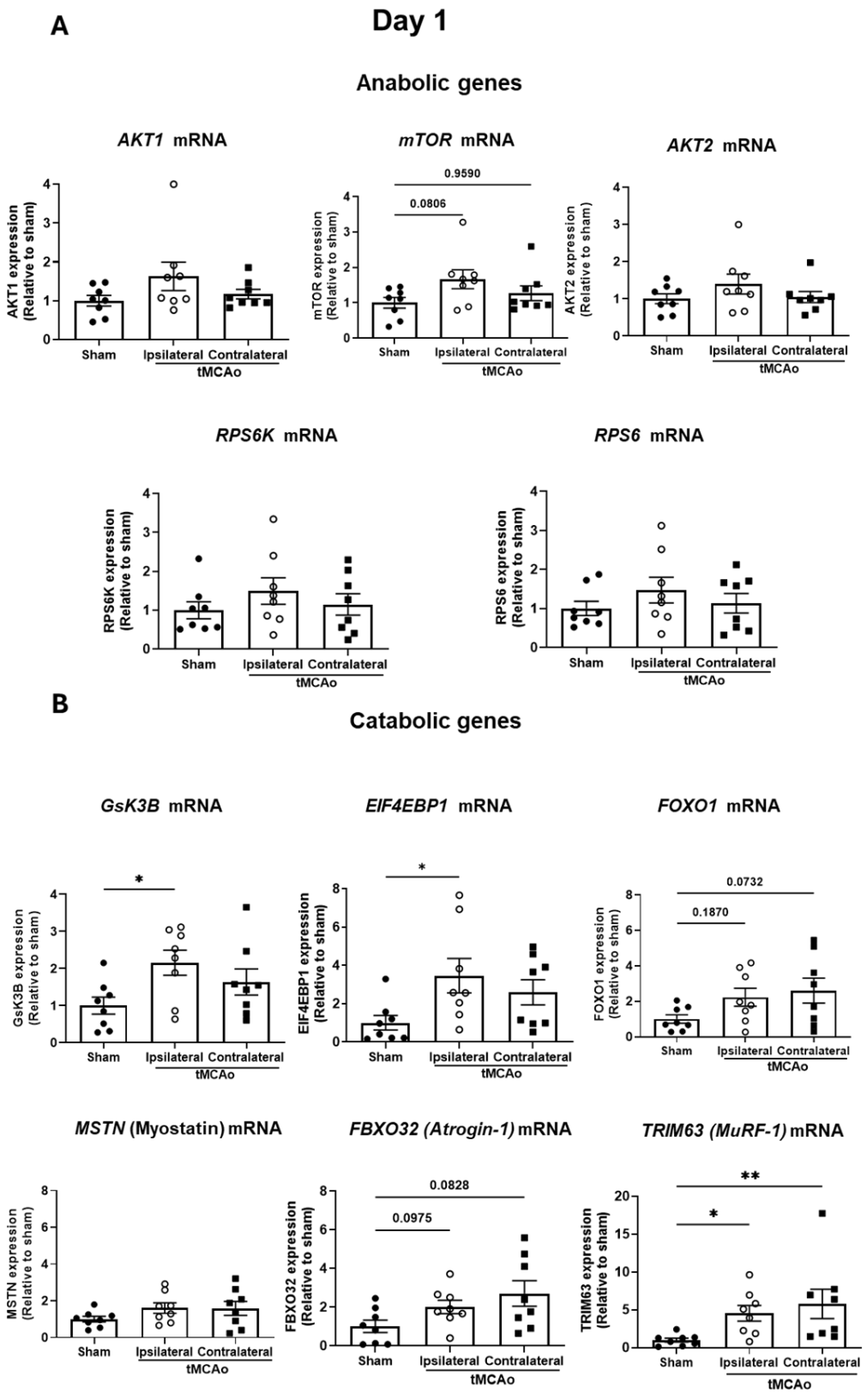

Figure 6-7 Expression levels of key anabolic and catabolic signalling genes on Day 1 after sham or 40-minute transient middle cerebral artery occlusion (tMCAo) surgery. mRNA expression levels of *AKT1, mTOR, AKT2, RPS6,* and *RPS6K* anabolic genes *(***A**); *and GsK3B, EIF4EBP-1, FOXO1, MSTN, FBXO32* and *TRIM63* catabolic genes *(***B***)* were assessed in the gastrocnemius from sham (right hindlimb) and tMCAo mice (ipsilateral [right] and contralateral [left – stroke affected]. For all genes, values were normalised to the housekeeping gene *r18s* and expressed relative to sham using the $2^{-\Delta\Delta Ct}$ method. Data is expressed as mean ± SEM. n=8 per group. *p<0.05, **p<0.01, one-way ANOVA followed by Dunnett's multiple comparisons test.

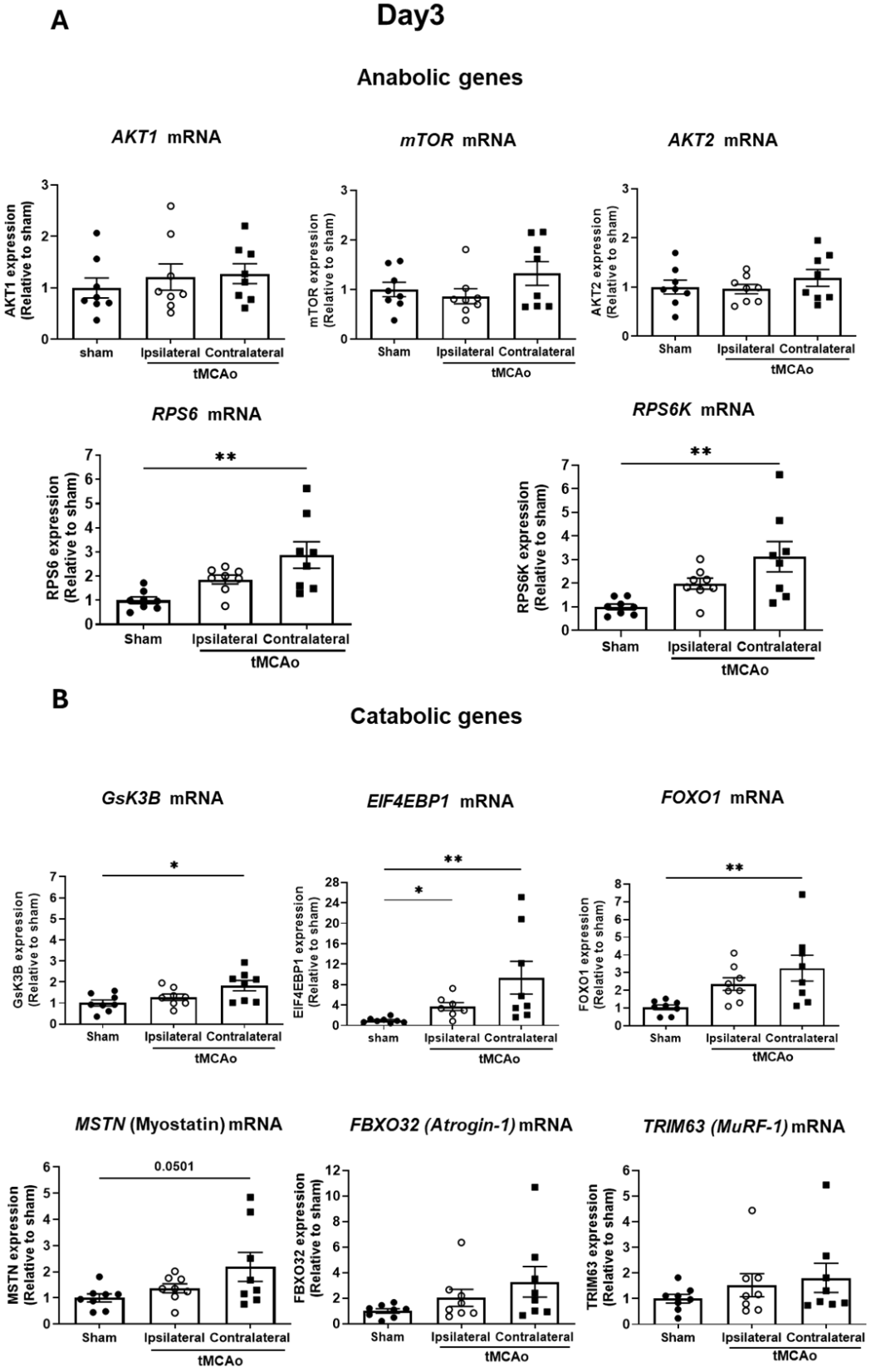

Figure 6-8 Expression levels of key anabolic and catabolic signalling genes on day 3 after sham or 40-minute transient middle cerebral artery occlusion (tMCAo) surgery. mRNA expression levels of *AKT1, mTOR, AKT2, RPS6,* and *RPS6K* anabolic genes *(***A**); *and GsK3B, EIF4EBP-1, FOXO1, MSTN, FBXO32* and *TRIM63* catabolic genes *(***B***)* were assessed in the gastrocnemius from sham (right hindlimb) and tMCAo mice (ipsilateral [right] and contralateral [left – stroke affected]. For all genes, values were normalised to the housekeeping gene *r18s* and expressed relative to sham using the $2^{-\Delta\Delta Ct}$ method. Data is expressed as mean ± SEM, n=8 per group. *p<0.05, **p<0.01, one-way ANOVA followed by Dunnett's multiple comparisons test.

6.3.6.2 Day 7, day 14, and 1-month post-surgery

As depicted in Figure 6-9 A, on day 7 post-surgery – a time point when muscle wasting persisted – expression levels of mRNA for *AKT1* and *mTOR* were significantly lower in the gastrocnemius from the ipsilateral hindlimb of tMCAo mice compared with sham. However, there were no statistical differences between the groups with respect to the other anabolic genes – *AKT2, RPS6, and RPS6K*. Similarly, for the genes involved in catabolic signalling, apart from *Atrogin-1* which was significantly lower in the ipsilateral hindlimb of tMCAo mice, there were no statistical differences between the groups for the other catabolic genes (Figure 6-9B).

Lastly, consistent with our finding of no differences in muscle mass on day 14 or 1 month in mice after tMCAo or sham surgery (Figure 6-4), there were no statistically significant differences between tMCAo and sham mice with respect to the expression of anabolic or catabolic genes at either time point (data for 1 month not shown) (Figure 6-10).

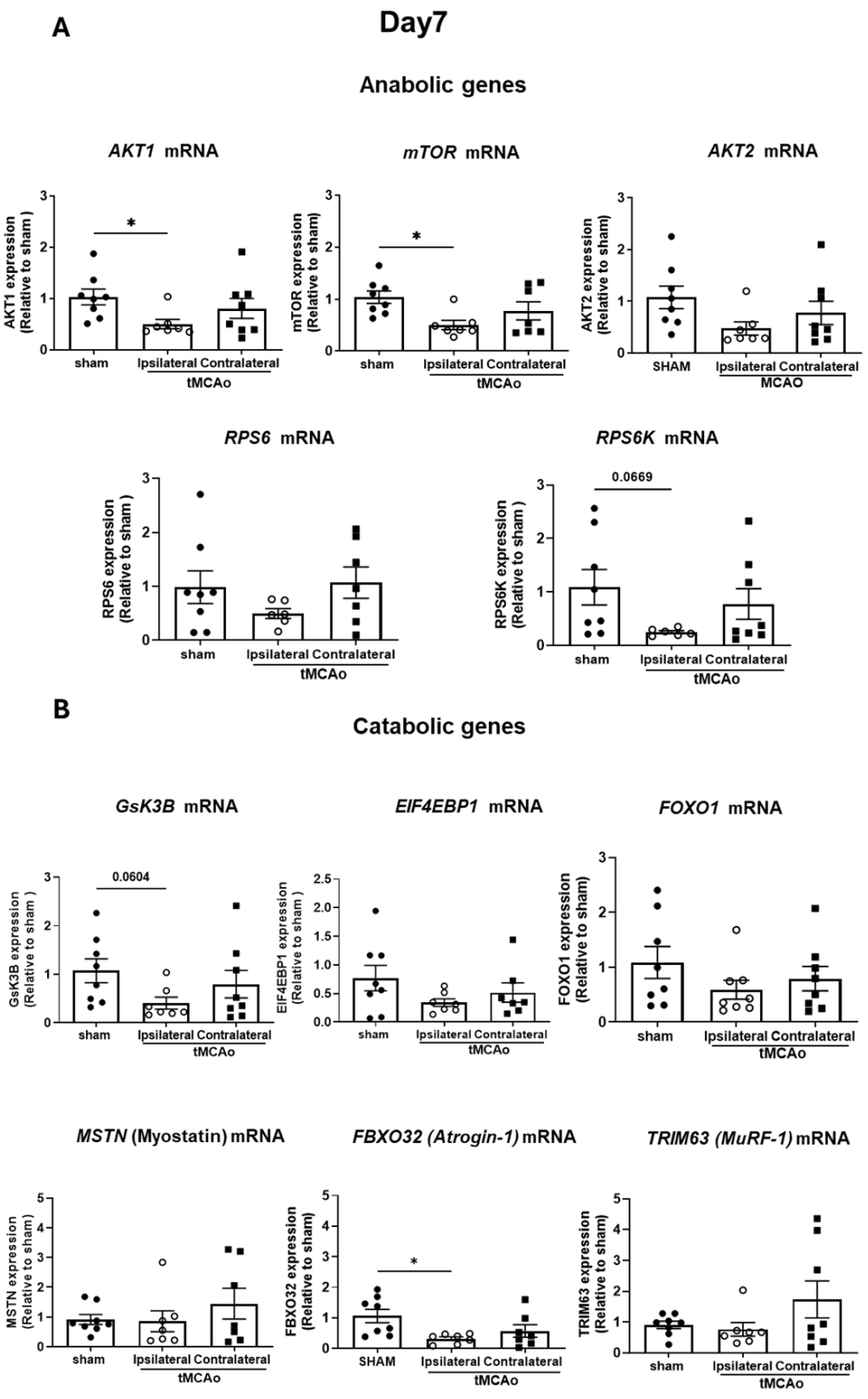

Figure 6-9 Expression levels of key anabolic and catabolic signalling genes on day 7 of sham or 40-minute transient middle cerebral artery occlusion (tMCAo) surgery. mRNA expression levels of *AKT1, mTOR, AKT2, RPS6,* and *RPS6K* anabolic genes *(***A**); *and GsK3B, EIF4EBP-1, FOXO1, MSTN, FBXO32* and *TRIM63* catabolic genes *(***B***)* were assessed in the gastrocnemius from sham (right hindlimb) and tMCAo mice (ipsilateral [right] and contralateral [left – stroke affected]. For all genes, values were normalised to the housekeeping gene *r18s* and expressed relative to sham using the $2^{-\Delta\Delta Ct}$ method. Data is expressed as mean ± SEM, sham n=8, tMCAo ipsilateral n=7, tMCAo contralateral n=8. *p<0.05, one-way ANOVA followed by Dunnett's multiple comparisons test.

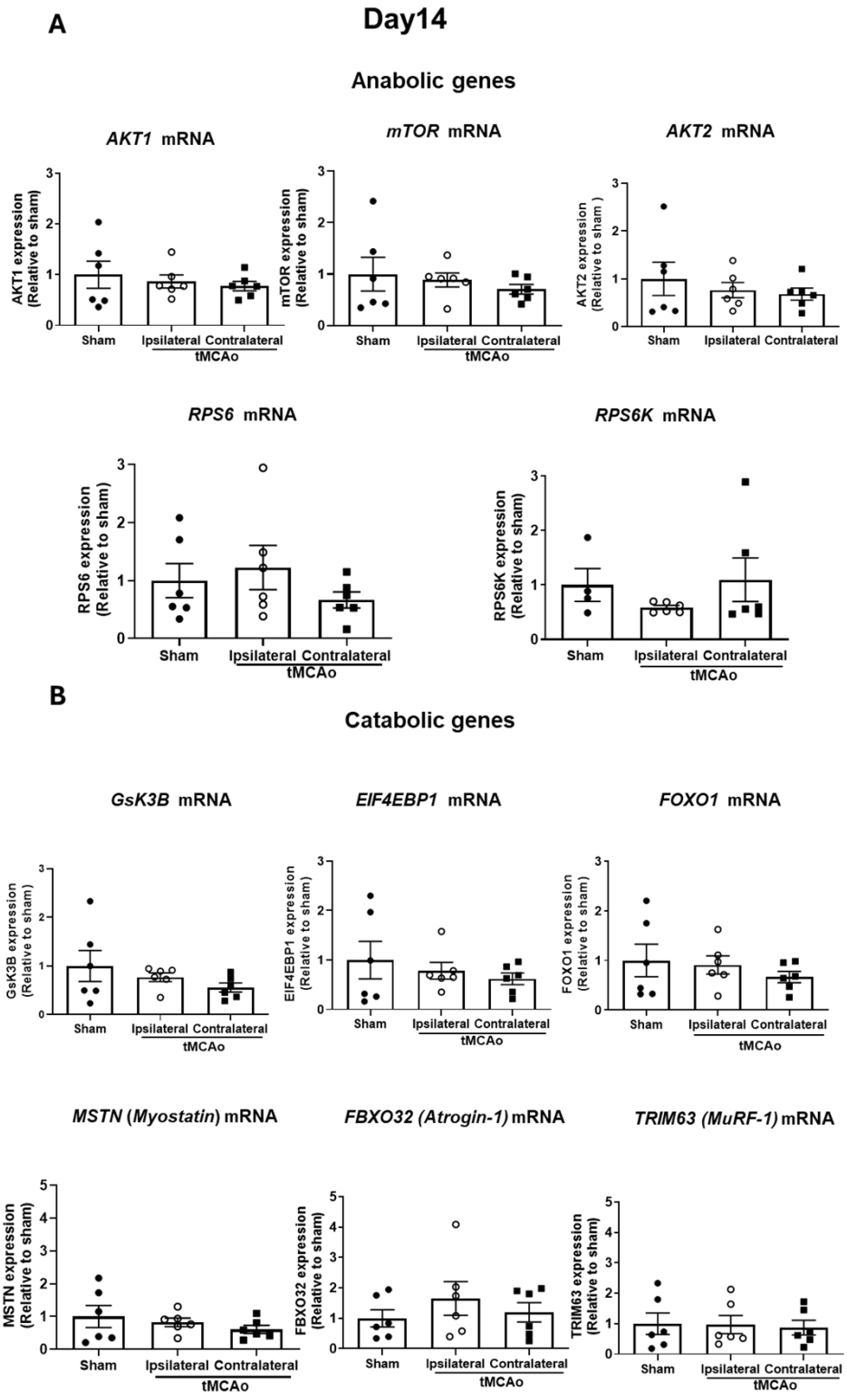

Figure 6-10 Expression levels of key anabolic and catabolic signalling genes at day 14 of sham or 40-minute transient middle cerebral artery occlusion (tMCAo) surgery. mRNA expression levels of *AKT1, mTOR, AKT2, RPS6,* and *RPS6K* anabolic genes *(***A**); *and GsK3B, EIF4EBP-1, FOXO1, MSTN, FBXO32* and *TRIM63* catabolic genes *(***B***)* were assessed in the gastrocnemius from sham (right hindlimb) and tMCAo mice (ipsilateral [right] and contralateral [left – stroke affected]. For all genes, values were normalised to the housekeeping gene *r18s* and expressed relative to sham using the $2^{-\Delta\Delta Ct}$ method. Data is expressed as mean ± SEM, n=6 per group. One-way ANOVA followed by Dunnett's multiple comparisons test.

Table 6-2 Summary of changes in gene expression after tMCAo

Gene	Day 1		Day 3		Day 7		Day 14		1 month	
	Ipsi	Contra	Ipsi	Contra	Ipsi	Contra	Ipsi	Contra	Ipsi	Contra
AKT1	=	=	=	=	-	=	=	=	=	=
AKT2	=	=	=	=	=	=	=	=	=	=
mTOR	+*	=	=	=	-	=	=	=	=	=
RPS6K	=	=	=	+	-*	=	=	=	=	=
RPS6	=	=	=	+	=	=	=	=	=	=
GsK3B	+	=	=	+	-*	=	=	=	=	=
EIF4EBP1	+	=	+	+	=	=	=	=	=	=
FOXO1	=	+*	=	+	=	=	=	=	=	=
MSTN	=	=	=	+*	=	=	=	=	=	=
FBXO32	+*	+*	=	=	-	=	=	=	=	=
TRIM63	+	+	=	=	=	=	=	=	==	

Abbreviations: Ipsi, ipsilateral; Contra, contralateral; +, upregulation; -, downregulation; *, trend; =, no change

6.3.7 Effect of tMCAo on gene expression of inflammatory cytokines involved in muscle wasting

To explore potential upstream mediators of muscle wasting after tMCAo, we next measured mRNA expression levels of cytokines - *TNF-α*, *IL-6*, and *IL-1β* – in gastrocnemius from sham and tMCAo (40 minutes) mice on day 3 and day 7 after stroke induction (time points when muscle wasting is evident). Our data revealed a statistically significantly higher expression level of *TNF-α* in gastrocnemius from both contralateral and ipsilateral hindlimbs of tMCAo compared to sham on day 3 after tMCAo (Figure 6-11A). Moreover, the expression of *TNF-α* was significantly higher in the gastrocnemius from the contralateral limb compared to the ipsilateral. In contrast, no statistical difference was observed between groups for *TNF-α* mRNA on day 7 after tMCAo (Figure 6-11A'). Similarly, *IL-6* mRNA expression in gastrocnemius was comparable between sham and tMCAo mice (both limbs) on day 3 and day 7 post-surgery (Figure 6-11B-B'). We also attempted to measure expression levels of mRNA for *IL-1β*; however, this cytokine was undetectable in muscle samples from sham and tMCAo mice at both time points.

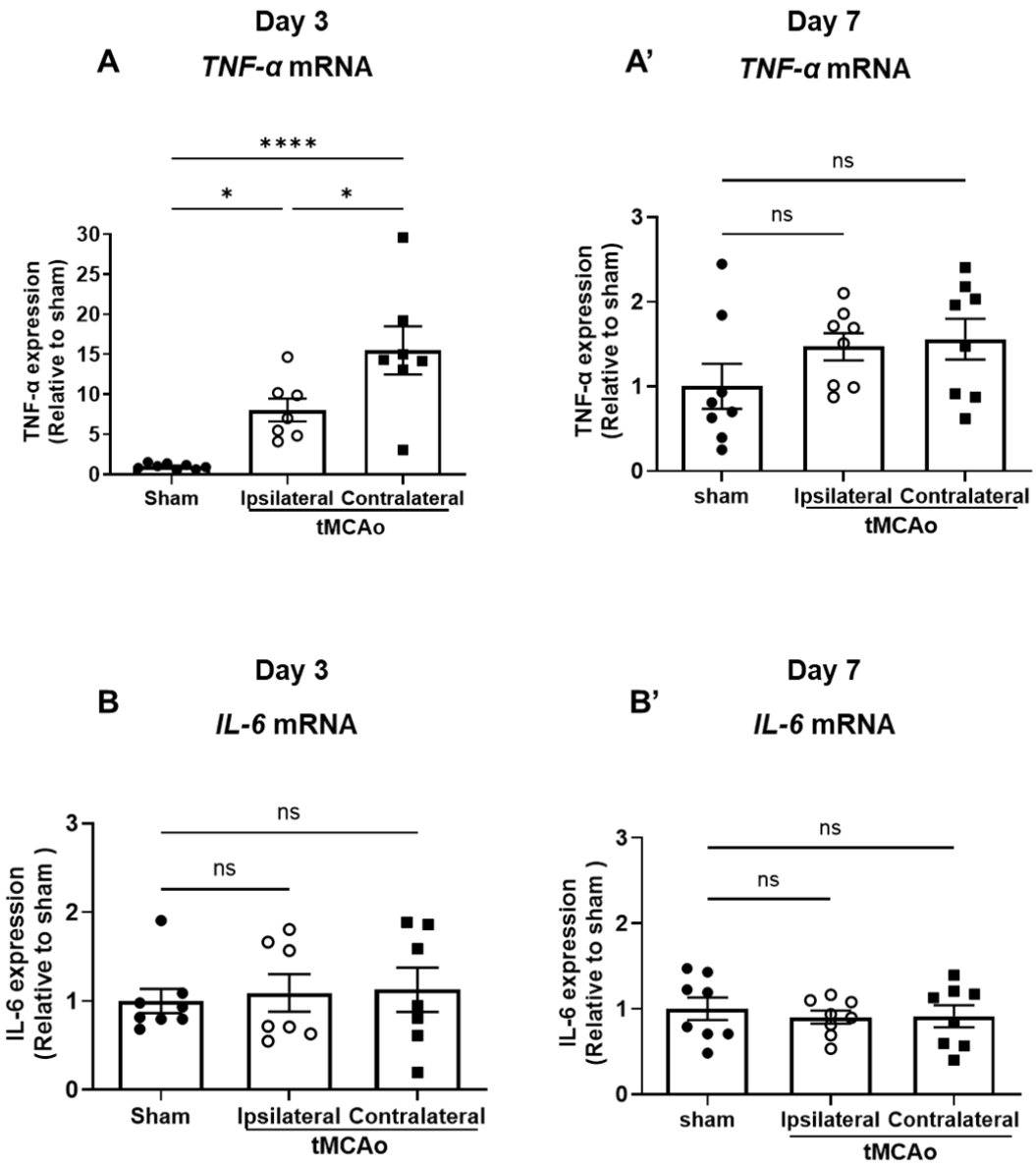

Figure 6-11 mRNA expression of cytokines on day 3 and day 7 after sham or 40-minute transient middle cerebral artery occlusion (tMCAo) surgery. mRNA expression of *TNF-α* at day 3 (**A**) and day 7 (**A'**), *IL-6* at day 3 (**B**) and day 7 **(B'**). For all genes, values were normalised to the housekeeping gene *r18s* and expressed relative to sham using the $2^{-\Delta\Delta Ct}$ method. Data is expressed as mean ± SEM, n=7-8 per group. *p<0.05, ****p<0.0001, ns=not significant, one-way ANOVA followed by Šídák's multiple comparisons test.

6.3.8 Effect of ageing on expression of genes involved in anabolic and catabolic signalling in skeletal muscle

An aim of this study was to determine whether stroke-induced muscle changes resemble those observed in natural age-related sarcopenia. As shown in Figure 6-12A, weights of gastrocnemius and tibialis anterior muscles were significantly lower in naïve (non-stroke) aged mice compared to muscles collected from naïve young mice. However, expression levels of anabolic genes - *mTOR*, *AKT-1*, and *RPS6* – in gastrocnemius muscle were comparable between young and aged mice (Figure 6-12B), suggesting that age-related muscle loss in this cohort of aged mice may not be primarily driven by suppression of protein synthesis pathways at the transcriptional level. With respect to catabolic genes, mRNA expression levels of *FOXO, FBXO32* and *TRIM63* were significantly higher in gastrocnemius from aged mice, whereas levels of *MSTN, GsK3B,* and *EIF4EBP-1* were comparable between the two groups (Figure 6-12C).

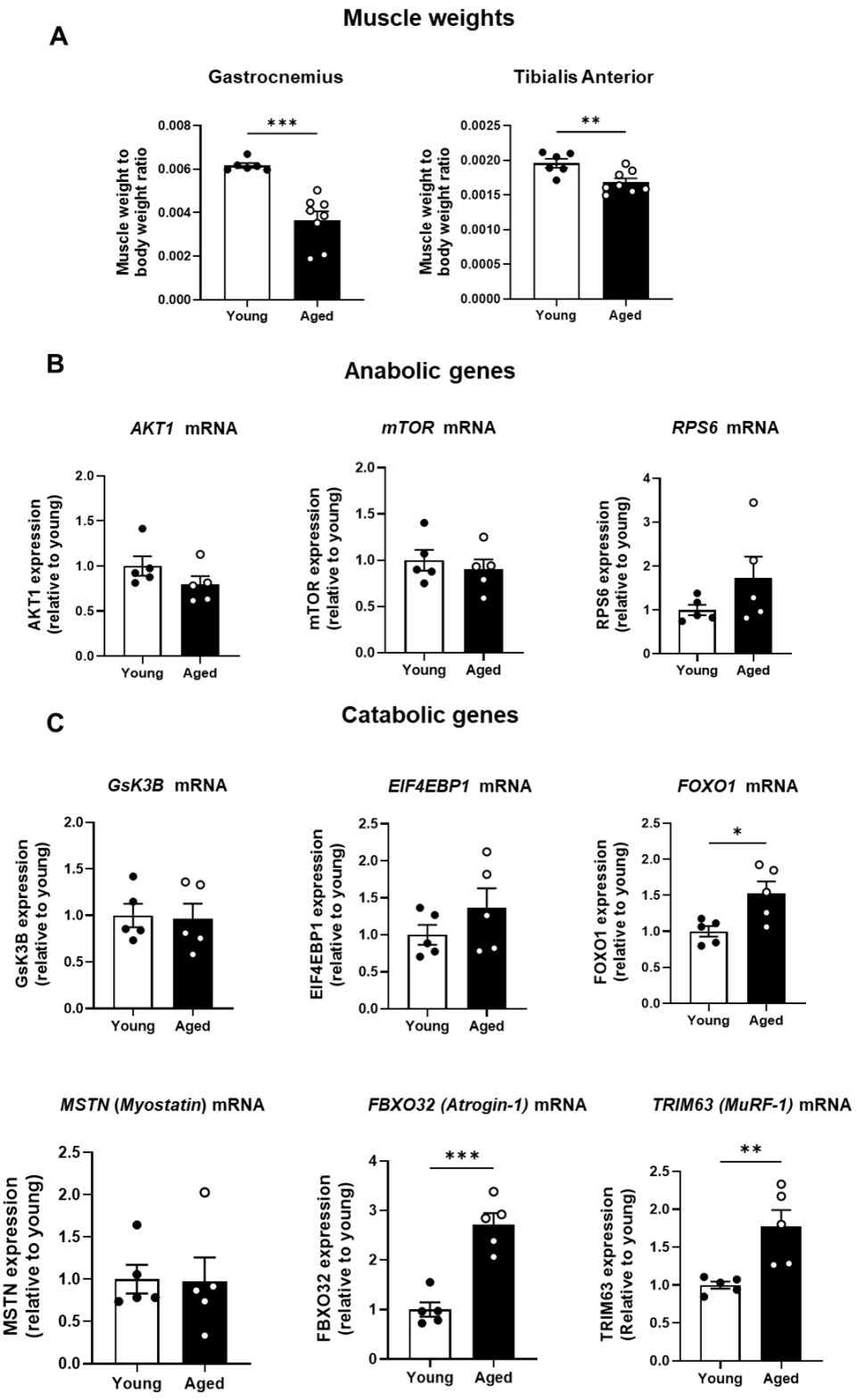

Figure 6-12 Muscle weights and expression levels of key anabolic and catabolic signalling genes in young and aged naïve mice. Ex vivo weights of the gastrocnemius and the tibialis anterior muscles from the right hindlimb of young and aged mice (**A**). Weights are normalised to body weight and given as mean ± SEM, n=6-8 per group, **p<0.01, ***p<0.001, unpaired Student's t-test. mRNA expression levels of *AKT1, mTOR,* and *RPS6 (***B***); and GsK3B, EIF4EBP-1, FOXO1, MSTN, FBXO32* and *TRIM63 (***C***)* in gastrocnemius from the right hindlimb of young and aged mice. For all genes, values were normalised to the housekeeping gene *r18s* and expressed relative to young mice using the $2^{-\Delta\Delta Ct}$ method. Data is expressed as mean ± SEM, n=5 per group, *p<0.05, **p<0.01, ***p<0.001, Mann-Whitney test.

6.3.9 Effect of tMCAo on expression of genes involved in anabolic and catabolic signalling in aged mice

Given that both stroke and ageing negatively impact muscle mass and function, whether through age-related sarcopenia or disuse and paresis after stroke onset, and because stroke is more common among the elderly, it is essential to examine the expression levels of genes involved in muscle homeostasis in aged mice after stroke. Our data revealed that expression levels of genes involved in anabolic signalling - *AKT1, mTOR, AKT2, RPS6K and RPS6* - in gastrocnemius from the ipsilateral and contralateral hindlimbs of aged tMCAo mice were not significantly different from those of sham aged mice (Figure 6-13A). With respect to catabolic genes, expression levels of *EIF4EBP-1* mRNA were significantly higher in the ipsilateral and contralateral gastrocnemius of aged tMCAo mice compared to sham (Figure 6-13B). Similarly, there was a significant increase (~3-fold) in *Atrogin-1* mRNA in muscle from both hindlimbs of aged tMCAo mice compared to aged sham controls (Figure 6-13B). However, *TRIM63* mRNA was significantly higher (~3-fold) in the ipsilateral muscle of aged tMCAo compared to aged sham (Figure 6-13B).

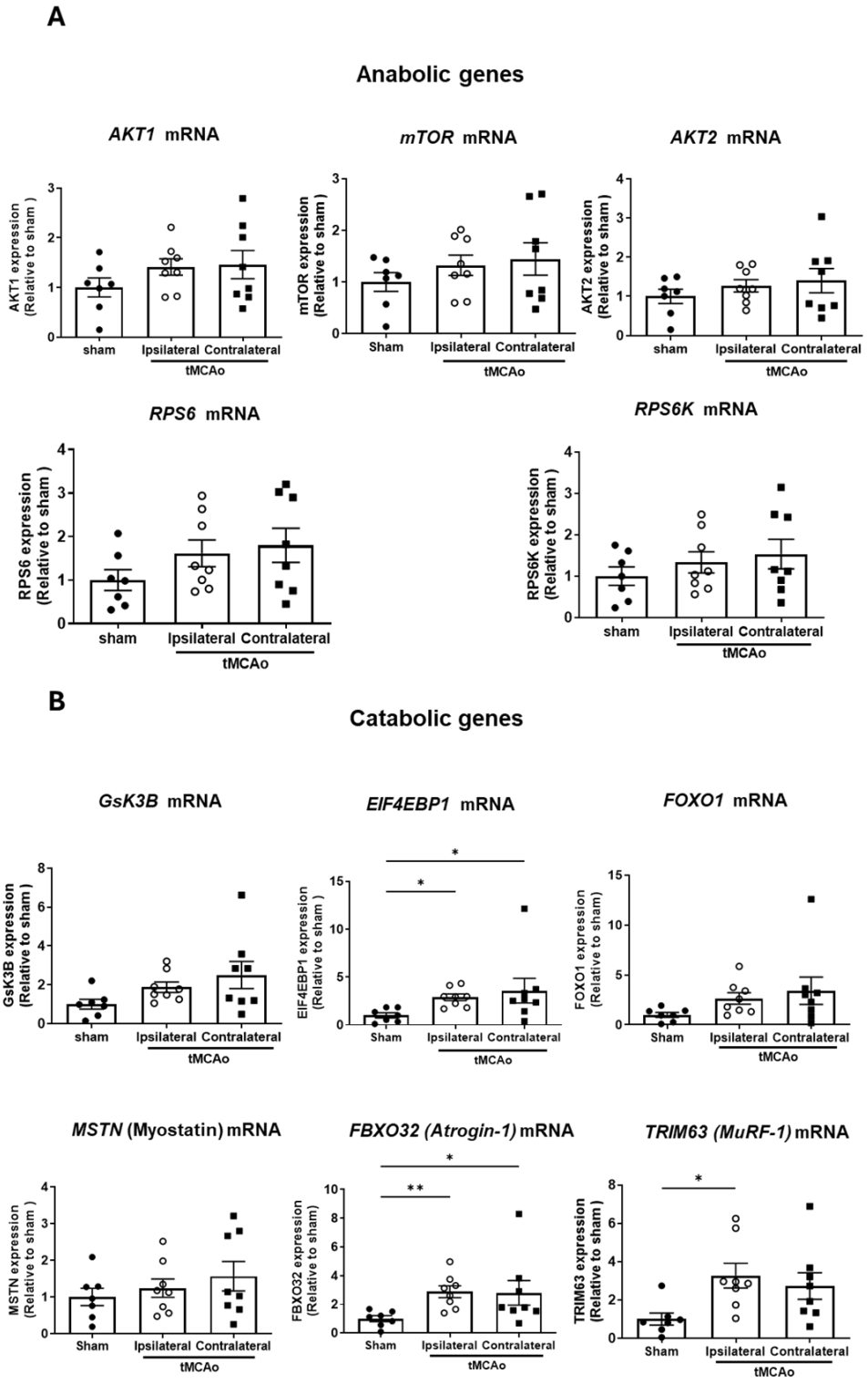

Figure 6-13 mRNA expression of key anabolic and catabolic signalling genes on day 1 after transient middle cerebral artery occlusion (tMCAo) or sham surgery in aged mice. mRNA expression levels of *AKT1, mTOR, AKT2, RPS6,* and *RPS6K* anabolic genes *(***A**); *and GsK3B, EIF4EBP-1, FOXO1, MSTN, FBXO32* and *TRIM63* catabolic genes *(***B***)* were assessed in the gastrocnemius from sham (right hindlimb) and tMCAo mice (ipsilateral [right] and contralateral [left – stroke affected]. For all genes, values were normalised to the housekeeping gene *r18s* and expressed relative to sham using the $2^{-\Delta\Delta Ct}$ method. Data is expressed as mean ± SEM, n=7-8 per group. *p<0.05, **p<0.01, one-way ANOVA followed by Dunnett's multiple comparisons test.

6.4 Discussion

The initial aims of this study were to investigate the effects of cerebral ischaemia on muscle wasting and to examine the underlying molecular mechanisms. The muscle weight, cross-sectional area, and the transcription levels of key genes involved in muscle homeostasis were assessed at different time points after tMCAo. We showed that the muscle mass loss was significant on days 3 and 7 post-experimental stroke, whereas by day 14, muscle weights in tMCAo mice were comparable to shams, inferring that muscle mass had been restored by this time. The expression profile of genes regulating muscle homeostasis revealed that some catabolic genes, such as MuRF-1, were upregulated on day 1 after experimental stroke. On day 3, the upregulation of some catabolic genes, including *FOXO1* and *MSTN,* was observed clearly in the contralateral limb of stroke-affected mice. Consistent with the muscle weights, no change in gene expression was observed on day 14 or 1 month after tMCAo in mice compared to the sham control. To investigate potential upstream mediators of this early catabolic response, we also assessed the expression of the pro-inflammatory cytokines *TNF-α* and *IL-6*. Notably, *TNF-α* was significantly upregulated on day 3 post-stroke, while no significant changes were detected on day 7. *IL-6*, on the other hand, did not show any significant transcriptional changes at either time point. Taken together, these findings suggest a transient inflammatory response, particularly mediated by *TNF-α*, may contribute to the early activation of muscle degradation pathways following cerebral ischaemia.

Although skeletal muscle atrophy is a common consequence of stroke and proper skeletal muscle function is crucial for restoring physical abilities in patients who have had a stroke (English et al., 2010), the underlying molecular mechanisms remain incompletely understood. One potential explanation involves an imbalance between protein synthesis and breakdown. Based on this, we hypothesised that stroke induces an upregulation of catabolic gene expression alongside a downregulation of anabolic gene expression, thereby contributing to muscle wasting. Our findings indicate that while muscle mass remained unchanged on day 1 following experimental stroke induced by tMCAo in mice, a significant loss of mass (weight and cross-sectional area) was observed by days 3 and 7 when compared to sham-operated controls. Notably, gene expression analysis at the early time point (day 1) revealed a significant upregulation of the key atrophy-

related gene *MuRF-1* in both the contralateral and ipsilateral limbs of stroke-affected mice. Additionally, there was a clear trend toward increased expression of *Atrogin-1*, although this did not achieve statistical significance. By day 3, the expression of both *MuRF-1* and *Atrogin-1* remained elevated, albeit without statistical significance. *MuRF-1* and *Atrogin-1* are muscle-specific E3 ubiquitin ligases that are typically expressed at low levels in healthy, resting skeletal muscle. However, numerous studies have shown that their transcription levels are markedly increased in conditions or diseases involving muscle atrophy, including disuse, chronic kidney disease, cancer and chronic obstructive pulmonary disease (Yoshida and Delafontaine, 2015, Bodine and Baehr, 2014). In line with these observations, our results demonstrate early transcriptional upregulation of at least one of these genes following stroke. This upregulation was accompanied by increased expression of the transcription factor *FOXO1,* which has been previously implicated in the regulation of both MuRF-1 and Atrogin-1 (Sandri et al., 2004), further supporting its role in stroke-induced muscle atrophy. Interestingly, the upregulation of *FOXO1* was statistically significant only in the contralateral limb on days 1 and 3 post-stroke, whereas *MuRF-1* and *Atrogin-1* were upregulated in both limbs. This may suggest that additional transcriptional regulators may be involved. One likely candidate is NF-κB, which has also been shown to induce the expression of these atrogenes (Bodine et al., 2001a, Bonaldo and Sandri, 2013). Supporting this hypothesis, Stitt et al. (2004) reported that activated *FOXO1* is necessary but not sufficient for the induction of *MuRF-1* and *Atrogin-1* in cultured myotubes, indicating the involvement of other transcription factors (Stitt et al., 2004). Furthermore, a substantial body of literature implicates *NF-κB* in muscle atrophy under various conditions, including disuse (Van Gammeren et al., 2009), denervation (Mourkioti et al., 2006), and cachexia (Cai et al., 2004), reinforcing the notion that multiple transcriptional pathways may act to drive muscle degradation following stroke.

It is worth noting that myostatin is primarily secreted by skeletal muscle and acts as a negative regulator of muscle growth. It exerts its effects through binding to activin receptors, leading to the initiation of a signalling cascade, causing inhibition of myoblast differentiation and proliferation (McPherron et al., 1997). *Myostatin* expression level is found to be upregulated in pathological conditions associated with muscle wasting, such as cancer, heart disease and HIV. Moreover,

it has been reported that systemic administration of myostatin caused cachexia in rodents (Zimmers et al., 2002, McPherron et al., 1997). It also acts by inhibiting *AKT1* activation, resulting in decreased protein synthesis and reduced muscle mass (Trendelenburg et al., 2009). In our study, we observed no significant change in *myostatin* expression on day 1 post-stroke; however, by day 3, its expression was upregulated in the contralateral limbs. This pattern suggests that signalling pathways inhibiting protein synthesis, such as the myostatin/Smad axis, may be activated later than those involved in protein degradation on day 1. Our findings, therefore, imply a sequential activation of muscle-wasting mechanisms following stroke, with early engagement of the ubiquitin–proteasome system (UPS), followed by delayed activation of the myostatin pathway.

It is worth noting that there was upregulation of *EIF4EBP1* and *GsK3B* on day 1 after experimental stroke in both limbs, but it was significant only in the ipsilateral limb (non-affected side). Notably, both *GsK3B* and *EIF4EBP1* are considered negative regulators of protein synthesis. GsK3B is a downstream target of *AKT1*, which acts to inhibit protein synthesis through suppression of translation initiation (Vyas et al., 2002). Under normal conditions, *AKT1* seems to enhance protein synthesis in many ways. One way *AKT1* phosphorylates *GsK3B*, leading to its inhibition which promotes translation initiation for protein synthesis (Vyas et al., 2002). *EIF4EBP1* is a downstream target of the *mTOR* pathway. Activation of *mTOR* enhances protein synthesis through the phosphorylation and inactivation of *EIF4EBP1*, a translational repressor, and through the phosphorylation and activation of *RPS6k* which promotes ribosomal activity (Hay and Sonenberg, 2004). Therefore, upregulation of *GSK3B* and *EIF4EBP1* suggests a suppression of the protein synthesis pathways early after experimental stroke. However, the upregulation of these two genes in the ipsilateral limb is quite interesting, as one might expect molecular changes to be more prominent in the contralateral limb given the likely additive contribution of neuromuscular disruption (denervation) to muscle wasting post-stroke (the stroke-affected side). This observation supports the notion that early post-stroke molecular alterations may be mediated by systemic mechanisms rather than localised effects alone. Furthermore, although genes associated with protein degradation, such as *MuRF-1* and *Atrogin-1*, were also upregulated on day 1, no significant change in muscle mass was observed at this time point. This potentially indicates that measurable muscle

atrophy likely requires more than 24 hours to develop and that early gene expression changes represent the initiation of catabolic processes that manifest structurally at later stages.

On day 3, our data showed a significant increase in the expression of RPS6K and RPS6 in the contralateral limbs. Since they are involved in the protein synthesis pathway through the regulation of mRNA translation, this upregulation may potentially reflect a compensatory mechanism aimed at restoring protein synthesis. Interestingly, a generalised downregulation (although not always supported by statistical differences) of both anabolic and catabolic pathways was observed on day 7 after experimental stroke, which may suggest the possibility of a shift to a transcriptional suppression state as an adaptive response due to prolonged stress as a result of cerebral ischaemia. However, this is just a speculation, and further studies are needed to support the observation.

On day 14 and 1-month post-stroke, muscle mass in tMCAo mice was comparable to that of sham-operated controls, and the gene expression profile appeared to return to baseline. Specifically, the expression levels of the key atrophy-related genes MuRF-1 and Atrogin-1 did not differ significantly from those observed in the sham group. Our findings up to day 3 post-stroke are in line with gene profile patterns from rodent models of muscle unloading and inactivity, in which both genes exhibit a rapid elevation within the first 48 hours, followed by a sustained upregulation over 7 to 10 days, and a gradual return to baseline by approximately day 14 (Bodine et al., 2001a, Li et al., 2014b, Hanson et al., 2013). Notably, the mechanisms underlying muscle mass restoration are unknown. In this study, food intake was not measured during this period, and therefore, it is unclear whether increased food consumption contributed to the recovery observed during this period.

Several studies have reported that inflammatory cytokines, such as TNF-α, IL-1ß, and IL-6, impair muscle regeneration and differentiation by suppressing the activity of myogenic transcription factors, particularly myogenic differentiation factor (MyoD), through activation of the NF-κB signalling pathway (Di Marco et al., 2005). In addition to inhibiting myogenesis, these pro-inflammatory mediators have also been shown to promote muscle wasting by upregulating the expression of key atrophy-related genes, including *Atrogin-1* and *MuRF-1* (Fang et al., 2021).

Based on these findings, we examined the expression of these genes in skeletal muscle following experimental stroke. In line with previous reports (Hafer-Macko et al., 2005), our data revealed a significant upregulation of *TNF-α* on day 3 post-stroke in both the contralateral and ipsilateral limbs. Given that *Atrogin-1* and *MuRF-1* were also upregulated bilaterally, it is plausible that their expression was mediated, at least in part, by TNF-α–dependent signalling. This interpretation is supported by previous work suggesting that TNF-α–induced NF-κB activation may represent one of the most potent stimuli driving muscle atrophy (Carda et al., 2013).

We also aimed to assess the effect of stroke and ageing on the molecular mechanisms of muscle homeostasis in aged mice. Given that it is well established that ageing is associated with muscle atrophy due to sarcopenia (age-related loss of muscle mass and strength), we found a reduced skeletal muscle mass in aged naïve mice compared to young mice. Then we assessed gene expression in aged naïve mice to examine the effect of ageing, independent of stroke, on muscle protein synthesis pathways. We found that the expression of atrophy-related genes (*MuRF-1* and *Atrogin-1*) was significantly higher in aged naïve mice compared to young mice. Moreover, the transcription factor *FOXO1*, which regulates their expression, was also upregulated. This suggests that the catabolic pathways represented by the ubiquitin-proteasomal system (UPS) were active in the basal state in the muscle of aged mice even in the absence of stroke. Notably, the gene expression profile associated with muscle wasting in ageing closely resembles that observed after stroke. Our findings are consistent with some studies that assessed protein homeostasis in aged rats. For instance, Clavel et al. (2006) reported that the loss of muscle mass in aged rats was accompanied by an upregulation of *MuRF-1* and *Atrogin-1* compared to young rats (Clavel et al., 2006). Similarly, Altun et al. (2010) demonstrated that MuRF-1 is overexpressed in the atrophied hindlimb muscles of aged rats compared to those of adult rats. Interestingly, Atrogin-1 was found to be downregulated in aged rats compared to adult rats (Altun et al., 2010). Another study revealed a different pattern of atrogenes expression, where both MuRF-1 and Atrogin-1 exhibited lower expression levels in aged rats compared to adult rats (Edström et al., 2006). The reason for these conflicts is unclear but may be related to differences in the muscles, as well as differences in the species and strains used across studies. In

Chapter 5 we found that like young tMCAo mice, skeletal muscle mass from aged mice on day 1 after tMCAo was comparable to muscles from aged sham mice, suggesting that ageing has no effect on post-stroke muscle atrophy at this early time point. In this chapter, we initially aimed to extend these findings by investigating whether ageing amplifies the impact of ischaemic stroke on genes regulating muscle homeostasis, through a comparison of gene expression in aged and young mice on day 1 after tMCAo. However, this was not possible because only had a single cohort of day 1 young tMCAo mice, which had been analysed and presented in Figure 6-7. Consequently, the present analysis focused on assessing the impact of stroke on gene expression in muscle from aged mice compared with age-matched sham controls. Consistent with our previous observations in the young tMCAo mice on day 1, there was an upregulation of the catabolic genes *Atrogin-1* and *MuRF-1* at 24 hours after tMCAo in aged mice whereas no changes were observed in the expression of anabolic genes.

The study has some limitations: it measured gene expression at the transcriptional level but did not assess protein activity or phosphorylation states. As a result, the functional implications of these molecular changes remain uncertain because mRNA levels do not always correlate with protein function. Future studies incorporating protein-level analyses will be essential to fully elucidate the mechanisms underlying stroke-induced changes in muscle homeostasis. Nevertheless, in conclusion, we have demonstrated that muscle loss after experimental cerebral ischaemia is observed on days 3 and 7 post-stroke but is restored by day 14. This muscle loss appears to be accompanied by the upregulation of atrophy-related genes, such as *MuRF-1*, on day 1 after stroke. Also, we found a similar pattern of gene expression upregulation in muscles from aged naïve and tMCAo mice, suggesting similarities between stroke-related and age-related changes in genes involved in muscle homeostasis.

Chapter 7 General discussion

7.1 Summary of main findings

The major findings of the research presented in this thesis are: (1) The estimated pooled prevalence of post-stroke weight loss or sarcopenia is 31% and 36% respectively, and both were associated with poor stroke outcomes; (2) Weight loss in young mice after experimental stroke is profound and encompasses global wasting of fat and skeletal muscles; and is not solely due to factors such as anaesthesia, surgical stress, and reduced food or liquid intake, suggesting other factors contribute to the observed weight loss. Interestingly, compared with young mice, aged mice were protected from post-stroke weight loss, at least during the first 24 hours following stroke onset; (3) Stroke severity rather than the anatomical location of the infarct largely determines the extent of weight loss after experimental stroke; (4) Using non-targeted metabolomics, multivariate and univariate analyses revealed no differences among sham or stroke mice or between the age groups. However, using a linear model we found potential stroke-associated metabolic alterations in metabolites involved in lipid, fatty acid, and tryptophan metabolism; and (5) Muscle wasting after experimental stroke is apparent during the acute phase (day 3 and 7) after stroke induction but is transient in nature as muscle mass was comparable between sham and stroke mice at day 14 post-surgery. The muscle atrophy occurs in association with upregulated expression of catabolic (e.g., MURF-1, Atrogin-1) and inflammatory (*TNF-α)* genes suggesting increased catabolic drive potentially by pro-inflammatory mediators. In this final chapter, I aim to discuss the overall findings of the thesis and provide recommendations for future research.

7.1.1 Post-stroke weight and muscle loss are dictated by stroke severity.

Post-stroke weight loss and sarcopenia are gaining attention as clinically important complications. Indeed, as demonstrated in our systematic review, the prevalence of weight loss or sarcopenia after stroke is relatively high (estimated to be 31% and 36%, respectively) and is related to poorer functional recovery, mortality and longer hospital stay. However, while this clinical evidence underscores the importance of post-stroke weight loss and sarcopenia on patient prognosis, very little is known about the mechanisms that drive tissue wasting after stroke. The key hypothesis underpinning this thesis was that the weight and

muscle loss observed after stroke are driven, at least in part, by systemic mechanisms triggered by cerebral ischaemia. Observations from this research support this hypothesis in many aspects: (1) consistent with published work, we found that weight loss after experimental stroke involves loss of both fat tissue and skeletal muscle of both limbs (stroke-affected and non-affected), indicating the weight loss arises from global wasting of tissues rather than a localised effect on stroke-affected muscles. Consistent with this, a previous study reported a loss in heart muscle after stroke as well (Springer et al., 2014a); (2) our data revealed a moderate, positive correlation between infarct volume and the extent of weight loss, indicating that larger infarcts, likely involving multiple brain regions, result in greater weight loss potentially by eliciting a 'stronger' metabolic response. We also provided evidence that the location of the infarct appears less important in dictating the extent of post-stroke weight loss. Indeed, weight loss occurred in two distinct pre-clinical models, one of which produces infarcts only in cortical brain regions. Furthermore, although the work was exploratory in nature, we found no relationship between infarct location and the extent of weight loss. Further studies using more sophisticated approaches are however needed to allow us to definitively conclude that stroke severity it is the key determining factor. (3) our findings showed upregulation of TNF-α in skeletal muscles of both limbs, providing further evidence for a systemic rather than a local response to stroke, since upregulation was observed not only on the affected side but also in both limbs.

Notably, an elevated level of TNF-α in cerebrospinal fluid and serum was also reported in patients after stroke, and was associated with infarct volume and poor neurological outcomes (Zaremba and Losy, 2001). TNF-α was first recognised as a potential cachectic factor in studies conducted on infected rabbits (Beutler et al., 1985). High concentrations of TNF-α have been detected in cachectic patients with chronic heart failure (Gullestad et al., 2012, Levine et al., 1990). Conversely, a previous study found that muscle protein loss in an animal model of cachexia was prevented or reduced when the infected animal was pretreated with pentoxifylline (TNF-α synthesis inhibitor) (Breuille et al., 1993). It is believed that TNF-α contributes to muscle atrophy via the TNF-α- NF-κB signalling pathway. TNF-α activates the transcription factor NF-κB, which, in turn, enhances the expression of atrogenes, specifically MuRF-1 and atrogin-1 (E3 ubiquitin ligases).

This accelerates protein breakdown through UPS (Li et al., 1998). Some researchers have proposed that TNF-α- NF-κB-mediated muscle wasting is the most potent driver of muscle atrophy (Carda et al., 2013). These observations support TNF-α's involvement in muscle wasting pathophysiology observed after stroke. In line with this, our data demonstrated significantly higher MuRF-1 expression and a trend toward higher Atrogin-1 expression in the skeletal muscle of mice on day 1 after stroke in both limbs. Similarly, on day 3, there was a non-significant trend for upregulation of these genes. Together, our findings provide additional evidence supporting the hypothesis that stroke triggers systemic catabolic pathways and implicates inflammatory and proteolytic signalling in early post-stroke muscle and tissue atrophy.

7.1.2 Treatment approaches

We have shown that post-stroke weight loss and sarcopenia significantly impact the quality of life of stroke patients and are associated with poor clinical outcomes and increased mortality, which highlights their clinical relevance and the need for medical attention and appropriate therapeutic management. Therefore, addressing these complications through interventions that maintain muscle mass and body weight is critical. However, treatment options available for these conditions are limited. In this context, some pharmacological drugs have emerged as promising therapeutic agents for counteracting cachexia.

Ghrelin is a peptide produced by the stomach and is an orexigenic (‘appetite stimulating’) hormone and numerous studies have shown its importance in stimulating growth hormone release by the pituitary and increases food intake by binding to the growth hormone secretagogue receptor to regulate energy homeostasis and body weight (Wren et al., 2001). Moreover, it has been found to inhibit the release of anorectic proinflammatory cytokines such as IL-1α, TNF-α, and IL-6 (Akamizu and Kangawa, 2010). It has been suggested that ghrelin-induced metabolic changes result in increased body weight and fat mass, accompanied by a concomitant increase in lean tissue mass, potentially mediated by reduced circulating myostatin levels (Akamizu and Kangawa, 2010). However, ghrelin has a short half-life in human plasma—approximately 10 minutes—and can only be administered by injection (IV or subcutaneous). In contrast, a ghrelin mimetic (Anamorelin) has a longer half-life, approximately 9 hours and can be taken orally,

making it a good substitute for ghrelin. Promising results in the treatment of cancer cachexia by using anamorelin were obtained in many clinical trials (Currow et al., 2017, Hamauchi et al., 2019, Temel et al., 2016). Recently, anamorelin has been approved and is on the market in Japan as a drug for cachexia treatment after it has passed three randomised clinical trials, but has not received approval elsewhere (Laird et al., 2025).

Another agent is Megestrol acetate (MA), which is a synthetic derivative of the progesterone hormone and is widely used for anorexia-cachexia syndrome therapy. It is used to increase appetite by its action on Neuropeptide Y (NPY) in the hypothalamus or by inhibiting the release of proinflammatory cytokines (Mantovani et al., 1997). However, its benefits are controversial, as some reports indicate that although cancer patients treated with MA exhibited a slight increase in body weight, they did not show improvement in quality of life (Ruiz-García et al., 2018).

Anabolic steroids, such as testosterone, are used to overcome skeletal muscle loss, and they exhibit clinical potential. However, the issue with the administration of anabolic steroids is that they are likely to be accompanied by side effects, and the risk outweighs their benefits. Notably, selective androgen receptor modulators (SARMs) are a class of therapeutics and are expected to have anabolic properties with minimal androgenic side effects such as testicular atrophy, gynecomastia and thrombotic incidents (Schmidt et al., 2009). Although SARMs such as enobosarm show the ability to increase muscle mass and stimulate muscle growth, there is no scientific evidence of their effectiveness in treating cachexia (Borecki et al., 2025).

Another group are steroidal and non-steroidal anti-inflammatory drugs. They function by reducing the production of pro-inflammatory cytokines. For steroidal anti-inflammatory drugs such as dexamethasone and prednisolone, it is important to monitor their potential to stimulate the appetite and increase weight due to their side effects.

It is important to consider nutritional support and rehabilitation exercise along with pharmacological interventions for managing post-stroke weight loss and sarcopenia. Adequate protein intake should be considered in stroke patients, as

leucine-rich amino acids supplementation has been shown to increase muscle mass and strength and improve daily activities in stroke patients with sarcopenia (Yoshimura et al., 2019a). Furthermore, krill oil supplementation has been shown to increase muscle size and function in healthy older adults (Alkhedhairi et al., 2022), suggesting its potential to support muscle health in stroke survivors, although this has yet to be investigated in stroke. Similarly, a study by Rabadi and colleagues (2008) in patients experiencing weight loss after stroke demonstrated that increased dietary intake through nutritional supplementation can facilitate functional recovery and exercise performance. However, supplementation alone appears insufficient if not accompanied by physical rehabilitation (Rabadi et al., 2008). Evidence suggests that leucin-enriched amino acid supplementation is most effective when combined with resistance exercise, indicating that nutritional interventions must be integrated with physical activity to achieve optimal improvements in muscle mass and functional outcomes.

Notably, however, post-stroke weight loss and sarcopenia, along with their associated clinical implications, are not currently acknowledged or addressed in stroke management guidelines for stroke survivors. Although clinical studies indicate that post-stroke weight and muscle loss are related to poor functional outcomes and reduced patient quality of life, the guideline recommendations do not recognise the prevention of muscle and tissue wasting after stroke as a therapeutic target. Additionally, our systematic review revealed how little attention these conditions received in the literature, identifying only nine studies specifically addressing post-stroke weight loss. This underexplored aspect of stroke management needs to be better appreciated within an integrated framework that combines rehabilitation, nutritional support, and pharmacological agents to prevent tissue loss, restore anabolic capacity, and improve patient outcomes.

7.1.3 Future directions

This thesis has provided valuable insights into the effect of stroke on body weight, systemic metabolism and muscle wasting. However, several aspects remain to be studied and explored by future investigations to improve our understanding of these conditions within the context of stroke. The following recommendations are suggested for future research:

As this study was conducted exclusively in male mice, it is essential to replicate these findings in female mice to assess potential sex-specific differences in metabolic and physiological responses to stroke. Future work should also focus on elucidating the upstream regulatory mediators that control muscle homeostasis, such as insulin-like growth factor (IGF-1) and glucocorticoids, as the downstream mediators in these pathways showed alterations in our dataset and could offer potential therapeutic approaches to prevent muscle wasting after stroke. Research should investigate how inflammatory and hormonal factors, including TNF-α and IL-6, and the ghrelin-leptin axis, affect post-stroke sarcopenia and weight loss. The TNF-α–NF-κB signalling pathway in skeletal muscle warrants further study, as our results show that TNF-α and E3 ubiquitin ligases increase after stroke, suggesting that proteolytic pathways are activated via FOXO or NF-κB signalling.

Extending metabolomics analysis to 72 hours post-stroke, when the infarct is fully developed, would provide valuable insight into the systemic metabolic consequences of cerebral ischaemia while minimising confounding factors such as anaesthesia and surgical stress. Furthermore, expanding metabolomic profiling beyond plasma to include brain and skeletal muscle tissues would enable identification of organ-specific contributions to post-stroke energy dysregulation. Additionally, complementary targeted lipidomics approaches could also yield a more accurate understanding of alterations in lipid and fatty acid metabolism, which were among the most significantly affected pathways in our dataset.

Lastly, future work using aged mice to determine whether the minimal weight loss observed at 24 hours persists over longer periods and to assess associated changes in neurological function and locomotor activity.

7.1.4 conclusions

In summary, we have found that weight loss and sarcopenia are prevalent among stroke survivors, estimated at 31% and 36% respectively, and they are related to poor functional outcomes and a longer hospital stay. In the experimental model, we found that post-stroke weight loss in young mice was characterised by loss of fat and skeletal muscle mass in both limbs (stroke-affected and non-affected), with the greatest loss observed on day 3 post-stroke. Additionally, the findings from this research suggest that stroke severity rather than infarct location determines the extent of post-stroke weight loss. The study on muscle wasting after acute stroke revealed upregulation of the pro-inflammatory cytokine TNF-α and ubiquitin E3 ligases (MuRF-1 and atrogin-1), which are believed to play a role in muscle degradation. Furthermore, cerebral ischaemia was found to affect the lipid and fatty acid metabolic profile, which is worth further investigation using more specific and targeted approaches such as lipidomics. Lastly, our data revealed that aged mice may be protected from post-stroke weight loss, despite being subjected to experimental conditions comparable to those of the young cohort. These findings underscore the complex interplay between cerebral ischaemia, systemic metabolism and peripheral tissue responses after stroke. They highlight the need to acknowledge post-stroke weight loss and sarcopenia as clinically significant complications that influence recovery and patients' quality of life.

Chapter 8 Appendix

8.1 Principal component analysis (PCA) of metabolites in plasma from sham or tMCAo mice.

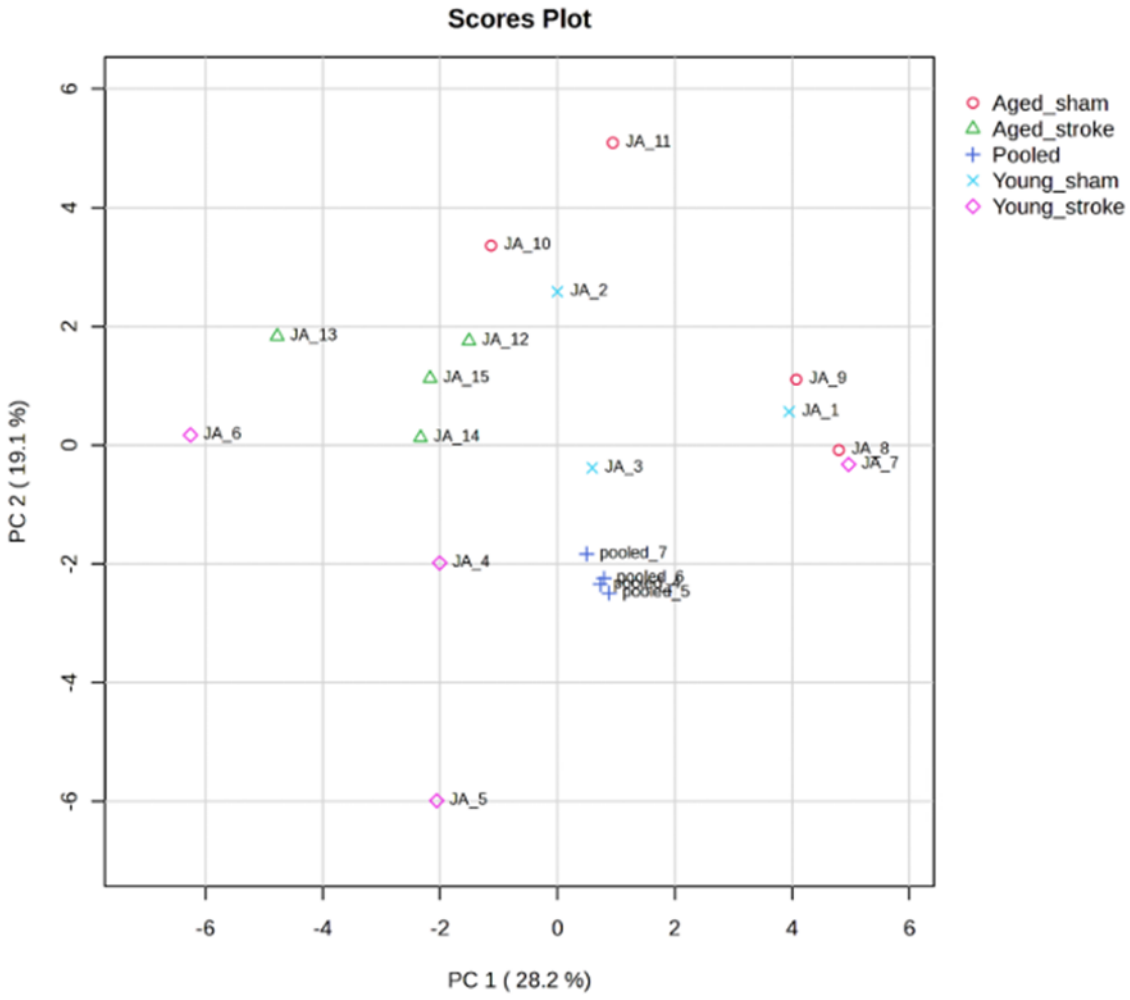

Figure 8-1 Plot of the first two principal components calculated for experimental and pooled samples. Graph generated in MetaboAnalyst 6.0 on on log_{10}-transformed data obtained in PiMP young mice: n=3 sham, 4 tMCAo; aged mice, n=4 sham, n=4 tMCAo.

8.2 List of significantly changed peaks for the effect of ischaemic stroke on the metabolic profile of aged and young mice

Table 8-1
List of significantly changed peaks at an adjusted p-value < 0.05 for the effect of stroke on the metabolome of young and aged mice in our linear model analysis. The data were processed in PiMP (Gloaguen, 2017), and statistical analyses were conducted in MetaboAnalyst 6.0.

Putative annotation(s)	Standard match	adj.P.Val
L-Carnitine;L-Carnitine;L-Carnitine;Malonyl-Carnitin;(S)-Carnitine	L-Carnitine	0.035646
Palmitoylsphingomyelin;SM(d18:1/16:0);SM(d18:0/16:1(9Z));PECer(d15:1(4E)/22:0);PE-Cer(d14:1(4E)/23:0);PE-Cer(d16:1(4E)/21:0);SM(d17:1/17:0);SM(d16:1/18:0)		0.035646
3-Oxohexanoic acid;3-Oxohexanoic acid;3-keto-n-caproic acid;2-Methyl-3-ketovaleric acid;3-Methyl-2-oxovaleric acid;3-Methyl-2-oxopentanoate;Ketoleucine;4-Methyl-2-oxopentanoate;Mevalonolactone;Pantolactone;2-Ketohexanoic acid;2-Oxohexanoic acid;2-keto-n-caproic acid;4-Acetylbutyrate;5-Oxohexanoic acid;5-keto-n-caproic acid;Adipate semialdehyde;Adipate semialdehyde;Methyl levulinate;Ethyl acetoacetate;Ethyl 3-oxobutanoate;Ethyl 3-oxobutanoate;5-Ethoxy-4,5-dihydro-2(3H)furanone;(4S,6S)-3,4,5,6-Tetrahydro-4-hydroxy-6-methyl-2H-pyran-2-one;Acetoin acetate;Sherry lactone;(3R)-3-Methyl-2-oxopentanoic acid;2oxo-3R-methyl-pentanoic acid;N-Butyryl-L-homoserine lactone;Crotanecine;1-Oxa-2-oxo-3-hydroxycycloheptane;(S)-3-Methyl-2-oxopentanoic acid;3S-methyl-2-oxo-pentanoic acid;2-Hydroxyethyl methacrylate;beta-Ketoisocaproate;3-oxo-4-methyl-pentanoic acid;(R)-Pantolactone;6-Hydroxyhexan-6-olide;4-Hydroxy-4-methyltetrahydro-2H-pyran-2-one;4-keto-n-caproic acid;N-butanoyl-lhomoserine lactone		0.037244
Pi-Methylimidazoleacetic-acid;(R)-Dihydromaleimide;Methylimidazoleacetic-acid;Methylimidazoleacetic-acid;Imidazolepropionic-acid;1,3-Dimethyluracil;Succinimide;Hymexazol;4,5,6,7-Tetrahydroisoxazolo(5,4-c)pyridin-3-ol;Dihydrourocanate		0.040043
4-Deoxyerythronic acid;Aminoadipic acid;Aminoadipic acid;(S)-3,4-Dihydroxybutyric acid;2,4-Dihydroxybutanoic acid;2,4-dihydroxy-butanoic acid;(±)-2,2'-Iminobispropanoic acid;Alanopine;Acetylhomoserine;Glutamate, gamma-methyl ester;A,b-Dihydroxyisobutyric acid;a,b-dihydroxy-isobutyric acid;Erythrose;D-Erythrose;4-Deoxythreonic acid;L-Erythrulose;L-Erythrulose;N-acetylthreonine;N-methyl-L-glutamic Acid;N-Methyl-L-glutamate;3-Amino-2,3-dideoxy-scyllo-inososе;4-Methyl-L-glutamate;D-Alanyl-(R)-lactate;D-Threose;L-Glutamate methylester;L-2-Aminoadipate;beta-Alanopine;O-Acetyl-L-homoserine;D-Erythrulose;3S,4-dihydroxy-butyric acid;4-deoxy-erythronic acid		0.049627

Acetylglycine;Glycolic acid;Glycolate;L-Aspartate-semialdehyde;L-Aspartate 4-semialdehyde;Peracetic acid;L-2-Amino-3-oxobutanoic acid;L-2-Amino-3-oxobutanoic acid;2S-amino-3-oxo-butanoic acid;(Z)-2-Methylperoxyaminoacrylate;2-Amino-3-oxobutanoate		0.037876
Pyrrolidonecarboxylic acid;5-Oxoprolinate;Pyroglutamic acid;Pidolic acid;N-Acryloylglycine;Pyrroline hydroxycarboxylic acid;dimethadione;1-Pyrroline-4-hydroxy-2-carboxylate;1-Pyrroline-4-hydroxy-2-carboxylate;(3R,5S)-1-pyrroline-3-hydroxy-5-carboxylic Acid;L-1-Pyrroline-3-hydroxy-5-carboxylate;N-Nitrosoguvacoline;4-Oxoproline;5-Oxo-D-proline		0.03564
Pyrrolidonecarboxylic acid;5-Oxoprolinate;Pyroglutamic acid;Pidolic acid;N-Acryloylglycine;Pyrroline hydroxycarboxylic acid;dimethadione;1-Pyrroline-4-hydroxy-2-carboxylate;1-Pyrroline-4-hydroxy-2-carboxylate;(3R,5S)-1-pyrroline-3-hydroxy-5-carboxylic Acid;L-1-Pyrroline-3-hydroxy-5-carboxylate;N-Nitrosoguvacoline;4-Oxoproline;5-Oxo-D-proline		0.03564
Indolelactic acid;Indolelactate;Phenylpyruvic acid;Phenylpyruvate;5-Methoxyindoleacetate;5-Methoxyindoleacetate;Cinnamoylglycine;3-Indolehydracrylic acid;m-Coumaric acid;trans-3-Hydroxycinnamate;cis-p-Coumaric acid;cis-p-Coumarate;Edulitine;2-Hydroxycinnamic acid;trans-2-Hydroxycinnamate;Enol-phenylpyruvate;2-Hydroxy-3-phenylpropenoate;4-Hydroxycinnamic acid;4-Coumarate;Coumaric acid;cis-2-Hydroxycinnamate;Methyl Phenylglyoxalate;Methyl 1-methoxy-1H-indole-3-carboxylate;Caffeic aldehyde;Gentianamine;Swietenidin B;3-Oxo-3-phenylpropanoate;9-hydroxy-7Z-Nonene-3,5-diynoic acid;9-hydroxy-7E-Nonene-3,5-diynoic acid		0.04206
Deoxyuridine;Deoxyuridine;Deoxyuridine;1-(Malonylamino)cyclopropanecarboxylic acid;(2S,4S)-4-Hydroxy-2,3,4,5-tetrahydrodipicolinate;2-(Acetamidomethylene)succinate	Deoxyruidine	0.03787
3-Succinoylpyridine;3-Succinoylpyridine;4-Hydroxybenzoic acid;4-Hydroxybenzoate;Hippuric acid;Hippurate;Gentisate aldehyde;Gentisate aldehyde;Sesamol;Sesamol;3,4-Dihydroxybenzaldehyde;3,4-Dihydroxybenzaldehyde;Salicylic acid;Salicylate;Methyl n-formylanthranilate;Adrenochrome;3-Hydroxybenzoic acid;3-Hydroxybenzoate;keratan sulfate II (core 2-linked), degradation product 1;alpha-Furyl methyl diketone;2-Methoxy-1,4-benzoquinone;1-(4-Methoxyphenyl)-2-nitroethylene;2-Hydroxy-5-methylquinone;2,5,6-Trihydroxy-5,6-dihydroquinoline;N-Acetylanthranilate		0.04004
Valerylglycine;3-Hydroxy-2-methyl-[S-(R,R)]-butanoic acid;2-Hydroxy-3-methylbutyric acid;3-Hydroxyvaleric acid;3-hydroxy valeric acid;Erythronilic acid;3-Hydroxy-2-methyl-[R-(R,S)]-butanoic acid;Isovalerylglycine;3-Hydroxyisovaleric acid;3-hydroxy-isovaleric acid;Medicanine;2-Ethylhydracrylic acid;2-ethyl-hydracrylic acid;2-Methylbutyrylglycine;2-Methyl-3-hydroxybutyric acid;2-methyl-3-hydroxybutyric acid;Calystegin A3;N-Acetylvaline;Diethyl carbonate;2-Hydroxyvaleric acid;DL-2-hydroxy valeric acid;2-Hydroxy-2-methylbutyric acid;2-hydroxy-2-methyl-butyric acid;Ethyl lactate;4-Hydroxystachydrine;Turicine;Betonicine;(-)-Betonicine;5-Hydroxypentanoic acid;5-Hydroxypentanoate;5-hydroxy valeric acid;Methyl 5-(hydroxymethyl)pyrrolidine-3-carboxylate;5-Acetamidovalerate;5-Acetamidopentanoate;3-Dehydrocarnitine;Calystegine A7;Methyl 3-hydroxybutyrate;4-Hydroxyisovaleric acid;4-hydroxy-isovaleric		0.03564

acid;Calystegine A6;(S)-2-hydroxy-3-methylbutyric Acid;2-hydroxy-3-methyl-butyric acid;Calystegin A3;3-Hydroxystachydrine;formyl 3-hydroxy-butanoate;4-hydroxy-valeric acid;3-Hydroxy-2-methyl-[S-(R,R)]-butanoic acid;3-hydroxy-2-methyl-[R-(R,S)]-butanoic acid		
3-Succinoylpyridine;3-Succinoylpyridine;4-Hydroxybenzoic acid;4-Hydroxybenzoate;Hippuric acid;Hippurate;Gentisate aldehyde;Gentisate aldehyde;Sesamol;Sesamol;3,4-Dihydroxybenzaldehyde;3,4-Dihydroxybenzaldehyde;Salicylic acid;Salicylate;Methyl n-formylanthranilate;Adrenochrome;3-Hydroxybenzoic acid;3-Hydroxybenzoate;keratan sulfate II (core 2-linked), degradation product 1;alpha-Furyl methyl diketone;2-Methoxy-1,4-benzoquinone;1-(4-Methoxyphenyl)-2-nitroethylene;2-Hydroxy-5-methylquinone;2,5,6-Trihydroxy-5,6-dihydroquinoline;N-Acetylanthranilate		0.04206
Methional diethyl acetal;Pentahomomethionine		0.03564
Taurocyamine;Taurocyamine		0.03564
(S)-3-Hydroxybutyric acid;(S)-3-Hydroxybutanoate;Alpha-Hydroxyisobutyric acid;alpha-hydroxy-isobutyric acid;4-Hydroxybutyric acid;4-Hydroxyacid;4-hydroxy-butyric acid;(S)-3-Hydroxyisobutyric acid;(S)-3-Hydroxyisobutyrate;(R)-3-Hydroxybutyric acid;(R)-3-Hydroxybutanoate;3R-hydroxy-butanoic acid;(R)-3-Hydroxybutanoate;2-Hydroxybutyric acid;(+/-)alpha-hydoxy butyric acid;(R)-3-Hydroxyisobutyric acid;3R-hydroxy-isobutyric acid;3-Hydroxybutyric acid;D(-)-beta-hydroxy butyric acid;2-Methyl-3-hydroxypropanoate;Ethoxyacetic acid;4-Hydroxybutanoic acid;Methyl methoxyacetate;3-Hydroxy-2-methylpropanoate;2-Hydroxybutanoic acid;2S-Hydroxybutanoic acid	(S)-3-Hydroxybutyric acid	0.02140
Linoleic acid;Linoleate;Linoleic acid;5-Octadecynoic acid;5-octadecynoic acid;Ethyl 2E,4Z-hexadecadienoate;Mangiferic acid;Linalyl caprylate;10E,12Z-Octadecadienoic acid;9E,11E-Octadecadienoic acid;9E,11E-octadecadienoic acid;Linoelaidic acid;Linoelaidic acid;Octadecadienoate;2,4-octadecadienoic acid;Bovinic acid;9-cis,11-trans-Octadecadienoate;Rumenic acid;6Z,9Z-octadecadienoic acid;6Z,9Z-octadecadienoic acid;Malvalic acid;Malvalic acid;Chaulmoogric acid;Stearolic acid;Stearolic acid;(Z)-3,7-Dimethyl-2,6-octadienyl octanoate;(E)-3,7-Dimethyl-2,6-octadienyl octanoate;Ethyl (Z,Z)-11,13-hexadecadienoate;10Z,12E-Hexadecadienyl acetate;11Z,13Z-Hexadecadienyl acetate;7Z,11Z-Hexadecadienyl acetate;8Z,10Z-Hexadecadienyl acetate;11-Hexadecynyl acetate;11Z,13E-Hexadecadienyl acetate;11Z,14E-Hexadecadienyl acetate;7Z,11E-Hexadecadienyl acetate;11E,13E-Hexadecadienyl acetate;10E,12E-Hexadecadienyl acetate;11E,13Z-Hexadecadienyl acetate;4E,6Z-Hexadecadienyl acetate;6E,11Z-Hexadecadienyl acetate;9E,11Z-Hexadecadienyl acetate;10E,12Z-Hexadecadienyl acetate;9Z-octadecadien-4R-olide;9-octadecen-4-olide;7-trans,9-cis-octadecadienoic acid;8-octadecynoic acid;6-octadecynoic acid;13-octadecynoic acid;12-octadecynoic acid;3-octadecynoic acid;2-octadecynoic acid;10-octadecynoic acid;7-octadecynoic acid;4-octadecynoic acid;11-octadecynoic acid;17-octadecynoic acid;16-octadecynoic acid;15-octadecynoic acid;14-octadecynoic acid;(S)-laballenic acid;(R)-laballenic acid;5E,12E-octadecadienoic acid;5E,12Z-octadecadienoic acid;5Z,12E-otadecadienoic		0.03724

acid;5Z,12Z-otadecadienoic acid;9Z,11Z-octadecadienoic acid;8Z,11Z-octadecadienoic acid;8E,10E-octadecadienoic acid;6, 8-octadecadienoic acid;10Z,12Z-octadecadienoic acid;9E,12Z-octadecadienoic acid;9Z,12E-octadecadienoic acid;10Z,13Z-octadecadienoic acid;10E,12E-octadecadienoic acid;10E,12Z-octadecadienoic acid;11Z,15Z-octadecadienoic acid;13Z,16Z-octadecadienoic acid;13E,17-octadecadienoic acid;12Z,15Z-octadecadienoic acid;12E,16E-octadecadienoic acid;2Z,5Z-octadecadienoic acid;2E,6E-octadecadienoic acid;14Z,17-octadecadienoic acid;2Z,6Z-octadecadienoic acid;3Z,12Z-octadecadienoic acid;3E,7E-octadecadienoic acid;4E,8E-octadecadienoic acid;4,9-octadecadienoic acid;3Z,7Z-octadecadienoic acid;3Z,6Z-octadecadienoic acid;5,11-octadecadienoic acid;5,10-octadecadienoic acid;4Z,8Z-octadecadienoic acid;4Z,7Z-octadecadienoic acid;5Z,11Z-octadecadienoic acid;5E,9Z-octadecadienoic acid;5,6-octadecadienoic acid;6,11-octadecadienoic acid;Taxoleic acid;5Z,9E-octadecadienoic acid;Sebaleic acid;6E,12E-octadecadienoic acid;6E,11Z-octadecadienoic acid;6E,10E-octadecadienoic acid;7E,12E-octadecadienoic acid;6Z,11Z-octadecadienoic acid;6E,9E-octadecadienoic acid;8,12-octadecadienoic acid;8,11-octadecadienoic acid;7Z,11Z-octadecadienoic acid;7Z,10Z-octadecadienoic acid;9,13-octadecadienoic acid;11Z,14Z-octadecadienoic acid;10Z,14Z-octadecadienoic acid;10E,14E-octadecadienoic acid;16-methyl-9Z,12Z-heptadecadienoic acid;16-methyl-6Z,9Z-heptadecadienoic acid;Chaulmoogric acid;16:2(2E,4E)(4Me,6Me[S]);16:2(2E,4E)(5Me,7Me[S])		
Levoglucosan;2-Hydroxyadipic acid;2-Hydroxyadipate;2-Hydroxyadipic acid;2(R)-Hydroxyadipic acid;3-Hydroxymethylglutaric acid;3-Hydroxy-3-methylglutarate;3-Hydroxyadipic acid;3-hydroxy-adipic acid;2-Hydroxy-2-ethylsuccinic acid;D-1-Deoxy-erythro-hexo-2,3-diulose;D-1,5-Anhydrofructose;Diethyl dicarbonate;Diethyl pyrocarbonate;1,5-Anhydro-D-fructose;2-Deoxy-scyllo-inososе;D-Fucono-1,4-lactone;2-Dehydro-3-deoxy-D-fuconate;L-Fucono-1,5-lactone;3,6-Anhydrogalactose;3,6-Anhydroglucose;Lichenin;L-Rhamnono-1,4-lactone;3-Ethylmalate;2-Dehydro-3-deoxy-L-rhamnonate;2-Dehydro-3-deoxy-L-fuconate;(R)-2-Ethylmalate;(R)-3,3-Dimethylmalate;(2R,3S)-2,3-Dimethylmalate;(S)-2-(Hydroxymethyl)glutarate;2S-hydroxyadipic acid;3-hydroxymethyl-glutaric acid		0.03564
(S)-3-Hydroxybutyric acid;(S)-3-Hydroxybutanoate;Alpha-Hydroxyisobutyric acid;alpha-hydroxy-isobutyric acid;4-Hydroxybutyric acid;4-Hydroxyacid;4-hydroxy-butyric acid;(S)-3-Hydroxyisobutyric acid;(S)-3-Hydroxyisobutyrate;(R)-3-Hydroxybutyric acid;(R)-3-Hydroxybutanoate;3R-hydroxy-butanoic acid;2-Hydroxybutyric acid;(+/-)alpha-hydoxy butyric acid;(R)-3-Hydroxyisobutyric acid;3R-hydroxy-isobutyric acid;3-Hydroxybutyric acid;D(-)-beta-hydroxy butyric acid;2-Methyl-3-hydroxypropanoate;Ethoxyacetic acid;4-Hydroxybutanoic acid;Methyl methoxyacetate;3-Hydroxy-2-methylpropanoate;2-Hydroxybutanoic acid;2S-Hydroxybutanoic acid		0.03564
Deoxyuridine;Deoxyuridine;Deoxyuridine	Deoxyuridine	0.03564
Amoritin;Isoamoritin		0.02140

Hydroxypropionylcarnitine		0.03083
Acetylglycine;L-Aspartate-semialdehyde;L-Aspartate 4-semialdehyde;L-2-Amino-3-oxobutanoic acid;L-2-Amino-3-oxobutanoic acid;2S-amino-3-oxo-butanoic acid;(Z)-2-Methylperoxyaminoacrylate;2-Amino-3-oxobutanoate		0.03564
Halomon		0.03564
Homocysteinesulfinic acid		0.03724
Dimethoate		0.03564
3,4-Dihydroxyhydrocinnamic acid;3,4-Dihydroxyphenylpropanoate;Hydroxyphenyllactic acid;3-(4-Hydroxyphenyl)lactate;Homovanillic acid;Homovanillate;Isohomovanillic acid;3-Methoxy-4-hydroxyphenylglycolaldehyde;3-Methoxy-4-hydroxyphenylglycolaldehyde;3,4-Dimethoxybenzoic acid;2,6-Dimethoxybenzoic acid;3-Hydroxyphenyllactate;2',6'-Dihydroxy-4'-methoxyacetophenone;2',6'-Dihydroxy-4'-methoxyacetophenone;3-(3-Hydroxyphenyl)-3-hydroxypropanoic acid;2',4'-Dihydroxy-6'-methoxyacetophenone;(±)-2-Hydroxy-3-(2-hydroxyphenyl)propanoic acid;Meta-hydroxyphenylhydracrylic Acid;Maltol propionate;3-(2,3-Dihydroxyphenyl)propanoate;cis-3-(3-Carboxyethenyl)-3,5-cyclohexadiene-1,2-diol;(R)-3-(4-Hydroxyphenyl)lactate		0.04536
MCPA-thioethyl		0.04527
Uracil;Uracil;4-Carboxypyrazole;Maleic hydrazide		0.03564
3-Hydroxy-9-(4-hydroxyphenyl)-1H,3H-naphtho[1,8-cd]pyran-1-one;3-Hydroxy-4-(4-hydroxyphenyl)-1H,3H-naphtho[1,8-cd]pyran-1-one;9-Methoxy-7-phenyl-5H-furo[3,2-g][1]benzopyran-5-one;Kanjone;Glabone;2-(4-Methoxyphenyl)-4H-furo[2,3-h]-1-benzopyran-4-one;Cauliflorin A;Pongone;2-(2-Methoxyphenyl)-4H-furo[2,3-h]-1-benzopyran-4-one;Pinnatin;Ponganone XI;Karanjin;4-Methoxyfurano[2",3":6,7]aurone;Derriobtusone A		0.04206
3-Succinoylpyridine;3-Succinoylpyridine;Hippuric acid;Hippurate;Methyl n-formylanthranilate;Adrenochrome;1-(4-Methoxyphenyl)-2-nitroethylene;2,5,6-Trihydroxy-5,6-dihydroquinoline;N-Acetylanthranilate		0.03564
Vinylacetylglycine;Trimethadione;Acrylamide-acrylic acid resin;6-Oxopiperidine-2-carboxylic acid;5-ethyl-5-methyl-2,4-oxazolidinedione;2-Hydroxymethylclavam		0.03564
3-Succinoylpyridine;3-Succinoylpyridine;Hippuric acid;Hippurate;Methyl n-formylanthranilate;Adrenochrome;1-(4-Methoxyphenyl)-2-nitroethylene;2,5,6-Trihydroxy-5,6-dihydroquinoline;N-Acetylanthranilate		0.03564
N-Butyryl-L-homoserine lactone;Crotanecine;N-butanoyl-lhomoserine lactone		0.03564

LysoPE(22:6(4Z,7Z,10Z,13Z,16Z,19Z)/0:0);PE(22:6(4Z,7Z,10Z,13Z,16Z,19Z)/0:0);LysoPE(0:0/22:6(4Z,7Z,10Z,13Z,16Z,19Z))		0.03724
Uracil;Uracil;4-Carboxypyrazole;Maleic hydrazide		0.03831
N-Butyrylglycine;Isobutyrylglycine;(S)-2-amino-6-oxohexanoate;L-2-Aminoadipate 6-semialdehyde;4-Acetamidobutanoate;4-Acetamidobutanoic acid;4-Acetamidobutanoate;Allysine;Methyl aminolevulinate;L-cis-4-(Hydroxymethyl)-2-pyrrolidinecarboxylic acid;L-trans-5-Hydroxy-2-piperidinecarboxylic acid;(S)-5-Amino-3-oxohexanoate;(S)-5-Amino-3-oxohexanoic acid;3-oxo-5S-amino-hexanoic acid;2-Keto-6-aminocaproate;6-Amino-2-oxohexanoate;N-(2-Carboxymethyl)-morpholine;2-Amino-5-oxohexanoate		0.03600
N2-Acetyl-L-aminoadipate		0.03724
L-Kynurenine;L-Kynurenine;L-Kynurenine;4-Aminobenzoyl-(beta)-alanine;Formyl-5-hydroxykynurenamine;Formyl-5-hydroxykynurenamine;Kynurenine	L-Kynurenine	0.04887
(2E,4E)-2,7-Dimethyl-2,4-octadienedioic acid;Guaifenesin;2,3-Methylene suberic acid;3,4-Methylene suberic acid;5-(3E-Pentenyl)tetrahydro-2-oxo-3-furancarboxylic acid;3-(4-Hydroxy-3-methoxyphenyl)-1,2-propanediol;cis-2,3-Dihydroxy-2,3-dihydro-p-cumate;Paeonilactone A;1,2-Dihydroxymint lactone;1-(3,4-Dimethoxyphenyl)ethane-1,2-diol		0.02140
Acetylcysteine;Acetylcysteine;Tiopronin		0.03593
Hydroxyanthraquinone		0.03083
DG(22:4n6/0:0/22:5n6);DG(22:4n6/0:0/22:5n3);PC(20:3(5Z,8Z,11Z)/16:1(9Z));PC(20:3(5Z,8Z,11Z)/16:1(9Z));PC(20:3(8Z,11Z,14Z)/16:1(9Z));PC(20:3(8Z,11Z,14Z)/16:1(9Z));PC(20:4(5Z,8Z,11Z,14Z)/16:0);PC(20:4(5Z,8Z,11Z,14Z)/16:0);PC(20:4(8Z,11Z,14Z,17Z)/16:0);PC(22:4(7Z,10Z,13Z,16Z)/14:0);PC(22:4(7Z,10Z,13Z,16Z)/14:0);PC(16:1(9Z)/20:3(8Z,11Z,14Z));PC(16:1(9Z)/20:3(8Z,11Z,14Z));PC(16:1(9Z)/20:3(5Z,8Z,11Z));PC(16:1(9Z)/20:3(5Z,8Z,11Z));PC(18:0/18:4(6Z,9Z,12Z,15Z));PC(18:0/18:4(6Z,9Z,12Z,15Z));PC(18:1(11Z)/18:3(9Z,12Z,15Z));PC(18:1(11Z)/18:3(9Z,12Z,15Z));PC(18:1(11Z)/18:3(6Z,9Z,12Z));PC(18:1(11Z)/18:3(6Z,9Z,12Z));PC(18:2(9Z,12Z)/18:2(9Z,12Z));PC(18:2(9Z,12Z)/18:2(9Z,12Z));PC(18:2(9Z,12Z)/18:2(9Z,12Z));PC(18:1(9Z)/18:3(9Z,12Z,15Z));PC(18:1(9Z)/18:3(9Z,12Z,15Z));PC(18:1(9Z)/18:3(6Z,9Z,12Z));PC(18:1(9Z)/18:3(6Z,9Z,12Z));PC(18:3(6Z,9Z,12Z)/18:1(9Z));PC(18:3(6Z,9Z,12Z)/18:1(9Z));PC(18:3(6Z,9Z,12Z)/18:1(11Z));PC(18:3(6Z,9Z,12Z)/18:1(11Z));PC(18:3(9Z,12Z,15Z)/18:1(9Z));PC(18:3(9Z,12Z,15Z)/18:1(9Z));PC(18:3(9Z,12Z,15Z)/18:1(11Z));PC(18:3(9Z,12Z,15Z)/18:1(11Z));PC(18:4(6Z,9Z,12Z,15Z)/18:0);PC(18:4(6Z,9Z,12Z,15Z)/18:0);PC(16:0/20:4(8Z,11Z,14Z,17Z));PC(16:0/20:4(8Z,11Z,14Z,17Z));PC(16:0/20:4(5Z,8Z,11Z,14Z));PC(16:0/20:4(5Z,8Z,11Z,14Z));DG(22:5(4Z,7Z,10Z,13Z,16Z)/22:4(7Z,10Z,13Z,16Z)/0:0);DG(22:4(7Z,10Z,13Z,16Z)/22:5(7Z,10Z,13Z,16Z,19Z)/0:0);DG(22:4(7Z,10Z,13Z,16Z)/22:5(7Z,10Z,13Z,16Z,19Z)/0:0)[iso2];DG(22:5(7Z,10Z,13Z,16Z,19Z)/22:4(7Z,10Z,13Z,16Z)/0:0);DG(22:4(7Z,10Z,13Z,16Z)/22:5(4Z,7Z,10Z,13Z,16Z)/0:0);PC(14:0/22:4(7Z,10Z,13Z,16Z));PC(14:0/22:4(7Z,10Z,13Z,16Z));PA(19:0/20:3(8Z,11Z,14Z));PA(19:1(9Z)/20:2(11Z,14Z));PA(20:2(11Z,14Z)/19:1(9Z));PA(20:3(8Z,11Z,14Z)/19:0);PA(17:1(9Z)/22:2(13Z,16Z));PA(17:2(9Z,12Z)/22:1(11Z));DG(22:3(10Z,13Z,16Z)/22:6(4Z,7Z,10Z,13Z,16Z,19Z)/0:0)[iso2];PA(18:3(6Z,9Z,12Z)/21:0);PA(18:3(9Z,12Z,15Z)/21:0);PA(21:0/18:3(6Z,9Z,12Z));PA(21:0/18:3(9Z,12Z,15Z));PA(22:1(11Z)/17:2(9Z,12Z));PA(22:2(13Z,16Z)/17:1(9Z));PE(22:4(7Z,10Z,13Z,16Z)/17:0);PE(22:2(13Z,16Z)/17:2(9Z,12Z));PE(21:0/18:4(6Z,9Z,12Z,15Z));PC(18:0/18:4(9E,11E,13E,15E));PC(18:2(2Z,4Z)/18:2(2Z,4Z));PC(18:2(2E,4E)/18:2(2E,4E));PC(18:2(6Z,9Z)/18:2(6Z,9Z));PC(18:2(9Z,11Z)/18:2(9Z,11Z));PC(16:0/20:4(5E,8E,11E,14E));PC(20:4(8E,11E,14E,17E)/16:0);PE(17:2(9Z,12Z)/22:2(13Z,16Z));PE(18:4(6Z,9Z,12Z,15Z)/21:0);PE(19:0/20:4(5Z,8Z,11Z,14Z));PE(17:0/22:4(7Z,10Z,13Z,16Z));PE(19:1(9Z)/20:3(8Z,11Z,14Z));PE(20:3(8Z,11Z,14Z)/19:1(9Z));PE(20:4(5Z,8Z,11Z,14Z)/19:0)		0.00356

References

ABE, T., YOSHIMURA, Y., SATO, Y., NAGANO, F. & MATSUMOTO, A. 2023. Validity of sarcopenia diagnosis defined by calf circumference for muscle mass to predict functional outcome in patients with acute stroke. *Archives of Gerontology & Geriatrics,* 105**,** 104854.

AKAMIZU, T. & KANGAWA, K. 2010. Ghrelin for cachexia. *Journal of cachexia, sarcopenia and muscle,* 1**,** 169-176.

AL-KHALED, M., MATTHIS, C. & EGGERS, J. R. 2013. Stroke Complications: Incidence and Effects on Stroke Outcomes–Data from the Stroke Registry in the Federal State in Schleswig-Holstein, Germany (P04. 071). Lippincott Williams & Wilkins.

ALBERS, G. W., MARKS, M. P., KEMP, S., CHRISTENSEN, S., TSAI, J. P., ORTEGA-GUTIERREZ, S., MCTAGGART, R. A., TORBEY, M. T., KIM-TENSER, M. & LESLIE-MAZWI, T. 2018. Thrombectomy for stroke at 6 to 16 hours with selection by perfusion imaging. *New England Journal of Medicine,* 378**,** 708-718.

ALKHEDHAIRI, S. A., ALKHAYL, F. F. A., ISMAIL, A. D., ROZENDAAL, A., GERMAN, M., MACLEAN, B., JOHNSTON, L., MILLER, A. A., HUNTER, A. M. & MACGREGOR, L. J. 2022. The effect of krill oil supplementation on skeletal muscle function and size in older adults: A randomised controlled trial. *Clinical Nutrition,* 41**,** 1228-1235.

ALLEN, J., RAMSDEN, M. & NISAR, S. 2024. Skeletal muscle structure, function and pathology. *Orthopaedics and Trauma,* 38**,** 137-144.

ALTUN, M., BESCHE, H. C., OVERKLEEFT, H. S., PICCIRILLO, R., EDELMANN, M. J., KESSLER, B. M., GOLDBERG, A. L. & ULFHAKE, B. 2010. Muscle wasting in aged, sarcopenic rats is associated with enhanced activity of the ubiquitin proteasome pathway. *Journal of Biological Chemistry,* 285**,** 39597-39608.

AMIROUCHE, A., DURIEUX, A.-C., BANZET, S., KOULMANN, N., BONNEFOY, R., MOURET, C., BIGARD, X., PEINNEQUIN, A. & FREYSSENET, D. 2009. Down-regulation of Akt/mammalian target of rapamycin signaling pathway in response to myostatin overexpression in skeletal muscle. *Endocrinology,* 150**,** 286-294.

ANDERSEN, K. K. & OLSEN, T. S. 2015. The obesity paradox in stroke: lower mortality and lower risk of readmission for recurrent stroke in obese stroke patients. *International Journal of Stroke,* 10**,** 99-104.

ANNE, M., JUHA, K., MAKIKALLIO, T., MIKKO, T., OLLI, V., KYOSTI, S., HEIKKI, H. & VILHO, M. 2007. Neurohormonal activation in ischemic stroke: effects of acute phase disturbances on long-term mortality. *Current Neurovascular Research,* 4**,** 170-175.

ARASAKI, K., IGARASHI, O., ICHIKAWA, Y., MACHIDA, T., SHIROZU, I., HYODO, A. & USHIJIMA, R. 2006. Reduction in the motor unit number estimate (MUNE) after cerebral infarction. *Journal of the neurological sciences,* 250**,** 27-32.

ARGILÉS, J. M., BUSQUETS, S., STEMMLER, B. & LÓPEZ-SORIANO, F. J. 2014. Cancer cachexia: understanding the molecular basis. *Nature Reviews Cancer,* 14**,** 754-762.

AWERE-DUODU, A., DARKWAH, S., OSMAN, A.-H. & DONKOR, E. S. 2024. A systematic review and meta-analysis show a decreasing prevalence of post-stroke infections. *BMC neurology,* 24**,** 479.

AYDIN, T., KESIKTAS, F. N., OREN, M. M., ERDOGAN, T., AHISHA, Y. C., KIZILKURT, T., CORUM, M., KARACAN, I., OZTURK, S. & BAHAT, G. 2021. Sarcopenia in patients following stroke: an overlooked problem. *International Journal of Rehabilitation Research,* 44**,** 269-275.

AYERBE, L., AYIS, S., CRICHTON, S., WOLFE, C. & RUDD, A. 2014. The long-term outcomes of depression up to 10 years after stroke; the South London Stroke Register. *Journal of Neurology, Neurosurgery & Psychiatry,* 85**,** 514-521.

BAIG, M. U. & BODLE, J. 2020. Thrombolytic therapy.

BANDA, K. J., CHU, H., KANG, X. L., LIU, D., PIEN, L.-C., JEN, H.-J., HSIAO, S.-T. S. & CHOU, K.-R. 2022. Prevalence of dysphagia and risk of pneumonia and mortality in acute stroke patients: a meta-analysis. *BMC geriatrics,* 22**,** 420.

BARUGH, A. J., GRAY, P., SHENKIN, S. D., MACLULLICH, A. M. J. & MEAD, G. E. 2014. Cortisol levels and the severity and outcomes of acute stroke: a systematic review. *Journal of neurology,* 261**,** 533-545.

BAZZANO, L. A., GU, D., WHELTON, M. R., WU, X., CHEN, C. S., DUAN, X., CHEN, J., CHEN, J. C. & HE, J. 2010. Body mass index and risk of stroke among Chinese men and women. *Annals of neurology,* 67**,** 11-20.

BEAR, M. H., REDDY, V. & BOLLU, P. C. 2022. Neuroanatomy, hypothalamus. *StatPearls [internet].* StatPearls Publishing.

BERGE, E., WHITELEY, W., AUDEBERT, H., DE MARCHIS, G. M., FONSECA, A. C., PADIGLIONI, C., PÉREZ DE LA OSSA, N., STRBIAN, D., TSIVGOULIS, G. & TURC, G. 2021. European Stroke Organisation (ESO) guidelines on intravenous thrombolysis for acute ischaemic stroke. *European stroke journal,* 6**,** I-LXII.

BERNHARDT, J., DEWEY, H., THRIFT, A. & DONNAN, G. 2004. Inactive and alone: physical activity within the first 14 days of acute stroke unit care. *Stroke,* 35**,** 1005-1009.

BERRIEL DIAZ, M., ROHM, M. & HERZIG, S. 2024. Cancer cachexia: multilevel metabolic dysfunction. *Nature Metabolism,* 6**,** 2222-2245.

BEUTLER, B., GREENWALD, D., HULMES, J., CHANG, M., PAN, Y.-C., MATHISON, J., ULEVITCH, R. & CERAMI, A. 1985. Identity of tumour necrosis factor and the macrophage-secreted factor cachectin. *Nature,* 316**,** 552-554.

BIOSE, I., CHASTAIN, W., WANG, H., OUVRIER, B. & BIX, G. 2022. Optimizing intraluminal monofilament model of ischemic stroke in middle-aged Sprague–Dawley rats. *BMC neuroscience,* 23**,** 75.

BIOSE, I. J., RUTKAI, I., CLOSSEN, B., GAGE, G., SCHECHTMAN, K., ADKISSON IV, H. D. & BIX, G. J. 2023. Recombinant human perlecan DV and its LG3 subdomain are neuroprotective and acutely functionally restorative in severe experimental ischemic stroke. *Translational stroke research,* 14**,** 941-954.

BISE, T., YOSHIMURA, Y., WAKABAYASHI, H., NAGANO, F., KIDO, Y., SHIMAZU, S., SHIRAISHI, A. & MATSUMOTO, A. 2022. Association between BIA-derived Phase Angle and Sarcopenia and Improvement in Activities of Daily Living and Dysphagia in Patients undergoing Post-Stroke Rehabilitation. *Journal of Nutrition, Health & Aging,* 26**,** 590-597.

BODINE, S. C. & BAEHR, L. M. 2014. Skeletal muscle atrophy and the E3 ubiquitin ligases MuRF1 and MAFbx/atrogin-1. *American Journal of Physiology-Endocrinology and Metabolism,* 307**,** E469-E484.

BODINE, S. C., LATRES, E., BAUMHUETER, S., LAI, V. K.-M., NUNEZ, L., CLARKE, B. A., POUEYMIROU, W. T., PANARO, F. J., NA, E. & DHARMARAJAN, K.

2001a. Identification of ubiquitin ligases required for skeletal muscle atrophy. *Science,* 294**,** 1704-1708.

BODINE, S. C., STITT, T. N., GONZALEZ, M., KLINE, W. O., STOVER, G. L., BAUERLEIN, R., ZLOTCHENKO, E., SCRIMGEOUR, A., LAWRENCE, J. C. & GLASS, D. J. 2001b. Akt/mTOR pathway is a crucial regulator of skeletal muscle hypertrophy and can prevent muscle atrophy in vivo. *Nature cell biology,* 3**,** 1014-1019.

BOEHME, A. K., ESENWA, C. & ELKIND, M. S. 2017. Stroke risk factors, genetics, and prevention. *Circulation research,* 120**,** 472-495.

BOHANNON, R. W. 2007. Muscle strength and muscle training after stroke. *Journal of rehabilitation Medicine,* 39**,** 14.

BONALDO, P. & SANDRI, M. 2013. Cellular and molecular mechanisms of muscle atrophy. *Disease models & mechanisms,* 6**,** 25-39.

BORECKI, R., BYCZKIEWICZ, P. & SŁOWIKOWSKA-HILCZER, J. 2025. Selective androgen receptor modulators (SARMs)—potential anabolic drugs for the treatment of cachexia and frailty syndrome. *Endokrynologia Polska*.

BORENSTEIN, M., HEDGES, L. V., HIGGINS, J. P. & ROTHSTEIN, H. R. 2010. A basic introduction to fixed-effect and random-effects models for meta-analysis. *Research synthesis methods,* 1**,** 97-111.

BOYKO, M., ZLOTNIK, A., GRUENBAUM, B. F., GRUENBAUM, S. E., OHAYON, S., GOLDSMITH, T., KOTZ, R., LEIBOWITZ, A., SHEINER, E. & SHAPIRA, Y. 2010. An experimental model of focal ischemia using an internal carotid artery approach. *Journal of neuroscience methods,* 193**,** 246-253.

BRANYAN, T. E. & SOHRABJI, F. 2020. Sex differences in stroke co-morbidities. *Experimental neurology,* 332**,** 113384.

BREUILLE, D., FARGE, M., ROSE, F., ARNAL, M., ATTAIX, D. & OBLED, C. 1993. Pentoxifylline decreases body weight loss and muscle protein wasting characteristics of sepsis. *American Journal of Physiology-Endocrinology and Metabolism,* 265**,** E660-E666.

CAI, D., FRANTZ, J. D., TAWA, N. E., MELENDEZ, P. A., OH, B.-C., LIDOV, H. G., HASSELGREN, P.-O., FRONTERA, W. R., LEE, J. & GLASS, D. J. 2004. IKKβ/NF-κB activation causes severe muscle wasting in mice. *Cell,* 119**,** 285-298.

CAMPBELL, J. E., PECKETT, A. J., D'SOUZA, A. M., HAWKE, T. J. & RIDDELL, M. C. 2011. Adipogenic and lipolytic effects of chronic glucocorticoid exposure. *American Journal of Physiology-Cell Physiology,* 300**,** C198-C209.

CANSELL, C., DENIS, R. G., JOLY-AMADO, A., CASTEL, J. & LUQUET, S. 2012. Arcuate AgRP neurons and the regulation of energy balance. *Frontiers in endocrinology,* 3**,** 169.

CARDA, S., CISARI, C. & INVERNIZZI, M. 2013. Sarcopenia or muscle modifications in neurologic diseases: a lexical or patophysiological difference. *Eur J Phys Rehabil Med,* 49**,** 119-130.

CARIN-LEVY, G., GREIG, C., YOUNG, A., LEWIS, S., HANNAN, J. & MEAD, G. 2006. Longitudinal changes in muscle strength and mass after acute stroke. *Cerebrovascular Diseases,* 21**,** 201-207.

CHE, B., CHEN, H., WANG, A., PENG, H., BU, X., ZHANG, J., JU, Z., XU, T., HE, J. & ZHONG, C. 2022. Association between plasma L-carnitine and cognitive impairment in patients with acute ischemic stroke. *Journal of Alzheimer's Disease,* 86**,** 259-270.

CHEN, L.-K., WOO, J., ASSANTACHAI, P., AUYEUNG, T.-W., CHOU, M.-Y., IIJIMA, K., JANG, H. C., KANG, L., KIM, M. & KIM, S. 2020. Asian Working Group for Sarcopenia: 2019 consensus update on sarcopenia diagnosis and

treatment. *Journal of the American Medical Directors Association,* 21**,** 300-307. e2.

CINTI, S. 2006. The role of brown adipose tissue in human obesity. *Nutrition, metabolism and cardiovascular diseases,* 16**,** 569-574.

CLAVEL, S., COLDEFY, A.-S., KURKDJIAN, E., SALLES, J., MARGARITIS, I. & DERIJARD, B. 2006. Atrophy-related ubiquitin ligases, atrogin-1 and MuRF1 are up-regulated in aged rat Tibialis Anterior muscle. *Mechanisms of ageing and development,* 127**,** 794-801.

COWLEY, M. A., PRONCHUK, N., FAN, W., DINULESCU, D. M., COLMERS, W. F. & CONE, R. D. 1999. Integration of NPY, AGRP, and melanocortin signals in the hypothalamic paraventricular nucleus: evidence of a cellular basis for the adipostat. *Neuron,* 24**,** 155-163.

CRUZ-FLORES, S., RABINSTEIN, A., BILLER, J., ELKIND, M. S., GRIFFITH, P., GORELICK, P. B., HOWARD, G., LEIRA, E. C., MORGENSTERN, L. B. & OVBIAGELE, B. 2011. Racial-ethnic disparities in stroke care: the American experience: a statement for healthcare professionals from the American Heart Association/American Stroke Association. *Stroke,* 42**,** 2091-2116.

CRUZ-JENTOFT, A. J., BAHAT, G., BAUER, J., BOIRIE, Y., BRUYÈRE, O., CEDERHOLM, T., COOPER, C., LANDI, F., ROLLAND, Y. & SAYER, A. A. 2019. Sarcopenia: revised European consensus on definition and diagnosis. *Age and ageing,* 48**,** 16-31.

CURIONI, C., ANDRÉ, C. & VERAS, R. 2006. Weight reduction for primary prevention of stroke in adults with overweight or obesity. *Cochrane Database of Systematic Reviews*.

CURROW, D., TEMEL, J., ABERNETHY, A., MILANOWSKI, J., FRIEND, J. & FEARON, K. 2017. ROMANA 3: a phase 3 safety extension study of anamorelin in advanced non-small-cell lung cancer (NSCLC) patients with cachexia. *Annals of Oncology,* 28**,** 1949-1956.

DABEK, A., WOJTALA, M., PIROLA, L. & BALCERCZYK, A. 2020. Modulation of cellular biochemistry, epigenetics and metabolomics by ketone bodies. *Implications of the ketogenic diet in the physiology of the organism and pathological states. Nutrients,* 12**,** 788.

DE DEYNE, P. G., HAFER-MACKO, C. E., IVEY, F. M., RYAN, A. S. & MACKO, R. F. 2004. Muscle molecular phenotype after stroke is associated with gait speed. *Muscle & Nerve: Official Journal of the American Association of Electrodiagnostic Medicine,* 30**,** 209-215.

DEINDL, E., BOENGLER, K., VAN ROYEN, N. & SCHAPER, W. 2002. Differential expression of GAPDH and ß-actin in growing collateral arteries. *Molecular and cellular biochemistry,* 236**,** 139-146.

DEMETRIUS, L. 2005. Of mice and men: when it comes to studying ageing and the means to slow it down, mice are not just small humans. *EMBO reports,* 6**,** S39-S44.

DETTORI, I., GAVIANO, L., MELANI, A., LUCARINI, L., DURANTE, M., MASINI, E. & PEDATA, F. 2018. A selective histamine H4 receptor antagonist, JNJ7777120, is protective in a rat model of transient cerebral ischemia. *Frontiers in Pharmacology,* 9**,** 1231.

DHEDA, K., HUGGETT, J. F., BUSTIN, S. A., JOHNSON, M. A., ROOK, G. & ZUMLA, A. 2004. Validation of housekeeping genes for normalizing RNA expression in real-time PCR. *Biotechniques,* 37**,** 112-119.

DI MARCO, S., MAZROUI, R., DALLAIRE, P., CHITTUR, S., TENENBAUM, S. A., RADZIOCH, D., MARETTE, A. & GALLOUZI, I.-E. 2005. NF-κB-mediated MyoD decay during muscle wasting requires nitric oxide synthase mRNA

stabilization, HuR protein, and nitric oxide release. *Molecular and cellular biology,* 25, 6533-6545.
DIRNAGL, U. 2010. Complexities, confounders, and challenges in experimental stroke research: a checklist for researchers and reviewers. *Rodent models of stroke*. Springer.
DIRNAGL, U., IADECOLA, C. & MOSKOWITZ, M. A. 1999. Pathobiology of ischaemic stroke: an integrated view. *Trends in neurosciences,* 22, 391-397.
DISORDERS, N. I. O. N. & GROUP, S. R.-P. S. S. 1995. Tissue plasminogen activator for acute ischemic stroke. *New England Journal of Medicine,* 333, 1581-1588.
DITTMAR, M., SPRUSS, T., SCHUIERER, G. & HORN, M. 2003. External carotid artery territory ischemia impairs outcome in the endovascular filament model of middle cerebral artery occlusion in rats. *Stroke,* 34, 2252-2257.
DOEHNER, W., SCHENKEL, J., ANKER, S. D., SPRINGER, J. & AUDEBERT, H. J. 2013. Overweight and obesity are associated with improved survival, functional outcome, and stroke recurrence after acute stroke or transient ischaemic attack: observations from the TEMPiS trial. *European heart journal,* 34, 268-277.
DONG, W., ZHAO, S., WEN, S., DONG, C., CHEN, Q., GONG, T., CHEN, W., LIU, W., MU, L. & SHAN, H. 2020. A preclinical randomized controlled study of ischemia treated with Ginkgo biloba extracts: Are complex components beneficial for treating acute stroke? *Current Research in Translational Medicine,* 68, 197-203.
DOUGHERTY, P. 2020. Chapter 1: Hypothalamus: Structural Organization. *Houston: University of Texas. Available onlin at: https://nba. uth. tmc. edu/neuroscience/m/s4/chapter01. html (accessed 2020)*.
DU, J., MIAO, M., LU, Z., CHEN, H., BAO, A., CHE, B., ZHANG, J., JU, Z., XU, T. & HE, J. 2022. Plasma l-carnitine and risks of cardiovascular events and recurrent stroke after ischemic stroke: A nested case-control study. *Nutrition, Metabolism and Cardiovascular Diseases,* 32, 2579-2587.
DYLLA, L., REISZ, J. A., POISSON, S. N., HERSON, P. S., SANSING, L. H. & MONTE, A. A. 2025. Elevated initial blood kynurenine is associated with increased odds of post-stroke infection: Kynurenine and post-stroke infection. *Journal of Stroke and Cerebrovascular Diseases,* 34, 108268.
EDSTRÖM, E., ALTUN, M., HÄGGLUND, M. & ULFHAKE, B. 2006. Atrogin-1/MAFbx and MuRF1 are downregulated in aging-related loss of skeletal muscle. *The Journals of Gerontology Series A: Biological Sciences and Medical Sciences,* 61, 663-674.
ELIA, M., RITZ, P. & STUBBS, R. 2000. Total energy expenditure in the elderly. *European journal of clinical nutrition,* 54, S92-S103.
ENGLISH, C., MCLENNAN, H., THOIRS, K., COATES, A. & BERNHARDT, J. 2010. Loss of skeletal muscle mass after stroke: a systematic review. *International Journal of Stroke,* 5, 395-402.
ESPOSITO, E., MANDEVILLE, E. T., HAYAKAWA, K., SINGHAL, A. B. & LO, E. H. 2013. Effects of normobaric oxygen on the progression of focal cerebral ischemia in rats. *Experimental neurology,* 249, 33-38.
ESSER, K. 2008. Regulation of mTOR signaling in skeletal muscle hypertrophy. *J Musculoskelet Neuronal Interact,* 8, 338-339.
ETTEHAD, D., EMDIN, C. A., KIRAN, A., ANDERSON, S. G., CALLENDER, T., EMBERSON, J., CHALMERS, J., RODGERS, A. & RAHIMI, K. 2016. Blood pressure lowering for prevention of cardiovascular disease and death: a systematic review and meta-analysis. *The Lancet,* 387, 957-967.

EVANS, W. J., MORLEY, J. E., ARGILÉS, J., BALES, C., BARACOS, V., GUTTRIDGE, D., JATOI, A., KALANTAR-ZADEH, K., LOCHS, H. & MANTOVANI, G. 2008. Cachexia: a new definition. *Clinical nutrition,* 27**,** 793-799.

FANG, W. Y., TSENG, Y. T., LEE, T. Y., FU, Y. C., CHANG, W. H., LO, W. W., LIN, C. L. & LO, Y. C. 2021. Triptolide prevents LPS-induced skeletal muscle atrophy via inhibiting NF-κB/TNF-α and regulating protein synthesis/degradation pathway. *British Journal of Pharmacology,* 178**,** 2998-3016.

FASSBENDER, K., SCHMIDT, R., MÖSSNER, R., DAFFERTSHOFER, M. & HENNERICI, M. 1994. Pattern of activation of the hypothalamic-pituitary-adrenal axis in acute stroke. Relation to acute confusional state, extent of brain damage, and clinical outcome. *Stroke,* 25**,** 1105-1108.

FATHALI, N., OSTROWSKI, R. P., HASEGAWA, Y., LEKIC, T., TANG, J. & ZHANG, J. H. 2013. Splenic immune cells in experimental neonatal hypoxia–ischemia. *Translational stroke research,* 4**,** 208-219.

FEARON, K. C., GLASS, D. J. & GUTTRIDGE, D. C. 2012. Cancer cachexia: mediators, signaling, and metabolic pathways. *Cell metabolism,* 16**,** 153-166.

FEIGIN, V. L., BRAININ, M., NORRVING, B., MARTINS, S., SACCO, R. L., HACKE, W., FISHER, M., PANDIAN, J. & LINDSAY, P. 2022. World Stroke Organization (WSO): global stroke fact sheet 2022. *International journal of stroke,* 17**,** 18-29.

FEIGIN, V. L., BRAININ, M., NORRVING, B., MARTINS, S. O., PANDIAN, J., LINDSAY, P., F GRUPPER, M. & RAUTALIN, I. 2025. World stroke organization: global stroke fact sheet 2025. *International Journal of Stroke,* 20**,** 132-144.

FENG, G., WU, Z., YANG, L., WANG, K. & WANG, H. 2024. Β-hydroxybutyrate and ischemic stroke: roles and mechanisms. *Molecular Brain,* 17**,** 48.

FISHER, M. 2011. New approaches to neuroprotective drug development. *Stroke,* 42**,** S24-S27.

FISHER, M., FEUERSTEIN, G., HOWELLS, D. W., HURN, P. D., KENT, T. A., SAVITZ, S. I. & LO, E. H. 2009. Update of the stroke therapy academic industry roundtable preclinical recommendations. *Stroke*.

FOLEY, N. C., MARTIN, R. E., SALTER, K. L. & TEASELL, R. W. 2009. A review of the relationship between dysphagia and malnutrition following stroke. *Journal of rehabilitation medicine,* 41**,** 707-713.

FONSECA, A. C., MERWICK, A., DENNIS, M., FERRARI, J., FERRO, J. M., KELLY, P., LAL, A., OIS, A., OLIVOT, J. M. & PURROY, F. 2021. European Stroke Organisation (ESO) guidelines on management of transient ischaemic attack. *European Stroke Journal,* 6**,** CLXIII-CLXXXVI.

FUGATE, J. E. & RABINSTEIN, A. A. Update on intravenous recombinant tissue plasminogen activator for acute ischemic stroke. Mayo Clinic Proceedings, 2014. Elsevier, 960-972.

GALLAGHER, D., VISSER, M., DE MEERSMAN, R. E., SEPÚLVEDA, D., BAUMGARTNER, R. N., PIERSON, R. N., HARRIS, T. & HEYMSFIELD, S. B. 1997. Appendicular skeletal muscle mass: effects of age, gender, and ethnicity. *Journal of applied physiology,* 83**,** 229-239.

GARCÍA-MARTÍNEZ, C., AGELL, N., LLOVERA, M., LÓPEZ-SORIANO, F. J. & ARGILÉS, J. M. 1993. Tumour necrosis factor-α increases the ubiquitinization of rat skeletal muscle proteins. *FEBS letters,* 323**,** 211-214.

GLARE, E. M., DIVJAK, M., BAILEY, M. & WALTERS, E. H. 2002. ß-Actin and GAPDH housekeeping gene expression in asthmatic airways is variable and not suitable for normalising mRNA levels. *Thorax,* 57**,** 765-770.

GLASS, D. J. 2010. Signaling pathways perturbing muscle mass. *Current opinion in clinical nutrition & metabolic care,* 13**,** 225-229.

GONZALES, R. A., BROWN, L. M., JONES, T. W., TRENT, R. D., WESTBROOK, S. L. & LESLIE, S. W. 1991. N-methyl-D-aspartate mediated responses decrease with age in Fischer 344 rat brain. *Neurobiology of aging,* 12**,** 219-225.

GONZÁLEZ-FERNÁNDEZ, M., OTTENSTEIN, L., ATANELOV, L. & CHRISTIAN, A. B. 2013. Dysphagia after stroke: an overview. *Current physical medicine and rehabilitation reports,* 1**,** 187-196.

GREIWE, J. S., CHENG, B., RUBIN, D. C., YARASHESKI, K. E. & SEMENKOVICH, C. F. 2001. Resistance exercise decreases skeletal muscle tumor necrosis factor α in frail elderly humans. *The FASEB Journal,* 15**,** 475-482.

GRUBERG, L., WEISSMAN, N. J., WAKSMAN, R., FUCHS, S., DEIBLE, R., PINNOW, E. E., AHMED, L. M., KENT, K. M., PICHARD, A. D. & SUDDATH, W. O. 2002. The impact of obesity on the short-term andlong-term outcomes after percutaneous coronary intervention: the obesity paradox? *Journal of the American College of Cardiology,* 39**,** 578-584.

GULLESTAD, L., UELAND, T., VINGE, L. E., FINSEN, A., YNDESTAD, A. & AUKRUST, P. 2012. Inflammatory cytokines in heart failure: mediators and markers. *Cardiology,* 122**,** 23-35.

HACKETT, M. & PICKLES, K. 2014. Frequency of depression after stroke: an updated systematic reviewandmeta-analysisofobservationalstudies. IntJStroke9.

HAFER-MACKO, C. E., YU, S., RYAN, A. S., IVEY, F. M. & MACKO, R. F. 2005. Elevated tumor necrosis factor-α in skeletal muscle after stroke. *Stroke,* 36**,** 2021-2023.

HALEY, M. J., MULLARD, G., HOLLYWOOD, K. A., COOPER, G. J., DUNN, W. B. & LAWRENCE, C. B. 2017. Adipose tissue and metabolic and inflammatory responses to stroke are altered in obese mice. *Disease models & mechanisms,* 10**,** 1229-1243.

HALEY, M. J., WHITE, C. S., ROBERTS, D., O'TOOLE, K., CUNNINGHAM, C. J., RIVERS-AUTY, J., O'BOYLE, C., LANE, C., HEANEY, O., ALLAN, S. M. & LAWRENCE, C. B. 2020a. Stroke Induces Prolonged Changes in Lipid Metabolism, the Liver and Body Composition in Mice. *Translational Stroke Research,* 11**,** 837-850.

HALEY, M. J., WHITE, C. S., ROBERTS, D., O'TOOLE, K., CUNNINGHAM, C. J., RIVERS-AUTY, J., O'BOYLE, C., LANE, C., HEANEY, O. & ALLAN, S. M. 2020b. Stroke induces prolonged changes in lipid metabolism, the liver and body composition in mice. *Translational stroke research,* 11**,** 837-850.

HALEY, M. J., WHITE, C. S., ROBERTS, D., O'TOOLE, K., CUNNINGHAM, C. J., RIVERS-AUTY, J., O'BOYLE, C., LANE, C., HEANEY, O. & ALLAN, S. M. 2020c. Stroke induces prolonged changes in lipid metabolism, the liver and body composition in mice. *Translational stroke research,* 11**,** 837-850.

HAMAUCHI, S., FURUSE, J., TAKANO, T., MUNEMOTO, Y., FURUYA, K., BABA, H., TAKEUCHI, M., CHODA, Y., HIGASHIGUCHI, T. & NAITO, T. 2019. A multicenter, open-label, single-arm study of anamorelin (ONO-7643) in advanced gastrointestinal cancer patients with cancer cachexia. *Cancer,* 125**,** 4294-4302.

HANKEY, G. J. 2006a. Is plasma homocysteine a modifiable risk factor for stroke? *Nature Clinical Practice Neurology,* 2**,** 26-33.

HANKEY, G. J. 2006b. Potential new risk factors for ischemic stroke: what is their potential? *Stroke,* 37, 2181-2188.

HANSON, A. M., HARRISON, B. C., YOUNG, M. H., STODIECK, L. S. & FERGUSON, V. L. 2013. Longitudinal characterization of functional, morphologic, and biochemical adaptations in mouse skeletal muscle with hindlimb suspension. *Muscle & nerve,* 48, 393-402.

HAY, N. & SONENBERG, N. 2004. Upstream and downstream of mTOR. *Genes & development,* 18, 1926-1945.

HERON, M. 2021. Deaths: leading causes for 2019. *National vital statistics reports: from the centers for disease control and prevention, national center for health statistics, national vital statistics system,* 70, 1-114.

HIGGINS, J. P. & THOMPSON, S. G. 2002. Quantifying heterogeneity in a meta-analysis. *Statistics in medicine,* 21, 1539-1558.

HOLLAND, S. A., WELLWOOD, I. & KUYS, S. 2024. Effect of abnormal body weight on mortality and functional recovery in adults after stroke: An umbrella review. *International Journal of Stroke,* 19, 397-405.

HOLLOSZY, J. O., CHEN, M., CARTEE, G. D. & YOUNG, J. C. 1991. Skeletal muscle atrophy in old rats: differential changes in the three fiber types. *Mechanisms of ageing and development,* 60, 199-213.

HU, Y., YANG, Z. H., YAN, F., HUANG, S. F., WANG, R. L., HAN, Z. P., FAN, J. F., ZHENG, Y. M., LIU, P. & LUO, Y. M. 2023. CCA repair or ECA ligation—Which middle cerebral artery occlusion is better in the reperfusion mouse model? *ibrain,* 9, 258-269.

HULTMAN, E. 1995. Fuel selection, muscle fibre. *Proceedings of the Nutrition Society,* 54, 107-121.

HUPPERTZ, V. A. L., PILZ, W., PILZ DA CUNHA, G., DE GROOT, L. C. P. G. M., VAN HELVOORT, A., SCHOLS, J. M. G. A. & BAIJENS, L. W. J. 2022. Malnutrition risk and oropharyngeal dysphagia in the chronic post-stroke phase. *Frontiers in Neurology,* 13.

HURD, M. D., GOEL, I., SAKAI, Y. & TERAMURA, Y. 2021. Current status of ischemic stroke treatment: From thrombolysis to potential regenerative medicine. *Regenerative Therapy,* 18, 408-417.

IBRAHIM, M. M. 2010. Subcutaneous and visceral adipose tissue: structural and functional differences. *Obesity reviews,* 11, 11-18.

IKEJI, R., NOZOE, M., YAMAMOTO, M., SEIKE, H., KUBO, H. & SHIMADA, S. 2023. Sarcopenia in patients following stroke: Prevalence and associated factors. *Clinical Neurology & Neurosurgery,* 233, 107910.

INOUE, T., MAEDA, K., SHIMIZU, A., NAGANO, A., UESHIMA, J., SATO, K. & MUROTANI, K. 2021. Calf circumference value for sarcopenia screening among older adults with stroke. *Archives of Gerontology & Geriatrics,* 93, 104290.

IZUMIYA, Y., HOPKINS, T., MORRIS, C., SATO, K., ZENG, L., VIERECK, J., HAMILTON, J. A., OUCHI, N., LEBRASSEUR, N. K. & WALSH, K. 2008. Fast/Glycolytic muscle fiber growth reduces fat mass and improves metabolic parameters in obese mice. *Cell metabolism,* 7, 159-172.

JACOB, L. & KOSTEV, K. 2020. Urinary and fecal incontinence in stroke survivors followed in general practice: A retrospective cohort study. *Annals of physical and rehabilitation medicine,* 63, 488-494.

JANG, A., BAE, C. H., HAN, S. J. & BAE, H. 2021. Association Between Length of Stay in the Intensive Care Unit and Sarcopenia Among Hemiplegic Stroke Patients. *Annals of Rehabilitation Medicine-Arm,* 45, 49-56.

JANG, Y., IM, S., HAN, Y., KOO, H., SOHN, D. & PARK, G. Y. 2020. Can initial sarcopenia affect poststroke rehabilitation outcome? *Journal of Clinical Neuroscience,* 71**,** 113-118.

JANSSEN, B., DEBETS, J., LEENDERS, P. & SMITS, J. 2002. Chronic measurement of cardiac output in conscious mice. *American Journal of Physiology-Regulatory, Integrative and Comparative Physiology,* 282**,** R928-R935.

JANSSEN, P. M., BIESIADECKI, B. J., ZIOLO, M. T. & DAVIS, J. P. 2016. The need for speed: mice, men, and myocardial kinetic reserve. *Circulation research,* 119**,** 418-421.

JANSSON, E., SJÖDIN, B. & TESCH, P. 1978. Changes in muscle fibre type distribution in man after physical training: a sign of fibre type transformation? *Acta Physiologica Scandinavica,* 104**,** 235-237.

JIA, J., ZHANG, H., LIANG, X., DAI, Y., LIU, L., TAN, K., MA, R., LUO, J., DING, Y. & KE, C. 2021. Application of metabolomics to the discovery of biomarkers for ischemic stroke in the murine model: a comparison with the clinical results. *Molecular Neurobiology,* 58**,** 6415-6426.

JOHANSSON, Å., OLSSON, T., CARLBERG, B., KARLSSON, K. & FAGERLUND, M. 1997. Hypercortisolism after stroke—partly cytokine-mediated? *Journal of the neurological sciences,* 147**,** 43-47.

JONKER, R., DEUTZ, N. E., ERBLAND, M. L., ANDERSON, P. J. & ENGELEN, M. P. 2017. Effectiveness of essential amino acid supplementation in stimulating whole body net protein anabolism is comparable between COPD patients and healthy older adults. *Metabolism,* 69**,** 120-129.

JØNSSON, A.-C., LINDGREN, I., NORRVING, B. & LINDGREN, A. 2008. Weight loss after stroke: a population-based study from the Lund Stroke Register. *Stroke,* 39**,** 918-923.

JONSSON, A. C., LINDGREN, I., NORRVING, B. & LINDGREN, A. 2008. Weight loss after stroke: a population-based study from the Lund Stroke Register. *Stroke,* 39**,** 918-23.

JOVIN, T. G., CHAMORRO, A., COBO, E., DE MIQUEL, M. A., MOLINA, C. A., ROVIRA, A., SAN ROMÁN, L., SERENA, J., ABILLEIRA, S. & RIBÓ, M. 2015. Thrombectomy within 8 hours after symptom onset in ischemic stroke. *New England Journal of Medicine,* 372**,** 2296-2306.

KAMEL, E. M., ALLAM, A. A., RUDAYNI, H. A., AHMED, N. A., ALKHAYL, F. F. A. & LAMSABHI, A. M. 2025. Uncoupling Toxic NO Signaling: Progress, Challenges, and Therapeutic Promise of Disrupting the PSD-95/nNOS Protein–Protein Interaction. *European Journal of Medicinal Chemistry***,** 117994.

KAMEYAMA, Y., ASHIZAWA, R., HONDA, H., TAKE, K., YOSHIZAWA, K. & YOSHIMOTO, Y. 2022. Sarcopenia Affects Functional Independence Measure motor Scores in Elderly Patients with Stroke. *Journal of Stroke & Cerebrovascular Diseases,* 31**,** 106615.

KANAI, M., NOZOE, M., OHTSUBO, T., YASUMOTO, I. & UENO, K. 2023. Relationship of Functional Outcome With Sarcopenia and Objectively Measured Physical Activity in Patients With Stroke Undergoing Rehabilitation. *Journal of Aging & Physical Activity,* 31**,** 1-6.

KAWAHARA, K., SUZUKI, T., YASAKA, T., NAGATA, H., OKAMOTO, Y., KITA, K. & MORISAKI, H. 2017. Evaluation of the site specificity of acute disuse muscle atrophy developed during a relatively short period in critically ill patients according to the activities of daily living level: A prospective observational study. *Australian Critical Care,* 30**,** 29-36.

KEEP, R., ANDJELKOVIC, A. & XI, G. 2017. Cytotoxic and vasogenic brain edema. *Primer on cerebrovascular diseases.* Elsevier.

KIM, H. J., KIM, H. J., YUN, J., KIM, K. H., KIM, S. H., LEE, S.-C., BAE, S. B., KIM, C. K., LEE, N. S. & LEE, K. T. 2012. Pathophysiological role of hormones and cytokines in cancer cachexia. *Journal of Korean medical science,* 27**,** 128-134.

KIM, S., PARK, E. S., CHEN, P. R. & KIM, E. 2022a. Dysregulated hypothalamic–pituitary–adrenal axis is associated with increased inflammation and worse outcomes after ischemic stroke in diabetic mice. *Frontiers in immunology,* 13**,** 864858.

KIM, Y., KIM, C. K., JUNG, S., KO, S.-B., LEE, S.-H. & YOON, B.-W. 2015a. Prognostic importance of weight change on short-term functional outcome in acute ischemic stroke. *International Journal of Stroke,* 10**,** 62-68.

KIM, Y., KIM, C. K., JUNG, S., KO, S. B., LEE, S. H. & YOON, B. W. 2015b. Prognostic importance of weight change on short-term functional outcome in acute ischemic stroke. *International Journal of Stroke,* 10 Suppl A100**,** 62-8.

KIM, Y. J., KANG, D., YANG, H. R., PARK, B. S., TU, T. H., JEONG, B., LEE, B. J., KIM, J. K. & KIM, J. G. 2022b. Metabolic profiling of the hypothalamus of mice during short-term food deprivation. *Metabolites,* 12**,** 407.

KISHIMOTO, H., NEMOTO, Y., MAEZAWA, T., TAKAHASHI, K., KOSEKI, K., ISHIBASHI, K., TANAMACHI, H., KOBAYASHI, N. & KOHNO, Y. 2022. Weight Change during the Early Phase of Convalescent Rehabilitation after Stroke as a Predictor of Functional Recovery: A Retrospective Cohort Study. *Nutrients,* 14**,** 09.

KITAZOE, Y., KISHINO, H., TANISAWA, K., UDAKA, K. & TANAKA, M. 2019. Renormalized basal metabolic rate describes the human aging process and longevity. *Aging Cell,* 18**,** e12968.

KLEINDORFER, D. O., TOWFIGHI, A., CHATURVEDI, S., COCKROFT, K. M., GUTIERREZ, J., LOMBARDI-HILL, D., KAMEL, H., KERNAN, W. N., KITTNER, S. J. & LEIRA, E. C. 2021a. 2021 guideline for the prevention of stroke in patients with stroke and transient ischemic attack: a guideline from the American Heart Association/American Stroke Association. *Stroke,* 52**,** e364-e467.

KLEINDORFER, D. O., TOWFIGHI, A., CHATURVEDI, S., COCKROFT, K. M., GUTIERREZ, J., LOMBARDI-HILL, D., KAMEL, H., KERNAN, W. N., KITTNER, S. J., LEIRA, E. C., LENNON, O., MESCHIA, J. F., NGUYEN, T. N., POLLAK, P. M., SANTANGELI, P., SHARRIEF, A. Z., SMITH, S. C., TURAN, T. N. & WILLIAMS, L. S. 2021b. 2021 Guideline for the Prevention of Stroke in Patients With Stroke and Transient Ischemic Attack: A Guideline From the American Heart Association/American Stroke Association. *Stroke,* 52**,** e364-e467.

KLOK, M. D., JAKOBSDOTTIR, S. & DRENT, M. L. 2007. The role of leptin and ghrelin in the regulation of food intake and body weight in humans: a review. *Obesity reviews,* 8**,** 21-34.

KNEZIC, A., BROUGHTON, B. R., WIDDOP, R. E. & MCCARTHY, C. A. 2022. Optimising the photothrombotic model of stroke in the C57Bl/6 and FVB/N strains of mouse. *Scientific Reports,* 12**,** 7598.

KNEZIC, A., BUDUSAN, E., SAEZ, N. J., BROUGHTON, B. R., RASH, L. D., KING, G. F., WIDDOP, R. E. & MCCARTHY, C. A. 2024. Hi1a Improves Sensorimotor Deficit following Endothelin-1-Induced Stroke in Rats but Does Not Improve Functional Outcomes following Filament-Induced Stroke in Mice. *ACS Pharmacology & Translational Science,* 7**,** 1043-1054.

KOIZUMI, J. 1986. Experimental studies of ischemic brain edema. 1. A new experimental model of cerebral embolism in rats in which recirculation can be introduced in the ischemic area. *Jpn. J. Stroke.,* 8**,** 1-8.

KORTEBEIN, P., FERRANDO, A., LOMBEIDA, J., WOLFE, R. & EVANS, W. J. 2007. Effect of 10 days of bed rest on skeletal muscle in healthy older adults. *Jama,* 297**,** 1769-1774.

KURIAKOSE, D. & XIAO, Z. 2020. Pathophysiology and treatment of stroke: present status and future perspectives. *International journal of molecular sciences,* 21**,** 7609.

LABAT-GEST, V. & TOMASI, S. 2013. Photothrombotic ischemia: a minimally invasive and reproducible photochemical cortical lesion model for mouse stroke studies. *Journal of visualized experiments: JoVE***,** 50370.

LAIRD, B. J., SKIPWORTH, R., BONOMI, P. D., FALLON, M., KAASA, S., GIORGINO, R., MCMILLAN, D. C. & CURROW, D. C. 2025. Anamorelin Efficacy in Non-Small-Cell Lung Cancer Patients With Cachexia: Insights From ROMANA 1 and ROMANA 2. *Journal of Cachexia, Sarcopenia and Muscle,* 16**,** e13732.

LANDIN, S., HAGENFELDT, L., SALTIN, B. & WAHREN, J. 1977. Muscle metabolism during exercise in hemiparetic patients. *Clinical Science and Molecular Medicine,* 53**,** 257-269.

LANSBERG, M. G., O'BRIEN, M. W., TONG, D. C., MOSELEY, M. E. & ALBERS, G. W. 2001. Evolution of cerebral infarct volume assessed by diffusion-weighted magnetic resonance imaging. *Archives of neurology,* 58**,** 613-617.

LAPCHAK, P. A., ZHANG, J. H. & NOBLE-HAEUSSLEIN, L. J. 2013. RIGOR guidelines: escalating STAIR and STEPS for effective translational research. *Translational stroke research,* 4**,** 279-285.

LARSON, T. 2025. Nissl Staining with Thionin.

LAVRIV, D. S., NEVES, P. M. & RAVASCO, P. 2018. Should omega-3 fatty acids be used for adjuvant treatment of cancer cachexia? *Clinical nutrition ESPEN,* 25**,** 18-25.

LEE, H., LEE, I. H., HEO, J., BAIK, M., PARK, H., LEE, H. S., NAM, H. S. & KIM, Y. D. 2022. Impact of Sarcopenia on Functional Outcomes Among Patients With Mild Acute Ischemic Stroke and Transient Ischemic Attack: A Retrospective Study. *Frontiers in Neurology,* 13.

LEE, S.-H., CHOI, H., KIM, K.-Y., LEE, H.-S. & JUNG, J.-M. 2023a. Appendicular skeletal muscle mass associated with sarcopenia as a predictor of poor functional outcomes in ischemic stroke. *Clinical Interventions in Aging***,** 1009-1020.

LEE, S. H., CHOI, H., KIM, K. Y., LEE, H. S. & JUNG, J. M. 2023b. Appendicular Skeletal Muscle Mass Associated with Sarcopenia as a Predictor of Poor Functional Outcomes in Ischemic Stroke. *Clinical Interventions In Aging,* 18**,** 1009-1020.

LEITE, M. O., SILVA, T. M. & MACHADO, M. 2021. IGF-1-PI3K-Akt-mTOR and myostatin-SMAD3 pathways signaling for muscle hypertophy. *J Endocrinol Thyroid Res,* 6**,** 555689.

LEVINE, B., KALMAN, J., MAYER, L., FILLIT, H. M. & PACKER, M. 1990. Elevated circulating levels of tumor necrosis factor in severe chronic heart failure. *New England Journal of Medicine,* 323**,** 236-241.

LI, H., ZHANG, N., LIN, H.-Y., YU, Y., CAI, Q.-Y., MA, L. & DING, S. 2014a. Histological, cellular and behavioral assessments of stroke outcomes after photothrombosis-induced ischemia in adult mice. *BMC neuroscience,* 15**,** 58.

LI, S., FRANCISCO, G. E. & ZHOU, P. 2018. Post-stroke hemiplegic gait: new perspective and insights. *Frontiers in physiology,* 9**,** 1021.

LI, S., GONZALEZ-BUONOMO, J., GHUMAN, J., HUANG, X., MALIK, A., YOZBATIRAN, N., MAGAT, E., FRANCISCO, G. E., WU, H. & FRONTERA, W. R. 2022. Aging after stroke: how to define post-stroke sarcopenia and what are its risk factors? *European journal of physical & rehabilitation medicine.,* 58**,** 683-692.

LI, W., CLAYPOOL, M. D., FRIERA, A. M., MCLAUGHLIN, J., BALTGALVIS, K. A., SMITH, I. J., KINOSHITA, T., WHITE, K., LANG, W. & GODINEZ, G. 2014b. Noninvasive imaging of in vivo MuRF1 expression during muscle atrophy. *PloS one,* 9**,** e94032.

LI, W., YUE, T. & LIU, Y. 2020. New understanding of the pathogenesis and treatment of stroke-related sarcopenia. *Biomedicine & Pharmacotherapy,* 131**,** 110721.

LI, Y. P., SCHWARTZ, R. J., WADDELL, I. D., HOLLOWAY, B. R. & REID, M. B. 1998. Skeletal muscle myocytes undergo protein loss and reactive oxygen-mediated NF-κB activation in response to tumor necrosis factorα. *The FASEB Journal,* 12**,** 871-880.

LIANG, D., BHATTA, S., GERZANICH, V. & SIMARD, J. M. 2007. Cytotoxic edema: mechanisms of pathological cell swelling. *Neurosurgical focus,* 22**,** 1-9.

LIAW, N. & LIEBESKIND, D. 2020. Emerging therapies in acute ischemic stroke. *F1000Research,* 9**,** F1000 Faculty Rev-546.

LICARI, C., TENORI, L., DI CESARE, F., LUCHINAT, C., GIUSTI, B., KURA, A., DE CARIO, R., INZITARI, D., PICCARDI, B. & NESI, M. 2022. Nuclear magnetic resonance-based metabolomics to predict early and late adverse outcomes in ischemic stroke treated with intravenous thrombolysis. *Journal of Proteome Research,* 22**,** 16-25.

LIU, F., SCHAFER, D. P. & MCCULLOUGH, L. D. 2009a. TTC, fluoro-Jade B and NeuN staining confirm evolving phases of infarction induced by middle cerebral artery occlusion. *Journal of neuroscience methods,* 179**,** 1-8.

LIU, F., YUAN, R., BENASHSKI, S. E. & MCCULLOUGH, L. D. 2009b. Changes in experimental stroke outcome across the life span. *Journal of Cerebral Blood Flow & Metabolism,* 29**,** 792-802.

LIU, M., ZHOU, K., LI, H., DONG, X., TAN, G., CHAI, Y., WANG, W. & BI, X. 2015. Potential of serum metabolites for diagnosing post-stroke cognitive impairment. *Molecular BioSystems,* 11**,** 3287-3296.

LONGO, N., FRIGENI, M. & PASQUALI, M. 2016. Carnitine transport and fatty acid oxidation. *Biochimica et biophysica acta (BBA)-molecular cell research,* 1863**,** 2422-2435.

LOO, D. T. 2002. TUNEL assay: an overview of techniques. *In situ detection of DNA damage: Methods and protocols***,** 21-30.

MAJUMDER, D. 2024. Ischemic stroke: pathophysiology and evolving treatment approaches. *Neuroscience Insights,* 19**,** 26331055241292600.

MANTOVANI, G., MACCIO, A., ESU, S., LAI, P., SANTONA, M., MASSA, E., DESSI, D., MELIS, G. & DEL GIACCO, G. 1997. Medroxyprogesterone acetate reduces the in vitro production of cytokines and serotonin involved in anorexia/cachexia and emesis by peripheral blood mononuclear cells of cancer patients. *European Journal of Cancer,* 33**,** 602-607.

MANWANI, B., LIU, F., SCRANTON, V., HAMMOND, M. D., SANSING, L. H. & MCCULLOUGH, L. D. 2013. Differential effects of aging and sex on stroke induced inflammation across the lifespan. *Experimental neurology,* 249**,** 120-131.

MANWANI, B., LIU, F., XU, Y., PERSKY, R., LI, J. & MCCULLOUGH, L. D. 2011. Functional recovery in aging mice after experimental stroke. *Brain, behavior, and immunity,* 25**,** 1689-1700.

MAPSTONE, M., CHEEMA, A. K., FIANDACA, M. S., ZHONG, X., MHYRE, T. R., MACARTHUR, L. H., HALL, W. J., FISHER, S. G., PETERSON, D. R. & HALEY, J. M. 2014. Plasma phospholipids identify antecedent memory impairment in older adults. *Nature medicine,* 20**,** 415-418.

MARGETIS, K. & SÁNCHEZ-MANSO, J. C. 2025. Neuroanatomy, middle cerebral artery. *StatPearls [Internet].* StatPearls Publishing.

MARINI, C., DE SANTIS, F., SACCO, S., RUSSO, T., OLIVIERI, L., TOTARO, R. & CAROLEI, A. 2005. Contribution of atrial fibrillation to incidence and outcome of ischemic stroke: results from a population-based study. *Stroke,* 36**,** 1115-1119.

MATSUSHITA, T., NISHIOKA, S., TAGUCHI, S. & YAMANOUCHI, A. 2019. Sarcopenia as a predictor of activities of daily living capability in stroke patients undergoing rehabilitation. *Geriatrics & gerontology international,* 19**,** 1124-1128.

MATSUSHITA, T., NISHIOKA, S., TAGUCHI, S., YAMANOUCHI, A., OKAZAKI, Y., OISHI, K., NAKASHIMA, R., FUJII, T., TOKUNAGA, Y. & ONIZUKA, S. 2021. Effect of Improvement in Sarcopenia on Functional and Discharge Outcomes in Stroke Rehabilitation Patients. *Nutrients,* 13**,** 25.

MCCULLER, C., JESSU, R. & CALLAHAN, A. L. 2023. Physiology, skeletal muscle. *StatPearls [Internet].* StatPearls Publishing.

MCPHERRON, A. C., LAWLER, A. M. & LEE, S.-J. 1997. Regulation of skeletal muscle mass in mice by a new TGF-p superfamily member. *Nature,* 387**,** 83-90.

MIWA, K., NAKAI, M., YOSHIMURA, S., SASAHARA, Y., WADA, S., KOGE, J., ISHIGAMI, A., YAGITA, Y., KAMIYAMA, K. & MIYAMOTO, Y. 2024. Clinical impact of body mass index on outcomes of ischemic and hemorrhagic strokes. *International Journal of Stroke,* 19**,** 907-915.

MOGAMIYA, T., OMORI, Y., KAWAGOE, J., KANEDA, T., MATSUSHIMA, S. & ONODERA, H. 2022. Association of Activities of Daily Living with Body Weight Change 3 Months After Stroke Onset. *Journal of Stroke & Cerebrovascular Diseases,* 31**,** 106573.

MOHAMMED, M. & LI, J. 2022. Stroke-Related Sarcopenia among Two Different Developing Countries with Diverse Ethnic Backgrounds (Cross-National Study in Egypt and China). *Healthcare,* 10.

MOHER, D., LIBERATI, A., TETZLAFF, J., ALTMAN, D. G. & GROUP, P. 2009. Preferred reporting items for systematic reviews and meta-analyses: the PRISMA statement. *BMJ,* 339**,** b2535.

MØLLER, N. 2020. Ketone body, 3-hydroxybutyrate: minor metabolite-major medical manifestations. *The Journal of Clinical Endocrinology & Metabolism,* 105**,** 2884-2892.

MORGAN, R. L., WHALEY, P., THAYER, K. A. & SCHÜNEMANN, H. J. 2018. Identifying the PECO: a framework for formulating good questions to explore the association of environmental and other exposures with health outcomes. *Environment international,* 121**,** 1027.

MORLEY, J. E., ARGILES, J. M., EVANS, W. J., BHASIN, S., CELLA, D., DEUTZ, N. E., DOEHNER, W., FEARON, K. C., FERRUCCI, L. & HELLERSTEIN, M. K. 2010. Nutritional recommendations for the management of sarcopenia. *Journal of the american Medical Directors association,* 11**,** 391-396.

MORLEY, J. E., THOMAS, D. R. & WILSON, M.-M. G. 2006. Cachexia: pathophysiology and clinical relevance1, 2. *The American journal of clinical nutrition,* 83, 735-743.

MORRIS, D. L. & RUI, L. 2009. Recent advances in understanding leptin signaling and leptin resistance. *American Journal of Physiology-Endocrinology and Metabolism,* 297, E1247-E1259.

MORTON, G. J. 2007. Hypothalamic leptin regulation of energy homeostasis and glucose metabolism. *The Journal of physiology,* 583, 437-443.

MOURKIOTI, F., KRATSIOS, P., LUEDDE, T., SONG, Y.-H., DELAFONTAINE, P., ADAMI, R., PARENTE, V., BOTTINELLI, R., PASPARAKIS, M. & ROSENTHAL, N. 2006. Targeted ablation of IKK2 improves skeletal muscle strength, maintains mass, and promotes regeneration. *The Journal of clinical investigation,* 116, 2945-2954.

MUNCK, A. & NÁRAY-FEJES-TÓTH, A. 1994. Glucocorticoids and stress: permissive and suppressive actions. *Annals of the New York Academy of Sciences,* 746, 115-30; discussion 131.

NAGANO, F., YOSHIMURA, Y., BISE, T., SHIMAZU, S. & SHIRAISHI, A. 2020. Muscle mass gain is positively associated with functional recovery in patients with sarcopenia after stroke. *Journal of Stroke & Cerebrovascular Diseases,* 29, 105017.

NAKLING, A. E., AARSLAND, D., NÆSS, H., WOLLSCHLAEGER, D., FLADBY, T., HOFSTAD, H. & WEHLING, E. 2017. Cognitive deficits in chronic stroke patients: neuropsychological assessment, depression, and self-reports. *Dementia and geriatric cognitive disorders extra,* 7, 283-296.

NEWGARD, C. B., AN, J., BAIN, J. R., MUEHLBAUER, M. J., STEVENS, R. D., LIEN, L. F., HAQQ, A. M., SHAH, S. H., ARLOTTO, M. & SLENTZ, C. A. 2009. A branched-chain amino acid-related metabolic signature that differentiates obese and lean humans and contributes to insulin resistance. *Cell metabolism,* 9, 311-326.

NEWMAN, J. C. & VERDIN, E. 2017. ß-Hydroxybutyrate: a signaling metabolite. *Annual review of nutrition,* 37, 51-76.

NG, Y. S., STEIN, J., NING, M. & BLACK-SCHAFFER, R. M. 2007. Comparison of clinical characteristics and functional outcomes of ischemic stroke in different vascular territories. *Stroke,* 38, 2309-2314.

NOGUEIRA, R. G., JADHAV, A. P., HAUSSEN, D. C., BONAFE, A., BUDZIK, R. F., BHUVA, P., YAVAGAL, D. R., RIBO, M., COGNARD, C. & HANEL, R. A. 2018. Thrombectomy 6 to 24 hours after stroke with a mismatch between deficit and infarct. *New England Journal of Medicine,* 378, 11-21.

O'COLLINS, V. E., DONNAN, G. A., MACLEOD, M. R. & HOWELLS, D. W. 2017. Animal models of ischemic stroke versus clinical stroke: comparison of infarct size, cause, location, study design, and efficacy of experimental therapies. *Animal models for the study of human disease*. Elsevier.

OESCH, L., TATLISUMAK, T., ARNOLD, M. & SARIKAYA, H. 2017. Obesity paradox in stroke–Myth or reality? A systematic review. *PloS one,* 12, e0171334.

OLSEN, T., SKRIVER, E. B. & HERNING, M. 1985. Cause of cerebral infarction in the carotid territory. Its relation to the size and the location of the infarct and to the underlying vascular lesion. *stroke,* 16, 459-466.

OLSEN, T. S., DEHLENDORFF, C., PETERSEN, H. G. & ANDERSEN, K. K. 2008. Body mass index and poststroke mortality. *Neuroepidemiology,* 30, 93-100.

OREOPOULOS, A., PADWAL, R., KALANTAR-ZADEH, K., FONAROW, G. C., NORRIS, C. M. & MCALISTER, F. A. 2008. Body mass index and mortality in heart failure: a meta-analysis. *American heart journal,* 156, 13-22.

PARK, J. G., LEE, K. W., KIM, S. B., LEE, J. H. & KIM, Y. H. 2019a. Effect of decreased skeletal muscle index and hand grip strength on functional recovery in subacute ambulatory stroke patients. *Annals of Rehabilitation Medicine,* 43, 535-543.

PARK, J. G., LEE, K. W., KIM, S. B., LEE, J. H. & KIM, Y. H. 2019b. Effect of Decreased Skeletal Muscle Index and Hand Grip Strength on Functional Recovery in Subacute Ambulatory Stroke Patients. *Ann Rehabil Med,* 43, 535-543.

PARK, S. S., KWON, E.-S. & KWON, K.-S. 2017. Molecular mechanisms and therapeutic interventions in sarcopenia. *Osteoporosis and sarcopenia,* 3, 117-122.

PASSMORE, L. A. & BARFORD, D. 2004. Getting into position: the catalytic mechanisms of protein ubiquitylation. *Biochemical Journal,* 379, 513-525.

PÉREZ-MATO, M., LÓPEZ-ARIAS, E., BUGALLO-CASAL, A., CORREA-PAZ, C., ARIAS, S., RODRÍGUEZ-YÁÑEZ, M., SANTAMARÍA-CADAVID, M. & CAMPOS, F. 2024. New perspectives in neuroprotection for ischemic stroke. *Neuroscience,* 550, 30-42.

PLOTKIN, D. L., ROBERTS, M. D., HAUN, C. T. & SCHOENFELD, B. J. 2021. Muscle fiber type transitions with exercise training: shifting perspectives. *Sports,* 9, 127.

PROKOPIDIS, K., IRLIK, K., HENDEL, M., PIAŚNIK, J., LIP, G. Y. & NABRDALIK, K. 2024. Prognostic Impact and Prevalence of Cachexia in Patients With Heart Failure: A Systematic Review and Meta-Analysis. *Journal of cachexia, sarcopenia and muscle,* 15, 2536-2543.

RABADI, M., COAR, P., LUKIN, M., LESSER, M. & BLASS, J. 2008. Intensive nutritional supplements can improve outcomes in stroke rehabilitation. *Neurology,* 71, 1856-1861.

RAPOSINHO, P., PIERROZ, D., BROQUA, P., WHITE, R., PEDRAZZINI, T. & AUBERT, M. 2001. Chronic administration of neuropeptide Y into the lateral ventricle of C57BL/6J male mice produces an obesity syndrome including hyperphagia, hyperleptinemia, insulin resistance, and hypogonadism. *Molecular and cellular endocrinology,* 185, 195-204.

RITZEL, R. M., LAI, Y.-J., CRAPSER, J. D., PATEL, A. R., SCHRECENGOST, A., GRENIER, J. M., MANCINI, N. S., PATRIZZ, A., JELLISON, E. R. & MORALES-SCHEIHING, D. 2018. Aging alters the immunological response to ischemic stroke. *Acta neuropathologica,* 136, 89-110.

RODRIGUEZ-CASTRO, E., RODRIGUEZ-YANEZ, M., ARIAS-RIVAS, S., SANTAMARIA-CADAVID, M., LOPEZ-DEQUIDT, I., HERVELLA, P., LOPEZ, M., CAMPOS, F., SOBRINO, T. & CASTILLO, J. 2019. Obesity Paradox in Ischemic Stroke: Clinical and Molecular Insights. *Translational Stroke Research,* 10, 639-649.

ROH, E. & KIM, M.-S. 2016. Brain regulation of energy metabolism. *Endocrinology and metabolism,* 31, 519.

ROMERO-CORRAL, A., SOMERS, V. K., SIERRA-JOHNSON, J., THOMAS, R. J., COLLAZO-CLAVELL, M., KORINEK, J., ALLISON, T. G., BATSIS, J., SERT-KUNIYOSHI, F. & LOPEZ-JIMENEZ, F. 2008. Accuracy of body mass index in diagnosing obesity in the adult general population. *International journal of obesity,* 32, 959-966.

ROMMEL, C., BODINE, S. C., CLARKE, B. A., ROSSMAN, R., NUNEZ, L., STITT, T. N., YANCOPOULOS, G. D. & GLASS, D. J. 2001. Mediation of IGF-1-induced skeletal myotube hypertrophy by PI (3) K/Akt/mTOR and PI (3) K/Akt/GSK3 pathways. *Nature cell biology,* 3, 1009-1013.

ROUBENOFF, R., PARISE, H., PAYETTE, H. A., ABAD, L. W., D'AGOSTINO, R., JACQUES, P. F., WILSON, P. W., DINARELLO, C. A. & HARRIS, T. B. 2003. Cytokines, insulin-like growth factor 1, sarcopenia, and mortality in very old community-dwelling men and women: the Framingham Heart Study. *The American journal of medicine,* 115**,** 429-435.

RUAS, J. L., WHITE, J. P., RAO, R. R., KLEINER, S., BRANNAN, K. T., HARRISON, B. C., GREENE, N. P., WU, J., ESTALL, J. L. & IRVING, B. A. 2012. A PGC-1α isoform induced by resistance training regulates skeletal muscle hypertrophy. *Cell,* 151**,** 1319-1331.

RUIZ-GARCÍA, V., LÓPEZ-BRIZ, E., CARBONELL-SANCHIS, R., BORT-MARTÍ, S. & GONZÁLVEZ-PERALES, J. L. 2018. Megestrol acetate for cachexia–anorexia syndrome. A systematic review. *Journal of Cachexia, Sarcopenia and Muscle,* 9**,** 444-452.

RYAN, A. S., BUSCEMI, A., FORRESTER, L., HAFER-MACKO, C. E. & IVEY, F. M. 2011a. Atrophy and intramuscular fat in specific muscles of the thigh: associated weakness and hyperinsulinemia in stroke survivors. *Neurorehabilitation and neural repair,* 25**,** 865-872.

RYAN, A. S., DOBROVOLNY, C. L., SILVER, K. H., SMITH, G. V. & MACKO, R. F. 2000. Cardiovascular fitness after stroke: role of muscle mass and gait deficit severity. *Journal of Stroke and Cerebrovascular Diseases,* 9**,** 185-191.

RYAN, A. S., IVEY, F. M., PRIOR, S., LI, G. & HAFER-MACKO, C. 2011b. Skeletal muscle hypertrophy and muscle myostatin reduction after resistive training in stroke survivors. *Stroke,* 42**,** 416-420.

RYAN, A. S., IVEY, F. M., SERRA, M. C., HARTSTEIN, J. & HAFER-MACKO, C. E. 2017. Sarcopenia and Physical Function in Middle-Aged and Older Stroke Survivors. *Archives of Physical Medicine & Rehabilitation,* 98**,** 495-499.

SALAUDEEN, M. A., BELLO, N., DANRAKA, R. N. & AMMANI, M. L. 2024. Understanding the pathophysiology of ischemic stroke: the basis of current therapies and opportunity for new ones. *Biomolecules,* 14**,** 305.

SAMANIEGO, E. A., ROA, J. A., LIMAYE, K. & ADAMS JR, H. P. 2018. Mechanical thrombectomy: emerging technologies and techniques. *Journal of Stroke and Cerebrovascular Diseases,* 27**,** 2555-2571.

SANDRI, M. 2008. Signaling in muscle atrophy and hypertrophy. *Physiology,* 23**,** 160-170.

SANDRI, M. 2013. Protein breakdown in muscle wasting: role of autophagy-lysosome and ubiquitin-proteasome. *The international journal of biochemistry & cell biology,* 45**,** 2121-2129.

SANDRI, M., SANDRI, C., GILBERT, A., SKURK, C., CALABRIA, E., PICARD, A., WALSH, K., SCHIAFFINO, S., LECKER, S. H. & GOLDBERG, A. L. 2004. Foxo transcription factors induce the atrophy-related ubiquitin ligase atrogin-1 and cause skeletal muscle atrophy. *Cell,* 117**,** 399-412.

SANTHOSHKUMAR, C. R., DEUTSCH, J. C., KOLHOUSE, J. C., HASSELL, K. L. & KOLHOUSE, J. F. 1994. Measurement of excitatory sulfur amino acids, cysteine sulfinic acid, cysteic acid, homocysteine sulfinic acid, and homocysteic acid in serum by stable isotope dilution gas chromatography-mass spectrometry and selected ion monitoring. *Analytical biochemistry,* 220**,** 249-256.

SAVITZ, S. I., BARON, J.-C., YENARI, M. A., SANOSSIAN, N. & FISHER, M. 2017. Reconsidering neuroprotection in the reperfusion era. *Stroke,* 48**,** 3413-3419.

SCHEFER, V. & TALAN, M. I. 1996. Oxygen consumption in adult and AGED C57BL/6J mice during acute treadmill exercise of different intensity. *Experimental gerontology,* 31**,** 387-392.

SCHERBAKOV, N., DIRNAGL, U. & DOEHNER, W. 2011a. Body weight after stroke: lessons from the obesity paradox. *Stroke,* 42**,** 3646-3650.

SCHERBAKOV, N., DIRNAGL, U. & DOEHNER, W. 2011b. Body weight after stroke: lessons from the obesity paradox. *Stroke,* 42**,** 3646-50.

SCHERBAKOV, N. & DOEHNER, W. 2011. Sarcopenia in stroke—facts and numbers on muscle loss accounting for disability after stroke. *Journal of cachexia, sarcopenia and muscle,* 2**,** 5-8.

SCHERBAKOV, N., PIETROCK, C., SANDEK, A., EBNER, N., VALENTOVA, M., SPRINGER, J., SCHEFOLD, J., VON HAEHLING, S., ANKER, S. & NORMAN, K. 2019a. Body weight changes and incidence of cachexia after stroke. J Cachexia Sarcopenia Muscle 10: 611–620.

SCHERBAKOV, N., PIETROCK, C., SANDEK, A., EBNER, N., VALENTOVA, M., SPRINGER, J., SCHEFOLD, J. C., VON HAEHLING, S., ANKER, S. D. & NORMAN, K. 2019b. Body weight changes and incidence of cachexia after stroke. *Journal of cachexia, sarcopenia and muscle,* 10**,** 611-620.

SCHERBAKOV, N., PIETROCK, C., SANDEK, A., EBNER, N., VALENTOVA, M., SPRINGER, J., SCHEFOLD, J. C., VON HAEHLING, S., ANKER, S. D., NORMAN, K., HAEUSLER, K. G. & DOEHNER, W. 2019c. Body weight changes and incidence of cachexia after stroke. *Journal of Cachexia, Sarcopenia and Muscle,* 10**,** 611-620.

SCHERBAKOV, N., SANDEK, A. & DOEHNER, W. 2015. Stroke-related sarcopenia: specific characteristics. *Journal of the American Medical Directors Association,* 16**,** 272-276.

SCHERBAKOV, N., VON HAEHLING, S., ANKER, S. D., DIRNAGL, U. & DOEHNER, W. 2013. Stroke induced Sarcopenia: muscle wasting and disability after stroke. *International journal of cardiology,* 170**,** 89-94.

SCHLUETER, N., DE STERKE, A., WILLMES, D. M., SPRANGER, J., JORDAN, J. & BIRKENFELD, A. L. 2014. Metabolic actions of natriuretic peptides and therapeutic potential in the metabolic syndrome. *Pharmacology & therapeutics,* 144**,** 12-27.

SCHMIDT, A., HARADA, S.-I., KIMMEL, D. B., BAI, C., CHEN, F., RUTLEDGE, S. J., VOGEL, R. L., SCAFONAS, A., GENTILE, M. A. & NANTERMET, P. V. 2009. Identification of anabolic selective androgen receptor modulators with reduced activities in reproductive tissues and sebaceous glands. *Journal of Biological Chemistry,* 284**,** 36367-36376.

SCOTT, W., STEVENS, J. & BINDER–MACLEOD, S. A. 2001. Human skeletal muscle fiber type classifications. *Physical therapy,* 81**,** 1810-1816.

SCRUTINIO, D., LANZILLO, B., GUIDA, P., PASSANTINO, A., SPACCAVENTO, S. & BATTISTA, P. 2020. Association between malnutrition and outcomes in patients with severe ischemic stroke undergoing rehabilitation. *Archives of physical medicine and rehabilitation,* 101**,** 852-860.

SHAHJOUEI, S., CAI, P. Y., ANSARI, S., SHARIFIFAR, S., AZARI, H., GANJI, S. & ZAND, R. 2016. Middle cerebral artery occlusion model of stroke in rodents: a step-by-step approach. *Journal of vascular and interventional neurology,* 8**,** 1.

SHI, K., WOOD, K., SHI, F.-D., WANG, X. & LIU, Q. 2018. Stroke-induced immunosuppression and poststroke infection. *Stroke and vascular neurology,* 3.

SHIRAISHI, A., YOSHIMURA, Y., WAKABAYASHI, H. & TSUJI, Y. 2018. Prevalence of stroke-related sarcopenia and its association with poor oral status in

post-acute stroke patients: Implications for oral sarcopenia. *Clinical Nutrition,* 37**,** 204-207.

SIBOLT, G., CURTZE, S., MELKAS, S., POHJASVAARA, T., KASTE, M., KARHUNEN, P. J., OKSALA, N. K., VATAJA, R. & ERKINJUNTTI, T. 2013. Post-stroke depression and depression-executive dysfunction syndrome are associated with recurrence of ischaemic stroke. *Cerebrovascular Diseases,* 36**,** 336-343.

SIMARD, J. M., KENT, T. A., CHEN, M., TARASOV, K. V. & GERZANICH, V. 2007. Brain oedema in focal ischaemia: molecular pathophysiology and theoretical implications. *The Lancet Neurology,* 6**,** 258-268.

SIMARD, J. M., WOO, S. K., SCHWARTZBAUER, G. T. & GERZANICH, V. 2012. Sulfonylurea receptor 1 in central nervous system injury: a focused review. *Journal of Cerebral Blood Flow & Metabolism,* 32**,** 1699-1717.

SIOTTO, M., GERMANOTTA, M., GUERRINI, A., PASCALI, S., CIPOLLINI, V., CORTELLINI, L., RUCO, E., KHAZRAI, Y. M., DE GARA, L. & APRILE, I. 2022. Relationship between Nutritional Status, Food Consumption and Sarcopenia in Post-Stroke Rehabilitation: Preliminary Data. *Nutrients,* 14**,** 15.

SKOLARUS, L. E., SANCHEZ, B. N., LEVINE, D. A., BAEK, J., KERBER, K. A., MORGENSTERN, L. B., SMITH, M. A. & LISABETH, L. D. 2014. Association of body mass index and mortality after acute ischemic stroke. *Circulation: Cardiovascular Quality and Outcomes,* 7**,** 64-69.

SMITH, S. M. & VALE, W. W. 2006. The role of the hypothalamic-pituitary-adrenal axis in neuroendocrine responses to stress. *Dialogues in clinical neuroscience,* 8**,** 383-395.

SONG, I.-U., KIM, J.-S., RYU, S.-Y., LEE, S.-B., LEE, S.-J., JEONG, D.-S., KIM, Y.-I. & LEE, K.-S. 2009. Are plasma homocysteine levels related to neurological severity and functional outcome after ischemic stroke in the Korean population? *Journal of the neurological sciences,* 278**,** 60-63.

SOSIAWATI, A. F., IRWAN, A. M. & ISNAH, W. O. N. 2021. Identifying sarcopenia among post-stroke older people. *Enfermeria Clinica,* 31**,** S847-S850.

SPRINGER, J., SCHUST, S., PESKE, K., TSCHIRNER, A., REX, A., ENGEL, O., SCHERBAKOV, N., MEISEL, A., VON HAEHLING, S. & BOSCHMANN, M. 2014a. Catabolic signaling and muscle wasting after acute ischemic stroke in mice: indication for a stroke-specific sarcopenia. *Stroke,* 45**,** 3675-3683.

SPRINGER, J., SCHUST, S., PESKE, K., TSCHIRNER, A., REX, A., ENGEL, O., SCHERBAKOV, N., MEISEL, A., VON HAEHLING, S., BOSCHMANN, M., ANKER, S. D., DIRNAGL, U. & DOEHNER, W. 2014b. Catabolic Signaling and Muscle Wasting After Acute Ischemic Stroke in Mice Indication for a Stroke-Specific Sarcopenia. *Stroke,* 45**,** 3675-+.

STERN, J. H., KIM, K. & RAMSEY, J. J. 2012. The influence of shc proteins and aging on whole body energy expenditure and substrate utilization in mice. *PloS one,* 7**,** e48790.

STITT, T. N., DRUJAN, D., CLARKE, B. A., PANARO, F., TIMOFEYVA, Y., KLINE, W. O., GONZALEZ, M., YANCOPOULOS, G. D. & GLASS, D. J. 2004. The IGF-1/PI3K/Akt pathway prevents expression of muscle atrophy-induced ubiquitin ligases by inhibiting FOXO transcription factors. *Molecular cell,* 14**,** 395-403.

STOKUM, J. A., GERZANICH, V. & SIMARD, J. M. 2016. Molecular pathophysiology of cerebral edema. *Journal of Cerebral Blood Flow & Metabolism,* 36**,** 513-538.

SU, Y., YUKI, M. & OTSUKI, M. 2020. Prevalence of stroke-related sarcopenia: a systematic review and meta-analysis. *Journal of Stroke and Cerebrovascular Diseases,* 29**,** 105092.

SUN, W., HUANG, Y., XIAN, Y., ZHU, S., JIA, Z., LIU, R., LI, F., WEI, J. W., WANG, J.-G. & LIU, M. 2017. Association of body mass index with mortality and functional outcome after acute ischemic stroke. *Scientific reports,* 7**,** 2507.

SUOFU, Y., JAUHARI, A., NIRMALA, E. S., MULLINS, W. A., WANG, X., LI, F., CARLISLE, D. L. & FRIEDLANDER, R. M. 2023. Neuronal melatonin type 1 receptor overexpression promotes M2 microglia polarization in cerebral ischemia/reperfusion-induced injury. *Neuroscience letters,* 795**,** 137043.

SUSSULINI, A. 2017. *Metabolomics: from fundamentals to clinical applications*, Springer.

SUTHERLAND, B. A., MINNERUP, J., BALAMI, J. S., ARBA, F., BUCHAN, A. M. & KLEINSCHNITZ, C. 2012. Neuroprotection for ischaemic stroke: translation from the bench to the bedside. *International Journal of Stroke,* 7**,** 407-418.

SZCZUDLIK, A., DZIEDZIC, T., BARTUS, S., SLOWIK, A. & KIELTYKA, A. 2004. Serum interleukin-6 predicts cortisol release in acute stroke patients. *Journal of endocrinological investigation,* 27**,** 37-41.

TEMEL, J. S., ABERNETHY, A. P., CURROW, D. C., FRIEND, J., DUUS, E. M., YAN, Y. & FEARON, K. C. 2016. Anamorelin in patients with non-small-cell lung cancer and cachexia (ROMANA 1 and ROMANA 2): results from two randomised, double-blind, phase 3 trials. *The Lancet Oncology,* 17**,** 519-531.

THELLIN, O., ZORZI, W., LAKAYE, B., DE BORMAN, B., COUMANS, B., HENNEN, G., GRISAR, T., IGOUT, A. & HEINEN, E. 1999. Housekeeping genes as internal standards: use and limits. *Journal of biotechnology,* 75**,** 291-295.

THIBAUT, M. M., SBOARINA, M., ROUMAIN, M., PÖTGENS, S. A., NEYRINCK, A. M., DESTRÉE, F., GILLARD, J., LECLERCQ, I. A., DACHY, G. & DEMOULIN, J. B. 2021. Inflammation-induced cholestasis in cancer cachexia. *Journal of cachexia, sarcopenia and muscle,* 12**,** 70-90.

TORRE-AMIONE, G., KAPADIA, S., LEE, J., DURAND, J.-B., BIES, R. D., YOUNG, J. B. & MANN, D. L. 1996. Tumor necrosis factor-α and tumor necrosis factor receptors in the failing human heart. *Circulation,* 93**,** 704-711.

TOUNG, T. J., CHEN, T.-Y., LITTLETON-KEARNEY, M. T., HURN, P. D. & MURPHY, S. J. 2004. Effects of combined estrogen and progesterone on brain infarction in reproductively senescent female rats. *Journal of Cerebral Blood Flow & Metabolism,* 24**,** 1160-1166.

TRAN, L. T., PARK, S., KIM, S. K., LEE, J. S., KIM, K. W. & KWON, O. 2022. Hypothalamic control of energy expenditure and thermogenesis. *Experimental & molecular medicine,* 54**,** 358-369.

TRENDELENBURG, A. U., MEYER, A., ROHNER, D., BOYLE, J., HATAKEYAMA, S. & GLASS, D. J. 2009. Myostatin reduces Akt/TORC1/p70S6K signaling, inhibiting myoblast differentiation and myotube size. *American Journal of Physiology-Cell Physiology,* 296**,** C1258-C1270.

TROTMAN-LUCAS, M., KELLY, M. E., JANUS, J., FERN, R. & GIBSON, C. L. 2017. An alternative surgical approach reduces variability following filament induction of experimental stroke in mice. *Disease Models & Mechanisms,* 10**,** 931-938.

TRUEMAN, R. C., HARRISON, D. J., DWYER, D. M., DUNNETT, S. B., HOEHN, M. & FARR, T. D. 2011a. A critical re-examination of the intraluminal filament

MCAO model: impact of external carotid artery transection. *Translational stroke research,* 2, 651-661.

TRUEMAN, R. C., HARRISON, D. J., DWYER, D. M., DUNNETT, S. B., HOEHN, M. & FARR, T. D. 2011b. A critical re-examination of the intraluminal filament MCAO model: impact of external carotid artery transection. *Translational stroke research,* 2, 651-661.

VAN GAMMEREN, D., DAMRAUER, J. S., JACKMAN, R. W. & KANDARIAN, S. C. 2009. The IκB kinases IKKα and IKKß are necessary and sufficient for skeletal muscle atrophy. *The FASEB Journal,* 23, 362.

VEMMOS, K., NTAIOS, G., SPENGOS, K., SAVVARI, P., VEMMOU, A., PAPPA, T., MANIOS, E., GEORGIOPOULOS, G. & ALEVIZAKI, M. 2011. Association between obesity and mortality after acute first-ever stroke. *Stroke*.

VERMA, R., HARRIS, N. M., FRIEDLER, B. D., CRAPSER, J., PATEL, A. R., VENNA, V. & MCCULLOUGH, L. D. 2016. Reversal of the detrimental effects of post-stroke social isolation by pair-housing is mediated by activation of BDNF-MAPK/ERK in aged mice. *Scientific reports,* 6, 25176.

VERMA, S. K., NAGASHIMA, K., YALIGAR, J., MICHAEL, N., LEE, S. S., XIANFENG, T., GOPALAN, V., SADANANTHAN, S. A., ANANTHARAJ, R. & VELAN, S. S. 2017. Differentiating brown and white adipose tissues by high-resolution diffusion NMR spectroscopy. *Journal of lipid research,* 58, 289-298.

VERMEER, S. E., SANDEE, W., ALGRA, A., KOUDSTAAL, P. J., KAPPELLE, L. J. & DIPPEL, D. W. 2006. Impaired glucose tolerance increases stroke risk in nondiabetic patients with transient ischemic attack or minor ischemic stroke. *Stroke,* 37, 1413-1417.

VON HAEHLING, S., LAINSCAK, M., SPRINGER, J. & ANKER, S. D. 2009. Cardiac cachexia: a systematic overview. *Pharmacology & therapeutics,* 121, 227-252.

VYAS, D. R., SPANGENBURG, E. E., ABRAHA, T. W., CHILDS, T. E. & BOOTH, F. W. 2002. GSK-3ß negatively regulates skeletal myotube hypertrophy. *American Journal of Physiology-Cell Physiology,* 283, C545-C551.

WANG, R., JIAO, H., ZHAO, J., WANG, X. & LIN, H. 2016. Glucocorticoids enhance muscle proteolysis through a myostatin-dependent pathway at the early stage. *PloS one,* 11, e0156225.

WANG, X., LIU, T., SONG, H., CUI, S., LIU, G., CHRISTOFOROU, A., FLAHERTY, P., LUO, X., WOOD, L. & WANG, Q. M. 2020. Targeted metabolomic profiling reveals association between altered amino acids and poor functional recovery after stroke. *Frontiers in Neurology,* 10, 1425.

WEBB, B. L. & PROUD, C. G. 1997. Eukaryotic initiation factor 2B (eIF2B). *The international journal of biochemistry & cell biology,* 29, 1127-1131.

WELLS, G., SHEA, B., O'CONNELL, D., PETERSON, J., WELCH, V., LOSOS, M. & TUGWELL, P. 2014. Newcastle-Ottawa quality assessment scale cohort studies. *University of Ottawa*.

WENK, G. L., WALKER, L. C., PRICE, D. L. & CORK, L. C. 1991. Loss of NMDA, but not GABA-A, binding in the brains of aged rats and monkeys. *Neurobiology of aging,* 12, 93-98.

WOHLFAHRT, P., LOPEZ-JIMENEZ, F., KRAJCOVIECHOVA, A., JOZIFOVA, M., MAYER, O., VANEK, J., FILIPOVSKY, J., LLANO, E. M. & CIFKOVA, R. 2015. The obesity paradox and survivors of ischemic stroke. *Journal of Stroke & Cerebrovascular Diseases,* 24, 1443-50.

WREN, A., SEAL, L., COHEN, M., BRYNES, A., FROST, G., MURPHY, K., DHILLO, W., GHATEI, M. & BLOOM, S. 2001. Ghrelin enhances appetite and increases food intake in humans. *J clin Endocrinol metab,* 86, 5992.

WU, C.-T., CHEN, M.-C., LIU, S.-H., YANG, T.-H., LONG, L.-H., GUAN, S.-S. & CHEN, C.-M. 2021. Bioactive flavonoids icaritin and icariin protect against cerebral ischemia–reperfusion-associated apoptosis and extracellular matrix accumulation in an ischemic stroke mouse model. *Biomedicines,* 9**,** 1719.

XIAO, X.-T., LUO, C., YUAN, Y., XIAO, L. & QU, W.-S. 2021. Systematic evaluation during early-phase ischemia predicts outcomes in middle cerebral artery occlusion mice. *Neuroreport,* 32**,** 29-37.

XU, C., HE, J., JIANG, H., ZU, L., ZHAI, W., PU, S. & XU, G. 2009. Direct effect of glucocorticoids on lipolysis in adipocytes. *Molecular endocrinology,* 23**,** 1161-1170.

XU, S.-Y. & PAN, S.-Y. 2013. The failure of animal models of neuroprotection in acute ischemic stroke to translate to clinical efficacy. *Medical science monitor basic research,* 19**,** 37.

XU, Z., LI, Y., TANG, S., HUANG, X. & CHEN, T. 2015. Current use of oral contraceptives and the risk of first-ever ischemic stroke: a meta-analysis of observational studies. *Thrombosis research,* 136**,** 52-60.

XUE, C., LI, G., ZHENG, Q., GU, X., SHI, Q., SU, Y., CHU, Q., YUAN, X., BAO, Z. & LU, J. 2023. Tryptophan metabolism in health and disease. *Cell metabolism,* 35**,** 1304-1326.

YAMAMOTO, M., NOZOE, M., MASUYA, R., YOSHIDA, Y., KUBO, H., SHIMADA, S. & SHOMOTO, K. 2022. Cachexia criteria in chronic illness associated with acute weight loss in patients with stroke. *Nutrition,* 96**,** 111562.

YANG, J., KIM, E., BELTRAN, C. & CHO, S. 2019. Corticosterone-mediated body weight loss is an important catabolic process for poststroke immunity and survival. *Stroke,* 50**,** 2539-2546.

YAO, R., YAO, L., RAO, A., OU, J., WANG, W., HOU, Q., XU, C. & GAO, B.-L. 2022. Prevalence and risk factors of stroke-related sarcopenia at the subacute stage: A case control study. *Frontiers in Neurology,* 13.

YOON, C. W. & BUSHNELL, C. D. 2023. Stroke in women: a review focused on epidemiology, risk factors, and outcomes. *Journal of Stroke,* 25**,** 2-15.

YOON, N., KIM, Y., KIM, S.-D., KIM, M., JUNG, B. H. & SONG, Y. S. 2022. Investigation of long-term metabolic alteration after stroke in tMCAO (transient middle cerebral artery occlusion) mouse model using metabolomics approach. *Neuroscience Letters,* 774**,** 136492.

YOSHIDA, T. & DELAFONTAINE, P. 2015. Mechanisms of cachexia in chronic disease states. *The American journal of the medical sciences,* 350**,** 250-256.

YOSHIDA, T. & DELAFONTAINE, P. 2020. Mechanisms of IGF-1-mediated regulation of skeletal muscle hypertrophy and atrophy. *Cells,* 9**,** 1970.

YOSHIMURA, Y., BISE, T., SHIMAZU, S., TANOUE, M., TOMIOKA, Y., ARAKI, M., NISHINO, T., KUZUHARA, A. & TAKATSUKI, F. 2019a. Effects of a leucine-enriched amino acid supplement on muscle mass, muscle strength, and physical function in post-stroke patients with sarcopenia: A randomized controlled trial. *Nutrition,* 58**,** 1-6.

YOSHIMURA, Y., WAKABAYASHI, H., BISE, T., NAGANO, F., SHIMAZU, S., SHIRAISHI, A., YAMAGA, M. & KOGA, H. 2019b. Sarcopenia is associated with worse recovery of physical function and dysphagia and a lower rate of home discharge in Japanese hospitalized adults undergoing convalescent rehabilitation. *Nutrition,* 61**,** 111-118.

YOSHIMURA, Y., WAKABAYASHI, H., BISE, T. & TANOUE, M. 2018. Prevalence of sarcopenia and its association with activities of daily living and dysphagia

in convalescent rehabilitation ward inpatients. *Clinical Nutrition,* 37**,** 2022-2028.

ZAREMBA, J. & LOSY, J. 2001. Early TNF-α levels correlate with ischaemic stroke severity. *Acta Neurologica Scandinavica,* 104**,** 288-295.

ZENG, C., WEN, B., HOU, G., LEI, L., MEI, Z., JIA, X., CHEN, X., ZHU, W., LI, J. & KUANG, Y. 2017. Lipidomics profiling reveals the role of glycerophospholipid metabolism in psoriasis. *Gigascience,* 6**,** gix087.

ZHANG, A., SUN, H. & WANG, X. 2014. Urinary metabolic profiling of rat models revealed protective function of scoparone against alcohol induced hepatotoxicity. *Scientific reports,* 4**,** 6768.

ZHANG, A., SUN, H., YAN, G., WANG, P. & WANG, X. 2015. Metabolomics for biomarker discovery: moving to the clinic. *BioMed research international,* 2015**,** 354671.

ZHANG, H. H., HALBLEIB, M., AHMAD, F., MANGANIELLO, V. C. & GREENBERG, A. S. 2002. Tumor necrosis factor-α stimulates lipolysis in differentiated human adipocytes through activation of extracellular signal-related kinase and elevation of intracellular cAMP. *Diabetes,* 51**,** 2929-2935.

ZHAO, L., DU, W., ZHAO, X., LIU, L., WANG, C., WANG, Y., WANG, A., LIU, G., WANG, Y. & XU, Y. 2014. Favorable functional recovery in overweight ischemic stroke survivors: findings from the China National Stroke Registry. *Journal of Stroke and Cerebrovascular Diseases,* 23**,** e201-e206.

ZHONG, H. & SIMONS, J. W. 1999. Direct comparison of GAPDH, β-actin, cyclophilin, and 28S rRNA as internal standards for quantifying RNA levels under hypoxia. *Biochemical and biophysical research communications,* 259**,** 523-526.

ZIMMERS, T. A., DAVIES, M. V., KONIARIS, L. G., HAYNES, P., ESQUELA, A. F., TOMKINSON, K. N., MCPHERRON, A. C., WOLFMAN, N. M. & LEE, S.-J. 2002. Induction of cachexia in mice by systemically administered myostatin. *Science,* 296**,** 1486-1488.